

The leucine-rich repeat immune protein family in malaria vector mosquitoes

Leanna Marie Upton

Supervised by Prof. George K. Christophides

Imperial College London

Division of Cell & Molecular Biology

Department of Life Sciences

A thesis submitted for the degree of Doctor of Philosophy, 2012

Declaration of originality

I certify that this thesis and the research upon which it is based are the product of my own work. Any ideas, quotations, results or publications from other authors are clearly stated in accordance with standard referencing practises and all scientific collaborations are acknowledged. This thesis contains some material modified from my MPhil/PhD transfer report. Some data has been published in Povelones et al., 2011.



Leanna Marie Upton

September 2012

Abstract

A novel mosquito-specific family of leucine-rich repeat immune proteins (LRIMs) was recently identified in *Anopheles gambiae*, the major vector of malaria in Africa. The founding family members, LRIM1 and APL1C, form a heterodimer circulating in the mosquito hemolymph and mediate killing of malaria parasites through their interaction with the complement C3-like effector, TEP1. This PhD thesis investigated the role of the LRIM family in mosquito immunity.

Transcriptional profiling demonstrated that different LRIMs show distinct responses to malarial, fungal, bacterial and viral infections as well as to blood feeding. Certain LRIMs are broadly induced whereas others respond specifically to particular immune challenges, suggesting that there is specificity within the LRIM family towards different infections. RNA interference-mediated gene silencing identified LRIM9 as a novel antagonist of the rodent malaria parasite, *Plasmodium berghei*, with a putative role in parasite melanisation. Silencing *LRIM9* partially inhibits the activity of phenoloxidase, a key enzyme in the melanisation pathway, but does not affect tissue melanisation. Unlike the LRIM1/APL1C heterodimer, LRIM9 circulates as a monomer in the mosquito hemolymph and is not involved in antibacterial defence. As LRIM9 does not interact with TEP1 and is not involved in TEP1 activity against *Plasmodium*, its precise function in the mosquito immune system remains unclear. Importantly, LRIM9 is highly upregulated in female mosquitoes after blood feeding but does not function in mosquito reproduction.

The findings reported in this thesis indicate that the LRIM family has diversified to respond to infections with different microbes that mosquitoes encounter in their blood feeding lifestyle. LRIM9 is an important novel candidate for involvement in defence against malaria parasites. We hypothesise that LRIM9 is induced after blood feeding in anticipation of blood-borne infections, which is an original concept in mosquito immunity.

Acknowledgements

I would firstly like to thank my supervisor, Prof. George K. Christophides, for his excellent scientific input, support and guidance throughout my PhD. I also wish to thank Dr Michael Povelones for his invaluable day-to-day supervision and his endless ideas, enthusiasm and patience. I am extremely grateful for all the time and effort you have both devoted to me and my project over the last four years. I have learnt so much from you both and feel very privileged to have had the opportunity to work with you.

I would like to thank all past and present members of the Christophides-Kafatos laboratory for making my PhD experience so enjoyable and for all their help along the way. I have very fond memories of our interesting discussions while injecting hundreds of mosquitoes, Christmas lunches (especially Secret Santa!) and trips to the opera/ballet. In particular, a special mention to Dr Lavanya Bhagavatula, Dr Mathilde Gendrin and Kasia Sala for their advice and support.

I am very grateful to all the colleagues and collaborators who have helped make this project possible. I wish to thank: Dr Lavanya Bhagavatula for producing a Sf9 cell line stably expressing LRIM9; Dr Joanna Waldock for assistance with viral infections; Dr Tibebe Habtewold for help with statistics and the mosquito fecundity experiment; Kasia Sala for mosquito rearing; Dr Fanny Turlure for providing *Beauveria bassiana* spores; Dr Anna Schnitger for bacterial stocks and protocols; Hassan Yassine for the phenoloxidase assay protocol. I would also like to thank Dr Alvaro Molina-Cruz for performing the *Plasmodium falciparum* infections at the National Institutes of Health (NIH), USA.

I would like to express my gratitude to all members of my new laboratory for being so supportive of my thesis writing, especially Dr Andrew Blagborough, Dr Michael Delves and Prof. Bob Sinden.

Finally, I would like to thank my family and friends for their encouragement and understanding. In particular, a massive thank you to my amazing parents and my wonderful husband, Andrew, for always being there for me and keeping me motivated throughout the highs and lows. I could not have made it without your love and support.

Funding

This PhD was funded by a BBSRC Doctoral Training Grant to the Division of Cell & Molecular Biology, Imperial College London.

Table of Contents

Declaration of originality	2
Abstract	3
Acknowledgements	4
Funding	4
Table of Figures	9
Table of Tables	11
Additional material.....	11
Abbreviations.....	12
1 Introduction	19
Mosquito-borne diseases	19
Mosquitoes and malaria	23
<i>Plasmodium</i> - the malaria parasite.....	23
<i>Anopheles</i> – the mosquito vector.....	27
Malaria control strategies.....	29
Vector control.....	30
Antimalarial drugs.....	32
Malaria vaccines	34
Genetically modified mosquitoes.....	36
Mosquito immunity	37
Pathogen recognition	40
Immune signalling pathways.....	42
The mosquito complement-like system.....	46
Melanisation and lysis.....	51
Cellular immunity	57
Local epithelial immunity.....	59
The LRIM family.....	64
2 Aims and Objectives	71
3 Materials and Methods.....	74
3.1 Mosquito experiments	74

Mosquito rearing	74
RNAi-mediated gene silencing	74
Hemolymph collection	74
Uninfected blood feeding	75
<i>P. berghei</i> infection.....	75
<i>P. yoelii</i> infection	75
<i>P. falciparum</i> infection.....	76
Fungal spore challenge	76
Bacterial infections	76
Injection of bioparticles	76
Bacterial proliferation assay.....	76
Bacterial survival assay	77
Antibiotic treatment	77
Phenoloxidase activity assay	77
Tissue melanisation assay	78
Viral challenge	78
Mosquito fecundity experiment.....	78
3.2 Molecular biology techniques	79
dsRNA synthesis	79
RNA extraction and cDNA synthesis	79
qRT-PCR analysis.....	80
NanoString analysis.....	80
Cloning LRIMs into pEx-10 expression vector	80
Cloning TEP3 and TEP4 C-terminal fragments into pET-41a(+) expression vector.....	81
Site-directed mutagenesis	81
3.3 Protein analysis and cell culture	81
Maintenance of insect cell lines	81
Transfection of cultured cells.....	81
LRIM9 peptide antibodies	82
LRIM9 whole protein antibody.....	82
Western blot analysis of hemolymph or conditioned media.....	82
Immunolocalisation of TEP1.....	83
Purification of His-tagged proteins from conditioned media	84
3.4 Statistical analysis and further data analysis.....	84

3.5	VectorBase gene identifiers.....	85
4	Transcriptional and functional analysis of the LRIM family	87
4.1	Background.....	87
4.2	Results	90
	Transcriptional profiling of the LRIMs and TEPs.....	90
	Screening the LRIMs for effects on <i>P. berghei</i> development.....	112
4.3	Discussion	117
5	LRIM9 – a novel antagonist of <i>Plasmodium berghei</i>	129
5.1	Background.....	129
5.2	Results	131
	LRIM9 and <i>P. berghei</i> infections.....	131
	Recombinant LRIM9 in insect cell culture.....	138
	Developing an antibody against LRIM9	139
	LRIM9 in the hemolymph.....	140
	LRIM9 expression in the midgut.....	145
	LRIM9 and TEP1-mediated parasite killing	146
	LRIM9 and other TEP family members	150
	Involvement of LRIM9 in antibacterial defence	153
	LRIM9 and the melanisation pathway	157
	LRIM9 and mosquito fecundity	162
5.3	Discussion	163
6	Functional analysis of other LRIMs.....	175
6.1	Background.....	175
6.2	Results	177
	Recombinant LRIM4, LRIM15 and LRIM17 in insect cell culture.....	177
	Analysing the role of cysteine residues in LRIM4 homodimerisation.....	179
	LRIM4 and parasite killing	181
	LRIM17 and parasite killing	183
6.3	Discussion	185
7	Final discussion and conclusions	190

8	Bibliography	195
9	Appendix	222
9.1	Supplementary figures	222
9.2	Tables of primers	224

Table of Figures

Figure 1.1 The dual life cycle of <i>Plasmodium</i> parasites.....	25
Figure 1.2 Changes in <i>Plasmodium</i> parasite population during its life cycle.....	26
Figure 1.3 Global distribution of <i>Anopheles</i> malaria vectors, past and present.....	27
Figure 1.4 World map of malaria transmission hotspots.....	30
Figure 1.5 Schematic overview of innate immunity in <i>An. gambiae</i>	40
Figure 1.6 Intracellular immune signalling pathways in <i>Drosophila melanogaster</i>	45
Figure 1.7 Proposed roles of TEP1, LRIM1 and APL1C in the complement-like system of <i>An. gambiae</i>	49
Figure 1.8 The prophenoloxidase activating system in arthropods.....	53
Figure 1.9 The four LRIM subfamilies.....	65
Figure 1.10 Functional modules of the LRIM1/APL1C complex.....	68
Figure 1.11 Phylogenetic relationships between LRIMs in three mosquito species.....	69
Figure 4.1 Schematic overview of NanoString technology.....	89
Figure 4.2 Transcriptional regulation of the LRIMs and TEPs after various immune challenges.....	94
Figure 4.3 Hierarchical clustering of LRIMs and TEPs based on transcriptional profile.....	96
Figure 4.4 Transcriptional responses of the short LRIMs to blood feeding.....	98
Figure 4.5 Transcriptional co-regulation of <i>LRIM1</i> , <i>APL1C</i> and <i>TEP1</i> after <i>P. berghei</i> infection.....	100
Figure 4.6 Transcriptional co-regulation of <i>LRIM4</i> , <i>LRIM17</i> , <i>TEP12</i> and <i>TEP14</i> after <i>Plasmodium</i> infection.....	101
Figure 4.7 Representative transcriptional responses to injection with PBS or conditioned media..	103
Figure 4.8 Responses to injected ONNV and blood fed ONNV.....	105
Figure 4.9 Viral load and tissue tropism in ONNV infected mosquitoes.....	106
Figure 4.10 A cluster of core immune genes induced by <i>E. coli</i> injection.....	108
Figure 4.11 Key genes responding to fungal infection.....	110
Figure 4.12 <i>P. berghei</i> oocysts and melanised ookinetes in the <i>An. gambiae</i> midgut.....	113
Figure 5.1 Schematic representation of LRIM9 protein structure.....	130
Figure 5.2 Orthologous genomic clusters of Short LRIMs in different mosquito species.....	131
Figure 5.3 Knockdown efficiency time course for <i>LRIM9</i> transcript.....	132
Figure 5.4 <i>LRIM9</i> knockdown in susceptible mosquitoes.....	133
Figure 5.5 <i>LRIM9</i> knockdown in L3-5 mosquitoes using two lines of <i>P. berghei</i>	136
Figure 5.6 <i>LRIM9</i> and <i>CTL4</i> double knockdown in susceptible mosquitoes.....	137
Figure 5.7 Expression of recombinant LRIM9 in insect cell lines.....	139
Figure 5.8 Testing LRIM9 whole protein antibody using conditioned media from mosquito cells...	140
Figure 5.9 Testing LRIM9 antibody with hemolymph after <i>LRIM9</i> knockdown.....	141
Figure 5.10 LRIM9 transcript and protein expression after feeding on rodent naïve blood.....	143
Figure 5.11 LRIM9 protein expression after feeding on human naïve blood.....	144
Figure 5.12 <i>LRIM9</i> transcript levels in the midgut.....	145
Figure 5.13 Binding assay to test interactions between LRIM9 and TEP1, LRIM1 and APL1C.....	147
Figure 5.14 Investigating the involvement of LRIM9 in TEP1 activity in the hemolymph.....	149
Figure 5.15 TEP1 localisation to <i>P. berghei</i> ookinetes after <i>LRIM9</i> silencing.....	149
Figure 5.16 TEP1 protein levels after <i>E. coli</i> bioparticle challenge after <i>LRIM9</i> silencing.....	150

Figure 5.17 The effect of <i>TEP3</i> and <i>TEP4</i> knockdown on <i>P. berghei</i> development.....	152
Figure 5.18 Double knockdowns of <i>CTL4</i> with <i>TEP3</i> and <i>TEP4</i>	153
Figure 5.19 Survival after <i>E. coli</i> injection in naïve and blood fed mosquitoes.	154
Figure 5.20 The effect of <i>LRIM9</i> knockdown on bacterial proliferation.....	155
Figure 5.21 The effect of antibiotics and bacterial injection on <i>LRIM9</i> expression.	156
Figure 5.22 Investigating the involvement of <i>LRIM9</i> in <i>CLIPA8</i> activation cleavage.....	158
Figure 5.23 <i>LRIM9</i> and phenoloxidase activity.	160
Figure 5.24 The effect of <i>LRIM9</i> knockdown on tissue melanisation.....	161
Figure 6.1 <i>LRIM4</i> and <i>LRIM17</i> expression in cell culture and hemolymph.....	178
Figure 6.2 Investigating the cysteine residue responsible for <i>LRIM4</i> homodimer formation.	180
Figure 6.3 Binding assay to investigate whether <i>LRIM4</i> interacts with <i>TEP1</i> and <i>LRIM1/APL1C</i>	182
Figure 6.4 <i>LRIM4</i> silencing and <i>P. berghei</i> infection.....	183
Figure 6.5 <i>LRIM17</i> silencing and <i>P. berghei</i> development in Keele mosquitoes.....	184
Figure 9.1 Evaluating <i>LRIM9</i> peptide antibodies using blood fed hemolymph.	222
Figure 9.2 Temporal profiling of <i>LRIM1/APL1C</i> and <i>TEP1</i> protein levels after <i>E. coli</i> bioparticle challenge in naïve mosquitoes.....	223

Table of Tables

Table 1.1 The LRIM family in <i>An. gambiae</i>	66
Table 4.1 Rank order of all genes based on average number of NanoString gene-specific reporters.	93
Table 4.2 Developmental profile of LRIMs and TEPs in <i>An. gambiae</i>	111
Table 4.3 The initial RNAi screen of LRIM genes upon <i>P. berghei</i> infection.	115
Table 5.1 The effect of <i>LRIM9</i> silencing on <i>P. berghei</i> development in susceptible mosquitoes.	134
Table 5.2 The effect of <i>LRIM9</i> knockdown on egg laying and larval hatching.....	163
Table 9.1 RNAi primer sequences.....	224
Table 9.2 qRT-PCR primer sequences.....	225
Table 9.3 NanoString probe sequences.	226
Table 9.4 Ek/LIC cloning primer sequences.	228

Additional material

An Appendix CD containing raw data from the transcriptional profiling is included in the CD pocket.

Abbreviations

A

ACT	Artemisinin-based combination theory
AMP	Antimicrobial peptide
ANK	Ankyrin
APL	<i>Anopheles Plasmodium</i> -responsive leucine-rich repeat
Apo	Apolipoprotein
ATP	Adenosine triphosphate
ATT	Attacin
AZ	Actin zone

B

BF	Blood feeding
BINT2	β 2-integrin
bp	Base pair
BSA	Bovine serum albumin
Bti	<i>Bacillus thuringiensis israelensis</i>

C

Cdc42	Cell division control protein 42
cDNA	Complementary DNA
CEC	Cecropin
CFU	Colony forming unit
CHIKV	Chikungunya virus
CLIP	Clip-domain serine protease
CM	Conditioned medium/media
CO ₂	Carbon dioxide
CS	Circumsporozoite protein
CTL	C-type lectin
CTLMA	C-type lectin: mannose binding

D

DAMP	Damage-associated molecular pattern
------	-------------------------------------

DAPI	4',6-diamidino-2-phenylindole
DCE	Dopachrome conversion enzyme
DD	Death domain
DDC	Dopa decarboxylase
DDT	Dichlorodiphenyltrichloroethane
DEF	Defensin
DEN	Dengue
DNA	Deoxyribonucleic acid
DNase	Deoxyribonuclease
DREDD	Death-related ced3/Nedd2-like death-domain
Dscam	Down syndrome cell adhesion molecule
dsRNA	Double stranded ribonucleic acid
Duox	Dual oxidase
E	
EDTA	Ethylenediaminetetraacetic acid
EST	Expressed sequence tag
F	
FADD	Fas-associated death-domain containing protein
FBN (or FREP)	Fibrinogen-like domain immunoelectin
FBS	Fetal bovine serum
Fz2	Frizzled2
G	
g	Gram
GALE	Galectin
GAM	Gambicin
GFP	Green fluorescent protein
GM	Genetically modified
GNBP	Gram-negative binding protein
GPELF	Global Programme to Eradicate Lymphatic Filariasis
GPI	Glycosylphosphatidylinositol
GSK	GlaxoSmithKline

GST	Glutathione S-transferase
H	
h	Hour
His	Histidine
I	
Imd	Immune deficiency
IMPer	Immunomodulatory peroxidase
IPT	Intermittent preventive treatment
IPTG	Isopropyl β -D-1-thiogalactopyranoside
IRS	Indoor residual spraying
ITN	Insecticide-treated bednet
J	
JAK-STAT	Janus kinase-signal transducer and activator of transcription
JEV	Japanese encephalitis virus
JNK	c-Jun N-terminal kinase
K	
kDa	KiloDalton
L	
L	Litre
L-DOPA	L-3,4-dihydroxyphenylalanine
LLIN	Long-lasting insecticide-treated bednet
LPS	Lipopolysaccharide
LRIM	Leucine-rich repeat immune protein
LRP	Lipoprotein receptor-related protein
LRR	Leucine-rich repeat
M	
MAPK	Mitogen-activated protein kinase
MEM	Minimum essential media

Min	Minute(s)
MMV	Medicines for Malaria Venture
Mnp	Membranes no protein
ModSP	Modular serine protease
mRNA	Messenger RNA
MVI	Malaria Vaccine Initiative
N	
NF- κ B/Rel	Nuclear factor-kappa B/reticuloendotheliosis
NLR	Nod-like receptor
NO	Nitric oxide
NOS	Nitric oxide synthase
O	
OD	Optical density
ONNV	O'nyong-nyong virus
P	
PAMP	Pathogen-associated molecular pattern
PBS	Phosphate buffered saline
PCR	Polymerase chain reaction
PFU	Plaque forming unit
PGN	Peptidoglycan
PGRP	Peptidoglycan-recognition protein
PO	Phenoloxidase
PPAE	Prophenoloxidase-activating enzyme
PPO	Prophenoloxidase
PRR	Pathogen recognition receptor
PVDF	Polyvinylidene difluoride
Q	
qRT-PCR	Quantitative real-time polymerase chain reaction
QTL	Quantitative trait locus

R

RBM	Roll Back Malaria
RHD	Rel homology domain
RNA	Ribonucleic acid
RNAi	RNA interference
RNase	Ribonuclease
ROS	Reactive oxygen species

S

ScFv	Single chain variable region antibody
SCR	Scavenger receptor
SDS-PAGE	Sodium dodecyl sulphate-polyacrylamide gel electrophoresis
SiRNA	Small interfering RNA
SNP	Single nucleotide polymorphism
SOD	Superoxide dismutase
SPE	Spätzle processing enzyme
SPH	Serine protease homologue
SRPN	Serpin
SURE	Stop Unwanted Rearrangement Events

T

TBV	Transmission blocking vaccine
TE	Thioester
TEP	Thioester-containing protein
TIR	Toll/Interleukin-1 receptor
TLR	Toll-like receptor
TNF	Tumour necrosis factor
TO	Theiler's original mice

V

VERO	African Green monkey kidney cells
VLR	Variable lymphocyte receptor

W

WHO World Health Organisation

WNV West Nile Virus

Y

YPP Yolk protein precursor

Chapter 1: Introduction

1 Introduction

Mosquito-borne diseases

Mosquitoes transmit numerous human and animal diseases with devastating consequences worldwide. These diseases are responsible for severe morbidity and mortality, especially in poorer, developing countries (Hill et al., 2005; Tolle, 2009; Weaver and Reisen, 2010). It is frequently young children, adolescents and pregnant women that are worst affected. As well as human suffering, death, ill health and disability have dramatic economic, political and social impacts.

The mosquito life cycle makes it an ideal disease vector. Mosquitoes, which are Dipteran insects of the family Culicidae, are phenomenally successful and have colonised every continent except Antarctica (Reiter, 2001). There are approximately 3,500 species of mosquito and almost three-quarters live in tropical or sub-tropical regions. Most adult female mosquitoes must feed on the blood of vertebrates to acquire nutrients for egg production (Attardo et al., 2005). The females use their elongated proboscis to pierce skin and inject saliva to facilitate feeding, which effectively disseminates protozoan parasites, viruses and nematode worms into their vertebrate host (Reiter, 2001). For most of these pathogens, the mosquito represents an essential stage in their life cycle. Feeding behaviour varies between mosquito species, with some preferring to feed on humans (anthropophilic) and others preferring animals, including mammals, birds and even reptiles (zoophilic). Female mosquitoes lay their eggs on or close to water and the larval and pupal stages are entirely aquatic (Reiter, 2001). A female mosquito can lay eggs more than once in her life, producing between 50 and 500 eggs per reproductive cycle (Clements, 2000). The mosquito life cycle is rapid and takes only 15-20 days from egg to adult (McGavin, 2001). Female mosquitoes have a life span of 2-4 weeks whereas males generally live for less than 10 days.

Many mosquito-borne diseases are resurging due to the complex interplay of human activity, vector biology and environmental factors. Population growth and uncontrolled urbanisation have led to humans infringing on traditional mosquito habitats (Weaver and Reisen, 2010). Mosquitoes, such as *Aedes aegypti*, are becoming increasingly anthropophilic (attracted to humans) and adapted to living in close proximity to humans. In developing countries, poorly managed water storage and inadequate disposal of waste water contribute to expansions in mosquito populations (Kyle and Harris, 2008; Reiter, 2001; Tolle, 2009). For example, water storage vessels, plastic containers and discarded tyres provide plentiful mosquito breeding sites. Increased agriculture has also affected mosquito populations, with irrigated rice fields and cattle hoof-prints providing excellent larval habitats (Reiter, 2001). Climate change and global warming strongly impact on mosquito ecology,

behaviour, development and survival, which can affect disease transmission and the geographical range of mosquitoes (Reiter, 2001).

The deadliest mosquito-borne disease is malaria, which exacts a devastating toll on developing countries. It is an acute febrile disease caused by protozoan *Plasmodium* parasites and transmitted to humans exclusively by infected female *Anopheles* mosquitoes. *Plasmodium falciparum* is the deadliest form of human malaria and *Anopheles gambiae* is its main African vector. According to the most recent figures from the World Health Organisation (WHO), 3.3 billion people were at risk of malaria in 2010, especially those in Sub-Saharan Africa (WHO, 2011b). There were approximately 216 million malaria cases in 2010, with 81% in Africa and 13% in South East Asia. An estimated 655,000 people died in the same year, although estimates vary from 537,000 and 907,000. 91% of these casualties were in Africa and 86% were children under 5 years of age. Pregnant women were also severely affected, with high rates of miscarriage and maternal death.

The second most important mosquito-borne parasitic disease is lymphatic filariasis, which is a major cause of permanent disability worldwide (Manguin et al., 2010). Lymphatic filariasis is caused by filarial parasites, which are tissue-dwelling nematodes transmitted to humans during a mosquito blood meal (Tolle, 2009). Over 90% of human lymphatic filariasis cases are caused by the nematode *Wuchereria bancrofti* (Manguin et al., 2010). More than 70 species of mosquito are known vectors of *W. bancrofti*, including *Culex* (in urban areas), *Anopheles* (in rural areas of Africa and other areas) and *Aedes* (in the Pacific islands) (Manguin et al., 2010; WHO, 2012b). Following an infectious mosquito bite, the parasites invade the human lymphatic system, disrupt the immune system and cause abnormal enlargement of body parts, severe pain and disability. The most common chronic manifestations are lymphoedema, elephantiasis and hydrocele (tissue swelling, skin thickening and fluid accumulation, respectively) (WHO, 2012b). Legs and genital organs are commonly affected. Over 120 million people were infected and 40 million were incapacitated by the disease in 2010 (WHO, 2012b). The socioeconomic impact of this disease is immense. WHO launched a Global Programme to Eradicate Lymphatic Filariasis (GPELF) in 2000, with the aim to eliminate the disease by 2020. This programme involves mass drug administration and morbidity management (WHO, 2012b).

Malaria and lymphatic filariasis are co-endemic in many parts of the tropics and concomitant human infections occur. In fact, many *Anopheles* mosquitoes are able to transmit both malaria parasites and filarial nematodes, including *An. gambiae* and *Anopheles arabiensis* in Africa (Muturi et al., 2008). Interactions between malaria parasites and filarial nematodes within the same mosquito are poorly understood. A recent study reported that filarial worms reduce the prevalence and intensity of

Plasmodium gallinaceum infections in dually infected *Anopheles* mosquitoes (Aliota et al., 2011). It is therefore possible that elimination of filarial parasites could inadvertently increase malaria transmission, which must be taken into careful consideration by the GPELF campaign.

Many arthropod-borne viruses (arboviruses) are also transmitted by mosquitoes, especially *Aedes* and *Culex*. Of these, dengue virus (of the genus *Flavivirus*) is the most prevalent and potentially severe arbovirus, with half of the world's population at risk (WHO, 2012a). The WHO currently estimates that there are 50-100 million infections every year, with 250,000-500,000 causing severe illness. Although many dengue cases are asymptomatic, symptomatic dengue is a debilitating febrile illness, which can develop into a life-threatening complication called severe dengue (Kyle and Harris, 2008). There are four distinct serotypes of dengue virus: DEN-1 to -4. Infection with one serotype is believed to result in life-long immunity to that particular serotype but not the others (WHO, 2012a). Furthermore, subsequent infections with different serotypes have an increased risk of progressing to severe dengue. This complexity has so far prevented the development of a successful vaccine. Worryingly, the incidence of dengue has been increasing dramatically and expanding geographically in the last 50 years (Kyle and Harris, 2008; WHO, 2011a). Population growth and uncontrolled urbanisation have been held largely responsible. Global travel has also spread dengue virus and its mosquito vectors to new locations. The primary dengue vector is *Ae. aegypti*, a previously forest-dwelling mosquito that has become highly anthropophilic and well adapted to living in urban areas. *Aedes albopictus* is a secondary dengue vector. Many arboviruses are maintained in wild animals (known as enzootic amplification), but dengue virus has largely lost this ability (Weaver and Reisen, 2010).

Yellow fever is another flavivirus transmitted to humans by *Ae. aegypti*. Yellow fever is an acute haemorrhagic disease, which gets its name from the jaundice experienced by some sufferers (WHO, 2012d). Even though an effective vaccine is available, the virus continues to cause a huge disease burden (Tolle, 2009). There are an estimated 200,000 cases each year, with 30,000 deaths. Yellow fever is a zoonotic disease that is sustained in a sylvatic cycle (also called forest or jungle cycle) involving monkeys, in which *Ae. aegypti* is not the main vector. *Aedes africanus* is the principle vector of the sylvatic cycle in Africa whereas *Haemagogus* mosquitoes take this role in the Americas. A potential threat is "spillover" transmission to humans or domestic animals when rural environments are invaded (Weaver and Reisen, 2010). Infected people carry the virus into villages and towns where *Ae. aegypti* spreads the virus through the population, resulting in urban outbreaks (Gould and Solomon, 2008). Interestingly, the virus cannot complete its developmental cycle in humans and domestic animals, which are incidental or dead-end hosts.

The Japanese encephalitis serogroup of flaviviruses includes Japanese encephalitis virus (JEV) and West Nile Virus (WNV). These viruses are zoonotic with avian hosts and are transmitted primarily by *Culex* mosquitoes. JEV is the most common cause of mosquito-borne encephalites, with around 50,000 infections every year (Weaver and Reisen, 2010). It is endemic to large parts of Asia and the Pacific but has shown widespread expansion in recent years (Erlanger et al., 2009). The disease often occurs in epidemics and can lead to permanent neurological damage. JEV is primarily transmitted by *Culex tritaeniorhynchus*, which breed in irrigated rice paddies, and its main reservoir is wading water birds. The virus is amplified in domestic pigs before spreading to humans and horses, which are dead-end hosts. Human population growth, intensified rice cultivation and increased pig rearing are all responsible for the rapid expansion of JEV (Erlanger et al., 2009). WNV can also cause severe neuroinvasive disease, although 80% of infections are asymptomatic (Tolle, 2009). Its primary vector is *Culex pipiens* and the virus has now spread across all continents, except Antarctica (Weaver and Reisen, 2010). Epidemics are rife across North America. WNV also causes severe illness and death in horses and corvid birds, such as crows and jays (Tolle, 2009).

Chikungunya virus (CHIKV) and O'nyong-nyong virus (ONNV) are members of the *Alphavirus* family. CHIKV was once seen as a debilitating but seldom fatal disease, which manifests as fever and severe joint pain (Weaver and Reisen, 2010). However, over the last decade, CHIKV has spread geographically, its virulence has dramatically increased and there have been major epidemics (Tolle, 2009); therefore, CHIKV is now classed as a dangerous emerging arbovirus. The virus no longer requires enzootic amplification (Weaver and Reisen, 2010). The primary CHIKV vector is *Ae. aegypti* but a recent amino acid mutation has enabled it to be transmitted effectively by *Ae. albopictus*, which has facilitated dissemination to new locations. It has been speculated that this mutation may be associated with increased virulence in the recent outbreaks. ONNV is unusual as it is the only arbovirus primarily transmitted by *Anopheles* mosquitoes (Waldock et al., 2012). ONNV was responsible for epidemics in East Africa in the 1960s and 1990s.

It is interesting that different mosquitoes have become adapted to transmit different pathogens. *Anopheles* mosquitoes, the exclusive vectors of malaria parasites, are very poor transmitters of viruses. *Aedes* and *Culex* are excellent vectors of viral infection but do not transmit *Plasmodium* parasites.

Mosquitoes and malaria

Plasmodium - the malaria parasite

Of all the mosquito-borne diseases, malaria is by far the most devastating. Of the 172 species of *Plasmodium* parasites known to infect mammals, birds and reptiles, the vast majority are incapable of infecting humans (Baird, 2005). Only five species are known to cause human malaria: *P. falciparum*, *Plasmodium vivax*, *Plasmodium malariae*, *Plasmodium ovale* and *Plasmodium knowlesi*. Each parasite causes a debilitating acute febrile disease. *P. falciparum* and *P. vivax* are responsible for the vast majority of infections. *P. falciparum* causes the vast majority of severe malaria infections and is the main perpetrator of malaria mortality and morbidity (WHO, 2012c). The five parasites are endemic to different regions worldwide. *P. falciparum* is prevalent in sub-Saharan Africa, where the disease burden is strongest, whereas *P. vivax* is more common in South and Southeast Asia, the Western Pacific and Central and South America (Price et al., 2007; Tolle, 2009). The geographical range of *P. vivax* is wider because it can develop at lower temperatures (Greenwood et al., 2005). *P. ovale* is restricted to West Africa. *P. knowlesi* was traditionally described as a parasite of macaque monkeys but it also naturally infects humans in certain areas, like Malaysia (Singh et al., 2004). In the laboratory, rodent parasites *Plasmodium berghei* and *Plasmodium yoelii* are used as convenient models of malaria parasite infection. These naturally infect thicket rats in central Africa (Frech and Chen, 2011).

Plasmodium parasites undergo a complex dual life cycle in the mosquito vector and the vertebrate host (Figure 1.1) (Wirth, 2002). Malaria transmission is reliant on successful completion of the parasite's sexual developmental cycle in the mosquito. The mosquito is the parasite's definitive host and an essential component of its life cycle whereas the vertebrate is a passage between mosquitoes (the intermediate host). The female mosquito ingests *Plasmodium* gametocytes upon blood feeding on an infected vertebrate. Based largely on studies in *P. berghei* (Sinden, 2002), within minutes of reaching the mosquito gut lumen, haploid male and female gametocytes leave their red blood cells and differentiate into gametes. Changes in temperature and exposure to mosquito-derived xanthurenic acid initiate gametogenesis in *P. berghei* (Billker et al., 1998; Billker et al., 1997) and *P. falciparum* (Ghosh et al., 2010). The male gametocyte undergoes an extraordinary process, called exflagellation, during which eight haploid flagellated gametes are generated within minutes. In contrast, the female gametocyte becomes activated and transforms into the female gamete without undergoing DNA replication (Guttery et al., 2012). Within one hour (h) of blood feeding, the male gamete fertilises the female to form a diploid zygote, which undergoes meiosis and becomes tetraploid within the subsequent 3 h (Kuehn and Pradel, 2010). Over the next 5-18 h, each zygote

develops into a single motile, elongated tetraploid ookinete (Sinden, 2002). Between 19-36 h after feeding, ookinetes use gliding motility (via an actin/myosin motor) to migrate out of the blood meal (Aly et al., 2009). Ookinetes traverse the peritrophic matrix, which surrounds the blood bolus, and penetrate the midgut epithelium intracellularly, often passing through several cells (Zieler and Dvorak, 2000). Midgut invasion causes a significant change in epithelial cell morphology and results in apoptosis and expulsion of the invaded cell(s) by wound repair mechanisms (Han et al., 2000). In the space between the epithelial layer and the basal lamina, the ookinete develops into a spherical, sessile oocyst. The basal lamina, which coats the entire body cavity (hemocoel) of the mosquito, is believed to trigger the ookinete-to-oocyst transition (Aly et al., 2009; Vlachou et al., 2006). Over the next 12-18 days, the oocyst undergoes many internal mitotic divisions and generates thousands of haploid sporozoites. Upon maturation, the oocyst bursts to release these sporozoites into the hemolymph (mosquito blood). The motile sporozoites migrate to and invade the mosquito's salivary glands, where they can be injected into a new vertebrate host upon the next blood feeding.

When sporozoites enter the circulation of the vertebrate host, they travel rapidly to the liver and invade hepatocytes (Aly et al., 2009; Tolle, 2009). Sporozoites use a membrane-associated actin-myosin motor to actively invade several hepatocytes before stopping in a final hepatocyte. A parasitophorous vacuole forms around the parasite for protection from the host cell. Within this vacuole, the sporozoite undergoes asexual reproduction (a process called schizony) producing a hepatic schizont that contains thousands of merozoites (Prudencio et al., 2006). The liver stage of infection is asymptomatic and lasts 5-6 days for *P. falciparum* and 10-14 days for *P. vivax* (although *P. vivax* can persist in the liver, as discussed later) (Tolle, 2009). After this incubation period, thousands of merozoites are released into the host bloodstream. The merozoites invade and develop within red blood cells (erythrocytes). Asexual blood stage parasites undergo many cycles of multiplication, which can produce up to 10^{13} merozoites per host (Greenwood et al., 2008). These asexual parasites are pathogenic and associated with the high fever, chills, headache and vomiting symptoms of a malaria infection. If not treated within 24 h, *P. falciparum* infections often progress to life-threatening disease. A proportion of merozoites develop into male and female gametocytes (sexual forms), which are not pathogenic but can be ingested by a blood feeding mosquito, spreading the disease.

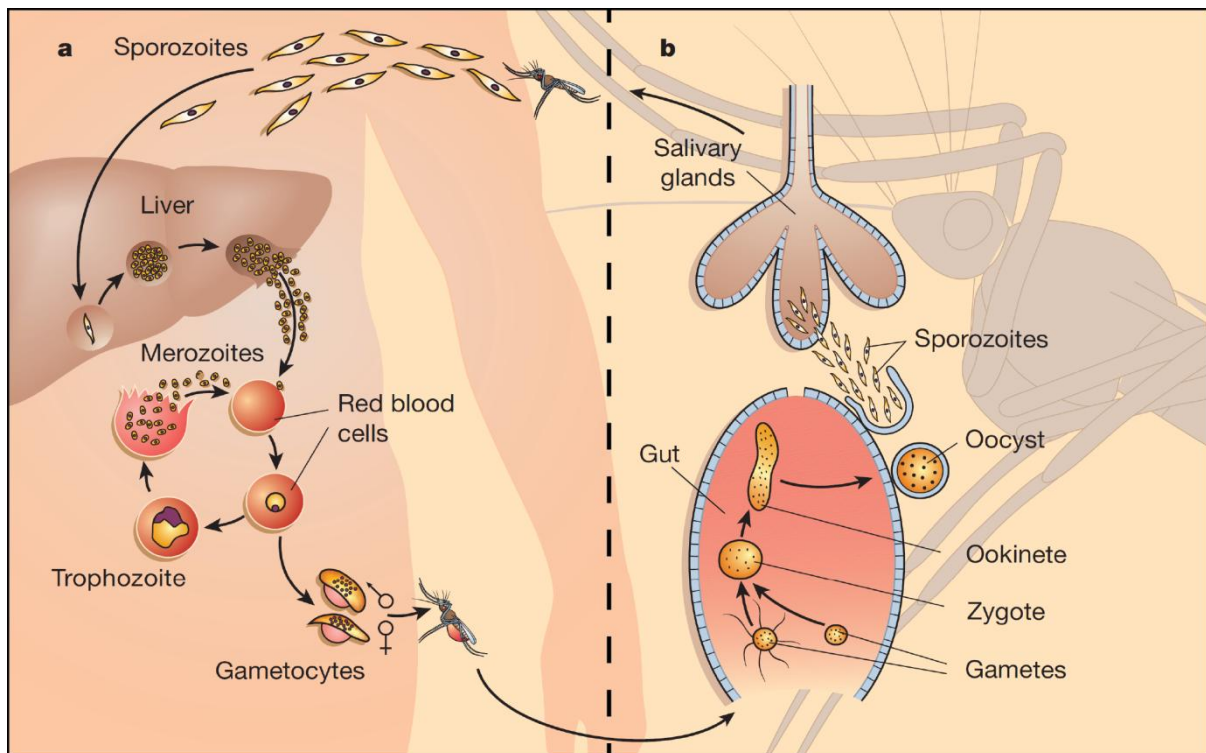


Figure 1.1 The dual life cycle of *Plasmodium* parasites.

Plasmodium parasites undergo asexual and sexual development in their vertebrate (a) and mosquito (b) hosts, respectively. A female mosquito becomes infected with *Plasmodium* gametocytes when blood feeding on an infected vertebrate. Inside the mosquito midgut, gametocytes differentiate into gametes that form a zygote upon fertilisation. The zygote develops into a motile ookinete, which traverses the peritrophic membrane (not shown) and penetrates the midgut epithelium intracellularly. In the space between the epithelial cells and the basal lamina, the ookinete develops into a sessile oocyst. Over the next two weeks, the oocyst undergoes many internal mitotic divisions and matures to release thousands of sporozoites into the hemolymph. The sporozoites migrate to the salivary glands and are injected into a naïve vertebrate host upon the next blood feeding. Inside the vertebrate host, the parasites travel to the liver and invade hepatocytes. The parasite asexually reproduces to form thousands of merozoites. These merozoites are released into the blood where they infect red blood cells and cause symptomatic disease. Some parasites differentiate into gametocytes that will continue the life cycle in the next mosquito host. Adapted from Wirth, 2002.

There are interesting differences in the behaviours of the five *Plasmodium* parasites that infect humans. The increased virulence of *P. falciparum* can be partly explained because this species can generate more merozoites per hepatocyte, increasing the disease burden (Tolle, 2009). In addition, *P. falciparum* can invade red blood cells of all ages whereas *P. vivax* and *P. ovale* prefer to invade only immature red blood cells (reticulocytes). Unlike the other *Plasmodium* species, *P. vivax* and *P. ovale* cause characteristic relapses months after the original illness. A subset of *P. vivax* and *P. ovale* sporozoites remain dormant in the liver, as hypnozoites, for prolonged periods of time before developing into schizonts and causing recurrent malaria symptoms (Price et al., 2007). *P. malariae* can persist in the blood for several years if poorly treated (Schlitzer, 2007).

The *Plasmodium* parasite's journey through the mosquito is a difficult and dangerous battle for survival, with the parasite population suffering substantial losses (Barillas-Mury and Kumar, 2005). Compared to the trillions of parasites in the human bloodstream, parasite numbers typically drop to single figures in the mosquito (Figure 1.2) (Vogel, 2010). The most important bottleneck in parasite numbers takes place in the mosquito midgut, with major parasite losses occurring during the gametocyte-to-ookinete and ookinete-to-oocyst transition (Alavi et al., 2003; Sinden, 1999). Remarkably, 90-99% of ookinetes are lost before becoming oocysts (Sinden, 2002). Although a blood meal can contain 10^5 gametocytes, as few as 1 to 5 oocysts usually develop. The mosquito innate immune system is largely responsible for eliminating the majority of invading ookinetes during the midgut stages of mosquito infection (Christophides et al., 2004). The second bottleneck occurs between release of sporozoites from the oocyst and invasion of the salivary glands, with only 20% of sporozoites completing the journey (Clements, 2012). Critically, *Plasmodium* parasites have evolved to cope with these population bottlenecks and even a single oocyst is sufficient to transmit malaria. Nevertheless, the parasite is extremely vulnerable in the mosquito host, which makes this an ideal time to control malaria – either by targeting the parasite or the mosquito. *P. falciparum* infections in wild mosquito populations are typically much lower than *P. berghei* infections in the laboratory (Tahar et al., 2002), which could facilitate control strategies.

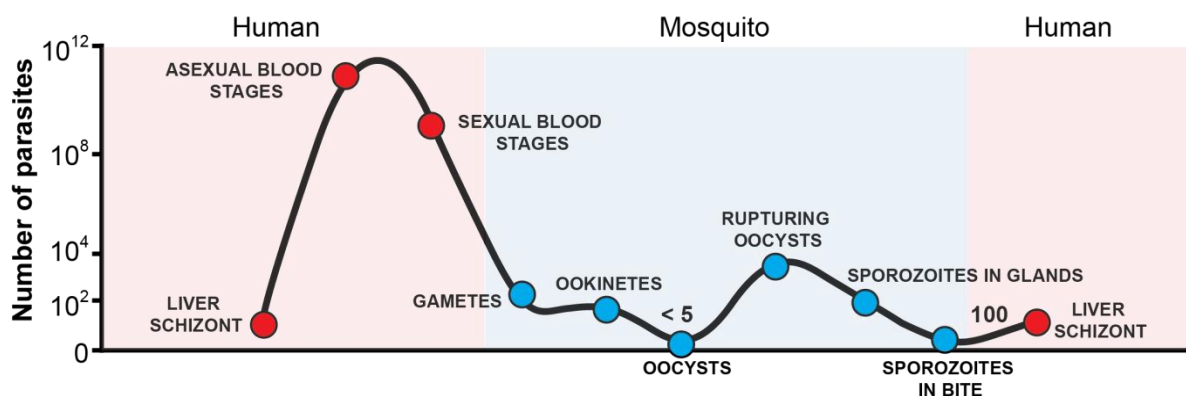


Figure 1.2 Changes in *Plasmodium* parasite population during its life cycle.

The parasite undergoes two serious bottlenecks in population size during its passage through the mosquito. Whereas up to 10^{13} asexual blood stage parasites can be found in the human host, only a few thousand parasites will be ingested by the mosquito. Of these, as few as 1 to 5 oocysts develop, with the vast majority of parasites killed in the journey from the midgut lumen to the basal labyrinth. Parasite numbers are boosted when each oocyst releases thousands of sporozoites into the hemolymph. However, most sporozoites do not make it to the salivary glands and only 10-20 parasites are typically injected with each infectious mosquito bite (Sinden, 1999). Adapted from Vogel, 2010.

Anopheles – the mosquito vector

Contrary to popular belief, the vast majority of mosquitoes are incapable of transmitting disease. *Plasmodium* parasites causing human malaria are only transmitted by mosquitoes of the genus *Anopheles*, and of the estimated 400 species of *Anopheles* mosquitoes, only about 40 are known to transmit malaria effectively so that they can be considered important vectors. Different *Anopheles* mosquitoes are the dominant vectors in specific geographic locations (Figure 1.3) (Kiszewski et al., 2004; Sinka et al., 2012). *An. gambiae* is the major malaria vector in sub-Saharan Africa, where the global disease burden is highest. *Anopheles culicifacies* and *Anopheles stephensi* are important in India. *Anopheles darlingi* is the chief vector in South America.

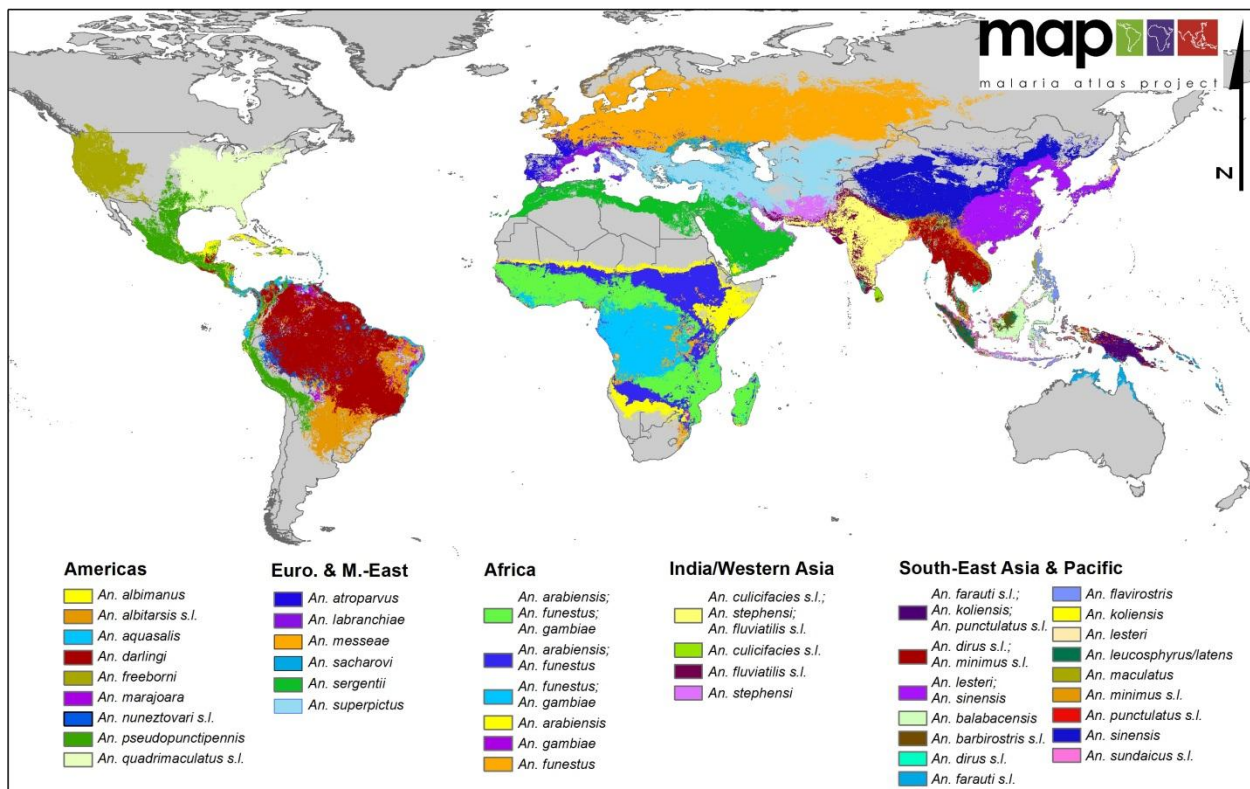


Figure 1.3 Global distribution of *Anopheles* malaria vectors, past and present.

Dominant *Anopheles* species transmit malaria parasites in different regions of the world, as indicated by colour-coding. This map includes regions where malaria is no longer transmitted but was transmitted in the past, such as most of Europe and North America. From Sinka et al., 2012.

Vector competence, the capacity of mosquitoes to allow development of a particular parasite, is species and context specific (Sinden et al., 2004). Each mosquito species is usually only an efficient vector of a limited number of *Plasmodium* species (Blandin et al., 2004). Additionally, there are wide variations in vectorial capacity even within the same species. There are even intraspecific differences in susceptibility between mosquitoes of the same strain, shown by the wide range of oocyst intensities in experimental infections. The mechanisms of vector competence are not well understood (Blandin et al., 2004). Genetic, behavioural, ecology and immunity components are important determinants of vectorial capacity (Catteruccia, 2007). Refractory mosquitoes can inhibit or reduce the progress of the malaria parasite at one or more points in its complex life cycle (Sinden et al., 2004). Some mosquitoes are completely refractory to *Plasmodium* development, others are partially refractory and some mosquitoes are highly susceptible. Even in mosquitoes susceptible to *Plasmodium* development, the vast majority of parasites are still killed at the ookinete-to-oocyst transition. Mosquito behaviour also determines whether a species will transmit a particular *Plasmodium* parasite in natural settings. For example, host preference, feeding behaviour, resting behaviour and breeding sites all influence malaria transmission (Besansky et al., 1994). Geographical distribution is also important in determining whether a mosquito species can vector a particular parasite.

Importantly, *An. gambiae* is a complex of seven closely related species and several incipient species that vary greatly in their ability to transmit malaria (Coetzee et al., 2000). The complex is officially called the *An. gambiae* Giles complex, named after the English entomologist George Michael James Giles. The seven species in the complex are *An. gambiae sensu stricto* (henceforth *An. gambiae*), *An. arabiensis*, *Anopheles bwambae*, *Anopheles merus*, *Anopheles melas* and *Anopheles quadriannulatus* Theobald species A and B. These species are morphologically indistinguishable but are genetically and behaviourally distinct. They are able to interbreed in the laboratory but hybrid males are sterile (Davidson, 1964). They were originally defined by polytene chromosome analysis but are now distinguished by PCR-based methods (Bass et al., 2007; Coluzzi et al., 2002; Fanello et al., 2002). Both *An. gambiae* and *An. arabiensis* are extremely efficient vectors of *P. falciparum* in sub-Saharan Africa and are sympatric across large regions. The other species are more localised malaria vectors: *An. melas* in West Africa, *An. merus* in East Africa and *An. bwambae* in Uganda. Interestingly, *An. quadriannulatus* species A and B, endemic to southern Africa and Ethiopia, respectively, are considered to be zoophilic and thus non-vectors of human malaria (Habtewold et al., 2008; Hunt et al., 1998).

Furthermore, *An. gambiae* has a complicated population structure, with several subdivisions (Holt et al., 2002; Neafsey et al., 2010). It is composed of at least two incipient species, known as the M and S molecular forms, initially defined based on fixed differences in ribosomal DNA (Lawniczak et al., 2010). M and S are morphologically identical at all life stages. M and S forms are sympatric across large parts of West and Central Africa but are partially reproductively isolated by assortative mating. Hybridisation still occurs and so there is gene flow between the forms. M and S differ in their larval breeding sites and reproductive behaviour. M and S forms are further subdivided into five chromosomal forms: Mopti (molecular form M), Savanna (S form), Bamako (S form), Bissau and Forest (Neafsey et al., 2010). This complexity poses significant challenges for malaria control (Lawniczak et al., 2010).

Malaria control strategies

Malaria is such a complex and widespread disease that an integrated approach, combining many strategies, must be taken to achieve eradication. Controlling the mosquito vector, employing antimalarial drugs and vaccines and developing new technologies are all important if we are to successfully fight this devastating disease. Thanks to a huge influx of new funding, notably from the Bill & Melinda Gates Foundation, the global malaria map is “shrinking” (Figure 1.4) (Feachem et al., 2010). Thirty two countries on the borders of the malaria transmission zone, such as Algeria, Egypt and Mexico, are making good progress towards eliminating malaria. However, other countries, particularly those close to the equator, such as Nigeria, Sudan, India, Brazil and Indonesia, are still battling to control transmission. Despite progress, malaria elimination in sub-Saharan Africa is not possible with the current tools and novel control strategies are urgently required. As well as new tools and techniques, malaria control needs socioeconomic and infrastructural advances to be truly effective (Enayati and Hemingway, 2010).

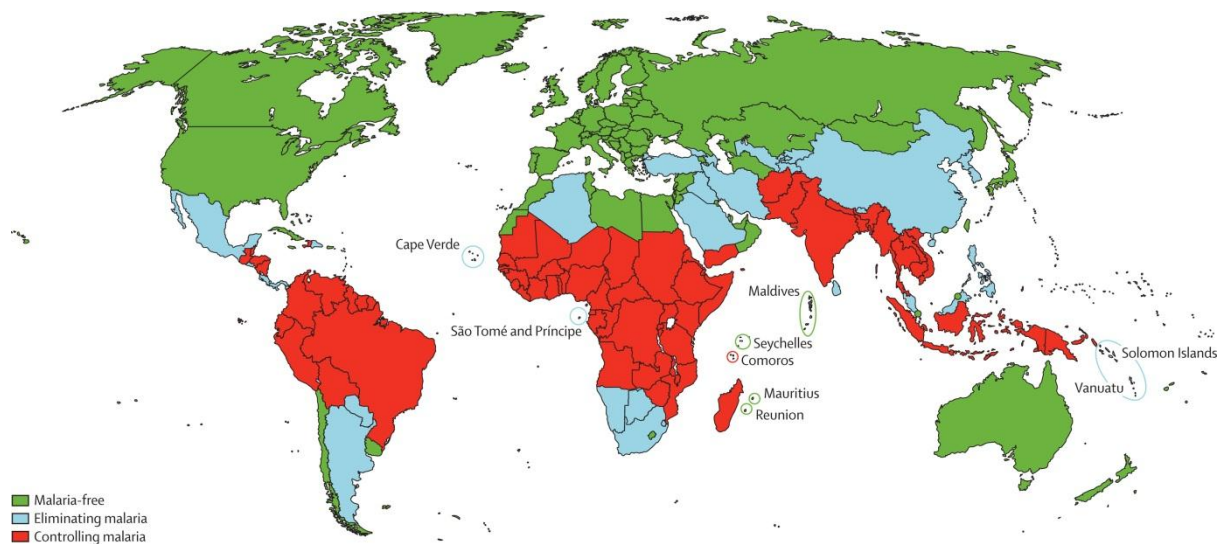


Figure 1.4 World map of malaria transmission hotspots.

Thanks to new funding and control efforts, the geographical regions affected by malaria are “shrinking”. Areas in green, such as much of Europe and Australia, have no malaria transmission. Areas in blue, such as Mexico and Algeria, are progressing towards eliminating the disease. However, countries at the central belt of malaria transmission close to the equator, shown in red, are still struggling to control the disease. From Feachem et al., 2010.

Vector control

Insecticides targeting the mosquito vector have played an important role in reducing the burden of malaria. Clearly, reducing the mosquito population can decrease malaria transmission. From 1955 to 1969, a Global Malaria Eradication Program employed insecticides to significantly reduce the population at risk of malaria from 77% in 1900 to 55% in 1975 (Hay et al., 2004). Malaria was eradicated from North America and much of Europe by the 1970s. However, the program excluded sub-Saharan Africa because transmission was phenomenally high (Enayati and Hemingway, 2010). The campaign relied heavily on the organochloride insecticide DDT (dichlorodiphenyl-trichloroethane), which was used for indoor residual spraying (IRS). IRS is the application of insecticides to the inside of human dwellings to kill resting mosquitoes. DDT delays the closure of voltage-gated sodium channels causing neurons to repetitively fire, resulting in paralysis and death. However, DDT is a persistent organic pollutant with the ability to bioaccumulate in food chains, poisoning predatory birds and other animals. DDT was subsequently banned, although it has recently been re-introduced in parts of Africa. The eradication campaign was abandoned in 1969 because of technical, logistical, economic and political complications (Enayati and Hemingway, 2010).

Today, both IRS and insecticide-treated nets (ITNs) are frequently used concurrently to reduce mosquito populations and malaria transmission. Modern IRS uses stable formulations of insecticides that last for 2 to 6 months before re-spraying is necessary (Enayati and Hemingway, 2010). ITNs are designed to prevent human-mosquito contact and therefore mosquito bites by covering humans whilst sleeping. A major improvement to ITNs was the development of long-lasting insecticide-treated nets (LLINs), which provide protection for 3 to 5 years (Okumu and Moore, 2011). Since 2005, there has been large-scale distribution of LLINs within sub-Saharan Africa to encourage wider coverage and usage, particularly in young children and pregnant women (Atieli et al., 2011). This has been organised by WHO and various partnerships, including Roll Back Malaria (RBM). Trials in Africa have demonstrated that LLINs and IRS reduce malaria morbidity and mortality (Akachi and Atun, 2011; Atieli et al., 2011; Lengeler, 2004).

However, LLINs and IRS alone are insufficient to eliminate malaria from high-transmission regions. Increased ownership of LLINs does not necessarily translate to increased coverage. A disadvantage of IRS and ITNs is that they only target endophilic (indoor-resting/biting) mosquitoes, allowing exophilic (outdoor-resting/biting) mosquitoes to continue transmitting disease. Persistent use of IRS and ITNs could even evolutionarily select for exophilic behaviour (Riehle et al., 2011). Another major problem is the development of insecticide resistance in mosquito populations. Vector control is currently extremely reliant on pyrethroids, a single class of insecticides (Ranson et al., 2011). Pyrethroids are the only class approved for use on ITNs and they are also widely used for IRS across Africa, largely because they have been shown to be non-toxic and efficacious (Zaim et al., 2000). Overuse of one particular insecticide selects for mosquitoes in the population with resistance phenotypes. Sadly, pyrethroid resistance is now widespread in *An. gambiae* in Africa. Like DDT, pyrethroids target voltage-gated sodium channels in mosquito neurons. Several methods of acquiring resistance have been documented, including target site alteration, metabolic resistance, penetration resistance and behavioural resistance (Ranson et al., 2011). In recent years, the frequency of resistance genes in *An. gambiae* has rapidly increased. One solution to combat resistance would be to use distinct insecticide classes for ITNs and IRS. For example, pyrethroid-treated nets could be employed in combination with organophosphate or carbamate IRS (Okumu and Moore, 2011). Importantly, a recently established product development partnership, called the Innovative Vector Control Consortium, is researching and developing novel or altered insecticides to provide options for the future (Hemingway et al., 2006).

Inventive new approaches to vector control are currently being investigated, including biological control agents. Biological control has many advantages over chemicals, including safety to humans

and non-target wildlife and lower risk of resistance development (Raghavendra et al., 2011). Instead of targeting adult mosquitoes, another way of reducing the vector population is to kill larvae. This could be advantageous for exophilic mosquito populations that avoid ITNs and IRS (Enayati and Hemingway, 2010). Predators have been successfully introduced into breeding sites to control anophelines, including larvivorous fish, such as *Poecilia*, *Tilapia*, *Gambusia* and *Aphanius* species (Haq and Yadav, 2011). *Bacillus thuringiensis israelensis (Bti)*, a toxin-producing bacterium, has been used as an effective larvicide in Northern Europe (Christophides, 2005; Raghavendra et al., 2011). Other biological control agents targeting adults or larvae include entomopathogenic fungi, such as *Beauveria bassiana* (Blanford et al., 2005; Bukhari et al., 2010; Scholte et al., 2005). Nematodes and insect-killing viruses have also been proposed. These additional control measures are yet to be deployed on a large scale (Enayati and Hemingway, 2010). Natural plant phytochemicals have also been demonstrated to have larvicidal effects (Raghavendra et al., 2011).

Antimalarial drugs

Antimalarial drugs are used for both the prevention and treatment of malaria. There are only a handful of available antimalarials and most target the pathogenic asexual blood stages of *Plasmodium*. Several drugs have been employed worldwide for prophylaxis and treatment of malaria but these efforts are being undermined by the emergence of resistant parasites. Excessive usage of non-lethal drug levels, poor compliance, self-treatment and counterfeit drugs have fuelled the emergence and spread of resistance (Baird, 2005), resulting in treatment failure and increased mortality and morbidity (WHO, 2010).

Various strategies have been utilised for the administration of antimalarial drugs. Chemoprophylaxis is successfully used by millions of non-immune people that travel to malaria regions for business or pleasure every year (Greenwood et al., 2005). For the inhabitants of endemic areas, chemoprophylaxis in children can significantly reduce malaria mortality and morbidity but this is difficult to sustain over prolonged periods, might encourage resistance and could prevent children from acquiring natural immunity (Greenwood, 2010). During pregnancy, intermittent preventative therapy (IPT) is the preferred approach. This involves the use of antimalarials two or three times during pregnancy to protect mother and baby. IPT has also been successfully employed in infants, with drugs administered at set points during their first year (Greenwood et al., 2005). In regions where malaria is very seasonal, vulnerable groups can be given antimalarials at intervals during the transmission season. Another approach is mass drug administration (MDA) in which entire populations are given drugs regardless of their disease status. This has been demonstrated to

facilitate the emergence of resistance and is not recommended for controlling malaria. MDA might, however, be useful for regions on the brink of malaria elimination (Greenwood, 2010).

In the 1940s, chloroquine became the first-line antimalarial for uncomplicated malaria worldwide. This asexual blood stage drug was very effective, safe, inexpensive and fast-acting (Baird, 2005). However, resistance in *P. falciparum* became widespread and this drug can no longer be used in many countries. Nevertheless, chloroquine is still used against *P. vivax* in areas without resistance (WHO, 2010). Sulfadoxine-pyrimethamine was employed in the 1970s to target chloroquine-resistant parasites but resistance also developed quickly. Mefloquine and quinine were then used, resulting in the appearance of multi-drug resistant parasites, especially in Southeast Asia (Eastman and Fidock, 2009). Subsequently, there was a global surge in malaria mortality and morbidity (Fidock, 2010). Primaquine is the only licensed tissue schizonticide available, which targets liver stage parasites (Baird, 2005; Schlitzer, 2007). It is the only classic drug capable of killing the hypnozoites of *P. vivax* and *P. ovale* (Enayati and Hemingway, 2010). Primaquine is also able to kill sexual blood stages (gametocytes), which prevents mosquito infection. However, safety concerns about this drug have limited its usage (Kiszewski, 2011).

For the last decade, artemisinin-based combination therapies (ACTs) have been recommended as the best first-line treatment for *P. falciparum* malaria (WHO, 2010). Combination therapies exploit two drugs with different modes of action against the same parasite developmental stage (Baird, 2005). Artemisinin is highly potent against the asexual blood stages, rapidly reducing parasitemia (Eastman and Fidock, 2009). It is also active against immature gametocytes, which reduces malaria transmission (Baird, 2005). However, artemisinin is promptly eliminated from the body and seven days of treatment would be required if the drug was used alone, which is deemed impractical. In combination with a slowly excreted blood schizonticide, like mefloquine, necessary treatment time is reduced to three days. Although combination therapies are more expensive, shorter treatment times increase patient compliance and slow the development of parasite resistance (Greenwood et al., 2005). Together with ITNs and IRS, ACTs have reduced malaria transmission in sub-Saharan Africa (Fidock, 2010). Worryingly though, artemisinin resistance in *P. falciparum* was recently reported in the Thai-Cambodia border (WHO, 2010). The WHO is battling to contain artemisinin resistance because few alternative antimalarials are available for the immediate future.

Public-private partnerships, like the Medicines for Malaria Venture (MMV), are currently trying to discover and develop new antimalarial drugs (Enayati and Hemingway, 2010). Drugs against the sporozoites, liver stages and sexual blood stages are seriously lacking (Kiszewski, 2011; Mazier et al., 2009). The development of high throughput screens of novel antimalarial drug candidates has been

a valuable step forward (Delves et al., 2012; Fidock, 2010). Unfortunately, drug development is a very slow process (Enserink, 2010). A key aim is to develop successful transmission blocking drugs that are effective against mature gametocytes and stop mosquitoes from being infected. The ideal antimalarial would require a single dose and target both asexual and sexual stages. Some promising candidates are currently undergoing development, such as Tafenoquine manufactured by GlaxoSmithKline (GSK) (Kiszewski, 2011; Schlitzer, 2007) and OX439 from MMV (Delves et al., 2012).

Malaria vaccines

A fully protective malaria vaccine has proven elusive. Hurdles to vaccine development have included lack of funding and the sheer complexity of the parasite biology and life cycle (Crompton et al., 2010). Notably, the parasite naturally undergoes extensive antigenic variation and has many redundant proteins to evade the host immune response. To eliminate malaria with a vaccine, it would need to be almost 100% efficacious and given to the population at risk with very high coverage, which may be unattainable (Enayati and Hemingway, 2010). Therefore, a vaccine would need to be used in coordination with other malaria control strategies, like ITNs.

The most clinically advanced malaria vaccine candidate by far is RTS,S, which is undergoing phase 3 trials in seven African countries. It is the world's first malaria vaccine candidate to reach large-scale phase 3 testing, which is the final stage of development before submission to the regulatory authorities (GlaxoSmithKline and PATH, 2012). GSK created RTS,S in 1987 and led its early development. In 2001, GSK went into a public-private partnership with the PATH Malaria Vaccine Initiative (MVI), supported by the Bill & Melinda Gates Foundation, to develop the vaccine for use in young children in Africa. RTS,S is a pre-erythrocytic (liver stage) subunit vaccine that targets the parasite's circumsporozoite (CS) protein, the most prominent surface protein of the sporozoite. The vaccine is a recombinant protein combining part of *P. falciparum* CS protein with a hepatitis B virus surface antigen, which improves immunogenicity. It is administered with patented GSK adjuvant systems called AS01 or AS02. Together, this induces production of CS-specific antibodies and CD4⁺ T-cells, which reduce the parasite's ability to invade and develop within liver cells. The phase 3 trials are investigating vaccine efficacy, safety and immunogenicity in young babies and older infants (Agnandji et al., 2011). Early results met the modest expectations set by the phase 2 trials. The risk of clinical malaria and severe malaria were reduced by 56% and 47%, respectively, in older infants. Safety of the vaccine was also promising, with few adverse effects reported. The vaccine's efficacy in young babies, its cost-effectiveness and longevity of the protective effect are yet to be determined.

Final results are not expected until 2014 but WHO has taken the unprecedented step of recommending the use of RTS,S in some African countries by 2015 (Tanne, 2011).

Other vaccine candidates are being developed against every parasite life stage, with most targeting the pre-erythrocytic stages (Greenwood and Targett, 2011). Whole parasite immunisation, using sporozoites attenuated by irradiation or genetic manipulation, was one of the earliest vaccine attempts and has recently been revived (Hill, 2011). It is hoped this pre-erythrocytic vaccine could induce significantly higher levels of efficacy than RTS,S but product development is challenging. Vectored vaccines, usually delivered in a prime-boost regime, use viral vectors or plasmid DNA to deliver pre-erythrocytic or blood stage antigens to induce an immune response. Progress with developing asexual blood stage vaccines has been disappointing and improved target antigens are required. One challenge for the future is developing multicomponent vaccines against all life stages (Hill, 2011; Vogel, 2010).

An exciting prospect for malaria control is the development of transmission blocking vaccines (TBVs), which prevent parasites infecting the mosquito vector. The aim would be to immunise humans with gametocyte, gamete, zygote or ookinete antigens so they produce antibodies which are transferred to the mosquito during blood feeding. These antibodies could prevent or reduce oocyst development in the mosquito gut and therefore malaria transmission (Crompton et al., 2010; Hill, 2011). This is a logical approach as the parasite is at its most vulnerable inside the mosquito because it is present extracellularly and in small numbers (Figure 1.2) (Crompton et al., 2010). These vaccines are known as “community vaccines” because they would benefit the local population rather than the immunised individuals. The entire population would need to be vaccinated to block transmission, which could be logistically difficult. Early trials of TBV candidates have been very promising, with some blocking parasite development by 96% (Vogel, 2010). Interestingly, mosquito midgut antigens have also been proposed for use in TBVs. An aminopeptidase N (AgAPN1) in the *An. gambiae* midgut was recently identified as a putative ligand for ookinete invasion (Dinglasan et al., 2007). It was demonstrated that antibodies against AgAPN1 could significantly inhibit *P. falciparum* invasion in several mosquito species, which implies a conserved role for AgAPN1 in ookinete invasion. Therefore, a major advantage of mosquito-stage vaccines is they could be effective against more than one *Plasmodium* species, such as *P. falciparum* and *P. vivax*, which is unlikely to be true for other types of vaccines (Hill, 2011; Vogel, 2010).

Genetically modified mosquitoes

Technological advances have led to the exciting prospect of exploiting genetically modified (GM) mosquitoes to control malaria transmission. Furthermore, this can also be applied to controlling arboviruses, like dengue and CHIKV (Alphey, 2009). Two different approaches are available: population suppression and population replacement. Population suppression aims to use GM mosquitoes to reduce mosquito numbers in natural populations. An important example is RIDL (release of insects with a dominant lethal), which is an advancement on the sterile insect technique (SIT). In SIT, mass-reared male insects are sterilised and released repeatedly into wild populations to mate with wild females. This results in few viable offspring and ultimately suppresses the population (Black et al., 2011). In RIDL, male GM mosquitoes are fertile but their female offspring are killed by a dominant lethal gene whereas male offspring pass the lethal gene on (Thomas et al., 2000). If sufficient numbers of males are released over a sustained period, this suppresses the local population. Expression of the lethal gene is conditional, usually in the absence of tetracycline, so females survive in the laboratory and are killed before release by withdrawing the drug. The conditional female-specific lethal gene removes any danger of accidental release and also the need to sterilise males. RIDL field trials using *Ae. aegypti* are ongoing (Alphey, 2009). It is believed that RIDL would be useful for suppressing isolated mosquito populations but not for large areas.

Population replacement involves replacing the natural mosquito population with GM mosquitoes refractory to *Plasmodium* parasites (Catteruccia, 2007; Christophides, 2005). Sequencing of the *An. gambiae* genome (Holt et al., 2002) has helped identify mosquito effector genes that could be exploited for population replacement programs. The mosquito immune system is an excellent target for manipulation as it plays an important role in naturally refractory mosquito strains or species. For example, the mosquito immune system could be enhanced by overexpressing a *Plasmodium* antagonist (Christophides, 2005). To date, no single gene is capable of completely blocking *Plasmodium* development and so multiple genes would need to be targeted (Catteruccia, 2007). This would also reduce the likelihood of resistance emerging in the parasite population.

Several examples of partially refractory GM mosquitoes have been created in the laboratory. Transgenic *An. stephensi* mosquitoes expressing the artificial peptide SM1 in the midgut significantly reduced capacity to transmit the rodent parasite, *P. berghei* (Ito et al., 2002). SM1 binds to the mosquito salivary gland and midgut epithelia, which inhibits parasite invasion. This was the first demonstration of stably transforming *Anopheles* mosquitoes to affect malaria transmission. In another study, ectopic overexpression of the antimicrobial peptide (AMP), cecropin A, in the *An. gambiae* midgut resulted in a 60% reduction in oocysts (Kim et al., 2004). *An. stephensi* have also

been engineered to express single-chain antibodies (scFvs), which significantly reduced *P. falciparum* infection levels (Isaacs et al., 2012; Isaacs et al., 2011). Expression of a synthetic antimalarial gene, *Vida3*, in the midgut of *An. gambiae* reduced rodent parasite *P. yoelii* infections by 85%, although results were inconsistent for *P. falciparum* (Meredith et al., 2011).

A genetic drive system is necessary to spread a new trait into field populations of mosquitoes (Christophides, 2005). Various different gene drive systems have been proposed, with some tested in the laboratory. Examples include transposable elements, meiotic drive, intracellular symbionts like *Wolbachia* and homing endonucleases (Sinkins and Gould, 2006). Tight linkage between the gene drive system and the engineered gene(s) is essential to prevent recombination from separating them, resulting in spread of an “empty” drive (Alphey et al., 2002; Catteruccia, 2007; Christophides, 2005).

Practical implementation of GM mosquitoes for malaria control is challenging, with technical, ethical and safety issues to overcome (Catteruccia, 2007). It is vital to have a thorough understanding of the population structure, behaviour and ecology of the mosquito population being targeted (Christophides, 2005). Detailed knowledge of local malaria transmission dynamics is also essential. Altering the mosquito immune system may have fitness or survival costs, which must be investigated if the GM mosquito is to successfully mate with wild insects (Catteruccia, 2007). Also, all GM mosquito strategies are species-specific and can be complicated by the intricate population structure of the *An. gambiae* complex.

An alternative approach to GM mosquitoes is paratransgenesis, the transformation of obligate insect symbionts. In a recent laboratory study, *Pantoea agglomerans*, a bacterial symbiont of *Anopheles* mosquitoes, was engineered to secrete anti-*Plasmodium* effector proteins (Bisi and Lampe, 2011). It remains to be determined whether this strategy is able to block malaria transmission in the field.

Mosquito immunity

The innate immune response is a powerful, fast-acting and primitive form of defence shared by all eukaryotes and is the sole defence mechanism of insects (Christophides et al., 2004). It is a broad defence system that allows organisms to quickly distinguish between self and infectious non-self to protect against infection (Michel and Kafatos, 2005). Once the danger is recognised, the signal is modulated, either amplified or dampened depending on its original intensity and the situation (Christophides et al., 2004). A diverse range of effector mechanisms, such as phagocytosis, lysis and melanisation are deployed to kill the invader. As well as detecting non-self, the innate immune

system can also be activated upon recognition of endogenous molecules released from injured or stressed cells, known as damage-associated molecular patterns (DAMPs) (Carta et al., 2009; Newton and Dixit, 2012). DAMPs, such as ATP, uric acid, DNA, heat-shock proteins and collagen, act as danger signals and trigger inflammatory responses to restore homeostasis. Unlike the adaptive immune response of vertebrates, innate immunity is largely independent of previous infections (Hoffmann, 2003; Meister et al., 2004). However, a memory-like response called “immune priming” has been reported in insects, whereby an initial challenge makes the immune system more responsive to subsequent challenges of the same or different type (Schmid-Hempel, 2005). This protection can be either generalised or pathogen-specific and persist for several weeks (Pham et al., 2007).

The *An. gambiae* innate immune response is a complex interplay between many effector mechanisms, including a complement-like system (Figure 1.5). Insect defence can be broadly divided into humoral and cellular reactions, although many immune molecules are shared between the two types of responses (Christophides et al., 2004). In humoral reactions, immune molecules are secreted into the hemolymph where they fight microbial invaders. Insects have an open circulatory system, which allows the hemolymph to bathe organs and tissues. The major immune tissues of insects are hemocytes (blood cells) and fat body, a diffuse organ analogous to the mammalian liver and adipose tissue. Cellular responses entail direct action by hemocytes, such as encapsulation and phagocytosis (Christophides et al., 2004). Some responses are acute and happen rapidly after infection, such as cellular responses or those involving immune effectors constitutively present in the hemolymph. Other responses are inducible and require activation of signalling pathways, resulting in induction of immune gene expression. Induction can also replace those molecules utilised in acute reactions.

The fruitfly, *Drosophila melanogaster*, has been an invaluable model for studying the innate immune system (Lemaitre and Hoffmann, 2007). A great deal of our knowledge about *An. gambiae* immunity originally stemmed from studies in *Drosophila*. Mosquitoes and fruitflies are both Dipteran insects, which are believed to have separated approximately 250 million years ago (Waterhouse et al., 2007). Classical genetics, the use of mutants and morphological markers and genetic manipulation have been perfected in the fly. However, in recent years, *An. gambiae* has emerged as an alternative model system to study innate immunity. Furthermore, as a major malaria vector, *An. gambiae* is ideal for studying natural host-parasite interactions.

The last decade or more has seen tremendous advances in the tools and techniques available to study the mosquito immune system. High throughput sequencing permitted the complete sequence

of the *An. gambiae* genome (Giles reference strain) to be published in 2002 (Holt et al., 2002) and further annotation continues. Comparative genomic analyses between *An. gambiae* and the well-studied *D. melanogaster* have been exploited to identify candidate immunity genes (Christophides et al., 2002). The genomes of *Ae. aegypti* and *Culex pipiens quinquefasciatus*, two other vector mosquitoes, have also been sequenced, which allows for further genomic comparisons (Baton et al., 2008). VectorBase has been developed as an online bioinformatic resource for analysing disease vector genomes and expression data (Lawson et al., 2009). Furthermore, genome sequencing of *P. falciparum*, *P. vivax*, *P. yoelii* and *P. berghei* has been successfully accomplished (Carlton et al., 2008; Carlton et al., 2002; Gardner et al., 2002; Hall et al., 2005).

Cultured cell lines derived from *An. gambiae* hemocyte-like cells were generated for analysing gene function *in vitro* (Muller et al., 1999). Expressed Sequence Tag (EST) libraries constructed from these cell lines were used for the first *An. gambiae* microarray to analyse gene expression (Dimopoulos et al., 2002). An important advancement was the development of whole-genome *An. gambiae* microarray platforms, which allow genome-wide transcriptional profiling. Microarrays have facilitated the discovery of genes differentially expressed by various immune challenges (Dong et al., 2006a; Marinotti et al., 2005; Vlachou et al., 2005). Recently, a high-density single nucleotide polymorphism (SNP) genotyping array has been employed to map genetic divergence between mosquitoes in a population or species (Lawniczak et al., 2010).

Germline transgenesis of mosquitoes has been successfully implemented in *An. stephensi* (Catteruccia et al., 2000) and *An. gambiae* (Grossman et al., 2001). This allows overexpression of candidate genes to elucidate their immune function. Nevertheless, producing and maintaining transgenic mosquitoes is technically and logistically demanding (Baton et al., 2008). Transient gene silencing using RNA interference (RNAi) has become the preferred method for functional characterisation of candidate genes. RNAi can silence a target gene in the whole mosquito by microinjection of specific double-stranded (ds) RNA (Blandin et al., 2002). Rather than a complete knockout, RNAi can significantly “knockdown” expression of the gene. The dsRNA is taken up by cells where it is cleaved into small interfering RNA fragments (siRNA) that induce degradation of endogenous target mRNA. This technique can be effectively used for cultured cells by transfecting the dsRNA (Levashina et al., 2001). Simultaneous RNAi silencing of two or more genes can be used to investigate epistatic interactions. RNAi is a form of reverse genetics: investigating the phenotype associated with a known gene. It has been pivotal in the discovery and characterisation of many novel anti-*Plasmodium* effectors. Transgenic *P. berghei* constitutively expressing green fluorescence

protein (GFP) throughout its life cycle is an excellent tool for screening candidate genes for a role in *Plasmodium* infections (Franke-Fayard et al., 2004).

Together, these powerful technological advances have transformed the study of molecular biology of the mosquito and enabled dissection of its innate immune system. Importantly, they led to the exciting discovery of a complement-like system in *An. gambiae* (Blandin et al., 2008), which will be discussed later in this Chapter.

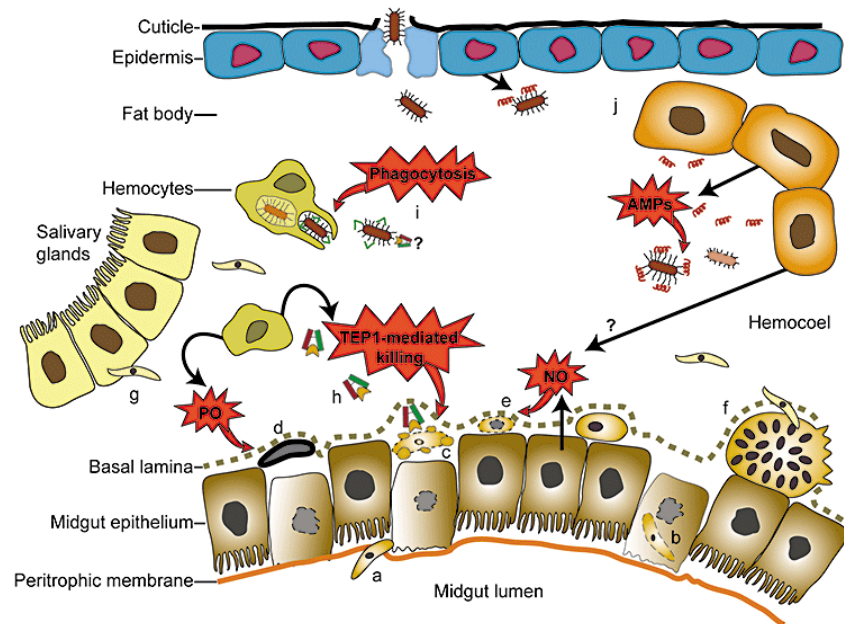


Figure 1.5 Schematic overview of innate immunity in *An. gambiae*.

Plasmodium ookinetes invade the mosquito midgut epithelium (a) and some are killed by nitration of epithelial cells (b). The vast majority of parasites are killed and lysed in the basal labyrinth by the mosquito complement-like system (c), which involves the effector TEP1 and its interaction with LRIM1/APL1C (h). In certain mosquito genetic backgrounds, ookinetes are melanised by the activity of phenoloxidase (PO) (d). Toxic nitric oxide (NO) generated by midgut epithelial cells and possibly fat body cells kills some early oocysts (e). Surviving oocysts develop in the basal labyrinth and rupture after approximately two weeks to release thousands of sporozoites into the hemolymph (f). These sporozoites travel to and invade the mosquito salivary glands (g). Bacteria that invade the hemolymph through the cuticle or from the midgut are phagocytosed by hemocytes after opsonisation by TEP1, possibly in complex with LRIM1/APL1C (i). Antimicrobial peptides (AMPs), produced by the fat body, hemocytes and barrier epithelia, play an important role in microbial killing in the hemolymph (j). From Yassine and Osta, 2010.

Pathogen recognition

Insects have an array of pattern recognition receptors (PRRs) that detect and bind to conserved pathogen-associated molecular patterns (PAMPs) and trigger immune responses (Christophides et al., 2002). PAMPs are crucial to microbial physiology but rare or absent from higher organisms

(Michel and Kafatos, 2005). Examples include peptidoglycan (PGN), lipopolysaccharide (LPS) and β -1,3 glucans, which are microbial cell wall or membrane components. The nature of *Plasmodium* PAMPs and how they are recognised by the mosquito is still unknown (Christophides et al., 2004). PRRs can be membrane bound, such as on the surface of hemocytes, or circulating in the hemolymph. Once a PRR has bound a PAMP, it can directly mediate microbial killing via phagocytosis and encapsulation or it can indirectly initiate killing by activating serine protease cascades in the hemolymph and intracellular signalling pathways (Warr et al., 2008).

The PGN recognition protein (PGRP) family are the best studied insect PRRs (Christophides et al., 2004). This family has central and diverse functions in triggering immune reactions, such as melanisation, phagocytosis and signal transduction (Christophides et al., 2002). There are two PGRP subfamilies: short (S) are secreted whereas long (L) are either transmembrane or intracellular. There are seven *An. gambiae* PGRP family members (three S and four L) compared to 13 in *Drosophila* (seven S and six L). PGRP-S proteins have amidase activity whereas PGRP-L proteins are catalytically inactive. PGRP-LC is essential for survival of gram-negative and gram-positive bacterial infections in *An. gambiae* (Meister et al., 2009). Like in *Drosophila*, *An. gambiae* PGRP-LC undergoes alternative splicing to form three isoforms with variant PGRP domains (LC1, LC2 and LC3) and different specificities (Christophides et al., 2002; Meister et al., 2009).

Another established family of insect PRRs are the gram-negative bacteria binding proteins (GNBPs), which are known to bind to LPS and β -1,3 glucans (Christophides et al., 2002). Three GNBPs have been discovered in *Drosophila* and the family has expanded to six in *An. gambiae*. Different GNBPs have been demonstrated to aid mosquito survival during gram-negative and gram-positive bacterial infections (Warr et al., 2008). Several GGBP family members are also antagonists of *P. falciparum* and *P. berghei*.

The C-type lectins (CTLs), which bind carbohydrates in a calcium-dependent manner, are also predicted to be PRRs (Christophides et al., 2004). There are 35 and 22 CTLs predicted in *Drosophila* and *Anopheles*, respectively (Christophides et al., 2002). CTLs have been implicated in innate immune reactions in various insects, including melanisation, cellular encapsulation and opsonisation (Ao et al., 2007; Jomori and Natori, 1992). In *An. gambiae*, CTL4 and CTLMA2 circulate in the hemolymph as a disulphide-bonded heterodimer and act as repressors of *P. berghei* ookinete melanisation (Osta et al., 2004a; Schnitger et al., 2009), although their role in *P. falciparum* infections is uncertain (Cohuet et al., 2006). The CTL4/CTLMA2 complex is also involved in defence against gram-negative bacteria (Schnitger et al., 2009).

Other potential insect PRR families include the Galectins (GALEs), the scavenger receptors (SCRs) and the fibrinogen-like domain immunoelectins (known as FBNs or FREPs).

Immune signalling pathways

Five intracellular immune signalling pathways have been identified in *Drosophila* and these are also found in mosquitoes. The two best studied, Toll and Immune deficiency (Imd), are fundamental to the *Drosophila* innate immune response and evolved early in metazoan evolution (Hoffmann, 2003). The Toll and Imd pathways in insects are homologous to the Toll-like receptor (TLR) and Tumour necrosis factor (TNF) signalling pathways in vertebrates, respectively. In *Drosophila*, the Toll pathway chiefly responds to infections with fungi and gram-positive bacteria whereas Imd is mainly activated by gram-negative bacteria. There is, however, significant cross-talk between pathways, which can therefore act synergistically (Ferrandon et al., 2007; Lemaitre and Hoffmann, 2007). The Toll pathway is also critical for embryogenesis in *Drosophila*. In the Toll pathway, PRRs convey an immune signal to a transmembrane receptor, resulting in intracellular signalling which culminates in nuclear translocation of a nuclear factor- κ B/reticuloendotheliosis (NF- κ B/Rel) transcription factor. In the Imd pathway, transmembrane PRRs directly initiate intracellular signalling. Depending on the signal, the NF- κ B/Rel transcription factor induces expression of a specific repertoire of immune genes, such as AMPs. Most AMPs are secreted, cationic effectors that kill microbes by binding to their lipid membranes and causing surface perturbation and cytoplasmic efflux (Broderick et al., 2009; Christophides et al., 2004). Many AMPs are differentially active against particular pathogens. For example, *Drosophila* diptericin is mainly active against gram-positive bacteria, defensin against gram-positive bacteria and drosomycin against fungi (Lemaitre and Hoffmann, 2007). Some AMP genes, for example drosomycin, are activated to different extents by both the Toll and Imd pathways under diverse circumstances (Lemaitre and Hoffmann, 2007).

In the *Drosophila* Toll pathway, the Lysine-type PGN of gram-positive bacteria is recognised by three circulating PRRs, PGRP-SA, PGRP-SD and GGBP1 (Figure 1.6) (Ganesan et al., 2011; Lemaitre and Hoffmann, 2007). GGBP3 detects β 1,3-glucans from fungal cell walls (Ferrandon et al., 2007). All these recognition events converge on the Toll pathway via activation of the same protease, Modular Serine Protease (ModSP) (Ganesan et al., 2011). ModSP triggers a serine protease cascade which activates Spätzle processing enzyme (SPE), which directly cleaves pro-Spätzle and releases the active extracellular ligand, Spätzle. Virulence factors, produced by some bacteria and fungi, can also stimulate the Toll Pathway by activating the serine protease, Persephone, which converges on SPE, independently of ModSP. The negative regulator of Persephone, a serpin called Necrotic, can act to

dampen Toll signalling (Govind, 2008). Mature Spätzle binds to the transmembrane Toll receptor, inducing its homodimerisation (Lemaitre and Hoffmann, 2007). Toll signals via its intracellular Toll-IL1 receptor (TIR) domain to recruit three intracellular Death-domain (DD) containing proteins, dMyD88, Tube and Pelle. The kinase Pelle is activated by auto-phosphorylation, which triggers the phosphorylation and degradation of the NF- κ B/Rel inhibitor, I κ B/Cactus. As a result, NF- κ B/Rel transcription factors Dif and Dorsal, which are usually sequestered by Cactus, are released and translocate to the nucleus. Here they induce the expression of specific antimicrobial genes, such as *drosomycin*. Dorsal is important for developmental processes whereas Dif is essential in adult immunity (Ganesan et al., 2011).

The *Drosophila* Imd pathway is triggered by the PRRs, PGRP-LC and PGRP-LE, which detect the DAP-type PGN of gram-negative bacterial cell walls (Figure 1.6) (Ganesan et al., 2011). PGRP-LC is membrane bound whereas PGRP-LE is usually intracellular but a cleaved PGRP-domain only form can be extracellular. In the cytoplasm, PGRP-LE recognises tiny PGN fragments that have entered the cell or PGN from intracellular bacterial pathogens, such as *Listeria monocytogenes*. Upon direct binding of PGN, the receptors recruit the adaptor Imd. Imd interacts with dFADD which itself recruits the caspase Dredd, all via their DDs. Next, Dredd is proposed to bind Relish, an NF- κ B/Rel transcription factor with a self-inhibitory ankyrin (ANK) repeat domain (Govind, 2008). Relish is phosphorylated by the IKK γ / β complex, which is itself believed to be activated by the TAK1-TAB2 complex in an Imd-dependent manner (Ferrandon et al., 2007; Lemaitre and Hoffmann, 2007). Phosphorylated Relish is cleaved by Dredd, releasing its NF- κ B/Rel domain from inhibition and allowing nuclear translocation. Relish stimulates the expression of a specific subset of genes, including *diptericin*.

Comparative genomics has shown that the majority of Toll and Imd pathway components are highly conserved between *D. melanogaster* and *An. gambiae* (Christophides et al., 2002; Waterhouse et al., 2007). In contrast, other immune genes are rapidly evolving (Waterhouse et al., 2007). There are most differences in recognition, modulation and effector molecules rather than signal transduction, which might reflect adaptation to different pathogens. As a blood feeding insect, *An. gambiae* is subjected to a diverse range of pathogens compared to *Drosophila*, which primarily feed on yeast and sugars (Dimopoulos, 2003). For example, of the seven AMP families present in *Drosophila*, only defensins (DEFs), cecropins (CECs) and attacins (ATTs) have been so far found in *An. gambiae* (Waterhouse et al., 2007). Mosquitoes have an additional AMP family called gambicins (GAMs). The Imd pathway PRR, PGRP-LE, is also absent in mosquitoes (Christophides et al., 2002).

The precise mechanisms and functions of the Toll and Imd pathways in mosquitoes are still being investigated (Garver et al., 2008). In *An. gambiae*, REL1 (orthologue of Dorsal) and REL2 (orthologue

of Relish) are the NF- κ B/Rel transcription factors in the Toll and Imd pathways, respectively (Christophides et al., 2004). Surprisingly, there is no orthologue of Dif in the *An. gambiae* genome (Christophides et al., 2002). *An. gambiae* REL2 undergoes alternative splicing to produce the full-length isoform REL2-F and a shorter version, REL2-S, without the inhibitory ANK repeats and DD (Meister et al., 2005). Whereas Relish in *Drosophila* is specific to gram-negative bacteria, REL2-F and REL2-S are involved in defence against gram-positive and gram-negative bacteria, respectively. It therefore seems that REL2-S substitutes for the role of Dif. Like *Drosophila*, the *An. gambiae* Toll pathway is primarily active against fungi and gram-positive bacteria (Hillyer, 2010). In *Ae. aegypti*, the Toll pathway has been shown to control dengue virus infection (Xi et al., 2008) but the pathway does not affect ONNV infections in *An. gambiae* (Waldock et al., 2012).

Both the Toll and Imd pathways have been implicated in defence against *Plasmodium*. Imd signalling and subsequent REL2-F activation limits the development of *P. berghei* oocysts in the *An. gambiae* midgut (Meister et al., 2005). REL2 regulates the expression of major *Plasmodium* antagonists and AMPs (Dong et al., 2011; Garver et al., 2009; Meister et al., 2005). Overexpression of REL2 causes increased expression of these anti-*Plasmodium* effectors, which almost completely blocks *P. falciparum* infection of *An. stephensi* (Dong et al., 2011). Furthermore, Caspar, a negative regulator of REL2, has been shown to control resistance to *P. falciparum* in the major malaria vectors, *An. gambiae*, *An. stephensi* and *An. albimanus* (Garver et al., 2009). The Toll pathway has also been suggested to play an anti-*Plasmodium* role. Several important effectors, like components of the complement-like pathway, are regulated by the Toll/REL1 pathway (Fraiture et al., 2009; Frolet et al., 2006). Silencing Cactus, a negative regulator of REL1, renders *An. gambiae* mosquitoes almost refractory to *P. berghei* infections (Frolet et al., 2006). Interestingly, REL1 and REL2 were shown to be most efficient against *P. berghei* and *P. falciparum*, respectively, highlighting species specificity (Garver et al., 2009). Other immune signalling pathways in *Drosophila* and other insects are poorly characterised (Lemaitre and Hoffmann, 2007). The Janus kinase (JAK)/signal transducers and activators of transcription (STAT) pathway is essential for hematopoiesis in mammals and embryonic development in *Drosophila* (Christophides et al., 2004). It also plays an immunity role in insects but little is known about the mechanisms involved. The JAK/STAT pathway is involved in antiviral immunity in mammals, *Drosophila* and *Ae. aegypti* but does not have a major role in *An. gambiae* defence against ONNV (Steinert and Levashina, 2011; Waldock et al., 2012). Signalling by AgSTAT-A was recently reported to mediate a late-phase response against *Plasmodium* (Gupta et al., 2009). Next, the c-Jun N-terminal kinase (JNK) pathway plays a key role in the regulation of many developmental processes in *Drosophila* and has been proposed to regulate immune gene expression (Lemaitre and Hoffmann, 2007). JNK signalling is thought to be a branch of the Imd pathway as it is

triggered by TAK1 (Figure 1.6). Finally, the mitogen-activated protein kinase (MAPK)/p38 stress pathway has been implicated in the immune response of plants, *Caenorhabditis elegans* and mammals but its role in insects is unknown (Lemaitre and Hoffmann, 2007).

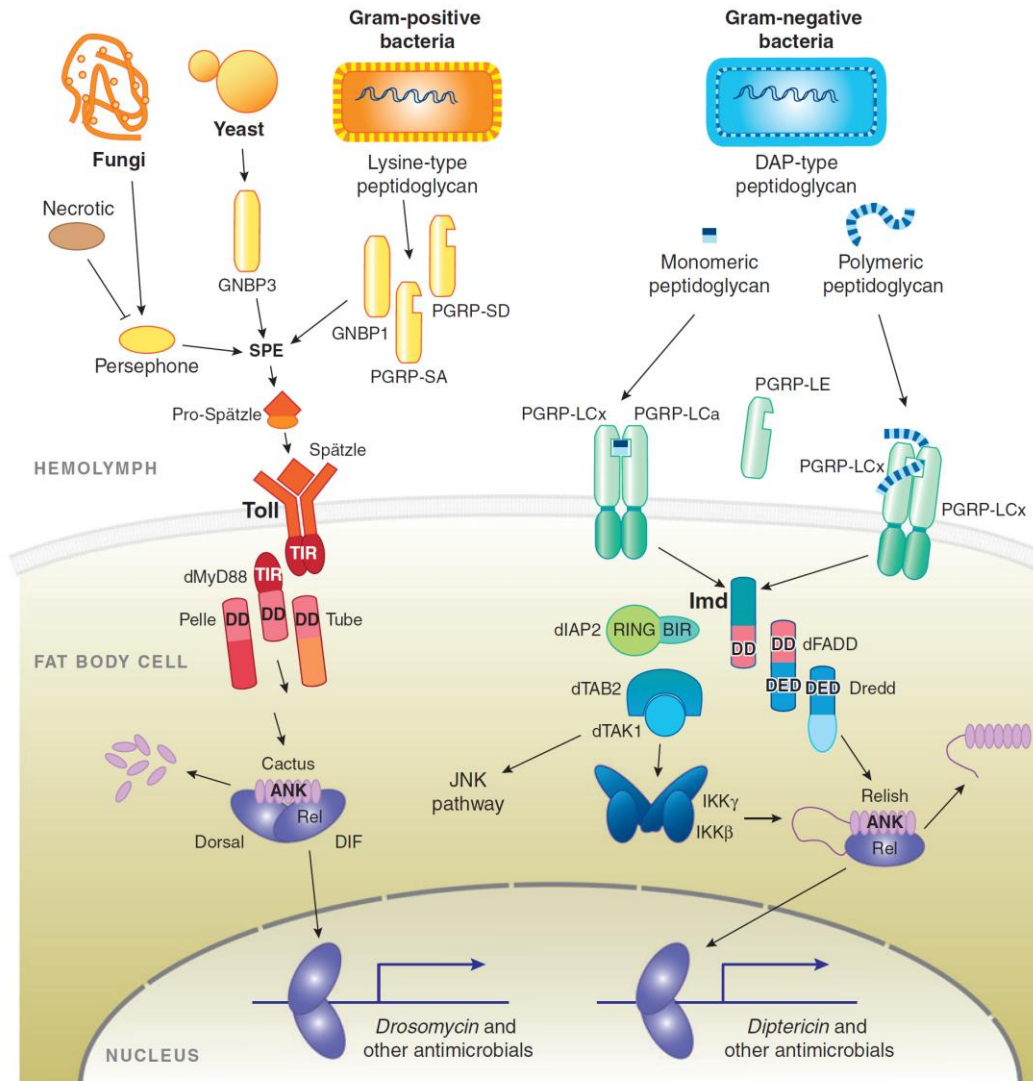


Figure 1.6 Intracellular immune signalling pathways in *Drosophila melanogaster*.

The Toll and Imd signalling pathways modulate expression of AMPs in *Drosophila*. In the fruitfly, the Toll pathway predominantly responds to fungal and gram-positive bacterial infections whereas the Imd pathway is largely activated by gram-negative bacteria. In the **Toll pathway**, PAMPs are recognised by soluble PRRs, including PGRP-SA, PGRP-SD, GNBPs and GNBPs. As well as the serine protease Persephone, these PRRs converge on SPE, which cleaves and activates Spätzle. Spätzle binds to the transmembrane receptor, Toll, inducing its dimerisation. MyD88, Tube and Pelle are recruited, resulting in phosphorylation and degradation of the inhibitor, Cactus. The NF- κ B/Rel transcription factors, Dif and Dorsal, are subsequently released and activate expression of immune genes, such as *drosomycin*. In the **Imd pathway**, the transmembrane PRR, PGRP-LC, directly binds to PAMPs and recruits intracellular adaptor, Imd. Imd interacts with dFADD and caspase Dredd. The Imd pathway NF- κ B/Rel transcription factor, Relish, has a self-inhibitory ankyrin (ANK) domain. After phosphorylation by the IKK γ / β complex, Relish is cleaved by Dredd and relieved from inhibition. The Rel domain of Relish translocates to the nucleus and activates specific genes, such as *dipthericin*. From Lemaitre and Hoffmann, 2007.

The mosquito complement-like system

Thioester-containing protein 1 (TEP1) and Leucine-rich repeat immune protein 1 (LRIM1) were the first major *Plasmodium* antagonists identified by RNAi (Blandin et al., 2004; Osta et al., 2004a). Silencing *TEP1* or *LRIM1* results in a dramatic increase in *P. berghei* oocysts in the midgut of susceptible mosquitoes, which suggests that wild-type mosquitoes actively control parasite development in a TEP1-LRIM1 dependent manner. Another important anti-*Plasmodium* effector related to LRIM1 named *Anopheles Plasmodium*-responsive leucine-rich repeat 1 (APL1) was discovered shortly after (Riehle et al., 2006). In a survey of natural *An. gambiae* populations in West Africa, *APL1* mapped to a genetic locus that controls resistance to *P. falciparum*. Silencing *APL1* gives the same antagonistic phenotype with *P. berghei* as *LRIM1* and *TEP1* (Povelones et al., 2009; Riehle et al., 2006). Manual re-annotation revealed that the *APL1* locus encompasses three independent yet closely related genes (*APL1A*, *APL1B* and *APL1C*); of these only *APL1C* is a *P. berghei* antagonist (Riehle et al., 2008) whereas all three paralogues have been implicated in defence against *P. falciparum* to varying degrees (Garver et al., 2012; Mitri et al., 2009).

TEP1, LRIM1 and APL1C are core members of the mosquito complement-like pathway, which plays a vital role in the killing and disposal of pathogens, including *Plasmodium* parasites and bacteria (Blandin et al., 2008). Melanisation, lysis and phagocytosis are all effector mechanisms of the complement-like system. The mosquito complement-like pathway, particularly its biochemical regulation, is still largely uncharacterised (Povelones et al., 2011). Interestingly, LRIM1 and APL1C do not have identifiable orthologues in *D. melanogaster* (Waterhouse et al., 2007). Evidence suggests that the LRIM1/APL1C/TEP1 module is conserved in *Ae. aegypti*, as their orthologues are upregulated following infection with a life-shortening *Wolbachia* strain (Kambris et al., 2009).

The TEPs are an important family of immune effectors, which are related to the vertebrate complement factors, C3, C4 and C5 and the universal protease inhibitors, α 2-macroglobulins (α 2Ms) (Christophides et al., 2004). There are 15 TEPs in *An. gambiae* compared to only six in *Drosophila* (Christophides et al., 2002). The highly reactive TE bond is exposed by proteolytic cleavage, either by a specific convertase protease complex or a general protease (Blandin and Levashina, 2004). Once proteolytically active, TEPs use their TE to covalently bind to pathogen surfaces, opsonising them for destruction (Levashina et al., 2001). Interestingly, nine *Anopheles* TEPs and two *Drosophila* TEPs lack the TE motif, which might suggest these TEPs have a regulatory role (Christophides et al., 2002). A TE motif is not essential for protein activity, as shown by vertebrate C5 complement factors. TEP family members are involved in anti-*Plasmodium* and antibacterial defence (Blandin and Levashina, 2004).

TEP1 displays considerable sequence, structural and functional similarities to C3, the central effector of the vertebrate complement system (Baxter et al., 2007; Levashina et al., 2001). Both are secreted glycoproteins with a conserved TE motif in comparable locations. The TE is sequestered and activated by cleavage in a protease-sensitive region of the protein (Baxter et al., 2007). TEP1 lacks the anaphylatoxin domain of C3, which triggers inflammatory responses in vertebrates. Vertebrate C3 is 180 kDa and composed of two chains, α and β , which are joined together by disulphide bridges. TEP1 circulates in the mosquito hemolymph as both the full length 165 kDa protein (TEP1-F) and a mature, proteolytically processed form (TEP1_{cut}). The two parts of TEP1_{cut} remain held together by a non-disulphide linkage and they can be separated by non-reducing SDS-PAGE into N- and C-terminal fragments (~75 kDa and ~85 kDa, respectively) (Levashina et al., 2001). The protease responsible for cleaving TEP1-F into mature TEP1_{cut} is still undetermined. *In vitro* experiments have indicated that the TE bond, found in the C-terminal fragment, is not spontaneously activated by this cleavage (Fraiture et al., 2009). It is unknown how the TE of TEP1_{cut} is activated *in vivo* and whether an additional cleavage is necessary.

TEP1 engages in complement-like activity, including opsonisation. Upon proteolytic activation, vertebrate C3 proteins covalently bind to pathogen surfaces via their active TE bond and trigger a cascade of events that culminates in pathogen killing by phagocytosis or cell lysis (Levashina 2001). Likewise, TEP1_{cut} covalently binds to the surface of bacteria and promotes their phagocytosis in a TE-dependent manner (Levashina et al., 2001). Chemical inactivation of the TE bond with methylamine or *TEP1* knockdown by RNAi impairs phagocytosis *in vitro* (Levashina et al., 2001). *TEP1* knockdown also severely impairs phagocytosis of *Escherichia coli* (gram-negative bacteria) and *Staphylococcus aureus* (gram-positive bacteria) in adult mosquitoes (Moita et al., 2005).

Plasmodium killing by *Anopheles* mosquitoes is mediated by direct binding of TEP1_{cut} to the ookinete surface, which triggers parasite lysis or melanisation (Blandin et al., 2004). TEP1_{cut} binds to parasites as they emerge from invaded midgut cells into the basal labyrinth, the space between the midgut epithelia and the basal lamina. The basal lamina is permeable to hemolymph proteins but not hemocytes. As mentioned earlier, silencing *TEP1* substantially increases *Plasmodium* infection intensity. A C-terminal TEP1 antibody was used to demonstrate TEP1 localisation on the surface of *P. berghei* ookinetes 24 to 48 h after an infected blood meal. Using transgenic *P. berghei*, the vast majority of TEP1-labelled parasites had lost GFP expression and were therefore dead. Importantly, not all ookinetes were TEP1-labelled but more labelled ookinetes were observed in refractory mosquitoes compared to susceptible mosquitoes. Binding of TEP1 also proceeded faster in refractory mosquitoes. TEP1 has also been observed on the surface of oocysts but not sporozoites,

highlighting the specificity of TEP1-parasite interactions. It should be noted that some parasites are killed in a TEP1-independent manner as parasites can be detected without GFP expression or TEP1 labelling.

LRIM1 and APL1C are related proteins that possess leucine-rich repeat (LRR) domains, which are found in host defence proteins of many phyla. LRIM1 and APL1C circulate in the hemolymph as a disulphide-linked heterodimeric complex (Baxter et al., 2010; Povelones et al., 2011). Using an antibody against LRIM1 or APL1C, a high molecular weight band is detected by non-reducing western blot that resolves into the predicted monomers under reducing conditions (Povelones et al., 2009). Upon silencing of *LRIM1*, APL1C is not secreted *in vivo*, and vice versa (Fraiture et al., 2009; Povelones et al., 2009). This suggests that complex formation is obligatory and occurs prior to secretion. The crystal structure of the LRIM1/APL1C heterodimer was recently solved, revealing that it is held together by a single intermolecular disulphide bond between conserved cysteine residues (Baxter et al., 2010). This has been confirmed with mutational analyses (Baxter et al., 2010; Povelones et al., 2011).

The LRIM1/APL1C complex interacts with TEP1_{cut} in the hemolymph, stabilising this processed form, maintaining it in circulation and promoting its localisation to parasite surfaces (Figure 1.7) (Fraiture et al., 2009; Povelones et al., 2009; Volohonsky et al., 2010). This interaction was demonstrated when the LRIM1/APL1C complex was able to co-immunoprecipitate endogenous TEP1_{cut} from the conditioned media of mosquito hemocyte-like cells (Povelones et al., 2009). His-tagged TEP1 injected into the mosquito hemocoel was also able to pull-down LRIM1 and APL1C (Fraiture et al., 2009). Furthermore, the complex prevents TEP1_{cut} from non-specifically reacting with self-tissues (Fraiture et al., 2009). RNAi-mediated depletion of LRIM1 or APL1C causes a significant decrease in levels of TEP1_{cut} but not TEP1-F in the hemolymph (Fraiture et al., 2009; Povelones et al., 2009). Immunofluorescence staining showed that TEP1_{cut} is deposited on mosquito tissues, such as the abdominal epidermis, in the absence of LRIM1/APL1C (Fraiture et al., 2009). Levels of TEP1_{cut} in the hemolymph can be rescued by injection of recombinant LRIM1/APL1C (Baxter et al., 2010). Interestingly, the LRIM1/APL1C complex is still detected in the hemolymph after *TEP1* knockdown, demonstrating that LRIM1/APL1C stability is not dependent on TEP1. Silencing of *LRIM1* or *APL1C* completely abolishes binding of TEP1_{cut} to *P. berghei* ookinetes and subsequent TEP1-mediated killing (Fraiture et al., 2009; Povelones et al., 2009). Therefore, TEP1 malfunction seems to be largely responsible for the increased parasite load observed upon *LRIM1* or *APL1C* knockdown (Osta et al., 2004a; Riehle et al., 2006). Furthermore, silencing *TEP1*, *LRIM1* or *APL1C* in *An. quadriannulatus*

transforms this refractory mosquito into a highly susceptible *Plasmodium* vector (Habtewold et al., 2008).

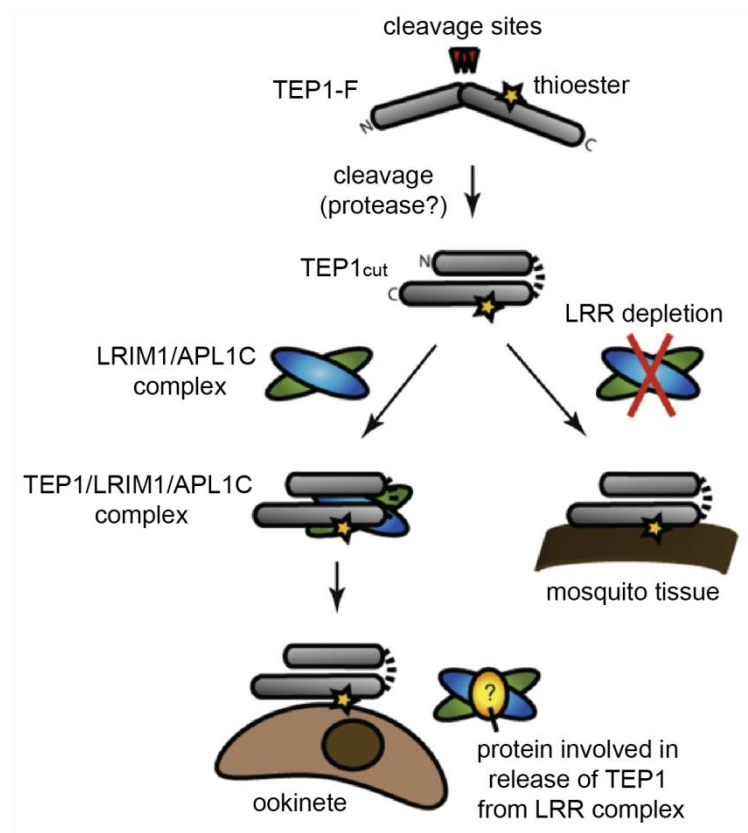


Figure 1.7 Proposed roles of TEP1, LRIM1 and APL1C in the complement-like system of *An. gambiae*.

Full-length TEP1 (TEP1-F) is constitutively cleaved in the mosquito hemolymph by an unknown protease. Cleavage generates TEP1-N and TEP1-C fragments, which remain together as a two-chain molecule called TEP1_{cut}. The LRIM1/APL1C complex binds to TEP1_{cut}, which stabilises TEP1_{cut} and maintains it in circulation. This LRR complex is proposed to direct TEP1_{cut} to pathogen surfaces during infection. During *P. berghei* infection, TEP1_{cut} is released from the LRIM1/APL1C complex by an unknown mechanism, possibly via another protein. TEP1_{cut} binds to the ookinete surface and promotes its destruction. When LRIM1 and/or APL1C are silenced by RNAi, TEP1_{cut} reacts with mosquito tissues and is unable to localise to parasite surfaces. This results in increased survival of live oocysts. Adapted from Volohonsky et al., 2010.

It is not clear whether the LRIM1/APL1C complex is able to recognise pathogen surfaces to control the specificity of TEP1 binding (Fraiture et al., 2009). One hypothesis is that TEP1 is released from the LRIM1/APL1C complex in close proximity to pathogens, which mediates activation of its TE bond and binding to the pathogen surface. To complicate matters, the LRIM1/APL1C complex was recently demonstrated to interact only with TEP1_{cut} possessing an inactive TE *in vitro*, although the relevance of this *in vivo* is unknown (Baxter et al., 2010). The authors speculated that TEP1_{cut} (with an inactive

TE) might act as a TEP1 convertase, activating free TEP1 molecules close to pathogen surfaces, under the regulation of LRIM1/APL1C. In addition to TEP1, the LRIM1/APL1C complex has been demonstrated to interact with other TEP family members *in vitro* (Povelones et al., 2011). The complex captured the N- and C-terminal fragments of TEP3, the C-terminal fragment of TEP4 and the N-terminal fragment of TEP9 from the conditioned media of mosquito hemocyte-like cells. As the LRIM1/APL1C complex is reported to interact with TEP1 with a 1:1 stoichiometry (Baxter et al., 2010), it seems probable that LRIM1/APL1C forms independent complexes with each of these TEPs in response to different infections (Povelones et al., 2011).

Basal immunity is an interesting concept related to the mosquito complement-like system and antiparasitic responses (Blandin et al., 2008; Frolet et al., 2006). It has been hypothesised that pre-formed immune components are permanently circulating in the hemolymph, ready for rapid action against invading pathogens. TEP1, LRIM1 and APL1C are all expressed and secreted by hemocytes (Levashina et al., 2001; Pinto et al., 2009). Under normal conditions, the complement components, *TEP1*, *LRIM1* and *APL1C*, are constitutively expressed under regulation of REL1 and REL2 (Fraiture et al., 2009; Frolet et al., 2006). TEP1, LRIM1 and APL1C are present in the hemolymph bathing the basal labyrinth poised to attack malaria parasites as they emerge through invaded cells (Blandin et al., 2008). Parasite invasion induces expression of these genes to replenish proteins utilised during the infection. Thus, acute response reactions play an important role in *An. gambiae* whereas *Drosophila* is highly dependent on inducible reactions. The role of constitutively expressed immune effectors in *Drosophila* is unclear.

The role of the LRIM1/APL1C/TEP1 module in defence against the deadliest human parasite, *P. falciparum*, remains uncertain. Most functional studies to date have used the rodent parasite, *P. berghei*, as a convenient laboratory model. However, *P. berghei* is naturally transmitted by *Anopheles durenii* and is unlikely to encounter the very anthropophilic *An. gambiae* in the wild (Cohuet et al., 2006). TEP1 has been shown to limit *P. falciparum* infections in *An. gambiae* (Dong et al., 2006a; Garver et al., 2012), although it remains undetermined whether TEP1 binds to *P. falciparum* ookinetes (Yassine and Osta, 2010). It was recently demonstrated that LRIM1 and APL1C are *P. falciparum* antagonists in an infection intensity-dependent manner (Garver et al., 2012). Silencing *LRIM1* or *APL1C* was found to significantly increase *P. falciparum* oocyst levels at medium and low infection intensities, respectively. Therefore, LRIM1 and APL1C are likely to play a context-specific role in *P. falciparum* defence, correlating well with the discovery of *APL1C* in a *P. falciparum* resistance island (Riehle et al., 2006). The dependence on infection intensity explains why earlier studies reported that *LRIM1* or *APL1C* knockdown in *An. gambiae* has no influence on *P. falciparum*

infections (Cohuet et al., 2006; Mitri et al., 2009). The varied impact of the LRIM1/APL1C/TEP1 module could highlight vector-parasite co-evolution and immune evasion by the parasite, presumably to enhance its transmission. Interestingly, LRIM1, APL1C and TEP1 are also antagonists of *P. yoelii* in *An. gambiae*, which is partially refractory to this rodent parasite, but not in *An. stephensi*, a natural vector of *P. yoelii* (Jaramillo-Gutierrez et al., 2009). It is possible that parasites in their natural vectors (*P. falciparum* in *An. gambiae* and *P. yoelii* in *An. stephensi*) have evolved to evade the LRIM1/APL1C/TEP1 pathway. In agreement, a recent study reported that the TEP1 pathway is unable to kill some sympatric strains of *P. falciparum* (Molina-Cruz et al., 2012). Alternatively, in line with the TEP1 convertase hypothesis discussed above, the putative TEP1 convertase could be under different regulation in specific contexts, which might explain why LRIM1 and APL1C exhibit a stronger phenotype with *P. berghei* than *P. falciparum* (Marois, 2011).

Melanisation and lysis

Melanisation is an important innate immune response exclusive to arthropods, which involves the production and deposition of melanin on invading pathogens and parasites (Christensen et al., 2005). It is sometimes referred to as melanotic encapsulation because the invader is encased in a melanin-containing capsule (Clements, 2012). In addition to immunity, melanisation plays a critical role in many invertebrate physiological processes, such as egg chorion hardening, cuticle sclerotisation and wound healing (Hillyer, 2010). Melanisation can be deployed against a variety of pathogens, including bacteria, fungi and *Plasmodium* parasites. However, the reaction is highly specific and only elicited against certain species or strains of pathogens. Melanisation often results in pathogen death but the killing mechanism is uncharacterised. It has been hypothesised that pathogens are killed by oxidative damage from cytotoxic intermediates or by starvation (Christensen et al., 2005; Hillyer, 2010). Melanisation is also utilised to dispose of pathogens killed by an independent mechanism (Blandin et al., 2004).

Melanisation is controlled by the enzyme, phenoloxidase (PO), which catalyses fundamental steps in the synthesis of melanin, a brown-black polymeric macromolecule (Christensen et al., 2005; Clements, 2012; Hillyer, 2010). The biochemical pathway of melanin synthesis in mosquitoes has not been fully elucidated (Clements, 2012). The putative pathway begins with the hydroxylation of phenylalanine into tyrosine. PO catalyses the hydroxylation of tyrosine to dopa and then the oxidation of dopa to dopaquinone, which is non-enzymatically converted to dopachrome (Hillyer, 2010). Dopachrome is converted to 5,6-dihydroxyindole by dopachrome conversion enzyme (DCE). 5,6-dihydroxyindole is oxidised to indole-5,6-quinone by PO and then cross-linked with hemolymph

proteins to form eumelanin. In an alternative pathway, dopa can produce dopamine via the action of dopa decarboxylase (DDC), which PO and other enzymes convert into melanin. Silencing either DCE or DDC impairs pathogen melanisation, highlighting the importance of both pathways (Hillyer, 2010).

PO is activated by a cascade of serine proteases and regulated by protease inhibitors and cofactors (Figure 1.8) (Cerenius and Soderhall, 2004). POs are synthesised as inactive precursors called prophenoloxidases (PPOs), which undergo limited proteolysis by a PPO-activating enzyme (PPAE) (Cerenius and Soderhall, 2004; Christensen et al., 2005). The *An. gambiae* genome encodes nine putative PPOs, with only one possessing a *Drosophila* orthologue (Christophides et al., 2002). Most PPOs lack a signal peptide and are thought to be released into the hemolymph via lysis of activated hemocytes rather than secretion (Castillo et al., 2006). It is hypothesised that each PO has a specific or primary function, such as in larvae or in adults after blood feeding (Christensen et al., 2005; Clements, 2012). PPAEs are also maintained as zymogens that are activated by an upstream cascade of extracellular serine proteases following infection or injury. This cascade modulates the initial signal, either amplifying a “danger signal” or dampening a false alarm (Christophides et al., 2004). Recognition events triggering melanisation are poorly understood but β -1,3-glucan-recognition proteins have been implicated (Christensen et al., 2005). As the quinone intermediates of the melanisation pathway are highly reactive and toxic, the process must be tightly regulated in both location and time to protect the host. Serpins (SRPNs), a family of irreversible serine protease inhibitors, prevent excessive or inappropriate PO activation (Cerenius and Soderhall, 2004). Different SRPNs inhibit both the serine protease cascade and PPAEs.

The clip-domain serine proteases and serine protease homologues (CLIPs) are an important family responsible for modulating and regulating melanisation. CLIPs possess a compact disulphide-bridged structure called the clip-domain, and a protease domain. After activation by proteolytic cleavage, the protein structure resembles a paperclip (Christophides et al., 2004). The precise function of the clip domain is unclear but it is believed to be important for regulating and localising the activity of the protease domain. There are five subfamilies of CLIPs in mosquitoes: A, B, C, D and E. Most CLIPB, D and C subfamily members have protease activity whereas CLIPA and E members are non-catalytic serine protease homologues (SPHs). CLIPBs are chiefly responsible for PPAE activation. They are sequentially cleaved in a proteolytic cascade, which culminates in the activation of PPAE and PPO. In contrast, CLIPAs are important positive and negative regulators of melanisation, sometimes acting as cofactors to help activate PO (Volz et al., 2006). There are predicted to be 10 CLIPAs and 17 CLIPBs in the *An. gambiae* genome (Christophides et al., 2002).

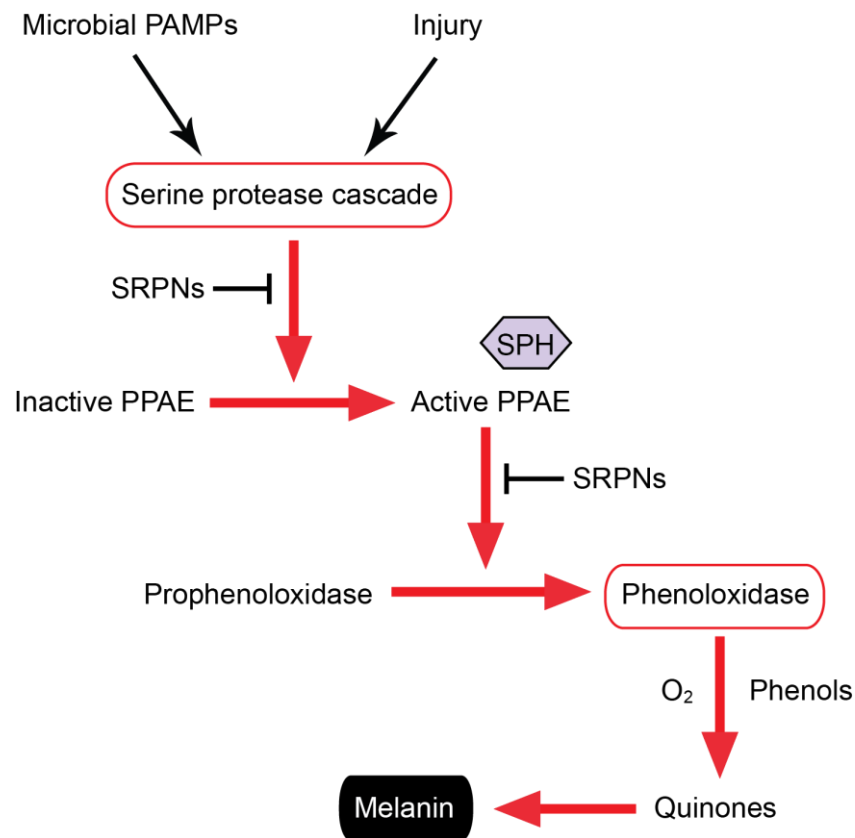


Figure 1.8 The prophenoloxidase activating system in arthropods.

Melanisation pathways in arthropods are triggered when PRRs detect microbial PAMPs or in response to injury. A cascade of serine proteases sequentially activate each other, culminating in cleavage and activation of PPAE. Active PPAE cleaves prophenoloxidase into active phenoloxidase. Phenoloxidase catalyses the major steps in melanin production, which generates cytotoxic intermediates, such as quinones. Melanin is deposited on pathogen surfaces as a killing or clearance mechanism. The process is tightly controlled by SRPN inhibitors and serine protease homologues (SPHs). Some PPAEs require SPHs to activate phenoloxidase. Adapted from Cerenius and Soderhall, 2004.

Melanisation is involved in the killing and clearance of *Plasmodium* parasites, but its role varies considerably between mosquito and parasite strains. Ookinetes are melanised once they have invaded the mosquito midgut and reached the basal labyrinth (Collins et al., 1986). Curiously, killed melanised parasites persist in the midgut tissues for the remainder of the mosquito's life but do not influence mosquito survival (Blandin et al., 2004). Certain mosquito genetic backgrounds are capable of blocking *Plasmodium* infection due to highly efficient melanisation. Such melanotic refractoriness is a complicated phenomenon requiring the coordinated function of a several genes, including *TEP1* (Blandin et al., 2004). The most famous example of melanotic refractoriness to *Plasmodium* infection is the L3-5 strain of *An. gambiae*. The L3-5 strain was genetically selected in the laboratory from *An. gambiae* G3, a susceptible strain colonised in Gambia in 1975 (Collins et al., 1986). L3-5 mosquitoes melanise virtually all invading ookinetes of various strains of rodent, primate, human and avian

parasites. This strain is almost completely refractory to the primate parasite *Plasmodium cynomolgi*, the rodent parasite *P. berghei* and allopatric (non-African) isolates of *P. falciparum*, *P. vivax* and *P. ovale*. Normal G3 mosquitoes are susceptible to all these parasites. Interestingly, L3-5 mosquitoes fail to melanise co-indigenous strains of human malaria parasites. It was recently shown that certain *P. falciparum* strains are able to evade TEP1-mediated antiparasitic responses to survive in the L3-5 strain (Molina-Cruz et al., 2012). Genetic mapping found that three quantitative trait loci (QTLs), named *Pen1*, *Pen2* and *Pen3*, are responsible for melanisation in L3-5 (Zheng et al., 1997). The contribution of each QTL varies depending on the parasite species (Zheng et al., 2003). Interestingly, the L3-5 strain has elevated levels of reactive oxygen species (ROS) (Kumar et al., 2003). Another example is a genetically selected strain of *Anopheles dirus*, a human malaria vector from Southeast Asia, which is completely refractory to the African rodent parasite, *P. yoelii nigeriensis* (Somboon et al., 1999; Wen-Yue et al., 2007). This refractory strain is capable of melanising ookinetes immediately after midgut invasion and fully encapsulated oocysts have also been observed. Interestingly, the same strain is fully susceptible to infections with *P. falciparum* and *P. vivax*, which both naturally infect *An. dirus*. Both these examples highlight the importance of host-pathogen co-evolution. It is likely that parasites have evolved to manipulate and evade the immune responses of their natural mosquito hosts.

The melanisation cascade in *An. gambiae* is poorly characterised but some major players have been identified. RNAi-mediated gene silencing has been used to determine the effect on *P. berghei* melanisation. Interestingly, phenotypes can vary considerably depending on the mosquito genetic background (Volz et al., 2006). Injection of abiotic Sephadex beads has also been utilised to test for genes influencing melanisation (Paskewitz et al., 2006; Warr et al., 2006). *Plasmodium*-refractory and susceptible strains of *An. gambiae* can both melanise beads, with a stronger response in refractory mosquitoes. CLIPB3, CLIPB4, CLIPB8 and CLIPB17 promote parasite melanisation whereas CLIPA2, CLIPA5 and CLIPA7 inhibit parasite melanisation (Volz et al., 2006). CLIPB4 and CLIPB8 are also involved in promoting bead melanisation (Paskewitz et al., 2006). CLIPA8, a non-catalytic SPH, is essential for PO activation and is a key regulator of both ookinete and bacterial melanisation in *An. gambiae* (Schnitger et al., 2007; Volz et al., 2006). This suggests there is overlap in the genetic modules regulating responses to both pathogens. There are 18 predicted SRPNs in *An. gambiae* and most of these possess inhibitory activity (Suwanchaichinda and Kanost, 2009). Knockdown of *SRPN2* results in the formation of spontaneous melanotic pseudotumours that reduce mosquito life span (Michel et al., 2005). Silencing *SRPN2* also strongly interferes with *P. berghei* midgut invasion because it usually inhibits parasite lysis and melanisation. *SRPN6* in *An. gambiae* also inhibits

parasite melanisation and potentially promotes parasite lysis (Abraham et al., 2005). The organisation of these genes in the melanisation cascade is yet to be elucidated.

Two potential *An. gambiae* pathogen recognition proteins of the CTL family are repressors of melanisation. CTL4 and CTLMA2 circulate as a disulphide-linked heterodimer in the hemolymph (Schnitger et al., 2009). Silencing either CTL results in a dramatic rise in melanised *P. berghei* ookinetes and decrease in live oocysts in the mosquito midgut (Osta et al., 2004a). The CTL4/CTLMA2 complex has been linked to the mosquito complement-like pathway and the promotion of parasite lysis. Silencing *LRIM1*, *APL1C* or *TEP1* simultaneously with *CTL4* in susceptible mosquitoes reverses the *CTL4* phenotype with *P. berghei*, indicating these genes are epistatic to *CTL4* (Osta et al., 2004a). Therefore, melanisation observed in *CTL4* knockdown mosquitoes depends on *LRIM1/APL1C/TEP1* function. Melanisation has been proposed as the killing mechanism in susceptible mosquitoes after *CTL4* knockdown (Volz et al., 2006). *CTL4* and *CTLMA2* knockdown had no effect on *P. falciparum* development when sympatric field isolates were used to infect *An. gambiae* (Cohuet et al., 2006). The CTL4/CTLMA2 complex plays a key role in defence against gram-negative bacteria in *An. gambiae* (Schnitger et al., 2009). Interestingly, CTL4 and CTLMA2 do not influence melanisation of Sephadex beads (Warr et al., 2006).

Melanisation is an effector mechanism of the complement-like cascade: *TEP1*, *LRIM1* and *APL1C* all influence melanisation. It has been hypothesised that binding of the *LRIM1/APL1C/TEP1* complex to pathogens initiates the melanisation cascade (Warr et al., 2006). Both *LRIM1* and *TEP1* are required for the melanisation of Sephadex beads (Warr et al., 2006). Silencing *LRIM1*, *APL1C* or *TEP1* can reverse the refractory L3-5 phenotype, abolishing parasite melanisation and making the mosquito susceptible to *P. berghei* infection (Blandin et al., 2004; Povelones et al., 2009). Therefore, it has been suggested that *TEP1*-mediated parasite killing (or damage) by an undetermined mechanism is a prerequisite for melanisation in L3-5 (Blandin et al., 2004). Melanisation in L3-5 is thought to be a clearance mechanism of dead or damaged parasites (Blandin et al., 2004; Volz et al., 2006).

The wide variability in the capacity of *An. gambiae* individuals to transmit *Plasmodium* parasites has been largely attributed to polymorphisms in the *TEP1* gene, which is exceptionally polymorphic (Blandin et al., 2009; Obbard et al., 2008). Interestingly, there are two distinct alleles of *TEP1* called *TEP1s* and *TEP1r*, which seem to be associated with susceptible and refractory mosquitoes, respectively (Blandin et al., 2004; Molina-Cruz et al., 2012). *TEP1r* has been associated with L3-5 mosquitoes (Blandin et al., 2004). The predicted *TEP1s* and *TEP1r* proteins share 93% identity and 96% similarity, with differences concentrated in one region close to the TE motif (Baxter et al., 2007). *TEP1r* has been shown to be more efficient at parasite killing (Blandin et al., 2009). It has been

hypothesised that TEP1r has a more reactive TE bond, which accelerates binding kinetics and efficiency (Baxter et al., 2007; Blandin et al., 2004).

The significance of melanisation in the mosquito immune response, including *P. falciparum* defence in the field, is still under investigation. Melanisation can negatively impact reproductive fitness and the toxic intermediates pose serious danger to the host (Whitten et al., 2006). *Anopheles punctulatus* uses melanisation to kill invading filarial worms (Aliota et al., 2011). However, melanisation is not essential for mosquito survival of bacterial infections and melanised bacteria are rarely observed in *An. gambiae* adults (Schnitger et al., 2007). Indeed, it has been suggested that melanisation might increase the effectiveness of other immune reactions, as seen in *Drosophila* (Schnitger et al., 2007; Tang et al., 2006). Melanised *P. falciparum* ookinetes are observed in field-caught *An. gambiae* mosquitoes although this is quite rare. Nevertheless, in one study in Tanzania, 90% of field-captured *An. gambiae* were able to melanise Sephadex beads prior to blood feeding (Schwartz and Koella, 2002). Furthermore, *APL1C* maps to a *Plasmodium* resistance island on chromosome 2L with significant effects on *P. falciparum* melanisation (Riehle et al., 2006), which suggests a role for the complement-like pathway in melanisation in field populations.

Recent studies in *Ae. aegypti* have suggested that immune melanisation and tissue melanisation have independent mechanisms of PPO activation (Zou et al., 2010). It is unknown whether this is also true for *An. gambiae*. However, CLIPA8 is critical for pathogen melanisation but is not required for wound melanisation (Schnitger et al., 2007), which implies the existence of distinct mechanisms in *An. gambiae*.

In addition to melanisation, lysis is a related *Plasmodium*-killing or clearance mechanism (Blandin et al., 2008). The term lysis was first adopted to account for the dramatic killing and subsequent disappearance of the vast majority of invading parasites. These “missing” parasites in wild-type mosquitoes become apparent as live oocysts in the midgut upon RNAi-mediated knockdown of particular effectors, like *LRIM1*. Both lysis and melanisation play an important role in refractory mosquitoes, such as *An. gambiae* L3-5 strain and *An. quadriannulatus* (Collins et al., 1986; Habtewold et al., 2008). Upon *TEP1* binding, dead or dying ookinetes appear morphologically deformed (Blandin et al., 2004). Ookinetes undergoing lysis exhibit organelle disintegration, cytoplasmic vacuolation and membrane blebbing (Whitten et al., 2006). An example of a lytic refractory *An. gambiae* strain is SUAF2, a laboratory selected line that lyses all *P. gallinaceum* parasites as they traverse the midgut epithelium (Vernick et al., 1995). As with melanisation, it is still undetermined whether lysis is predominantly a mechanism of killing or a means to clear dead or

dying parasites. It has been proposed that parasites are killed by TEP1 via an unidentified mechanism and then cleared by lysis (Blandin et al., 2004).

The underlying mechanism of lysis is very poorly understood. It is unknown whether TEP1 binding recruits a membrane attack complex akin to the vertebrate complement system. The *TEP1r* allele has been linked to more efficient lysis of parasites (Blandin et al., 2009). CLIPB14 and CLIPB15 promote *P. berghei* lysis in susceptible and refractory mosquitoes (Volz et al., 2005). In addition to inhibiting melanisation, SRPN6 promotes parasite lysis (Abraham et al., 2005).

Cellular immunity

As well as humoral defences, mosquitoes exhibit a range of cellular innate immune responses mediated by hemocytes, which act as immunosurveillance cells (Hillyer, 2010). Hemocytes also play a crucial role in humoral responses by producing immune proteins, such as PRRs, melanisation components and AMPs (Hillyer, 2009; Pinto et al., 2009). Mosquitoes possess an open circulatory system whereby hemolymph bathes all internal tissues and organs. Some hemocytes circulate in the hemolymph whereas most are found attached to visceral surfaces, such as the tracheae, Malpighian tubules and the basal surface of the midgut (Blandin and Levashina, 2007). Hemocyte abundance progressively decreases with mosquito age, which has been linked to increased susceptibility to septic infection (Castillo et al., 2006). Interestingly, a brief rise in circulating hemocytes is observed following blood feeding, which could represent mobilisation of sessile hemocytes or increased hematopoiesis. Three types of hemocytes have been identified in mosquito larvae, pupae and adults: granulocytes, oenocytoids and prohemocytes. Granulocytes are by far the most abundant whereas oenocytoids and prohemocytes usually account for less than 10%. Oenocytoids constitutively express PPO for the melanisation cascade, which is stored in the cytoplasm and released when the cell is activated and lysed upon immune challenge. Prohemocytes are small progenitors of granulocytes (Blandin and Levashina, 2007).

Phagocytosis is the engulfment of pathogens by circulating hemocytes, which results in their killing and degradation (Michel and Kafatos, 2005). It is triggered by PRRs that opsonise pathogens and induce intracellular signalling cascades, resulting in actin-dependent internalisation of the invader (Christophides et al., 2004). Granulocytes are the only insect hemocyte capable of phagocytosis (Castillo et al., 2006). The phagocytic response is very rapid and can occur within 5 minutes of exposure to microorganisms. As the infection advances, the granulocytes increase in size as they engulf hundreds of invaders (Hillyer, 2010). Apoptotic bodies and melanised pathogens can also be

cleared by phagocytosis (Clements, 2012; Osta et al., 2004b). Interestingly, distinct molecular mechanisms are believed to control phagocytosis of gram-negative and gram-positive bacteria. The uptake of gram-negative bacteria is faster and more efficient than gram-positive bacteria, with more gram-negative bacteria engulfed per cell (Blandin and Levashina, 2007). Inactivation of phagocytosis components results in rapid bacterial accumulation within 8 h of infection (Moita et al., 2005). However, similar to melanisation, blocking phagocytosis does not usually compromise mosquito survival during bacterial infection. This suggests that, although phagocytosis plays an important role in the early stages of infection, the powerful repertoire of AMPs take over once they have been induced.

The potential role of phagocytosis in *Plasmodium* defence remains unclear. Direct contact between ookinetes and hemocytes is prevented by the basal lamina. Therefore, phagocytosis by hemocytes is not involved in ookinete killing or clearance of dead ookinetes (Blandin and Levashina, 2007). Sporozoites are the only parasite stage that circulates freely in the hemolymph. Between 80 and 90% of sporozoites are cleared before reaching the salivary glands but the mechanisms responsible are unknown. Phagocytosis of *Plasmodium* sporozoites is observed *in vivo* but it is not believed to make a substantial contribution to sporozoite clearance in *An. gambiae* (Hillyer et al., 2007). It has been hypothesised that phagocytosis of a small number of sporozoites could trigger systemic immune signalling and other antiparasitic defences, such as lysis.

Several major players involved in phagocytosis in *An. gambiae* have been identified by RNAi and a semiquantitative *in vivo* assay (Moita et al., 2005). TEP1 is essential for promoting phagocytosis of gram-negative and gram-positive bacteria (Levashina et al., 2001; Moita et al., 2005). TEP1 opsonises bacterial surfaces in a TE-dependent manner, reminiscent of vertebrate complement factors. In contrast, LRIM1 has been demonstrated to be involved in phagocytosis of gram-negative not gram-positive bacteria (Moita et al., 2005). As LRIM1 and APL1C form an obligate complex, it can be assumed that APL1C is also important for gram-negative bacterial phagocytosis. Presumably, LRIM1/APL1C delivers TEP1_{cut} to the surface of gram-negative bacteria. It is not known whether TEP1 has a different partner for gram-positive bacteria. Other hemolymph proteins, TEP3 and TEP4, have also been implicated in efficient bacterial phagocytosis. TEP3 is involved with only gram-negative bacteria whereas TEP4 is important for both gram-types (Moita et al., 2005). Three intracellular molecules, CED2, CED5 and CED6, had a strong effect on phagocytosis of both gram-types. These CED proteins are homologues of components of the apoptotic and necrotic cell removal pathways in *C. elegans*. PGRP-LC, the transmembrane PRR of the Imd pathway, is important for gram-negative bacterial phagocytosis. Putative transmembrane receptors, lipoprotein receptor-related protein

(LRP) and β 2-integrin (BINT2), also affect bacterial phagocytosis of both gram-types and gram-negative bacteria, respectively. Finally, the Down syndrome cell adhesion molecule (Dscam), a hypervariable immunoglobulin-like transmembrane receptor, significantly affects phagocytosis of both gram-negative and gram-positive bacteria (Dong et al., 2006b).

Two partially redundant phagocytosis pathways have been proposed in *An. gambiae*, with each involving hemolymph proteins, transmembrane receptors and intracellular molecules (Blandin and Levashina, 2007; Moita et al., 2005). The pathways are named CED5 and CED6 after their main intracellular component. Epistasis experiments assigned TEP4, BINT2 and CED2 as putative components of the CED5 pathway (Moita et al., 2005). Likewise, TEP1, TEP3, LRIM1 and LRP are predicted to be in the CED6 pathway.

Cellular encapsulation is deployed against pathogens too large for engulfment, such as parasitoid eggs and nematodes (Clements, 2012; Michel and Kafatos, 2005). It involves aggregation of hemocytes around the invader to form a multi-layered capsule (Osta et al., 2004b). The invader is then isolated, immobilised and subsequently killed by asphyxiation, oxidation or the deposition of melanin. The mechanisms leading to cellular encapsulation are not well understood.

Local epithelial immunity

The mosquito's first line of defence against infection is the presence of structural barriers, such as the cuticle and the midgut (Meister et al., 2004). Barrier epithelia, such as the gut and reproductive tract, are constantly exposed to both indigenous and environmental microbes and are major potential routes of infection (Broderick et al., 2009). As well as being a physical barrier, epithelial cells mount powerful immune responses against microorganisms, such as secretion of AMPs. Local epithelial responses play an important role in the substantial loss of ookinetes during midgut invasion (Vlachou and Kafatos, 2005). Nevertheless, as barrier epithelia have to accommodate native microbiota, there must be a compromise between immune activation and tolerance (Broderick et al., 2009).

The peritrophic matrix is a thick acellular chitinous membrane that coats the luminal side of the midgut epithelium after blood ingestion (Whitten et al., 2006). Matrix components, such as chitin proteins and proteoglycans, are secreted by midgut epithelial cells during feeding and are polymerised within 24 h (Cirimotich et al., 2010; Meister et al., 2004). The peritrophic matrix is expelled after blood digestion and re-synthesised upon subsequent blood meals (Rodrigues et al., 2010). The matrix forms a physical barrier around the blood bolus, preventing midgut bacteria and

vertebrate blood cells from coming into direct contact with the epithelia. Nevertheless, malaria parasites have chitinases to digest the membrane and continue their journey through the mosquito (Clements, 2000).

Midgut epithelial cells play an active role in anti-*Plasmodium* defence by forming actin-based cytoplasmic protrusions during midgut invasion. It was reported that ookinetes emerging from the basal side of invaded midgut cells were covered by a specialised epithelial structure named a “hood” (Vlachou et al., 2004). The hood was thought to be an actin-based lamellipodia protrusion extended by the invaded cell to envelope the parasite. Previously, similar structures had been observed in the SUAF2 lytic refractory strain of *An. gambiae* (Vernick et al., 1995). In agreement with these findings, microarray analysis of midgut epithelial responses to *P. berghei* invasion discovered that the largest functional class upregulated encodes actin- and microtubule-cytoskeleton reorganisation proteins (Vlachou et al., 2005). Furthermore, silencing *WASP*, an important regulator of cytoskeleton dynamics, increases the intensity of *P. berghei* and *P. falciparum* infections (Mendes et al., 2008; Vlachou et al., 2005). It was therefore hypothesised that *WASP*-mediated cytoskeleton reorganisation contributes to *Plasmodium* killing. An independent study reported an “organelle-free actin zone” (AZ) at the base of midgut epithelial cells, partially surrounding dead or dying ookinetes in both susceptible and refractory mosquitoes (Shiao et al., 2006). In contrast to the previous reports, the AZ was reported to derive from epithelial cells adjacent to the invaded cell. Interestingly, AZ formation was associated with melanised parasites in the L3-5 refractory strain of *An. gambiae* and both were dependent on TEP1. Instead of parasite killing, these authors speculated that AZ formation was involved in clearance of dead or dying parasites.

An important mosquito defence is the production of ROS, which has been shown to modulate bacterial and *Plasmodium* infections (Molina-Cruz et al., 2008). ROS, such as superoxide anion and hydrogen peroxide, are generated as by-products of mitochondrial respiration or in response to pathogens (DeJong et al., 2007; Molina-Cruz et al., 2008). Production of ROS is massively increased in response to an uninfected blood meal and exacerbated further by *Plasmodium* infection (Kumar et al., 2003; Molina-Cruz et al., 2008). Hemocytes and epithelial cells both contribute to ROS generation. As ROS are highly reactive and toxic, insects protect themselves by producing detoxification enzymes, including superoxide dismutase (SOD), catalase and peroxidase (Clements, 2012). SOD converts superoxide anion into hydrogen peroxide, which is less toxic (DeJong et al., 2007). Both catalase and peroxidase convert hydrogen peroxide to water and oxygen. Detoxification enzymes are induced in midgut epithelial cells and fat body 24 h after blood feeding to reduce global ROS levels. However, as ROS are toxic to *Plasmodium*, catalase expression is specifically suppressed

in *P. berghei*-infected midguts, which keeps local hydrogen peroxide levels high and reduces parasite numbers (Molina-Cruz et al., 2008). Silencing *catalase* by RNAi significantly decreases *P. berghei* infection by lysis. Interestingly, L3-5 mosquitoes are in a chronic state of oxidative stress, which is intensified by blood feeding, resulting in increased ROS in the hemolymph and promoting melanisation (Kumar et al., 2003). This is probably due to a systemic deficiency in ROS detoxification. Dietary supplements of antioxidants in L3-5 can lower ROS levels and inhibit melanisation (Kumar et al., 2003). Mosquitoes with higher systemic ROS levels are also better at surviving bacterial infections (Molina-Cruz et al., 2008). ROS have also been shown to act as a signalling molecule in the JNK, NF- κ B and MAPK pathways (Jaramillo-Gutierrez et al., 2010; Surachetpong et al., 2011). Nevertheless, cumulative exposure to ROS is detrimental to mosquito fecundity and longevity, so there must be a trade-off between immunity and physiology (DeJong et al., 2007).

In a related defence mechanism, nitric oxide (NO), generated by NO synthase (NOS), also plays a role in anti-*Plasmodium* responses (Luckhart et al., 1998). Like ROS, NO is extremely toxic and reactive. Ookinetes induce tyrosine nitration in invaded midgut epithelial cells, which ultimately triggers apoptosis of these individual cells. NOS is induced in invaded midgut cells upon *P. berghei* and *P. falciparum* infection (Han et al., 2000; Luckhart et al., 1998). Parasite molecules, such as hemozoin and glycosylphosphatidylinositol (GPI), have been proposed to trigger this induction (Akman-Anderson et al., 2007; Lim et al., 2005). NOS generates NO, which is readily converted into nitrites and other reactive nitrogen species. After a short time delay, epithelial peroxidases are induced and these use nitrites and hydrogen peroxide to generate nitrogen dioxide, which mediates tyrosine nitration (Kumar et al., 2004; Oliveira Gde et al., 2012). Invaded cells, expressing elevated NO levels and undergoing extensive nitration, are “budded off” into the midgut lumen via a purse-string mechanism that maintains epithelial integrity (Han et al., 2000; Kumar et al., 2004). NO is important for limiting parasite infections and the administration of NOS inhibitors promotes parasite development (Luckhart et al., 1998). *Plasmodium* invasion is said to trigger a “time bomb” as the parasite has a limited opportunity to traverse the cell safely before nitrogen dioxide is produced (Han et al., 2000; Kumar et al., 2004). The observed lateral movement between epithelial cells might be a parasite escape strategy. In susceptible mosquitoes, the time delay between NOS and peroxidase induction allows many ookinetes to exit the epithelial cell before nitration takes place (Kumar et al., 2004). As hydrogen peroxide levels are constitutively higher in L3-5 mosquitoes, accelerated nitration might contribute to refractoriness. Upregulation of NOS has been implicated in natural refractoriness within *An. culicifacies* sibling species (Vijay et al., 2011). One exciting hypothesis is that epithelial nitration modifies or damages ookinetes, which facilitates their recognition by the mosquito complement-like system and promotes TEP1-mediated lysis (Oliveira

Gde et al., 2012). Furthermore, the STAT pathway, via AgSTAT-A, has been reported to activate NOS transcription and mediate a late-phase antiparasitic response, which reduces the survival of early oocysts (Gupta et al., 2009). In addition to antagonising *Plasmodium* infections, NO is crucial for hemocyte-mediated immune responses against bacteria (Hillyer and Estevez-Lao, 2010).

Finally, the mosquito midgut microbiota plays a key role in activating epithelial immunity and limiting *Plasmodium* infections. Mosquito guts harbour a diverse community of commensal bacteria encompassing a variety of genera and species (Dong et al., 2009). Gram-negative bacteria of the class *Proteobacteria* and family *Enterobacteriaceae* are most predominant (Cirimotich et al., 2011b). Common genera include *Enterobacter*, *Microbacterium*, *Sphingomonas*, *Serratia*, *Chryseobacterium*, *Asaia* and *Pseudomonas* (Dong et al., 2009). These endogenous bacteria are involved in the maintenance of host physiology, including metabolism and immune homeostasis. Blood feeding causes dramatic proliferation of the midgut microbiota, apparently due to the increase in nutrient availability (Cirimotich et al., 2010; Kumar et al., 2010). Bacterial levels can rise to 10^7 colony-forming units (CFU) per mL of blood by 24 h post blood feeding, returning to normal within 3 to 5 days (Cirimotich et al., 2010; Wang et al., 2011). Bacterial species composition changes drastically after blood feeding as well as between larvae, pupae and adults (Wang et al., 2011). Interestingly, bacterial load and species composition varies considerably between individual mosquitoes, which might contribute to susceptibility and refractoriness to *Plasmodium* infection (Cirimotich et al., 2010). For instance, gram-negative bacteria usually inhibit parasite development more strongly than gram-positive bacteria.

Gut bacteria can indirectly affect *Plasmodium* infections by priming the basal immune response. Mosquitoes cleared of their natural microbiotic flora by antibiotics are more susceptible to *Plasmodium* infections (Dong et al., 2009; Meister et al., 2009). This can be reversed by re-introducing bacteria into antibiotic-treated mosquitoes. Co-feeding bacteria and *P. falciparum* parasites reduces oocyst numbers, suggesting the inhibitory effect occurs before the oocyst stage (Dong et al., 2009). The mosquito immune response constitutively controls bacterial load in the midgut. Besides defending against systemic bacterial infections, PGRP-LC signalling controls the size of midgut bacterial populations, including their proliferation after blood feeding (Meister et al., 2009). This signalling modulates infections with *P. berghei* and field isolates of *P. falciparum*. Silencing *PGRP-LC* increases *P. berghei* and *P. falciparum* oocyst intensities, but only in the presence of normal midgut flora. Known *Plasmodium* effectors, such as TEP1, are elevated in control mosquitoes compared to antibiotic-treated mosquitoes (Dong et al., 2009). The majority of mosquito immune responses are active against both bacteria and parasites, so it is unsurprising that

responses mounted against endogenous bacteria can modulate *Plasmodium* infections (Cirimotich et al., 2010). Furthermore, particular midgut bacterial isolates have been shown to reduce susceptibility to dengue virus in *Ae. aegypti* by activating the mosquito immune system (Ramirez et al., 2012). It has been proposed that the mosquito's basal immune response is primed by previous encounters with bacteria, even as larvae. A recent study described a mechanism of innate immune memory in adult mosquitoes involving bacteria-mediated hemocyte differentiation (Rodrigues et al., 2010). Bacterial exposure triggered an increase in granulocytes that persisted for the mosquito's life span and enhanced antibacterial responses upon re-challenge. This immune priming indirectly suppressed *Plasmodium* development.

To prevent the proliferation of midgut bacteria after blood feeding from over-stimulating epithelial immunity, a cross-linked protein network is formed between the peritrophic matrix and midgut epithelial cells (Kumar et al., 2010). Dityrosine bonds are catalysed by immunomodulatory peroxidase (IMPer), which is secreted by epithelial cells in response to blood feeding, and dual oxidase (Duox), a transmembrane protein that produces hydrogen peroxide. The dityrosine network renders the gut less permeable to soluble immune elicitors and prevents activation of epithelial immunity. This shields the midgut microbiota from antibacterial responses but also protects *Plasmodium* parasites by preventing NOS induction. Immune responses are only elicited when parasites breach the peritrophic matrix and the dityrosine barrier. Silencing *IMPer* or *Duox* strongly elicits NOS production and dramatically reduces parasite survival.

Gut bacteria have also been shown to directly interfere with *Plasmodium* development. In a recent study, an *Enterobacter* species was isolated from wild Zambian mosquito populations (Cirimotich et al., 2011a). When introduced into laboratory-reared *An. gambiae* and *An. stephensi*, this bacterium rendered mosquitoes almost refractory to *P. falciparum* development. This was independent of the mosquito Imd pathway as knockdown of *PGRP-LC*, *Imd* or *REL2* failed to rescue parasite development. It was elucidated that the *Enterobacter* species was directly inhibiting parasite development in the mosquito midgut lumen by generating ROS. Furthermore, bacterial proliferation after blood feeding has been proposed to stimulate NOS induction in the midgut (Luckhart et al., 1998). Commensal bacteria may also prevent parasite interactions with the mosquito epithelium, such as physically blocking receptors for invasion (Cirimotich et al., 2011b).

Wolbachia, an intracellular bacterial symbiont of many insects, has been stably introduced into *Ae. aegypti* and inhibits infections with *Plasmodium*, dengue, CHIKV and filarial nematodes (Bian et al., 2010; Hoffmann et al., 2011; Kambris et al., 2009; Moreira et al., 2009; Walker et al., 2011). The disease vectors *Ae. aegypti* and *Anopheles* species do not naturally harbour *Wolbachia* (Moreira et

al., 2009). In stably infected *Ae. aegypti*, *Wolbachia* primes the immune response by inducing constitutive upregulation of immune genes, such as TEPs, CLIPs and PGRPs (Kambris et al., 2009). Transient somatic *Wolbachia* infections of *An. gambiae* have shown comparable effects, including induction of *TEP1* and *LRIM1* (Kambris et al., 2010) and inhibition of *P. falciparum* infections (Hughes et al., 2011). *Wolbachia* has been proposed as a novel malaria control strategy, especially as infections can shorten the mosquito life span (McMeniman et al., 2009). However, *Wolbachia* has yet to be stably introduced into *An. gambiae*, which remains a significant hurdle to overcome.

The LRIM family

Bioinformatic searches discovered a novel mosquito-specific family of proteins related to LRIM1 and APL1C, using their shared structural features (Povelones et al., 2009; Waterhouse et al., 2010). To date, 24 members of this LRR immune protein (LRIM) family have been identified in *An. gambiae* (Table 1.1). Orthologues of most LRIMs and additional homologous proteins were discovered in the available genomes of mosquitoes, *Ae. aegypti* and *C. quinquefasciatus*, which have 29 and 30 LRIMs, respectively (Waterhouse et al., 2010). However, no LRIM-related genes were found in other organisms, including *Drosophila*, the honeybee and body louse. Each LRIM member shares a distinct genomic organisation and protein domain architecture, which distinguishes them from the larger superfamily of LRR genes. The majority of LRIM genes are composed of a small exon and intron followed by a larger exon encoding most of protein. Typical LRIM proteins comprise a signal peptide, LRR motifs, a conserved pattern of cysteines and a coiled-coil domain. LRR domains are often involved in pattern recognition whereas coil-coils are generic protein-protein interaction domains. Both the LRR domain and coiled-coil can tolerate high levels of sequence variation, which makes them flexible in their binding properties but hinders the discovery of ancestral LRIM-like genes in other organisms (Povelones et al., 2009; Waterhouse et al., 2010). The LRIM members have been grouped into four subfamilies based on variations to this core structure (Figure 1.9, Table 1.1). Two of these subfamilies are classified by the number of LRR domains: Long (10 to 13 LRRs) and Short (6 or 7 LRRs). There are 6 Long LRIMs, including LRIM1 and APL1C, and 9 Short LRIMs in *An. gambiae*. Transmembrane LRIMs, with 3 members in *An. gambiae*, contain a C-terminal transmembrane region and are predicted to be membrane localised with the majority of the protein extracellular. In Transmembrane LRIMs, one of the cysteines in a conserved cysteine pair has been substituted with a tyrosine. Coil-less LRIMs possess all the characteristic LRIM features but lack the coiled-coil domain, which may affect how these proteins are organised into complexes and interact with other proteins.

There are 6 Coil-less LRIMs in *An. gambiae*. Apart from Transmembrane LRIMs, the other subfamilies are believed to be secreted into the hemolymph.

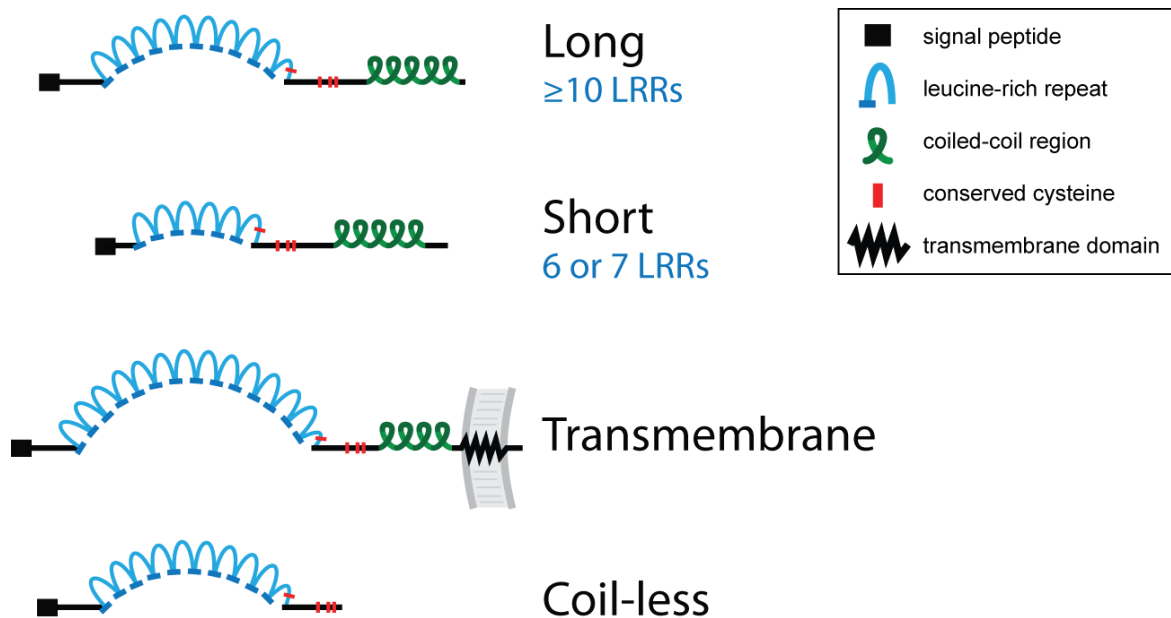


Figure 1.9 The four LRIM subfamilies.

A typical LRIM family member is comprised of a signal peptide, leucine-rich repeat (LRR) motifs, a conserved pattern of cysteine residues and a coiled-coil domain. The coiled-coil domain is often split into two parts. The family is divided into four subfamilies with different variations of this typical structure. The Short LRIMs have 6 or 7 LRR motifs whereas the long LRIMs have 10 to 13. Transmembrane LRIMs have a C-terminal transmembrane region and one cysteine in a conserved cysteine pair has been replaced with a tyrosine. Coil-less LRIMs lack the C-terminal coiled-coil domain but meet all the other LRIM selection criteria. Adapted from Waterhouse et al., 2010.

Table 1.1 The LRIM family in *An. gambiae*.

Subfamily	Gene ID or genomic location	LRIM name	Alternative name(s)
Long	AGAP006348	LRIM1	
	AGAP007036	APL1A	APL1, LRIM2
	AGAP007035	APL1B	APL1, LRIM2
	AGAP007033	APL1C	APL1, LRIM2, LRRD19
	AGAP007037	LRIM3	
	AGAP007039	LRIM4	LRRD5
Short	2R:17513769-4965	LRIM5	
	AGAP006327	LRIM6	
	AGAP007457	LRIM7	LRRD17
	AGAP007454	LRIM8A	
	AGAP007456	LRIM8B	LRRD4, LRRd-1
	AGAP007453	LRIM9	
	AGAP007455	LRIM10	LRRD9
	AGAP007034	LRIM11	
Transmembrane	AGAP005496	LRIM12	
	AGAP007045	LRIM15	
	3R: 317336-9560	LRIM16A	AGAP007758
Coil-less	3R: 322657-4842	LRIM16B	AGAP007758
	AGAP005693	LRIM17	APL2, LRRD7
	AGAP010675	LRIM18	
	AGAP011117	LRIM19	
	AGAP002542	LRIM20	
	AGAP005744	LRIM26	
	2R: 17512465-3625	LRIM27	

The LRIM family in *An. gambiae* currently has 24 members, each belonging to one of four subfamilies: Long, Short, Transmembrane and Coil-less. Adapted from Povelones et al., 2009 and Waterhouse et al., 2010. Refer to these papers for references of alternative names.

The LRR is a structural motif of 20-30 amino acids with a distinctive consensus sequence rich in hydrophobic leucine residues (Bella et al., 2008). This 11-residue sequence is typically $LxxLxLxxNxL$ (where x is any amino acid), although leucine and asparagine residues can be replaced with other hydrophobic residues. Most LRIM LRRs are 24 amino acids in length, although some LRIMs have an unusually short 19-residue LRR (Waterhouse et al., 2010). An LRR domain is composed of two or more repeats in tandem and forms a curved solenoid or “horseshoe” shape. This versatile shape has a high surface area that is ideal for protein-protein interactions (Kobe and Kajava, 2001; Padmanabhan et al., 2009). LRIMs with many LRR motifs are predicted to form extended arcs whereas Short LRIMs are likely to have shallow curves (Waterhouse et al., 2010). The concave side of an LRR domain is usually a parallel β -sheet, with each LRR motif providing a single strand (Bella et al., 2008). The convex side is composed of various secondary helical structures, including α -helices and polyproline II helices. Ligand binding sites are typically found on the concave surface, with some LRR

proteins able to interact with multiple structurally unrelated ligands (Bell et al., 2003). LRR domains are typically flanked by N- and C-terminal structures called “caps”, which protect the hydrophobic core (Bell et al., 2003; Kobe and Kajava, 2001). In extracellular proteins, these flanking regions are often cysteine-rich and form stabilising intramolecular disulphide-bonds (Bella et al., 2008; Buchanan and Gay, 1996). Most LRIMs have a leucine-rich leader sequence that precedes the LRR domain (Waterhouse et al., 2010).

Proteins with LRR domains have known roles in host defence in many phyla and mediate recognition of a diverse array of PAMPs. Mammalian innate immunity uses LRR-containing extracellular Toll-like receptors (TLRs) and intracellular Nod-like receptors (NLRs) to mediate pathogen recognition (Istomin and Godzik, 2009; Sirard et al., 2007). The LRR domains of different TLRs specifically interact with a vast range of ligands, including bacterial flagellin, LPS and peptidoglycan (Bell et al., 2003). Activation of TLRs and NLRs results in inflammatory responses (Wilmanski et al., 2008). Insect Toll transmembrane receptors, which are critical for intracellular immune signalling, also contain extracellular LRRs but do not directly interact with PAMPs (Christophides et al., 2002). LRR-containing proteins are also crucial in plant host defence. Plant NB-LRRs function analogously to the mammalian adaptive immune system by recognising specific pathogen-encoded effectors (Padmanabhan et al., 2009). Jawless vertebrates, such as lamprey and hagfish, possess a repertoire of variable lymphocyte receptor (VLR) antibodies generated by combinatorial assembly of LRR gene segments (Guo et al., 2009; Han et al., 2008; Herrin et al., 2008). Like LRIM1/APL1C, VLR antibodies are secreted as disulphide-bonded multimeric complexes (Herrin et al., 2008).

Structure-function analyses recently elucidated that LRIM1 and APL1C have a distinct modular organisation (Figure 1.10) (Povelones et al., 2011). The LRIM1/APL1C crystal structure and *in vitro* mutational analyses revealed that the conserved cysteines are important for heterodimer formation (Baxter et al., 2010; Povelones et al., 2011). Homologous cysteines in LRIM1 and APL1C form a single disulphide bond to stabilise the complex. This bond might also act as a hinge to release TEP1 at pathogen surfaces (Povelones et al., 2011). Additional conserved cysteines form two intramolecular disulphide bonds that are probably involved in protein folding and maybe even formation of a C-terminal cap. LRIM1 and APL1C are not secreted upon mutation of any of these additional cysteines. The coiled-coil regions of LRIM1 and APL1C are essential for the complex to interact with TEP1 and other TEP cargoes. Both LRIM1 and APL1C have coiled-coil regions split into two parts. The most C-terminal part of the coiled-coil also plays a role in regulating the specificity of LRIM1/APL1C heterodimerisation. The function of the LRR domain is still undetermined but it is hypothesised to be

involved in activation of LRIM1/APL1C/TEP complexes. The LRR domain may directly recognise pathogen surfaces or it may interact with other immune receptors.

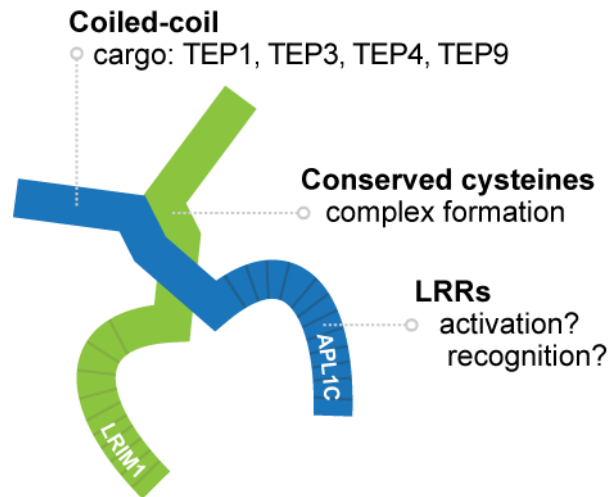


Figure 1.10 Functional modules of the LRIM1/APL1C complex.

LRIM1 and APL1C are believed to contain three distinct modules. The coiled-coil domain is required for interaction with effector proteins, such as TEP1, TEP3, TEP4 and TEP9. The conserved cysteine residues form a disulphide bond to stabilise the LRIM1/APL1C complex and intramolecular bonds to ensure correct protein folding. The LRR domain is predicted to function in pathogen recognition and activation of the LRIM1/APL1C/TEP complex. From Povelones et al., 2011.

Many LRIMs have 1:1:1 orthologues in *An. gambiae*, *Ae. aegypti* and *C. quinquefasciatus* (Figure 1.11) (Povelones et al., 2009). Interestingly, several LRIMs are encoded within tight genomic clusters. Comparison of orthologous genomic regions between the three sequenced mosquitoes has revealed evidence of local gene shuffling and duplication (Waterhouse et al., 2010). A cluster of Short LRIMs found in all three mosquitoes comprises *LRIM7*, *LRIM8*, *LRIM9* and *LRIM10*. *LRIM8* has duplicated in *An. gambiae* (*LRIM8A* and *LRIM8B*) whereas *LRIM10* has duplicated in *Ae. aegypti* (*LRIM10A* and *LRIM10B*). In *An. gambiae*, *APL1A*, *APL1B* and *APL1C* were previously annotated as a single gene (*APL1* or *LRIM2*) (Riehle et al., 2006) but are actually three distinct genes derived from recent duplications (Riehle et al., 2008). There are also three *LRIM2* genes in *C. quinquefasciatus* but only one in *Ae. aegypti* (Povelones et al., 2009). *An. gambiae* *APL1A*, *APL1B* and *APL1C* cluster with *LRIM3* and *LRIM11* on chromosome 2L, in close proximity to *LRIM4*. This synteny is partially retained in *Ae. aegypti* and *C. quinquefasciatus*. *LRIM16* has duplicated in *An. gambiae* and *LRIM16A* and *LRIM16B* are clustered together on chromosome 3R.

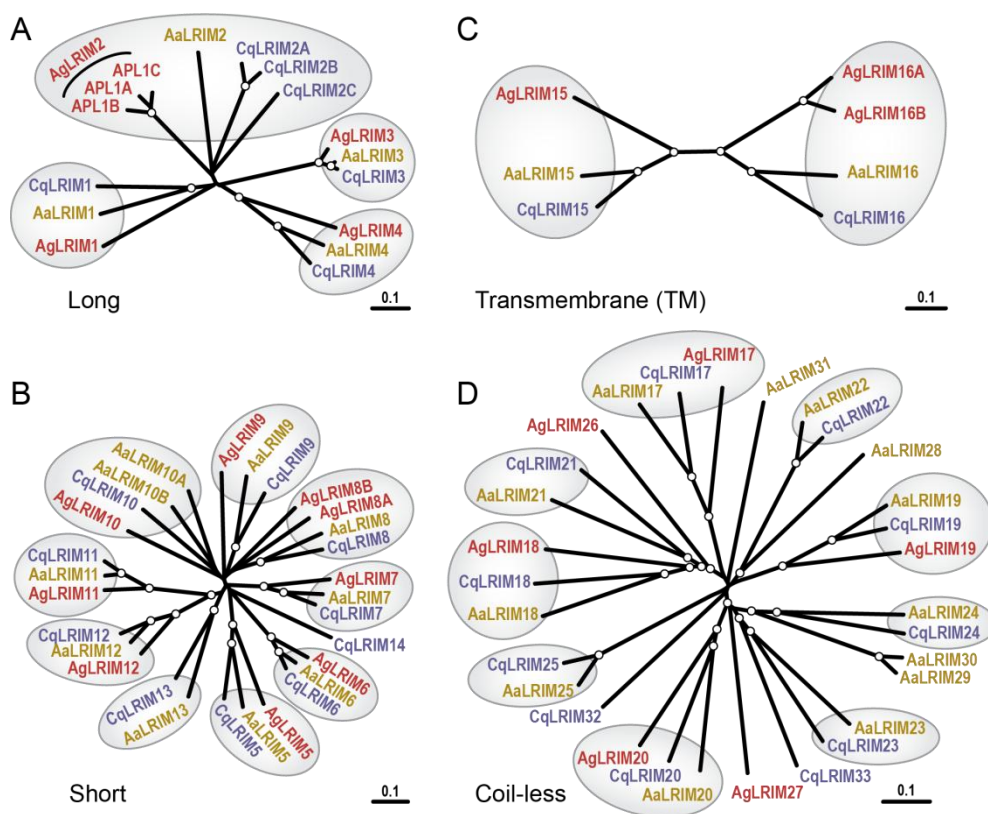


Figure 1.11 Phylogenetic relationships between LRIMs in three mosquito species.

Phylogenetic trees demonstrating the relationships between LRIM family members in *An. gambiae* (Ag, red), *Ae. aegypti* (Ae, yellow) and *C. quinquefasciatus* (Cq, blue). Long (A), Short (B), Transmembrane (C) and Coil-less (D) subfamilies are shown. Predicted orthologous groups are shown in shaded ovals. White dots indicate bootstrap values of >70%. From Povelones et al., 2009.

We hypothesise that the LRIM family has diversified to recognise different microbes that mosquitoes encounter, including human pathogens. It is unclear whether the LRIM family represents an adaptation to the hematophagous lifestyle of mosquitoes. With their versatile LRR domains, LRIMs are predicted to be pathogen recognition proteins. Apart from LRIM1 and APL1C (members of the Long subfamily), the other LRIM members have not been well characterised to date. Preliminary analyses have implicated certain LRIMs in innate immunity, as discussed further in Chapter 4 (Aguilar et al., 2005b; Dong et al., 2006a; Marinotti et al., 2005; Mitri et al., 2009; Vlachou et al., 2005). It is not known whether these LRIMs function in the same biochemical cascade as LRIM1/APL1C and TEP1 or if they have unique specificity and protein partners. Meta-analysis of all extant microarray data suggests some family members are transcriptionally co-regulated and present in clusters distinct from LRIM1, APL1C and TEP1 (Maccallum et al., 2011).

Chapter 2: Aims and Objectives

2 Aims and Objectives

The overall aim of this PhD thesis was to investigate the role of the LRIM family in *An. gambiae* immunity. This is a mosquito-specific family that is hypothesised to be involved in defence against blood-borne pathogens. The founding members, LRIM1 and APL1C, form a heterodimer and play important roles in defence against *Plasmodium* parasites and bacteria (Garver et al., 2012; Moita et al., 2005; Osta et al., 2004a; Riehle et al., 2006). However, the other 22 LRIMs in *An. gambiae* were largely uncharacterised at the start of this project. The reason for the huge expansion of LRIMs in mosquitoes was unknown and it was unclear whether different LRIMs function specifically against distinct pathogens.

The first objective was to transcriptionally profile all LRIMs to determine their responses to various immune challenges, including blood feeding and infections with *Plasmodium*, bacteria, fungi and virus. There is known to be a correlation between gene expression and protein function, although this is not true for all genes. Therefore, this profiling would determine whether there is transcriptional specificity in the family towards different pathogens and provide important clues to the immune function of the LRIMs. If certain LRIMs are transcriptionally co-regulated, this could highlight novel functional relationships or interactions. The next aim was to silence uncharacterised LRIMs using RNAi and investigate the resulting phenotypes during infections with the rodent malaria parasite, *P. berghei*. This simple screen would identify novel *Plasmodium* antagonists in the family, similar to LRIM1 and APL1C.

The next objective was to biochemically and phenotypically characterise interesting candidates from the transcriptional and RNAi screens to provide further insights into their function in *An. gambiae* immunity. This would include investigating their roles in melanisation and during bacterial infections. Another objective was to investigate whether formation of LRIM complexes (similar to the LRIM1/APL1C heterodimer) is a general characteristic of LRIM family members and which structural features govern complex formation. A representative from each LRIM subfamily would be expressed in insect cell lines to monitor expression levels, protein mobility and complex formation. If LRIM complexes are identified, mutational analyses would be performed to identify the amino acid residues responsible for complex formation. Furthermore, antibodies would be raised against the most promising candidate LRIMs to investigate their behaviour in the mosquito hemolymph after different immune challenges.

The final objective was to attempt to identify other mosquito proteins interacting with candidate LRIMs. This would indicate whether these LRIMs function in known immune pathways. In particular,

as the LRIM1/APL1C complex interacts with the complement C3-like effector TEP1 (Fraiture et al., 2009; Povelones et al., 2011; Povelones et al., 2009), it was planned to investigate whether any other LRIMs are linked to the mosquito complement-like system.

Chapter 3: Materials and Methods

3 Materials and Methods

3.1 Mosquito experiments

Mosquito rearing

An. gambiae (susceptible strains Ngousso, Yaoundé, G3 and Keele and refractory strain L3-5) adult mosquitoes were maintained as previously described (Sinden et al., 2002). G3 is a long-term laboratory strain that was colonised from field collections in The Gambia in 1975 and L3-5 was selected from G3 (Collins et al., 1986). The Keele strain was produced in 2005 at Keele University, UK, by interbreeding four strains of *An. gambiae* (Hurd et al., 2005). Yaoundé was established from the Yaoundé region of Cameroon in 1988 (Tchuinkam et al., 1993). Ngousso was colonised in 2006 from the urbanised Ngousso district of Yaoundé, Cameroon (Boissiere et al., 2012). As the most recently colonised strain, Ngousso was used for the majority of experiments, unless mentioned otherwise. Briefly, adult mosquitoes were maintained at 28 °C, 80% humidity in a 12 h light/dark cycle and provided with 10% sugar solution. For gene knockdown experiments, mosquitoes were used 0-2 days after emergence. Mosquitoes were 3-6 days old at the time of blood feeding. For experimental purposes, mosquitoes were kept in netted pots of 60-80 mosquitoes.

RNAi-mediated gene silencing

Female mosquitoes were anaesthetised under carbon dioxide (CO₂) and injected intrathoracically with dsRNA using a Nanoject II injector (Drummond Scientific). For single gene knockdown experiments, mosquitoes were injected with 69 nL dsRNA at 3 µg/µL. *GFP* (non-specific dsRNA) and *LRIM1* were used as negative and positive controls, respectively. To knockdown two genes simultaneously (“double knockdowns”), 138 nL of pooled dsRNA was injected per mosquito and controls were injected with 138 nL of *dsGFP*. Knockdown efficiency was monitored by quantitative real-time PCR (qRT-PCR) 4-5 days post injection.

Hemolymph collection

Prior to hemolymph collection, mosquitoes were briefly anaesthetised using CO₂ and kept on ice. Groups of 10 mosquitoes were positioned with their ventral side up on a glass plate chilled on ice. Fine scissors were used to cut the proboscis of all 10 mosquitoes. Forceps were used to gently squeeze the thorax and a clear drop of hemolymph was collected by capillary action into a pipette tip containing 5 µL 2X non-reducing Lane Marker sample buffer (Pierce) and transferred immediately to an Eppendorf tube. Hemolymph was collected from between 20-90 mosquitoes per group and the final sample volume was adjusted to 1 mosquito/µL (or 1.5 mosquitoes/µL for CLIPA8 western blots

to increase protein abundance). For gene knockdown experiments, hemolymph was collected 4 days after dsRNA injection. Hemolymph was snap frozen on dry ice and stored at -80 °C prior to analysis.

Uninfected blood feeding

After being deprived of sugar for 2-6 h, female mosquitoes were permitted to feed on a terminally anaesthetised uninfected (“naïve”) Theiler’s original (TO) or CD1 mouse (Harlan, UK). Non blood fed mosquitoes were removed between 3 and 48 h, when the blood meal is visible through the abdominal cuticle.

For human blood feeding, an artificial membrane feeding system was utilised. Briefly, compacted human red blood cells were washed twice with phosphate buffered saline (PBS) and resuspended in human AB serum at a 1:1 ratio. Perspex membrane feeders were warmed to 37 °C via connection to a water bath. Parafilm was stretched across the bottom of the feeders to provide a compartment for introduction of human blood with a 24 Gauge blunt needle (500 µL per feeder). Each feeder was rested on top of a pot of mosquitoes and they were allowed to feed for 30 min.

***P. berghei* infection**

Female mosquitoes were allowed to feed on a mouse infected with the *P. berghei* CON_{GFP} strain (a transgenic parasite constitutively expressing GFP (Franke-Fayard et al., 2004)), as previously described (Osta et al., 2004a). An uninfected (naïve) mouse was used as a control. Infected and control mosquitoes were stored at 19 °C, the optimum temperature for *P. berghei* development.

For gene knockdown experiments, mosquitoes were infected with *P. berghei* 3-4 days after dsRNA injection and parasite load was quantified 7-10 days later. Midguts were dissected into PBS, fixed in 4% formaldehyde for 30-60 min, washed three times in PBS and mounted on glass slides in Vectashield (Vector Labs). Live oocysts and melanised ookinetes were counted by direct microscopic observation using a Leica DMR microscope. Photographs were taken with a Zeiss digital camera and AxioVision software. Both infection intensity and prevalence (the percentage of guts with at least one oocyst or melanised parasite) were analysed.

***P. yoelii* infection**

As described for *P. berghei*, female mosquitoes were allowed to feed on mice infected with the transgenic GFP-*P. yoelii yoelii* 17X strain (Ono et al., 2007). Infected mosquitoes were stored at 25 °C, along with control mosquitoes fed on uninfected blood.

***P. falciparum* infection**

Female G3 mosquitoes were fed on *P. falciparum* gametocyte cultures (NF-54 strain) using an artificial membrane feeding system, as previously described (Jaramillo-Gutierrez et al., 2009), by Dr Alvaro Molina-Cruz at the NIH. Mosquitoes were fed on the same blood without gametocytes as a control. Infected and control mosquitoes were stored at 27 °C.

Fungal spore challenge

B. bassiana spores were extracted from 3-week old cultures on malt agar plates, washed, resuspended and quantified by Dr Fanny Turlure (as described in Fanny Turlure, PhD thesis, 2010). The stock of *B. bassiana* spores was stored at -80 °C and, on the day of each experiment, it was serially diluted in PBS so that 69 nL would equate to 100 spores. Female mosquitoes were injected intrathoracically with 69 nL of the spore dilution. For the fungal time courses, control mosquitoes were injected with sterile PBS and uninjected mosquitoes were used as “time zero”.

Bacterial infections

Ampicillin-resistant *E. coli* OP-50 and tetracycline-resistant *S. aureus* were cultured overnight in Luria-Bertani (LB) broth at 37 °C. Overnight cultures were re-cultured at 1/50 or 1/100 dilution (for *S. aureus* and *E. coli*, respectively) for 2-3 h until the optical density at 600 nm (OD₆₀₀) reached 0.7-0.8, which is indicative of logarithmic growth phase. Harvested cells were washed three times with sterile PBS and then resuspended in PBS to give an OD₆₀₀ of 0.4 (Schnitger et al., 2009). Female mosquitoes were injected with 69 nL of this final bacterial suspension (approximately 10,000-20,000 bacteria per mosquito). Bacterial viability was confirmed by plating onto agar at 1/10,000 dilution and incubating at 37 °C overnight (30-100 colonies expected). For bacterial time courses, control mosquitoes were injected with sterile PBS and uninjected mosquitoes were used as “time zero”.

Injection of bioparticles

Bioparticles are heat- or chemically-killed bacteria, usually fluorescently labelled, which can be used to provoke an immune response without the complication of bacterial proliferation. *E. coli* (K-12 strain) and *S. aureus* (Wood strain, without protein A) fluorescein-labelled bioparticles (Invitrogen) were resuspended in sterile PBS to 20 mg/mL. Female mosquitoes were intrathoracically injected with 69 nL of bioparticle suspension (equating to approximately 400,000 bioparticles).

Bacterial proliferation assay

Female mosquitoes were injected with dsRNA and, 4 days later, were inoculated with 69 nL viable ampicillin-resistant *E. coli* (OD₆₀₀ of 0.4). After 24 h, three to five batches of 10 mosquitoes per dsRNA treatment were surface-sterilised with 70% ethanol, washed twice with sterile PBS,

homogenised and plated on ampicillin-agar at 1/10 dilution. After an overnight incubation at 37 °C, colonies were counted and CFU per mosquito calculated. This protocol was adapted from Schnitger et al., 2009. As controls, 10 mosquitoes from each dsRNA-treatment were not injected with bacteria and were surface-sterilised and plated to check for bacterial contamination.

Bacterial survival assay

4 days after injection of dsRNA, female mosquitoes were inoculated with 69 nL viable ampicillin-resistant *E. coli* (OD₆₀₀ of 0.4). The number of dead mosquitoes was monitored daily for 10 days. In one experiment, mosquitoes were blood fed on a naïve mouse 24 h prior to bacterial inoculation.

Antibiotic treatment

Newly emerged mosquitoes were treated daily with a cocktail of antibiotics (10 U/mL penicillin, 10 µg/mL streptomycin and 15 µg/mL gentamicin) in their 10% sugar solution for 4 days prior to blood feeding. To test the efficacy of antibiotic treatment, cohorts of 5 mosquitoes were collected after 5 days of treatment, surface-sterilised in 70% ethanol and rinsed in sterile molecular biology grade water. Mosquitoes were homogenised in LB broth, plated at 1/100 dilution onto LB agar and incubated at 27 °C for 2 days.

Phenoloxidase activity assay

Genes of interest were silenced by RNAi in female mosquitoes 4 days prior to the assay. 1 mL of overnight cultures of *E. coli* and *S. aureus* were pelleted and washed twice with 1X PBS. Pellets were resuspended in PBS and suspensions were diluted to OD₆₀₀ of 0.5. Equal volumes of *E. coli* and *S. aureus* suspensions were mixed together and 69 nL injected into at least 90 mosquitoes per gene knockdown. After 4-5 h, hemolymph was collected from 90 mosquitoes per gene knockdown into 45 µL PBS supplemented with 2X protease inhibitors without EDTA (Roche). Each hemolymph sample was divided into 5 µL and 40 µL portions for protein quantification and the phenoloxidase assay, respectively. Samples were snap frozen and stored at -80 °C; they were used immediately after thawing. Each hemolymph sample was quantified using the Coomassie Plus (Bradford) Assay kit (Thermo Scientific) and the manufacturer's Micro Microplate Protocol (working range = 1-25 µg/µL). The samples were adjusted to equal protein concentration in a total volume of 40 µL and the same volume of hemolymph collection buffer was used for a blank. In a 96-well plate, the 40 µL samples were mixed with 120 µL of 3 mg/mL L-3,4-dihydroxyphenylalanine (L-DOPA). The assay plate was covered with foil and OD₄₉₀ was read immediately at kinetic intervals of 10 min for a total of 90 min. This assay measures dopachrome production by phenoloxidase.

Tissue melanisation assay

Female mosquitoes were injected with dsRNA and were allowed to feed on an anaesthetised naïve mouse 3 days later. Approximately 24 h post blood feeding, mosquito thoraxes were pricked multiple times with a sterile needle. The needle was sterilised with 70% ethanol between each mosquito. Live mosquitoes were examined for tissue melanisation 24 h after injury. To this end, mosquitoes were anaesthetised using CO₂ and immobilised by removal of their wings and legs. Immobilised mosquitoes were lined up on their sides on a glass slide and a large coverslip was secured on top using adhesive putty. Thoraxes were observed using a Leica DMR microscope and photographs were taken with a Zeiss digital camera and AxioVision software. This protocol was adapted from Schnitger et al., 2007.

Viral challenge

ONNV infectious clones (5'-ONNVic-eGFP) were produced by Dr Joanna Waldock from African green monkey kidney (VERO) cells (Waldock et al., 2012). VERO cells were grown in Minimum Essential Medium (MEM) supplemented with 10% fetal bovine serum (FBS), L-glutamine, non-essential amino acids, penicillin/streptomycin and fungizone (amphotericin B). Second passage 5'-ONNVic-eGFP (1.73×10^8 plaque-forming units (PFU)/mL) was used for the viral time courses. For viral injection, female mosquitoes were injected with 69 nL of virus (11,937 PFU/mosquito) and control mosquitoes were injected with conditioned media from uninfected VERO cells. For blood feeding, 69 µL of virus was mixed with 465.5 µL human red blood cells and 465.5 µL human AB serum and female mosquitoes were fed using a membrane feeder. Assuming a mosquito ingests 1 µL during a blood meal, each mosquito was infected with the same viral titre as via injection. Control mosquitoes were fed on uninfected blood from the same batch. Untreated mosquitoes were used for “time zero”. Virally infected mosquitoes were double-contained in a 28 °C incubator to prevent escape. After 6 days, entire guts from remaining ONNV blood fed mosquitoes were dissected to determine infection prevalence. Standard plaque assays were performed on individual mosquitoes 6 days after ONNV injection to determine viral titre, as described in Waldock et al., 2012.

Mosquito fecundity experiment

Upon emergence, mosquitoes were permitted to mate in a large cage for 3 days before being injected with dsRNA. Female mosquitoes were fed on an anaesthetised naïve mouse 3 days after injection. After 48 h, a random sample of mosquitoes was dissected to examine blood meal digestion and ovary development. 72 h after blood feeding, individual females were carefully placed in 50 mm petri dishes on top of wet filter paper (0.1% salt water). They were stored in darkness at 27 °C for 24 h to encourage oviposition. Female mosquitoes were then removed and the number of eggs laid was

counted by direct observation under a dissecting microscope. The egg dishes were half-filled with 0.1% salt water, dusted with fish food and returned to 27 °C for 3 days to allow hatching. Gentle movement of the dishes and the addition of drops of salt water were used to encourage hatching. Larvae were counted by direct observation under a dissecting microscope.

3.2 Molecular biology techniques

dsRNA synthesis

Primers were designed for 150-500 bp regions of each gene of interest, with 5' T7 promoter sequences, using the e-RNAi online software (Horn and Boutros, 2010). Primer sequences are shown in Appendix Table 9.1. RNAi probes were checked to ensure no significant sequence homology with other *An. gambiae* genes. Gene fragments were amplified by Polymerase Chain Reaction (PCR) using *An. gambiae* cDNA or plasmid template and purified using the QIAquick PCR Purification kit (Qiagen). The amplicons were analysed by agarose gel electrophoresis and NanoDrop (Thermo Scientific) to verify size and concentration, respectively. dsRNA was synthesised from the gene fragments using the MegaScript T7 kit (Ambion), according to manufacturer's guidelines. dsRNA was purified using the RNeasy Mini kit (Qiagen), eluting twice in 30 µL RNase-free water, and adjusted to 3 µg/µL. Purified dsRNA was stored at -80 °C until use.

RNA extraction and cDNA synthesis

Total RNA was extracted from 10 whole mosquitoes collected per sample and the TRIzol Reagent (Invitrogen) was used, according to manufacturer's instructions. Briefly, mosquitoes were homogenised in 200 µL TRIzol before a further 800 µL TRIzol was added (1 mL total volume). After removing debris by centrifugation, 200 µL chloroform was added to extract RNA from genomic DNA and protein. RNA was precipitated using 480 µL isopropanol. The RNA pellet was washed with 70% ethanol and resuspended in 90 µL RNase-free water. Total RNA was treated with DNase using Turbo DNA-free kit (Ambion) to remove genomic DNA contamination. cDNA was synthesised from 1 µg RNA using either SuperScript II or SuperScript III kits with oligo(dT)₁₂₋₁₈ primers (Invitrogen), according to manufacturer's instructions.

For transcriptional time courses, 10 adult mosquitoes were collected at 24, 48 or 72 h post challenge (except day 1, 3 and 6 for viral time courses) and untreated mosquitoes were used as "time zero". For other mosquito life stages, 10 larvae or pupae were collected per sample, surface-sterilised with 70% ethanol, washed twice with water and RNA was extracted in 1 mL TRIzol, as above. For midgut

RNA extraction, 20 guts were used per sample in a total volume of 600 μL TRIzol, with other reagent volumes reduced accordingly.

qRT-PCR analysis

The ABI Prism 7500 Fast Real-Time PCR System was used with Fast SYBR Green Master Mix (Applied Biosystems) to perform qRT-PCR, according to manufacturer's instructions. All qRT-PCR samples were analysed in duplicate, using 1 μL of 1/10 dilution of cDNA per reaction. The ribosomal "house-keeping" gene *S7* was used as the endogenous reference to normalise samples according to the amount of total cDNA added to the reaction. Gene expression was quantitated relative to a calibrator control sample (e.g. untreated mosquitoes, *dsGFP*-treated mosquitoes). If the efficiency of target gene amplification was approximately equal to the efficiency of *S7* amplification, the Comparative C_T ($\Delta\Delta C_T$) Method was used (refer to User Bulletin #2). Otherwise, the Relative Standard Curve Method was used and standard curves were prepared from serially diluted cDNA (pooled cDNA from each sample or *dsGFP*-treated mosquito cDNA for knockdown experiments). Primers were designed using Primer3 online software (Rozen and Skaletsky, 2000) and optimised according to User Bulletin #5. Refer to Appendix Table 9.2 for qRT-PCR primer sequences.

NanoString analysis

NanoString nCounter Gene Expression Analysis (NanoString Technologies, Inc.) is a high-throughput digital technology for determining gene expression from total RNA, as described in detail in Chapter 4 (Fortina and Surrey, 2008; Geiss et al., 2008). Gene-specific probes were designed and manufactured by NanoString Technologies Inc. to cover 100 bp of coding sequence (Appendix Table 9.3). For each gene, a capture and a reporter probe (~50 bp each) were used to target the 100 bp region. Total RNA samples (after DNase-treatment) were diluted to 100 ng/ μL and shipped on dry ice for NanoString analysis. Raw data was first normalised using positive "spike-in" controls to account for assay based variation and subsequently normalised using the mosquito reference gene, *S7*, to account for differences in total RNA abundance.

Cloning LRIMs into pIEx-10 expression vector

The *LRIM9* open reading frame, without the endogenous signal peptide, was amplified by PCR, initially from genomic DNA using gLRIM9 forA and tLRIM9 revA primers followed by LRIM9 LIC for and LRIM9 LIC rev primers (Appendix Table 9.4). The open reading frames of *LRIM4*, *LRIM17* and *LRIM15*, without the endogenous signal peptides, were amplified by PCR from cDNA template using primers in Table 9.4. The resulting products were cloned into the pIEx-10 insect expression plasmid using the Enterokinase/Ligase-independent cloning (Ek/LIC) system (Novagen), according to manufacturer's instructions. This plasmid incorporates a mouse IgM signal peptide, an N-terminal

Strep-tag and a C-terminal His-tag. pEx-10-LRIM9, -LRIM4 and -LRIM17 were transformed into NovaBlue GigaSingles competent cells (Novagen) and pEx-10-LRIM15 was transformed into SURE competent cells (Stratagene), which reduce unwanted rearrangement events. Plasmid DNA from one sequence-verified clone per LRIM was prepared using the HiSpeed Plasmid Midi kit (Qiagen).

Cloning TEP3 and TEP4 C-terminal fragments into pET-41a(+) expression vector

C-terminal fragments of *TEP3* and *TEP4* were cloned into pET-41a(+) expression vector (Novagen), which incorporates an N-terminal GST-tag, with the aim of raising antibodies against the purified fragments after expression in *E. coli*. C-terminal fragments were amplified by PCR from existing plasmid templates (see Appendix Table 9.4 for primers) and cloned into pET-41a(+) using the Ek/LIC system (Novagen). pET41a(+)-TEP3 and -TEP4 were transformed into NovaBlue GigaSingles cells, sequence verified and re-transformed into BL21-pLysS competent cells (Novagen), which are isopropyl β -D-1-thiogalactopyranoside (IPTG) inducible and optimised for protein expression.

Site-directed mutagenesis

A cysteine (TGC) to serine (AGC) missense mutation at position 535 in *LRIM4* was generated using the QuikChange II Site-Directed Mutagenesis protocol (Stratagene), according to manufacturer's instructions. The following PAGE-purified primers were used:

- C535S for 5'-gcagctgaccaagagcacctcgaccgt-3'
- C535S rev 5'-acggtcgaggtgctcttggtcagctgc-3'

3.3 Protein analysis and cell culture

Maintenance of insect cell lines

Spodoptera frugiperda (Lepidoptera)-derived Sf9 cells were cultured in serum-free Sf-900 medium (Gibco). Sua4.0 cells, derived from minced neonate *An. gambiae* larvae (Muller et al., 1999), were cultured in Schneider's medium (Gibco) supplemented with 10% heat-inactivated FBS, 10 U/mL penicillin and 10 μ g/mL streptomycin. All insect cells were maintained at 27 °C in 75 cm² flasks and were split by diluting 1/10 in fresh media every 7 days.

Transfection of cultured cells

Sf9 and Sua4.0 cells were seeded at 1×10^6 and 3×10^6 cells in 2 mL of medium per well, respectively, in 6-well plates. Cells were transfected with 2 μ g plasmid DNA, using a GFP-expressing plasmid as a control. Escort IV (Sigma-Aldrich) and Effectene (Qiagen) were used to transfect Sf9 and Sua4.0 cells, respectively, according to manufacturers' instructions. For one well, the following volumes of

reagents were used: 4 μ L Escort IV (for Sf9 cells) or 100 μ L EC buffer, 3.2 μ L Enhancer and 10 μ L Effectene (for Sua4.0 cells). The day after transfection, Sf9 media was replaced with fresh Sf-900 whereas Sua4.0 cells were washed (to remove serum) and placed in 2 mL serum-free Schneider's medium. Conditioned media were collected after 3-4 days and filtered using a 0.45 μ M syringe filter to remove cells and debris. Samples were stored at 4 °C (protected from light) and used within 7 days.

LRIM9 peptide antibodies

Rabbit polyclonal antibodies were raised against the following peptides by Eurogentec using the "Super Speedy" 28 day immunisation programme:

- Peptide 70: NH₂-CDYARRLEVASEPSAK-COOH (the real C-terminus with an ectopic cysteine)
- Peptide 71: NH₂-DSDGTLDDKSTDGTDCCOOH (amino acids 269-284; between LRRs and coiled-coil)

Antibodies were affinity purified by Eurogentec and then verified by western blotting analysis of conditioned media from cultured cells and hemolymph (see below for details).

LRIM9 whole protein antibody

A Sf9 cell line stably expressing LRIM9 was produced by Dr Lavanya Bhagavatula by co-transfecting pIEx-10-LRIM9 and the pIE1-neo selection plasmid (Novagen), following the manufacturer's protocol. Over 2 L of LRIM9-containing conditioned medium was collected and 0.22 μ M sterile-filtered. LRIM9 was purified from the media using a His Trap FF column on an ÄKTA purifier (fast protein liquid chromatography or FPLC; GE Healthcare), according to the manufacturer's protocol.

LRIM9 protein was analysed by Coomassie staining, concentrated using Amicon Ultra Centrifugal filter units (Millipore) and quantified by Bradford assay. 214 μ g of purified LRIM9 was sent to Eurogentec for immunisation of two guinea pigs (named 59 and 60). Pre-immune serum (PPI) was collected from each animal before immunisation, as a control for antibody specificity. A large bleed (GP) and final bleed (SAB) were collected 3 weeks and 4 weeks, respectively, after immunisation. Antisera from both animals were characterised. SAB from guinea pig 59 at 1/500 dilution (in 3% milk) produced the strongest signal and was chosen for use in subsequent experiments.

Western blot analysis of hemolymph or conditioned media

Proteins were separated on an 8% SDS-PAGE gel before transfer to a PVDF membrane using a Trans-Blot SD Semi-Dry Transfer Cell (Bio-Rad). Non-reduced samples were prepared in Lane Marker sample buffer (Pierce) without heating. Reduced samples were prepared by adding tris(2-

carboxyethyl)phosphine (TCEP) solution (Pierce) to non-reduced samples to a final concentration of 25 mM and heating at 95 °C for 5 min. Membranes were blocked with PBS containing 3% milk and 0.05% Tween-20 and probed at room temperature for 1 h (or overnight at 4 °C) with primary antibody. Primary antibodies were used at the following dilutions: guinea pig α -LRIM9 (1/500), rabbit α -LRIM1-w (1/1000), rabbit α -LRIM2-300 (for APL1C; 1/2000), rabbit α -SRPN3 (1/1000), rabbit C-terminal α -TEP1 (1/1000), mouse α -CLIPA8 monoclonal (1/50) and mouse α -Strep-tag (1/1000). PBS-Tween containing 3% bovine serum albumin (BSA) was used as blocking buffer for α -Strep-tag. Membranes were washed three times with PBS-Tween and incubated with horseradish peroxidase (HRP)-conjugated rabbit secondary antibody for 1 h at room temperature. α -rabbit (1/12,000), α -guinea pig (1/10,000) and α -mouse (1/12,000) secondary antibodies (Promega) were used, diluted in blocking buffer. Finally, blots were washed three times with PBS-Tween. For detection of the His-tag, blots were blocked with 3% BSA and probed for 1 h at room temperature with HRP-conjugated His probe (1/5000 dilution; Pierce), without the need for a secondary antibody. For visualisation, Western Lightning Chemiluminescence Reagent Plus (Perkin-Elmer) was applied and the ChemiDoc XRS+ System with Image Lab software (Bio-Rad) was used. Protein abundance was measured semi-quantitatively using Image Lab software, normalising to the SRPN3 loading control.

A MiniBlotter (Immunectics) was used to test the new LRIM9 antibodies, according to manufacturer's guidelines. This allows multiple antibody dilutions to be tested on the same western blot. Antibody concentration and blocking buffer were optimised accordingly.

Immunolocalisation of TEP1

Mosquito midguts were dissected in ice-cold PBS 27-30 h after a *P. berghei* infected blood meal (Povelones et al., 2009). Micro-dissection scissors were used to cut along the length of the midgut and the bloodmeal was gently removed from the midgut epithelium. The epithelia were fixed in 4% formaldehyde for 45 min, washed three times in PBS for 15 min and permeabilised for 10 min in PBS with 0.05% Triton X-100. They were blocked for 30 min in PBS-Triton supplemented with 3% BSA and then incubated overnight at 4 °C with rabbit α -TEP1 antibody (diluted 1/500 in blocking buffer). After three more washes with PBS-Triton, midgut epithelia were incubated with an Alexa Fluor 546 conjugated goat α -rabbit secondary antibody (Molecular Probes) at 1/1500 dilution in blocking buffer. The epithelia were washed three more times with PBS-Triton; the second 15 min wash was supplemented with 1 μ g/ μ L DAPI (Boehringer Mannheim). Finally, they were mounted on glass slides in Vectashield. 4-7 midguts were analysed for each gene knockdown using the Leica DMR fluorescent microscope. One representative photograph (comprised of Alexa, GFP and DAPI channels) was taken per gut using the 40X objective. Green (live, GFP-labelled) and red (dead, TEP1-

labelled) parasites were counted manually from the photographs, labelling each “counted” parasite with a brush mark in Adobe Photoshop to reduce error.

Purification of His-tagged proteins from conditioned media

Sua4.0 cells were transfected with pEx-10-GFP, -LRIM1, -APL1C and either -LRIM9 or -LRIM4. Conditioned media were collected after 3.5 days and analysed by western blot using the His probe. Depending on the abundance of each His-tagged protein, between 400 μ L and 1 mL of conditioned media were supplemented with 0.05% Triton X-100 in a Protein LoBind tube (Eppendorf). 50 μ L of 1:1 slurry of Talon Metal Affinity Resin (Clontech) in PBS was added to each sample. Samples were gently agitated for 1 h at room temperature before centrifugation for 2 min at 2500 rpm and removal of the supernatant. Beads were washed with 500 μ L Talon wash buffer (50 mM NaH_2PO_4 , 300 nM NaCl, 10 mM imidazole) containing 0.05% Triton X-100. A further 500 μ L Talon wash buffer (without Triton) was added to the beads and the entire solution was transferred to a Microcentrifuge spin column in a 2 mL collection tube (Pierce). Beads were washed five times with Talon wash buffer, centrifuging for 2 min at 2500 rpm each time. The column was transferred to a clean Protein LoBind tube and beads were incubated for 10 min with 35 μ L 2X non-reducing Lane Marker sample buffer (Pierce). Eluates were recovered by centrifugation and samples were stored at -20°C prior to western blot analysis.

3.4 Statistical analysis and further data analysis

Statistical analyses were performed using GraphPad Prism 5 software, unless otherwise noted. *P. berghei* infection intensity (number of oocysts or melanised ookinetes) was analysed by the Mann Whitney U-test whereas prevalence was analysed by Fisher’s exact test. However, if prevalence was zero for one gene knockdown, the Wilcoxon signed-rank test was used instead, which compares a median to a hypothetical value (i.e. 0.0). Bacterial survival assays were analysed using the Log-rank (Mantel-Cox) test. Bacterial proliferation assays were analysed using Meta-Analysis (Comprehensive Meta-Analysis, Biostat).

Log_2 -transformed NanoString transcriptional data was analysed using Cluster 2.11 and Treeview (Eisen Laboratory). Average data for each time course was used to create a heat map and individual biological replicates were used to hierarchically cluster the genes tested (see Chapter 4).

3.5 VectorBase gene identifiers

For the LRIM family, refer to Table 1.1.

TEP1, AGAP010815; TEP2, AGAP008366; TEP3, AGAP010816; TEP4, AGAP010812; TEP5, AGAP010818; TEP6, AGAP010814; TEP8, AGAP010831; TEP9, AGAP010830; TEP10, AGAP010819; TEP12, AGAP008654; TEP13, AGAP008407; TEP14, AGAP008368; TEP15, AGAP008364; S7, AGAP010592; CTL4, AGAP005335; CLIPA8, AGAP010731; Polyubiquitin, AGAP001971.

Chapter 4: Transcriptional and functional analysis of the LRIM family

4 Transcriptional and functional analysis of the LRIM family

4.1 Background

The LRIMs are a novel mosquito-specific protein family recently discovered in *An. gambiae* (Povelones et al., 2009; Waterhouse et al., 2010). The family shares characteristic protein domain architecture and LRIMs have been divided into four subfamilies: Long, Short, Transmembrane and Coil-less. The founding members, LRIM1 and APL1C, form a heterodimer and function in the mosquito complement-like pathway (Blandin et al., 2008; Povelones et al., 2011). The LRIM1/APL1C complex binds to and stabilises the complement-like effector, TEP1, delivering it to *Plasmodium* surfaces, which results in parasite killing, lysis and melanisation (Fraiture et al., 2009; Povelones et al., 2009). The LRIM1/APL1C complex also plays a key role in bacterial defence and phagocytosis (Moita et al., 2005). Apart from LRIM1 and APL1C, the other 22 LRIMs in *An. gambiae* have been poorly characterised to date. Microarray analyses have revealed expression changes in certain *An. gambiae* LRIMs after blood feeding, *Plasmodium* invasion and other immune challenges (Aguilar et al., 2005a; Dong et al., 2006a; Marinotti et al., 2005; Vlachou et al., 2005). For example, *LRIM4*, *LRIM8B*, *LRIM10* and *LRIM17* were shown to be upregulated in the *An. gambiae* midgut during *P. falciparum* infection (Dong et al., 2006a). *LRIM10* was also highly induced in the midgut after *P. berghei* invasion (Vlachou et al., 2005) whereas *LRIM8B* was also downregulated by infection with *Salmonella typhimurium*, a gram-negative bacterium (Aguilar et al., 2005b). A few novel LRIMs have been putatively described as *Plasmodium* antagonists. The Coil-less LRIM17 was reported to antagonise infections with *P. berghei* and *P. falciparum* (Dong et al., 2006a; Garver et al., 2012), although this has not been supported by other studies (Riehle et al., 2006). The Long APL1A has been demonstrated to influence the prevalence of *P. falciparum* infections but not the infection intensity (Mitri et al., 2009). The Long APL1B was recently shown to influence *P. falciparum* oocyst levels at medium infection intensities (Garver et al., 2012).

The importance of LRIM1 and APL1C in the mosquito immune response led to the hypothesis that the LRIM family has expanded and diversified in mosquitoes to provide protection against different pathogens they encounter. To determine whether there is specificity in the LRIM family, this PhD aimed to provide a complete transcriptional profile for all LRIMs after various immune challenges using NanoString nCounter Gene Expression Analysis (NanoString Technologies, Inc.). As most previous experiments focused on expression in the mosquito midgut, this current study used whole mosquitoes. Transcriptional regulation often reflects protein function and so profiling will provide

candidates for involvement in defence against certain pathogens. Genes that function in the same biochemical pathways are frequently transcriptionally co-regulated and therefore profiling can identify putative functional relationships between LRIMs. For instance, co-regulation of *LRIM1*, *APL1C* and *TEP1* has previously been demonstrated after *P. berghei* infection (Blandin et al., 2004; Fraiture et al., 2009; Frolet et al., 2006).

As NanoString allows many genes to be assayed using the same RNA sample in a single reaction, the TEP family was also included for analysis. The TEPs are predicted to be interacting partners of the LRIMs because TEP1, TEP3, TEP4 and TEP9 have been demonstrated to interact with the LRIM1/APL1C complex (Povelones et al., 2011). The TEPs are related to the vertebrate complement factors, C3, C4 and C5 (Christophides et al., 2004). They contain highly reactive TE bonds, which allow TEPs to covalently bind to and opsonise pathogen surfaces (Blandin and Levashina, 2004). However, most mosquito TEPs, including TEP3, lack an active TE bond and could play regulatory roles in immunity (Christophides et al., 2002). TEP1 is an essential component of the mosquito complement-like pathway and other *An. gambiae* TEPs have been implicated in *Plasmodium* and bacterial defence (Blandin and Levashina, 2004). Microarrays have reported that *TEP4* is upregulated by gram-negative and gram-positive bacteria and *TEP4* knockdown decreases survival upon bacterial challenge (Dong et al., 2006a; Dong et al., 2009). TEP4 also functions in phagocytosis of both bacterial gram-types whereas TEP3 is only involved in phagocytosis of gram-negative bacteria (Moita et al., 2005).

The NanoString nCounter System is a novel digital technology for high-throughput mRNA expression profiling (Fortina and Surrey, 2008; Geiss et al., 2008). The assay uses unique molecular “barcodes” for each gene of interest and hundreds of different transcripts can be multiplexed in a single reaction (Figure 4.1). Specific pairs of 50 bp capture and reporter probes are designed to be complementary to each transcript of interest. The reporter probe carries a directional fluorescent barcode made from combinations of four spectrally distinct dyes at seven regions. The capture probe enables immobilisation required for data collection. Both probes are mixed with the total RNA sample and allowed to hybridise in solution. Complexes composed of one mRNA transcript, one capture probe and one reporter probe form and excess probes are removed by purification. Complexes bind to the imaging surface via their capture probes; they are oriented by electrophoresis and then immobilised. A digital analyser detects and counts the number of reporter probes for each gene, providing quantitation of gene expression. The technique is highly precise and sensitive with the equivalent of less than one transcript per cell detectable, which is superior to microarrays and comparable to qRT-PCR. Detection of low abundance transcripts is considerably improved compared

to microarrays. Unlike qRT-PCR and microarrays, NanoString analysis does not require cDNA synthesis or enzymatic reactions, which avoids unnecessary bias.

A large subset of samples was verified by qRT-PCR, a traditional technique for gene expression profiling. Unlike the NanoString, qRT-PCR requires a single reaction per target gene and is considerably more laborious.

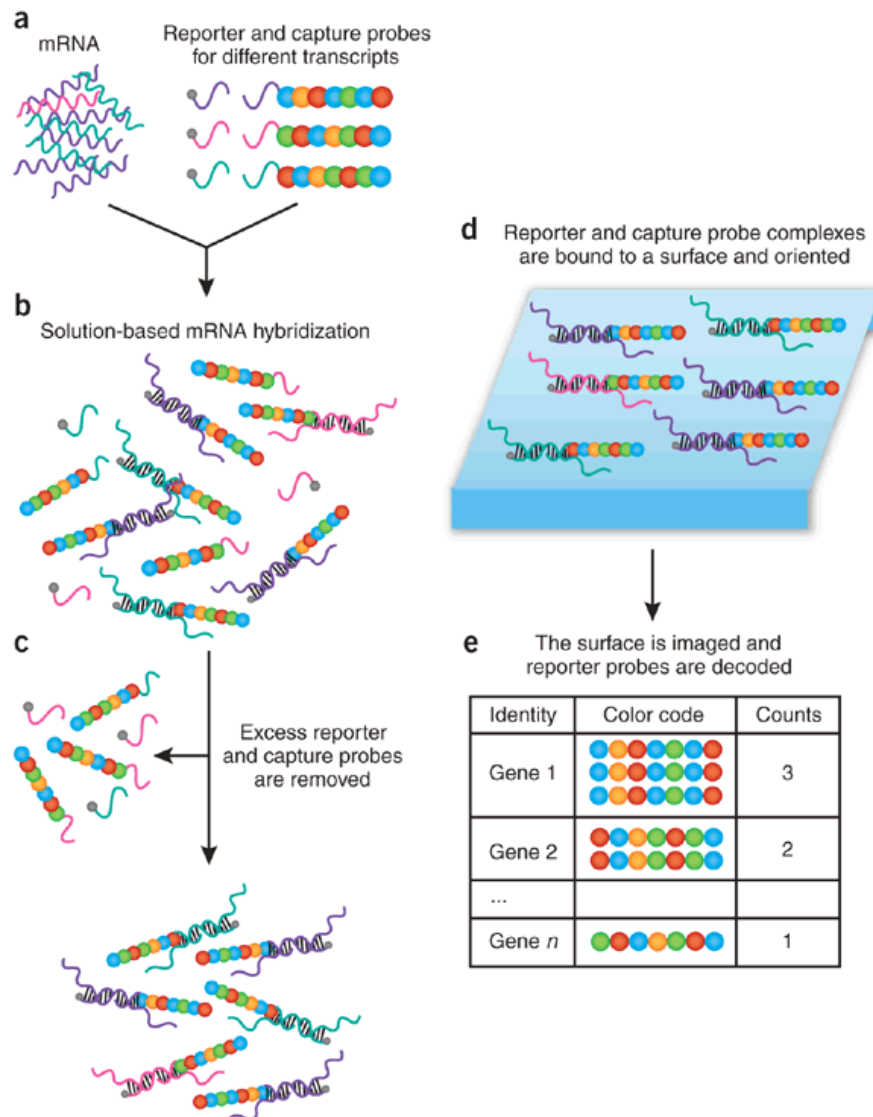


Figure 4.1 Schematic overview of NanoString technology.

The total RNA sample is mixed with reporter and capture probes complementary to the different genes being assayed (**a**). Specific mRNA transcripts hybridise with their unique probes in solution (**b**). Purification is utilised to remove unhybridised probes (**c**). mRNA-probe complexes bind to the imaging surfaces and are immobilised in the correct orientation (**d**). The number of reporter probes per gene (corresponding to the number of transcripts) is counted (**e**). From Fortina and Surrey, 2008.

As LRIM1 and APL1C are potent antagonists of *P. berghei*, the uncharacterised LRIMs were screened for a similar phenotype. A functional screen was used to determine whether silencing any novel LRIMs influences malaria parasite development, using *P. berghei* as a laboratory model.

4.2 Results

Transcriptional profiling of the LRIMs and TEPs

To investigate transcriptional specificity in the LRIM family, expression was monitored after various immune challenges. It was hoped that transcriptional profiling would provide clues about the function of novel LRIMs and also the relationships between LRIMs. The TEPs were included in the analysis because they are known to be interacting partners of LRIMs: as well as its main functional partner TEP1, the LRIM1/APL1C complex has been demonstrated to interact with TEP3, TEP4 and TEP9 *in vitro* (Povelones et al., 2011).

The Ngousso strain of *An. gambiae* was used for all transcriptional experiments and RNA was extracted from a group of 10 whole mosquitoes per sample. A wide range of immune challenges were selected to represent the variety of pathogens that mosquitoes encounter in their blood feeding lifestyle. *An. gambiae* females were infected with three *Plasmodium* parasites – two murine parasites (*P. berghei* and *P. yoelii*) and the human malaria parasite, *P. falciparum*. Interestingly, these parasites have different optimal growth temperatures (19 °C for *P. berghei*, 25 °C for *P. yoelii* and 27 °C for *P. falciparum*). To gain a temporal understanding of transcriptional changes, mosquitoes were collected at three time points (24, 48 and 72 h). To ensure parasite-specific responses, *Plasmodium* infections were normalised against naïve blood feeding performed at the same temperature. Transcriptional responses to naïve blood feeding at each temperature were also analysed, relative to unfed mosquitoes.

Viral responses were monitored using ONNV, an alphavirus related to CHIKV. ONNV is the only arbovirus that is commonly transmitted by *An. gambiae* (Powers et al., 2000). Most arboviruses are transmitted by Culicine mosquitoes (Sim et al., 2005). The virus is ingested with a blood meal, replicates in midgut epithelial cells and then disseminates through the hemocoel to the salivary glands, fat body, muscles and other tissues (Pierro et al., 2003). In the transcriptional profiling, mosquitoes were either infected by injection into the hemocoel or by ingestion in a blood meal of virus that had been harvested in the conditioned media of infected VERO cells. This would allow comparison of systemic and midgut dissemination responses. Samples were collected at day 1, 3 and 6 after infection to account for the slower process of viral infection and dissemination. Mosquitoes

injected with conditioned media from uninfected VERO cells were used to normalise viral injection. The response to conditioned media injection was also monitored, relative to uninjected mosquitoes. Results from mosquitoes infected by ONNV blood feeding were normalised using naïve blood feeding.

Mosquitoes were challenged with bacteria and fungi, both organisms that the immune system commonly encounters, and samples were collected 24, 48 and 72 h post challenge. Challenges included injection of spores of *B. bassiana*, an entomopathogenic fungus, and live suspensions of *E. coli* (gram-negative) and *S. aureus* (gram-positive) bacteria. Results were normalised against sterile PBS injection. To monitor injury responses, PBS injection alone was also analysed, relative to uninjected mosquitoes. In total, four PBS injection time courses were examined by NanoString (two from the fungi experiments and two from bacteria).

Finally, RNA from 10 fourth instar larvae and 10 pupae was extracted and analysed to provide an initial insight into the developmental expression profiles of the LRIMs and TEPs.

Two independent biological experiments were tested by NanoString for each experiment except the developmental profiling, for which only one replicate was performed. Raw NanoString data was first normalised using positive “spike-in” controls to account for assay based variation. These controls are used to monitor and adjust for slight differences in hybridisation, purification and binding efficiency due to differences in RNA quality. Next, samples were normalised based on a mosquito reference gene to account for differences in total RNA quantity between samples. Probes for three potential reference genes, *S7*, *polyubiquitin* and *actin5C*, were included in the analysis. These “housekeeping” genes were chosen because they are expressed by virtually all cells. *S7* is a ribosomal gene, polyubiquitin is involved in protein turnover and actin is a cytoskeletal component. Of the three potential reference genes, *S7* showed the least variation over all the RNA samples and was chosen to normalise all samples. For a large subset of RNA samples and genes, NanoString results were verified by qRT-PCR. Four replicates of blood feeding and *P. berghei* infection, three *B. bassiana* infection and three bacteria experiments were tested by qRT-PCR. Overall, there was very good agreement between NanoString and qRT-PCR in terms of fold changes in expression and patterns of expression across time courses.

The LRIMs and TEPs were ranked according to their average number of NanoString reporter counts over all experiments to give a guide to expression levels (Table 4.1). Interestingly, *LRIM1*, *APL1C* and *TEP1* were amongst the most highly expressed. *LRIM11* and *TEP11* were excluded from further analysis because their average reporter counts fell within the negative controls. Both were less than

the average reporter counts for the negative controls across all experiments plus 2 standard deviations. In support of the NanoString data, seven attempts to generate qRT-PCR primers against *LRIM11* failed and this is likely due to very poor or complete lack of expression. Other poorly expressed genes that were not excluded included *LRIM18*, *LRIM19*, *LRIM20*, *APL1B*, *TEP5*, *TEP9* and *TEP10*. Although very low detection in whole mosquito RNA may indicate low transcription levels in immune tissues or limited tissue-specific expression, caution should be taken when interpreting fold changes for these poorly expressed genes as a large fold change is not necessarily biologically meaningful. It was decided to focus on the transcriptional responses of genes with stronger expression but these poorly expressed genes will be discussed further in section 4.3.

Fold change gene expression data is presented in a heat map to highlight the specific responses of each gene to different immune challenges (Figure 4.2). A complete data set is available on the Appendix CD. Overall, both the LRIM and TEP families showed a variety of transcriptional profiles, with different genes upregulated by distinct immune challenges.

Table 4.1 Rank order of all genes based on average number of NanoString gene-specific reporters.

Rank	Gene	Average	Minimum	Maximum
1	<i>Polyubiquitin</i>	39543	7474	84197
2	<i>Actin5C</i>	16811	5079	68431
3	<i>APL1C</i>	4589	1313	19233
4	<i>TEP1</i>	4255	928	13142
5	<i>LRIM17</i>	3182	302	11768
6	<i>TEP15</i>	3017	538	7545
7	<i>LRIM1</i>	2432	472	7949
8	<i>LRIM9</i>	2248	2	12142
9	<i>LRIM8B</i>	2002	5	5618
10	<i>LRIM8A</i>	870	47	2149
11	<i>LRIM15</i>	852	31	7856
12	<i>LRIM4</i>	818	57	3523
13	<i>TEP4</i>	763	86	2846
14	<i>TEP14</i>	745	134	2505
15	<i>LRIM10</i>	506	7	2285
16	<i>LRIM16B</i>	489	221	1465
17	<i>LRIM6</i>	482	166	1268
18	<i>TEP12</i>	456	68	1594
19	<i>LRIM26</i>	432	122	1092
20	<i>LRIM3</i>	354	143	907
21	<i>TEP3</i>	273	54	1184
22	<i>LRIM16A</i>	258	67	800
23	<i>LRIM27</i>	249	34	773
24	<i>TEP2</i>	240	94	521
25	<i>APL1A</i>	175	26	1467
26	<i>TEP13</i>	156	38	867
27	<i>LRIM7</i>	155	16	1380
28	<i>LRIM12</i>	139	11	623
29	<i>LRIM5</i>	133	7	396
30	<i>TEP6</i>	111	3	525
31	<i>LRIM20</i>	88	15	414
32	<i>LRIM18</i>	62	20	262
33	<i>LRIM19</i>	62	0	455
34	<i>APL1B</i>	36	2	477
35	<i>TEP5</i>	31	2	509
36	<i>TEP9</i>	28	3	189
37	<i>TEP10</i>	27	0	201
38	<i>NEG_G(0)</i>	20	5	49
39	<i>LRIM11</i>	15	1	55
40	<i>TEP11</i>	9	0	140
41	<i>NEG_C(0)</i>	8	0	61
42	<i>NEG_A(0)</i>	8	0	22
43	<i>NEG_F(0)</i>	8	0	18
44	<i>NEG_D(0)</i>	7	0	52
45	<i>NEG_H(0)</i>	7	0	30
46	<i>NEG_E(0)</i>	6	0	18
47	<i>NEG_B(0)</i>	5	0	18

All genes analysed by NanoString were ranked according to their average number of NanoString reporter counts across all experiments, after normalisation to the reference gene, *S7. Polyubiquitin* and *Actin5C* were analysed as potential reference genes but were not used for normalisation because they showed higher variation between RNA samples than *S7*. Genes are shown in blue and negative controls (NEG) in red. The minimum and maximum number of reporter counts in any experiment is shown.

Hierarchical gene clustering

Individual transcriptional profiles were utilised to identify potentially co-regulated LRIM and TEP genes by employing hierarchical clustering analysis. Co-regulated genes are hypothesised to function together, either in the same immune pathway or in defence against the same pathogen(s). It was hoped that this analysis would provide clues as to which LRIMs and TEPs interact with each other or work together in the mosquito immune system.

Hierarchical clustering analysis revealed distinct groups of LRIMs and TEPs with similar expression profiles (Figure 4.3). Four members of the short LRIM genomic cluster (*LRIM8A*, *LRIM8B*, *LRIM9* and *LRIM10*) were tightly clustered. As expected, functional partners *LRIM1*, *APL1C* and *TEP1* were found in the same cluster. *LRIM1*, *APL1C* and *TEP1* were co-regulated with *APL1A*, *TEP3* and *TEP4*. This supports the previous finding that *TEP3* and *TEP4* interact with the *LRIM1/APL1C* complex (Povelones et al., 2011). Interestingly, *APL1A* and *APL1C* were in a different cluster to *APL1B* despite being derived from recent gene duplication (Riehle et al., 2008). *LRIM5* and *LRIM27* are adjacent to each other on chromosome 2R and were also hierarchically clustered together. Another interesting cluster was *LRIM4*, *LRIM17*, *TEP12* and *TEP14*, which might reflect a novel functional relationship.

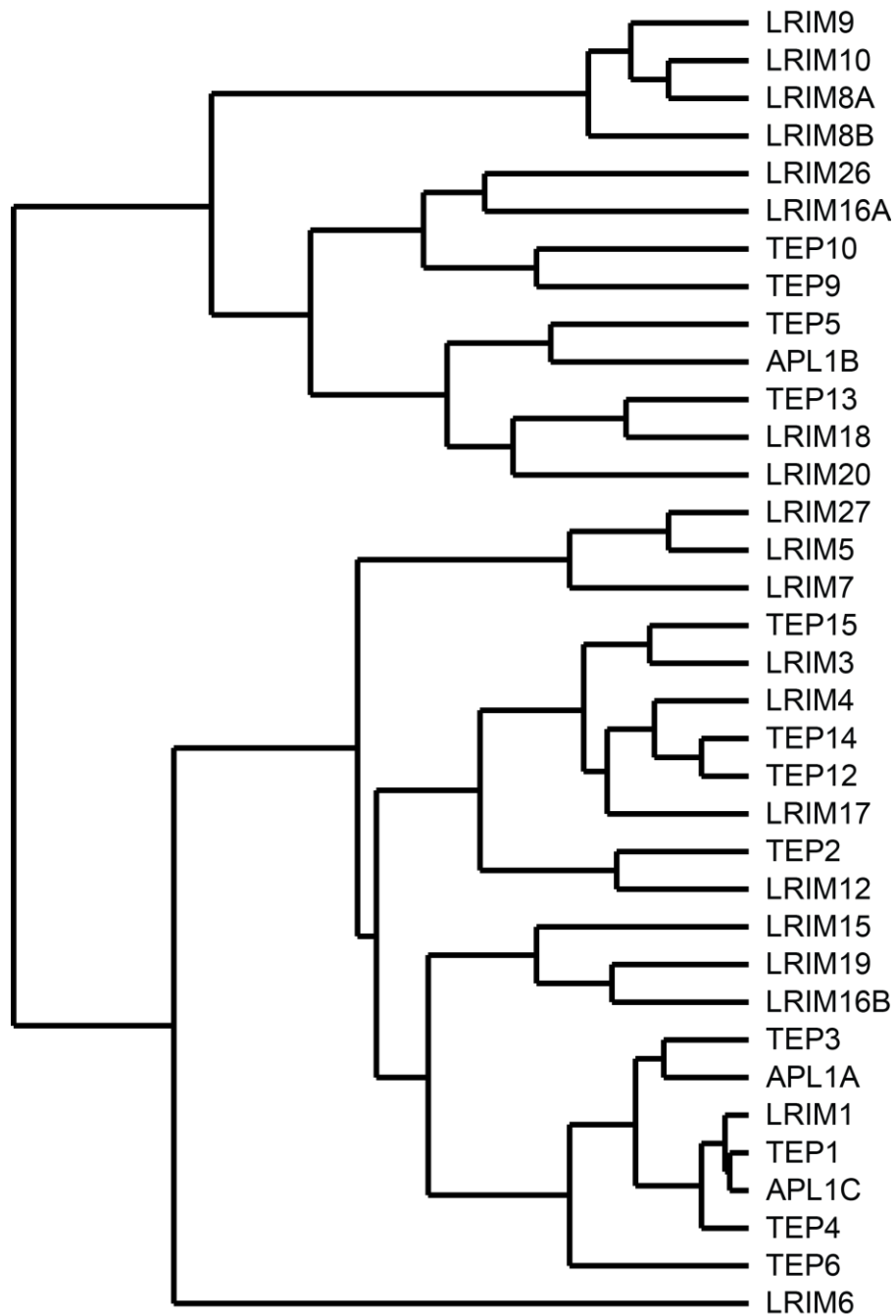


Figure 4.3 Hierarchical clustering of LRIMs and TEPs based on transcriptional profile.

Individual biological replicates of NanoString expression data were \log_2 -transformed and clustered using Cluster 2.11 and Treeview. Complete linkage clustering analysis was performed using un-centred correlation. Branches indicate clusters of co-regulated genes. The data included infections with *P. berghei*, *P. yoelii*, *P. falciparum*, injected ONNV, blood fed ONNV, *E. coli*, *S. aureus* and *B. bassiana* (two replicates each). Other challenges were naïve blood feeding (8 replicates), PBS injection (4 replicates) and conditioned media injection (2 replicates).

Transcriptional responses to blood feeding

Specific LRIMs responded strongly to naïve blood feeding, in the absence of parasite infection. The most dramatically induced genes were the Short LRIMs: *LRIM8A*, *LRIM8B*, *LRIM9* and *LRIM10*. Interestingly, these genes are found clustered together on *An. gambiae* chromosome 2L and were also hierarchically clustered in Figure 4.3. All genes were upregulated by mouse and human blood and at all three temperatures (19, 25 and 27 °C). These genes seem to be largely blood feeding specific LRIMs. *LRIM8A*, *LRIM8B*, *LRIM9* and *LRIM10* were all induced between 2- and 10-fold within 24 to 48 h of naïve blood feeding at 19 °C (Figure 4.4 A), with good agreement between NanoString and qRT-PCR.

Differences in the peak and duration of upregulation were observed at different temperatures. For example, *LRIM9* and *LRIM10* peaked at 48 h after feeding on mouse blood at 19 °C, with expression rising steadily from 24 h (Figure 4.4 B). After feeding on mouse blood at 25 °C or human blood at 27 °C, expression of *LRIM9* and *LRIM10* peaked rapidly at 24 h. As responses to mouse blood at 25 °C and human blood at 27 °C were more similar than mouse blood at 25 °C and 19 °C, this suggests that the vertebrate species has little influence. It is likely that the higher temperature accelerates gene expression.

Curiously, *LRIM7*, the fifth member of the genomic cluster, was not co-clustered with the other Short LRIMs in Figure 4.3 and was largely uninduced by blood feeding. Although *LRIM7* was upregulated 48 h after human blood feeding in some replicates, it showed a completely distinct pattern of induction to the other Short LRIMs.

Other LRIMs upregulated by blood feeding included Coil-less *LRIM26*, which was strongly induced at all time points, all temperatures and all blood types. *LRIM26* was in a neighbouring cluster to *LRIM8A*, *LRIM8B*, *LRIM9* and *LRIM10* in Figure 4.3, which might suggest they function in related pathways. Transmembrane *LRIM15* was also upregulated by naïve blood feeding and seemed to be very sensitive to changes in temperature. Strikingly, *LRIM15* was induced at 72 h at 19 °C, 48 h at 25 °C and 24 h at 27 °C. As with the Short LRIMs, higher temperatures caused more rapid responses. Many genes were downregulated in response to taking a blood meal. This included *LRIM12* and *TEP2*, which were hierarchically clustered together in Figure 4.3.

The TEPs were less responsive to blood feeding compared to the LRIMs. The only TEP with a strong and consistent response to blood feeding was *TEP13*. Interestingly, *TEP13* gave a more pronounced response to mouse blood feeding, compared to human blood feeding.

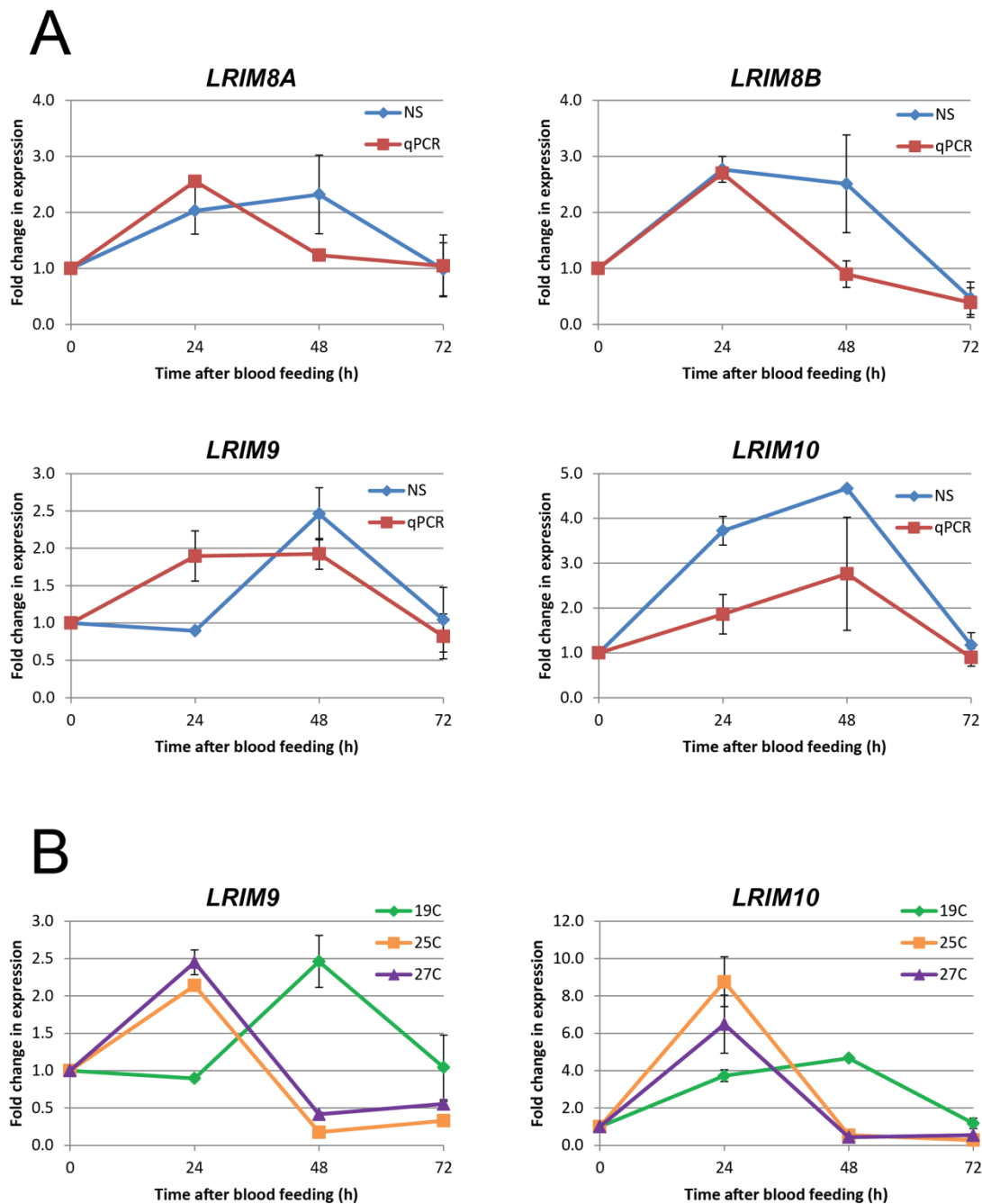


Figure 4.4 Transcriptional responses of the short LRIMs to blood feeding.

A) Transcriptional responses of *LRIM8A*, *LRIM8B*, *LRIM9* and *LRIM10* were measured 24, 48 and 72 h after feeding on naïve mouse blood at 19 °C. Expression was measured by NanoString (blue line) and qRT-PCR (red line), normalising to *S7*. Average fold change in expression from 2 independent replicates is shown with standard error bars. Results are calculated relative to unfed mosquitoes (time “0 h”). **B)** Transcriptional responses of *LRIM9* and *LRIM10* to naïve blood feeding were monitored at different temperatures. Mosquitoes were fed on mouse blood at 19 °C (green line) or 25 °C (orange line) or human blood at 27 °C (purple line). Average fold change in expression and standard error bars from 2 replicates are shown (4 replicates for human blood feeding at 24 h and 72 h), measured by NanoString.

Transcriptional responses to Plasmodium infection

Distinct subsets of LRIMs were induced by *Plasmodium* infection, with differences observed for infections with different malaria parasite species. Mosquitoes were infected with two rodent parasites, *P. berghei* and *P. yoelii*, and one human parasite, *P. falciparum*. Key players induced by all three parasite species included *LRIM1*, *APL1C* and *TEP1*, which are known to function together as major antagonists of *P. berghei* (Fraiture et al., 2009; Povelones et al., 2009) and *P. yoelii* (Jaramillo-Gutierrez et al., 2009). *LRIM1*, *APL1C* and *TEP1* demonstrated tight co-regulation in all *Plasmodium* responses, suggesting they function together against all *Plasmodium* species. Expression after *P. berghei* infection was also monitored by qRT-PCR, which showed excellent correlation with the NanoString. Strong co-regulation of *LRIM1*, *APL1C* and *TEP1* after *P. berghei* infection is demonstrated in Figure 4.5. *APL1A*, *TEP3* and *TEP4*, which hierarchically clustered with *LRIM1*, *APL1C* and *TEP1* in Figure 4.3, also shared a similar pattern of regulation after *Plasmodium* infection, suggesting a functional relationship between these 6 genes in *Plasmodium* defence. However, *TEP3* and *APL1A* were only weakly induced in response to *P. yoelii* infection, which implies that these genes come into play under specific circumstances.

The *Plasmodium* time courses showed intrinsic variability between replicates due to uncontrollable biological factors, such as infection levels, minor temperature fluctuations and mosquito rearing conditions. For the *P. berghei* time courses in particular, peak gene expression for particular LRIMs occurred at different time points in the two replicates. In replicate 1, most LRIMs peaked at 48 h post infectious blood meal whereas they peaked at 72 h in replicate 2. Despite this temporal shift, *LRIM1*, *APL1C* and *TEP1* remained tightly co-regulated in replicate 1 and 2 (Figure 4.5). Importantly, peak fold change in replicates 1 and 2 were of the same magnitude – it seems there was a 24 h lag in response time in replicate 2. The parasitemia (percentage of infected red blood cells in a blood smear) of the mouse used for replicate 1 was higher than in replicate 2, therefore it is likely that the level of infection was lower in replicate 2. *LRIM15* was an interesting exception, peaking at 48 h in both *P. berghei* experiments. Perhaps *LRIM15* was induced by the quality of infected blood rather than the parasite *per se*. LRIMs were considerably less responsive in *P. yoelii* infection replicate 2 compared to replicate 1, indicating the infection was much lower in replicate 2. Indeed, surviving mosquitoes from the *P. yoelii* time courses were dissected 7 days after infection and both median parasite load and prevalence were lower in replicate 2 (data not shown).

LRIM4, *LRIM17*, *TEP12* and *TEP14* clustered together in Figure 4.3, which implied the possibility of cooperative function. Interestingly, *LRIM4*, *LRIM17*, *TEP12* and *TEP14* showed similar transcriptional responses to *Plasmodium* (Figure 4.6), supporting the hypothesis that these genes work together in the mosquito immune response. These genes were induced at 48 h after *P. berghei* infection, 24 h

after *P. yoelii* infection and 48 h after *P. falciparum* infection. *LRIM17* was the only exception as it was not induced by *P. falciparum*. This was surprising as *LRIM17* has previously been reported as a major antagonist of *P. berghei* and *P. falciparum* in the *An. gambiae* Keele strain (Dong et al., 2006a; Garver et al., 2012).

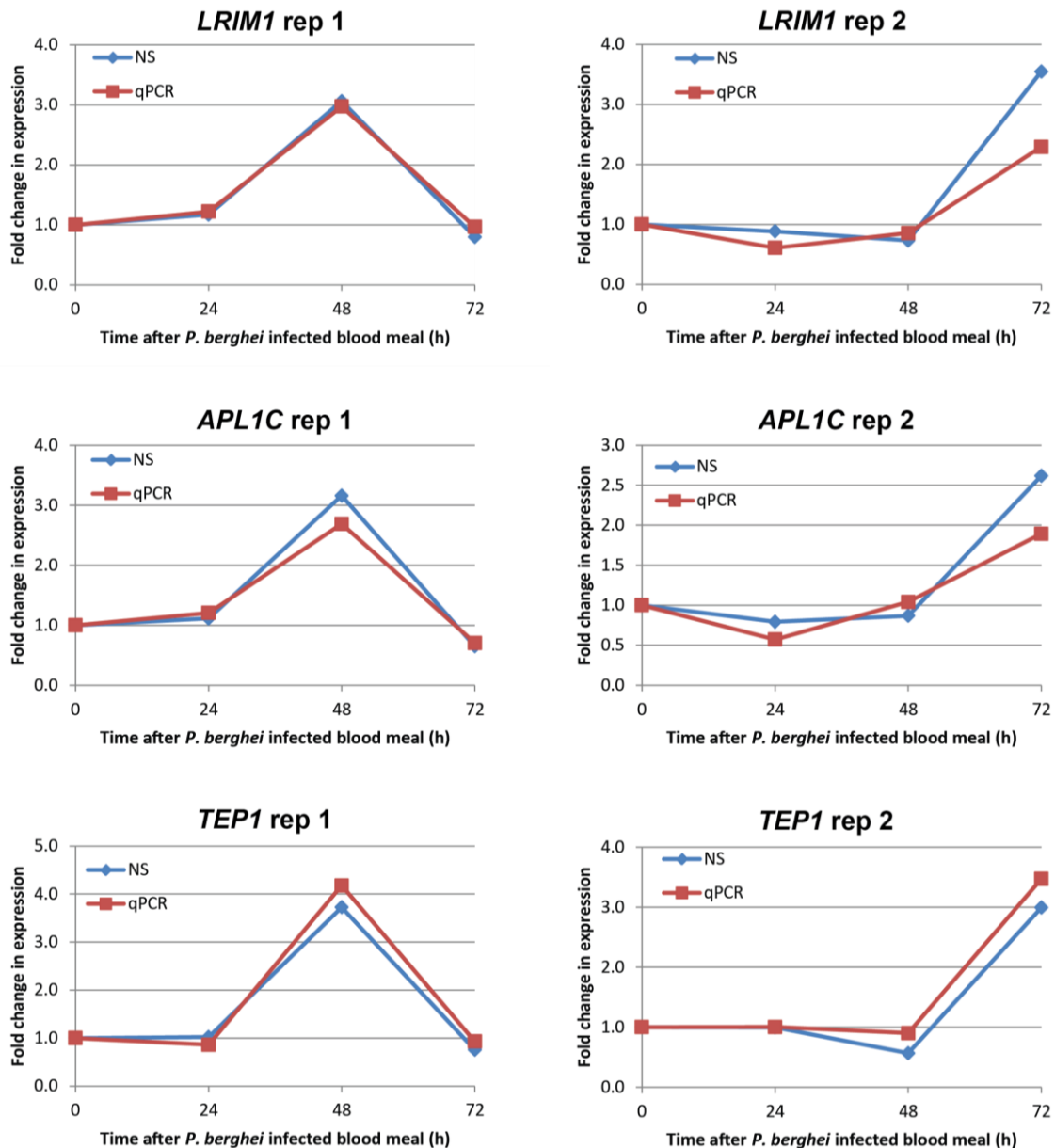


Figure 4.5 Transcriptional co-regulation of *LRIM1*, *APL1C* and *TEP1* after *P. berghei* infection.

Expression of *LRIM1*, *APL1C* and *TEP1* was measured 24, 48 and 72 h after taking a *P. berghei* infected blood meal. Both NanoString (blue line) and qRT-PCR (red line) were used, normalising to *S7*. Fold change in expression from 2 independent experiments is shown separately (replicate 1 on the left, replicate 2 on the right). Expression was normalised to naïve blood feeding at each time point. Fold change in expression was calculated relative to unfed mosquitoes (time “0 h”).

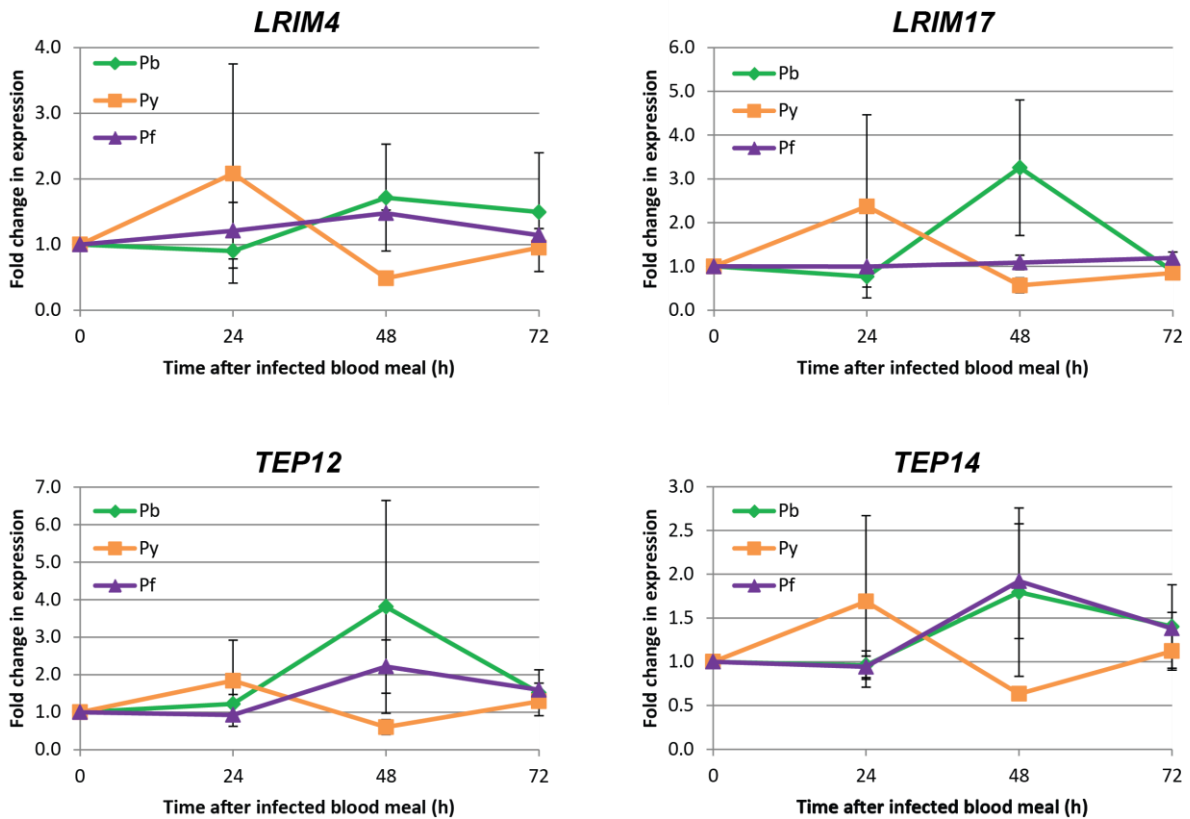


Figure 4.6 Transcriptional co-regulation of *LRIM4*, *LRIM17*, *TEP12* and *TEP14* after *Plasmodium* infection.

Mosquitoes were infected with *P. berghei* at 19 °C (green line), *P. yoelii* at 25 °C (orange line) or *P. falciparum* at 27 °C (purple line). Expression of *LRIM4*, *LRIM17*, *TEP12* and *TEP14* was measured after 24, 48 and 72 h by NanoString, normalising to S7. Average relative expression from 2 independent experiments is shown, with standard error bars. Expression was normalised to naïve blood feeding (at the appropriate temperature) at each time point. Fold change in expression was calculated relative to unfed mosquitoes (time “0 h”).

In addition to *LRIM17*, other LRIMs showed distinct responses to particular parasite species. Although parasite infections were performed at different temperatures (19 °C for *P. berghei*, 25 °C for *P. yoelii* and 27 °C for *P. falciparum*), responses should be specific to the parasite and independent of temperature because each time point was normalised against naïve blood feeding at the same temperature. *TEP3*, *APL1A*, *LRIM5*, *LRIM7* and *TEP15* responded to *P. berghei* and *P. falciparum* but not *P. yoelii*. Curiously, *LRIM5* and *LRIM7* were hierarchically clustered in Figure 4.3, with *TEP15* in a neighbouring cluster.

The Short LRIMs, *LRIM8A*, *LRIM8B*, *LRIM9* and *LRIM10*, were not transcriptionally responsive to any of the three *Plasmodium* species tested. Only very minor responses were observed. To clarify, these LRIMs were induced during a *Plasmodium* infection but the responses were no higher than after

naïve blood feeding, suggesting that these LRIMs do not specifically respond to parasites in a blood meal.

Transcriptional responses to injection of sterile PBS and conditioned media

PBS injection was performed as a control for bacterial and fungal injection, while injection of conditioned media from uninfected VERO cells was performed to normalise ONNV injection. Both were also analysed separately to give an indication of injury responses. Overall, most genes did not respond to injection of sterile solutions; however, distinct weak responses were observed for some genes (Figure 4.7). *LRIM6* showed the strongest upregulation after PBS injection, with a 2-4-fold induction compared to uninjected mosquitoes. Interestingly, *LRIM6* demonstrated no response to conditioned media injection.

LRIMs and TEPs were more responsive to injection of conditioned media compared to PBS. *LRIM15* was non-responsive to PBS but 2.5-fold induced by conditioned media injection (Figure 4.7). *LRIM12* and *TEP6* were also induced by conditioned media not PBS injection. VERO cells were grown in MEM supplemented with 10% FBS, L-glutamine, non-essential amino acids, penicillin/streptomycin and fungizone (amphotericin B). The conditioned media would contain the supplemented MEM and any host proteins secreted by the VERO cells. It is likely that this protein-rich content was responsible for the increased induction of genes. The Short LRIM cluster, *LRIM8A*, *LRIM8B*, *LRIM9* and *LRIM10*, were weakly induced by conditioned media injection. As these four LRIMs were highly induced by blood feeding, this was probably a response to the serum in the conditioned media. It should be noted that the conditioned media injection time course used one different time point to PBS. Samples were collected at day 1 (24 h), day 3 (72 h) and day 6 (144 h) to match the slower process of viral infection. Despite this discrepancy, it is still reasonable to compare PBS and conditioned media injection.

Many LRIMs and TEPs were not induced by PBS or conditioned media injection. *LRIM1* was downregulated in response to PBS injection and neutral in response to conditioned media injection (Figure 4.7), as were its functional partners, *APL1C* and *TEP1*. In fact, most genes were downregulated by PBS injection.

It is not clear whether either of these experiments highlights injury responses rather than responses to the introduction of PBS or conditioned media into the hemocoel. Injection of sterile PBS is likely to be closest to an injury response because of its basic content, however, mosquitoes could be responding to changes in salt balance. For example, *LRIM6* could be involved in maintenance of salt homeostasis.

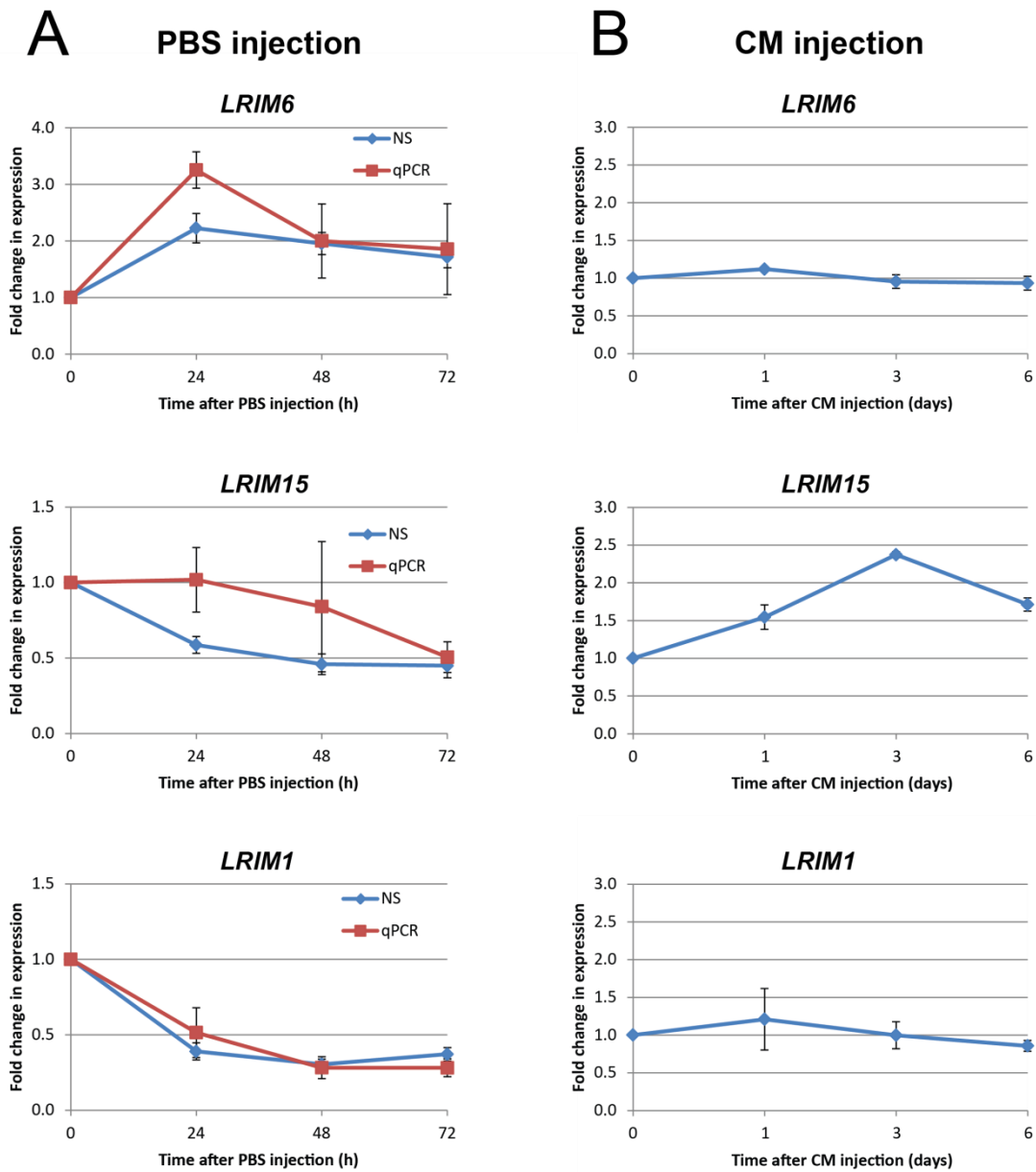


Figure 4.7 Representative transcriptional responses to injection with PBS or conditioned media.

A) Transcriptional responses of *LRIM6*, *LRIM15* and *LRIM1* were monitored 24, 48 and 72 h after sterile PBS injection. Expression was measured by NanoString (blue line) and qRT-PCR (red line), normalising to *S7*. Average fold change in expression from 4 independent experiments is shown (only 3 by qRT-PCR), with standard error bars. Results were calculated relative to uninjected mosquitoes (time “0 h”).

B) Expression of *LRIM6*, *LRIM15* and *LRIM1* was determined 1, 3 and 6 days after injection of conditioned media from uninfected VERO cells. Expression was measured by NanoString only, normalising to *S7*. Average relative expression from 2 biological replicates is shown.

Transcriptional responses to viral infection

Expression of LRIMs and TEPs was analysed after infection by ONNV, both by injection and blood feeding. Responses were more conservative than expected, with few genes upregulated above 2-fold. Genes induced by both injection and blood feeding of ONNV included *LRIM1*, *LRIM4*, *LRIM7*, *LRIM8A*, *LRIM12*, *LRIM15*, *TEP3* and *TEP4*. These genes are candidates for roles in viral immunity. Of these, *LRIM7* and *LRIM15* showed the most consistent upregulation across the two independent experiments (Figure 4.8). Overall, biological replicate 2 produced a stronger transcriptional response and some genes only responded to virus in this replicate, including *LRIM4*, *LRIM12* and *LRIM8A* (Figure 4.8). Plaque assays using individual virally injected mosquitoes showed that the average PFU per mosquito was slightly higher in this second replicate (Figure 4.9 A; not significant using Mann Whitney U-test). Furthermore, prevalence of viral infection was 67% in replicate 1 and 74% in replicate 2. Therefore, virus load had a strong influence over LRIM expression in response to ONNV.

Differences were observed between systemic infection of virus via injection and oral infection via blood feeding. After intrathoracic injection, the virus is dispersed through the hemolymph and infects various tissues, such as the head, salivary glands and muscle, with the initial acute phase of infection peaking at day 6-8 before declining (Joanna Waldock, PhD thesis, 2011). In contrast, after oral infection, the virus first infects the gut about 24 h after ingestion of the blood meal and there is a low frequency of dissemination via the hemolymph to secondary tissues in the following days (Brault et al., 2004). Mosquitoes were predominantly infected in the cardia (foregut-midgut junction) and the anterior gut following ONNV blood feeding (Figure 4.9 B), consistent with previous reports (Joanna Waldock, PhD thesis, 2011). Interestingly, *LRIM17* was only induced after viral infection by blood feeding (Figure 4.8). *LRIM7* also showed a stronger response after oral infection. Other LRIMs, like *LRIM15*, showed a delayed response after blood feeding compared to injection, with expression peaking at day 3 and day 1, respectively (Figure 4.8). Expression of *LRIM7* peaked at day 3 after injection and day 6 after blood feeding. This time lag probably represents the delay in virus dissemination into the hemolymph after oral infection.

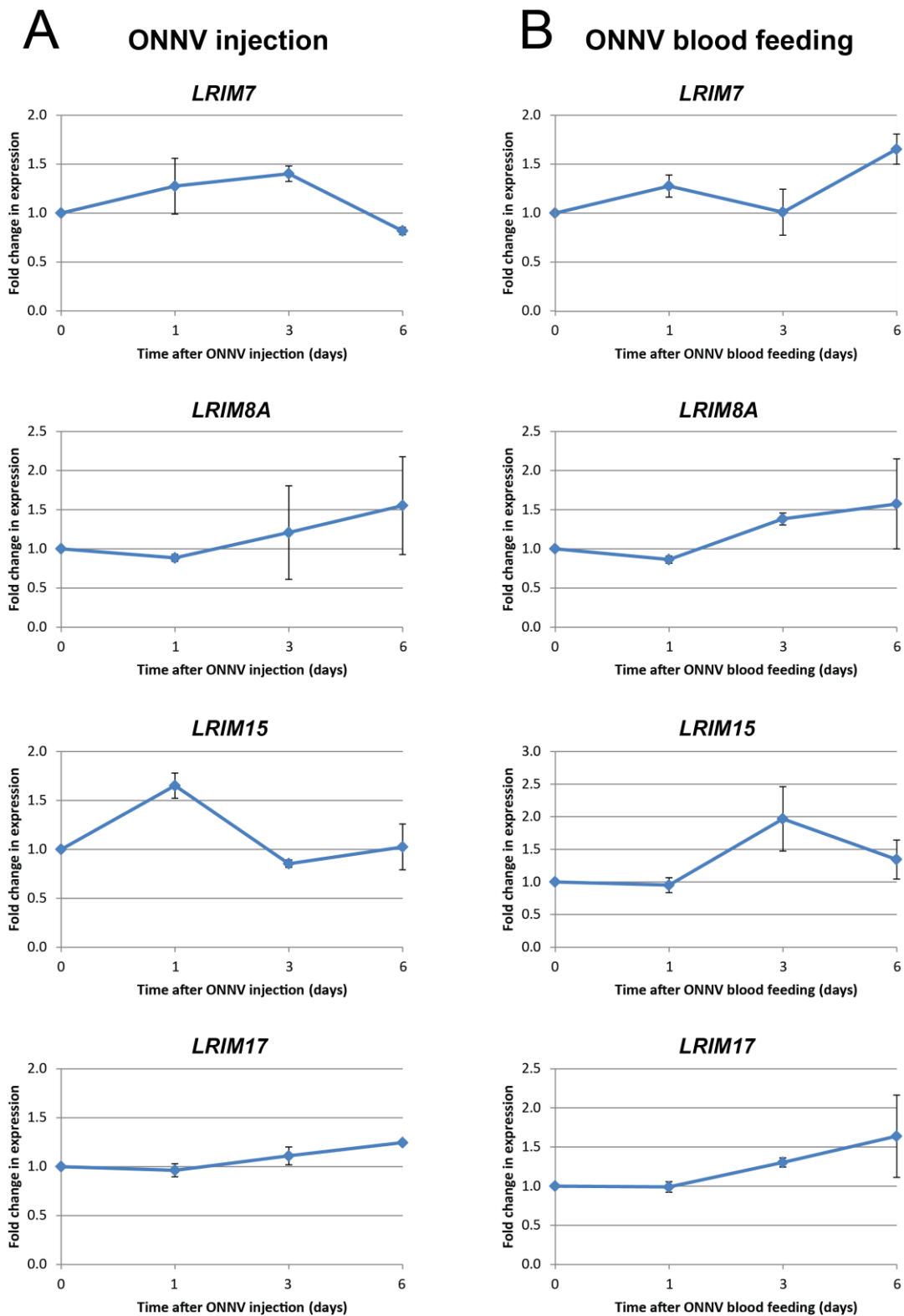


Figure 4.8 Responses to injected ONNV and blood fed ONNV.

A) Transcriptional responses of *LRIM7*, *LRIM8A*, *LRIM15* and *LRIM17* were monitored 1, 3 and 6 days after injection with ONNV (collected in conditioned media of infected VERO cells). Expression was measured by NanoString, normalising to *S7*. Average relative expression from 2 independent experiments is shown, with standard error bars. Expression was normalised to injection of conditioned media from uninfected cells at each time point. Fold change in expression was calculated relative to uninjected mosquitoes (time “0 h”). **B)** As above, but mosquitoes were given an ONNV infected blood meal and expression was normalised to naïve blood fed mosquitoes.

No particular hierarchical cluster appeared to be strongly viral specific (Figure 4.3). It is interesting that *LRIM1* responded to ONNV but its usual partners, *APL1C* and *TEP1*, did not. Also, *LRIM8A* was the only member of the Short LRIM cluster to be induced by viral infection. *LRIM4* and *LRIM17*, which are co-clustered, were both induced by replicate 2 of the viral infection, although *LRIM17* was only responsive to oral infection. *LRIM4* and *LRIM17* also clustered with *TEP12* and *TEP14* (Figure 4.3). *TEP12* was mildly induced by oral infection but *TEP14* was non-responsive to all viral challenges.

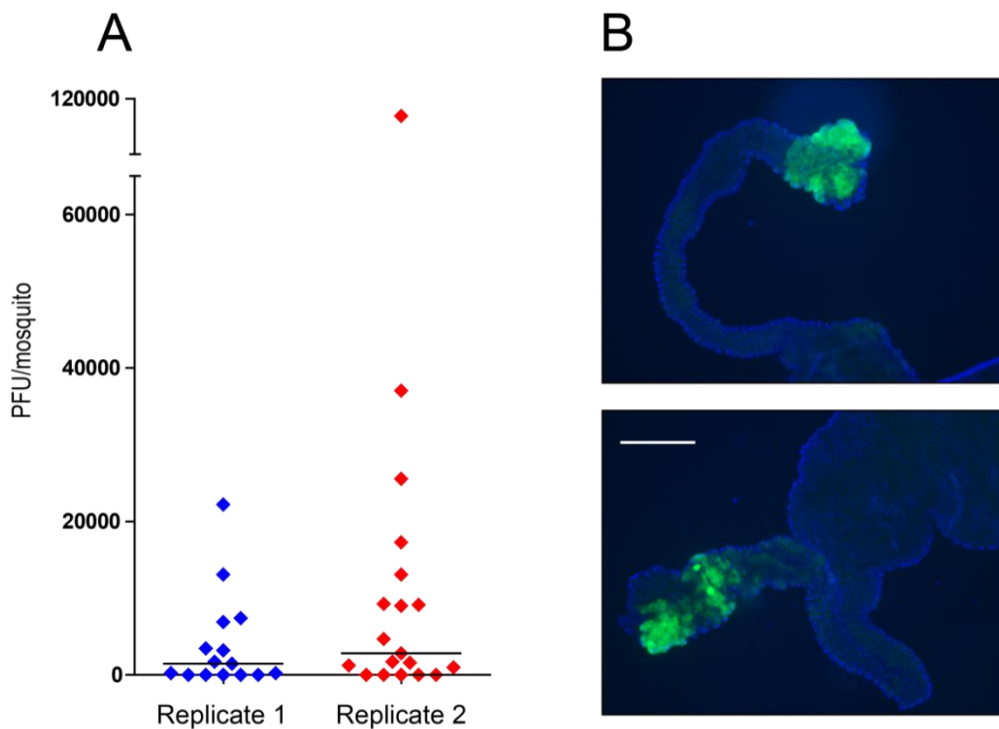


Figure 4.9 Viral load and tissue tropism in ONNV infected mosquitoes.

A) Plaque assays were performed on individual mosquitoes 6 days after ONNV injection. PFU per mosquito, which demonstrates viral titre, is shown for 2 independent replicates. Horizontal lines indicate the median. **B)** Entire guts were dissected 6 days after feeding on ONNV infected blood and analysed using fluorescent microscopy to determine tissue tropism of infection. Two representative guts are shown with GFP-expressing virus in green and gut cells in blue (DAPI staining). Scale bar (bottom panel) represents 250 μM.

Transcriptional responses to bacteria

Many LRIMs and TEPs showed strong induction following injection with live *E. coli* (gram-negative bacteria) and *S. aureus* (gram-positive bacteria). In fact, of all the challenges performed, the TEPs responded most highly to bacterial injection. Key genes upregulated by both bacterial species were *LRIM1*, *APL1A*, *APL1C*, *TEP1*, *TEP3* and *TEP4*, which co-cluster as shown in Figure 4.3. Expression of these genes peaked rapidly between 4- and 10-fold 24 h after *E. coli* injection (Figure 4.10), with similar responses to *S. aureus*. Of the 6 co-regulated genes, *APL1A* showed a slightly delayed response to bacterial challenge and peaked at 48 h in some experiments. These 6 genes were also co-regulated in response to *Plasmodium* infection, which might suggest they function together as core immune genes that protect mosquitoes from many pathogens.

NanoString fold changes in expression of the LRIMs and some TEPs were verified by qRT-PCR. Unfortunately, the matching qRT-PCR data for biological replicate 1 had to be excluded because of technical problems. Nevertheless, the qRT-PCR results for replicate 2 correlated well with the NanoString data. Although some differences in fold change were observed, overall trends were preserved.

Another hierarchical cluster, *LRIM4*, *LRIM17*, *TEP12* and *TEP14*, was also induced by *E. coli* and *S. aureus* injection. This strengthens the hypothesis of a functional relationship between these genes. *TEP2* and *LRIM12*, another cluster, also shared a similar pattern of induction following bacterial challenge. Interestingly, whilst *LRIM8A* was the only member of the Short LRIM cluster induced by viral infection, *LRIM8B* was the sole member upregulated by *E. coli* and *S. aureus*. Other genes induced by bacteria included *LRIM16A*, *TEP6*, *TEP13* and *TEP15*.

Overall, very similar responses were observed to *E. coli* and *S. aureus*, suggesting that the responsive genes are regulated by the same signalling pathway(s) that can be activated by gram-negative and gram-positive bacteria. Whether there are functional differences at the protein level remains to be determined. One exception was *TEP9*, which seemed to be specifically induced by *E. coli*.

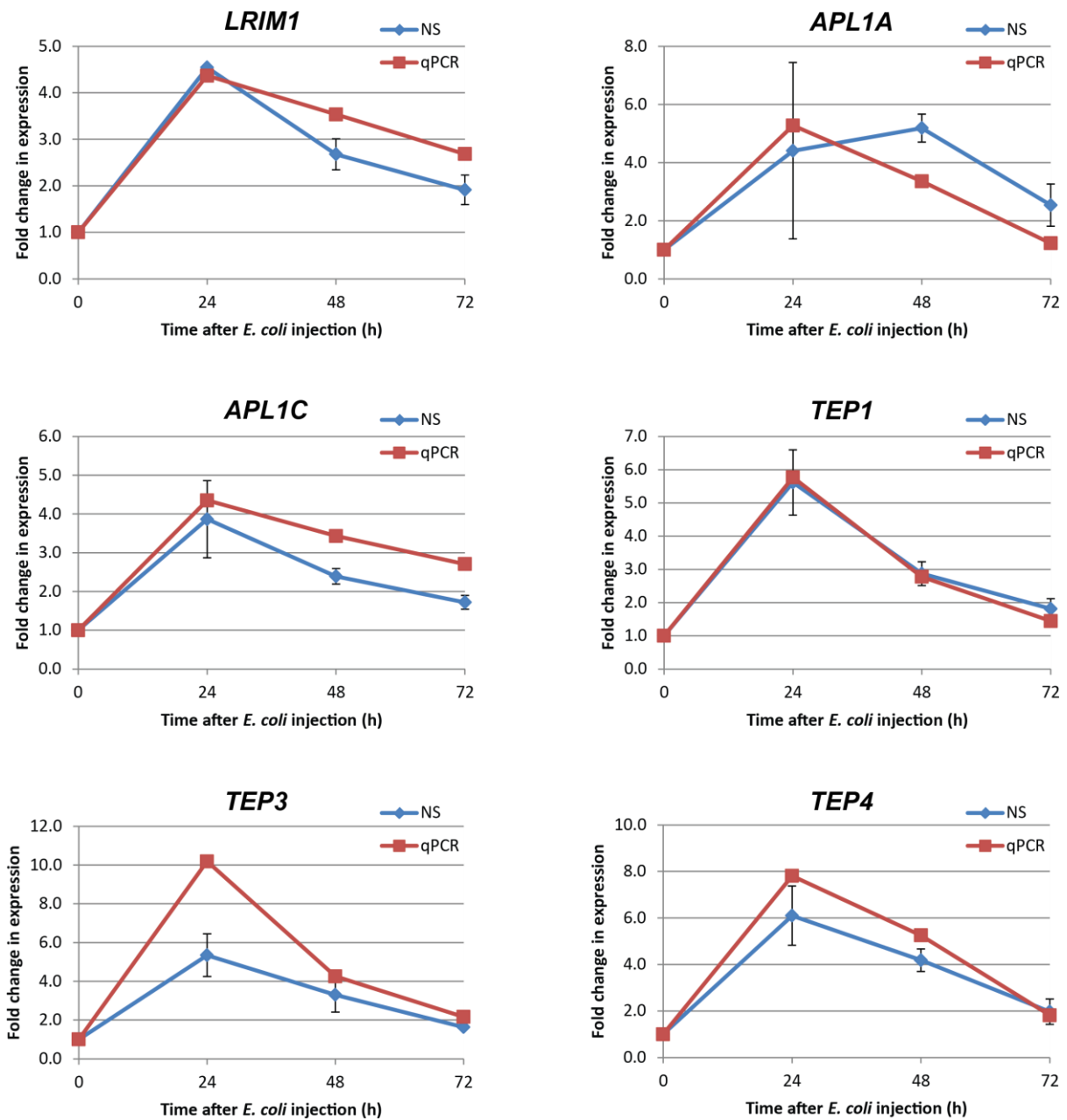


Figure 4.10 A cluster of core immune genes induced by *E. coli* injection.

Mosquitoes were injected with live *E. coli* and expression of *LRIM1*, *APL1A*, *APL1C*, *TEP1*, *TEP3* and *TEP4* was monitored after 24, 48 and 72 h. Expression was measured by NanoString (blue line) and qRT-PCR (red line), normalising to *S7*. Average fold change in expression by NanoString from 2 independent experiments is shown, with standard error bars. Only one replicate was measured by qRT-PCR. Expression was normalised to injection of sterile PBS at each time point. Results were calculated relative to uninjected mosquitoes (time “0 h”).

Transcriptional responses to fungi

A subset of the genes that responded to bacterial infection also responded to injection of *B. bassiana* spores. Four key genes induced by fungal infection, *LRIM1*, *APL1A*, *LRIM17* and *TEP3*, are shown in Figure 4.11. NanoString results were verified by qRT-PCR, with good correlation between both methods. Some differences in fold changes were observed between the two independent replicates. Genes belonging to the core cluster of *LRIM1*, *APL1A*, *APL1C*, *TEP1*, *TEP3* and *TEP4* were all induced by *B. bassiana*. These genes were also all induced by *Plasmodium* and bacteria, suggesting they are core immune genes that protect mosquitoes from many pathogens. *TEP6*, which was upregulated by fungi and bacteria, resided in a neighbouring hierarchical cluster to these 6 genes (Figure 4.3).

LRIM17 was strongly induced by injection of fungal spores. To a lesser extent, *LRIM4*, *TEP12* and *TEP14*, which co-clustered with *LRIM17*, were also upregulated. This is another example of co-regulation between these genes and further evidence to imply a functional relationship.

Overall, LRIMs and TEPs were less responsive to fungi than bacteria. Gene expression also peaked later after fungal infection, with most genes reaching their maximum induction after 48 to 72 h compared to 24 h for bacterial infection. This was probably because germination of fungal spores and proliferation of fungal hyphae takes considerably longer than bacterial proliferation.

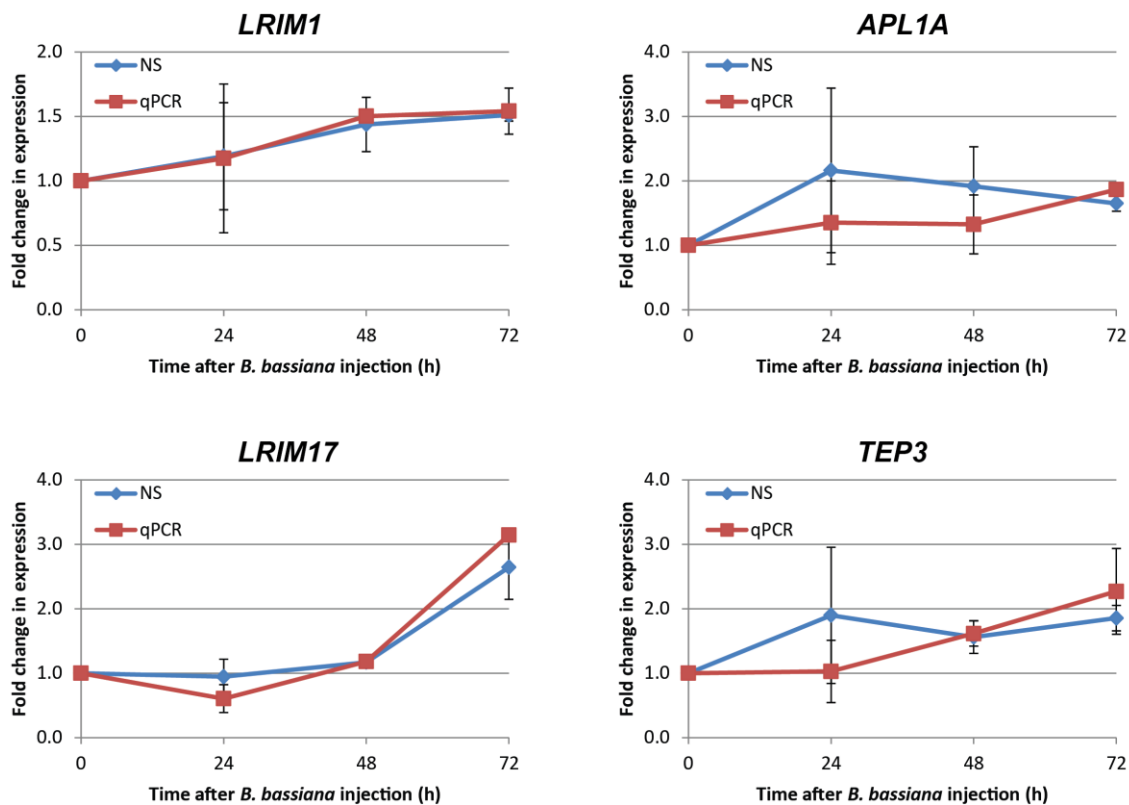


Figure 4.11 Key genes responding to fungal infection.

Expression of *LRIM1*, *APL1A*, *LRIM17* and *TEP3* was monitored 24, 48 and 72 h after injection with *B. bassiana* spores. Both NanoString (blue line) and qRT-PCR (red line) were used, normalising to *S7*. Average fold change in expression from 2 independent replicates is shown, with standard error bars. At each time point, expression was normalised to injection of sterile PBS. Results were calculated relative to uninjected mosquitoes (time “0 h”).

Expression in larvae and pupae

In an initial experiment, expression of LRIMs and TEPs was monitored in RNA extracted from fourth instar larvae and early pupae of *An. gambiae*. Rather than fold changes in expression, the number of times each gene-specific reporter was detected were compared (Table 4.2). Interestingly, some LRIMs and TEPs displayed distinct transcriptional profiles during the developmental cycle of the mosquito.

Some genes were highly expressed throughout all life stages, with high NanoString reporter counts in larvae, pupae and adults (Table 4.2). This included *LRIM1*, *APL1C* and *TEP1*, which suggests the mosquito complement-like system plays a key role in mosquito immunity at all life stages. *LRIM17* and *TEP15* were also highly expressed in larvae, pupae and adults, suggesting they also have an important immune function in these life stages.

Table 4.2 Developmental profile of LRIMs and TEPs in *An. gambiae*.

Gene	Larvae	Pupae	Adult			
			Sugar fed	BF 24 h	BF 48 h	BF 72 h
LRIM1	3454	777	3207	1876	2016	1459
APL1A	211	91	267	106	170	97
APL1B	367	11	25	83	61	11
APL1C	6260	1638	6274	3077	4228	2850
LRIM3	252	584	514	197	256	262
LRIM4	310	205	1119	395	579	644
LRIM5	32	172	155	105	122	118
LRIM6	249	603	606	375	522	337
LRIM7	62	109	154	39	294	129
LRIM8A	47	263	893	1611	916	534
LRIM8B	5	75	2093	4171	2209	923
LRIM9	2	22	2229	2942	3551	1484
LRIM10	7	28	472	1261	777	199
LRIM12	343	58	231	139	53	61
LRIM15	31	92	880	402	810	1674
LRIM16A	120	194	256	199	272	228
LRIM16B	271	575	599	436	494	420
LRIM17	3068	2361	4490	911	2298	2817
LRIM18	93	111	62	100	75	57
LRIM19	0	168	152	21	23	30
LRIM20	171	217	84	88	140	79
LRIM26	370	349	278	636	578	607
LRIM27	34	94	320	115	167	211
TEP1	6928	2024	5564	3377	4635	2818
TEP2	338	134	342	185	174	214
TEP3	243	181	336	262	236	148
TEP4	509	186	832	700	964	574
TEP5	20	23	18	90	52	21
TEP6	192	65	144	33	103	69
TEP9	52	28	20	50	63	18
TEP10	15	9	19	57	41	18
TEP12	690	424	652	186	330	266
TEP13	451	867	160	252	167	128
TEP14	395	134	1138	365	529	461
TEP15	3924	3463	4130	1406	2484	2123

NanoString gene-specific reporter counts, after normalisation to *S7*, are shown for LRIM and TEP genes in RNA samples extracted from larvae, pupae and adult *An. gambiae*. Per sample, RNA was extracted from a pool of 10 whole insects. Larvae and pupae reporter counts are from a single experimental replicate. Reporter counts for sugar fed (untreated) adults are averaged from 12 experiments. Reporter counts for blood feeding (BF) at 24 h, 48 h and 72 h are averaged from 8, 6 and 8 experiments, respectively. Experiments using different temperatures (19, 25 and 27 °C) were pooled together.

Others genes showed extremely low expression in larvae and pupae but very high expression in adult mosquitoes (Table 4.2). These included the Short LRIMs, *LRIM8B*, *LRIM9* and *LRIM10*, which were silent in larvae, slightly higher in pupae and very high in adults. Strikingly, average reporter counts for *LRIM8B* and *LRIM9* in adults were three orders of magnitude above those in larvae. *LRIM8A* showed a similar profile except with slightly greater expression in larvae and pupae than the others. Reporter counts in larvae were the minimum recorded for each of these genes across all experiments (Table 4.1), with *LRIM8B*, *LRIM9* and *LRIM10* expressed at the level of the negative control probes. Interestingly, these four Short LRIMs were massively induced by blood feeding, a behaviour exclusive to adult females. Unfortunately, expression in males was not determined and the sex of the larvae and pupae used was unknown. *LRIM15* was also relatively low in larvae and pupae compared to adults (one order of magnitude lower).

Screening the LRIMs for effects on *P. berghei* development

LRIM1 and *APL1C* are potent antagonists of *P. berghei* development in the mosquito, shown by striking increases in live parasites upon gene silencing (Osta et al., 2004a; Riehle et al., 2006; Riehle et al., 2008). To elucidate whether any other LRIM family members play a role in defence against *P. berghei*, the entire family was screened for a similar phenotype upon gene knockdown. Novel LRIM genes were silenced by RNA interference (RNAi), mosquitoes were infected with GFP-expressing *P. berghei* and parasite load monitored after 7 days. Both fluorescent live oocysts (parasites embedded in the mosquito midgut wall) and melanised ookinetes (dead parasites coated in black melanin) were analysed (Figure 4.12). Prevalence, the percentage of midguts with at least one oocyst or ookinete, was also calculated. *LRIM1* was used as a positive control because silencing *LRIM1* dramatically increases oocyst load (Osta et al., 2004a). Non-specific dsRNA against *GFP*, a gene which does not naturally exist in mosquitoes, was used as a negative control.

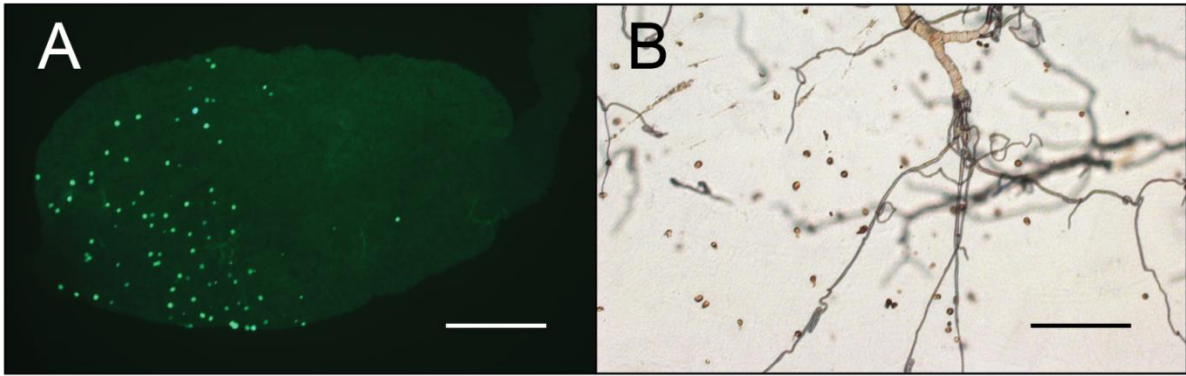


Figure 4.12 *P. berghei* oocysts and melanised ookinetes in the *An. gambiae* midgut.

A) Live GFP-expressing oocysts in the mosquito midgut observed 7 days after infection using fluorescent microscopy. Scale bar represents 500 μ M. **B)** Melanised ookinetes observed 7 days after infection using light microscopy. Scale bar represents 100 μ M.

20 novel LRIM family members were screened and results are reported in Table 4.3. APL1A and APL1B were excluded from the screen as both were previously reported to have no phenotype with *P. berghei* (Riehle et al., 2008). APL1C was not included because its role as a *P. berghei* antagonist is well documented (Riehle et al., 2006; Riehle et al., 2008). Unfortunately, some experiments suffered problems with mosquito death after infected blood feeding and low infection levels. Therefore, these results give a preliminary indication of antagonistic or agonistic phenotypes and further verification is required.

The only novel LRIM with a significant effect on *P. berghei* development was LRIM9, a Short LRIM that was strongly upregulated by blood feeding in the transcriptional analysis (Figure 4.4). Silencing *LRIM9* resulted in a significant increase in the median number of live oocysts, compared to *dsGFP*-treated control mosquitoes (experiment C of Table 4.3). *LRIM9* knockdown also significantly reduced the prevalence of melanisation and the number of melanised ookinetes. However, the effect of *LRIM9* was not as dramatic as upon *LRIM1* or *APL1C* silencing.

Also in experiment C, *LRIM7* and *LRIM10* showed a significant decrease in the number of melanised ookinetes compared to *dsGFP* controls. *LRIM10* also showed a significant reduction in prevalence of melanisation. However, prevalence of melanisation in *dsGFP* was unusually high in this experiment and so the melanisation phenotypes of *LRIM7*, *LRIM9* and *LRIM10* require verification. In experiment E, low prevalence of parasites and failure of the *LRIM1* positive control makes results for *LRIM5*, *LRIM15* and *LRIM20* particularly unreliable.

Knockdown efficiency varied between genes, although the majority of novel LRIMs were silenced by more than 50%. Knockdown efficiency of *LRIM1* was consistently high, averaging 90% across all experiments. Silencing of *LRIM7*, *LRIM8B*, *LRIM18*, *LRIM19* and *LRIM26* was particularly poor. For *LRIM7* and *LRIM8B*, this might explain the marginal increase in live oocysts observed for these genes. At least for *LRIM8B*, sequencing of the PCR product used for dsRNA synthesis ruled out abundant polymorphism for the inefficient knockdown. Knockdown efficiencies for *LRIM18* and *LRIM19* were -18 and -5%, respectively. This unusual result might reflect problems with the qRT-PCR primers or the poor expression of these genes.

In summary, LRIM9 emerged as a novel candidate for a role in *Plasmodium* defence and will be further investigated in Chapter 5. *LRIM9* knockdown did not influence *P. berghei* development to the same dramatic extent as *LRIM1* and *APL1C*. None of the other LRIMs screened changed the outcome of infection, however, these preliminary experiments must be replicated and knockdown efficiencies optimised before firm conclusions are drawn.

Table 4.3 The initial RNAi screen of LRIM genes upon *P. berghei* infection.

Expt (Strain)	Knock-down	N	Live oocysts				Melanised ookinetes				Knockdown efficiency (%)
			Prevalence		Infection intensity		Prevalence		Infection intensity		
			%	P-value	Median (Range)	P-value	%	P-value	Median (Range)	P-value	
A (Y)	GFP	14	79	N/A	2 (0-73)	N/A	43	N/A	0 (0-42)	N/A	N/A
	LRIM1	6	100	NS	462 (46-552)	< 0.001	50	NS	1 (0-3)	NS	80
	LRIM8A	17	65	NS	3 (0-29)	NS	59	NS	2 (0-77)	NS	89
	LRIM8B	16	88	NS	6 (2-160)	NS	31	NS	0 (0-34)	NS	28
B (Y)	GFP	23	91	N/A	9 (0-130)	N/A	39	N/A	0 (0-30)	N/A	N/A
	LRIM1	15	100	NS	367 (64-647)	< 0.0001	13	NS	0 (0-2)	NS	94
	LRIM4	23	96	NS	20 (0-153)	NS	26	NS	0 (0-16)	NS	80
	LRIM17	15	80	NS	6 (0-182)	NS	20	NS	0 (0-24)	NS	92
C (Y)	GFP	17	76	N/A	2 (0-89)	N/A	88	N/A	4 (0-85)	N/A	N/A
	LRIM1	10	100	NS	243 (46-805)	< 0.0001	0	< 0.0001	0	< 0.001 [#]	79
	LRIM7	11	91	NS	13 (0-167)	NS	55	NS	1 (0-10)	< 0.05	26
	LRIM9	14	93	NS	44 (0-285)	< 0.001	14	< 0.0001	0 (0-2)	< 0.0001	65
	LRIM10	18	94	NS	12 (0-92)	NS	44	< 0.05	0 (0-22)	< 0.01	76
D (Ng)	GFP	16	75	N/A	4 (0-22)	N/A	13	N/A	0 (0-3)	N/A	N/A
	LRIM1	13	100	NS	326 (225-748)	< 0.0001	0	NS	0	NS [#]	ND
	LRIM6	10	90	NS	11 (0-33)	NS	0	NS	0	NS [#]	69
	LRIM12	13	69	NS	3 (0-104)	NS	15	NS	0 (0-2)	NS	85
E (Ng)	GFP	29	59	N/A	1 (0-42)	N/A	0	N/A	0	N/A	N/A
	LRIM1	30	37	NS	0 (0-435)	NS	0	N/A	0	N/A	95
	LRIM5	36	11	< 0.0001	0 (0-8)	< 0.0001	0	N/A	0	N/A	77
	LRIM15	38	45	NS	0 (0-86)	NS	0	N/A	0	N/A	78
	LRIM20	37	32	< 0.05	0 (0-61)	NS	0	N/A	0	N/A	92
F (Ng)	GFP	31	100	N/A	60 (1-225)	N/A	26	N/A	0 (0-24)	N/A	N/A
	LRIM1	21	100	N/A	264 (11-642)	< 0.0001	5	NS	0 (0-1)	< 0.05	96
	LRIM16A+B	39	95	NS	46 (0-398)	NS	28	NS	0 (0-25)	NS	62(A) + 39(B)
	LRIM18	41	88	NS	32 (0-238)	NS	22	NS	0 (0-32)	NS	-18
	LRIM19	22	100	N/A	21 (1-235)	NS	23	NS	0 (0-5)	NS	-5

Expt (Strain)	Knock-down	N	Live oocysts				Melanised ookinetes				Knockdown efficiency (%)
			Prevalence		Infection intensity		Prevalence		Infection intensity		
			%	P-value	Median (Range)	P-value	%	P-value	Median (Range)	P-value	
G (Ng)	GFP	31	97	N/A	18 (0-93)	N/A	19	N/A	0 (0-27)	N/A	N/A
	LRIM1	27	96	NS	151 (0-449)	< 0.0001	0	< 0.05	0	< 0.05	95
	LRIM26	35	91	NS	12 (0-60)	NS	9	NS	0 (0-2)	NS	27
	LRIM27	30	87	NS	12 (0-245)	NS	20	NS	0 (0-2)	NS	58
H (Ng)	GFP	38	92	N/A	15 (0-191)	N/A	18	N/A	0 (0-11)	N/A	N/A
	LRIM1	31	94	NS	104 (0-313)	< 0.0001	0	< 0.05	0	< 0.05	92
	LRIM3	46	96	NS	18 (0-210)	NS	11	NS	0 (0-4)	NS	37
	LRIM11	37	76	NS	13 (0-147)	NS	8	NS	0 (0-2)	NS	45

Novel LRIM genes were silenced using RNAi, mosquitoes were infected with fluorescent *P. berghei* and parasite load was monitored after 7 days. Individual experimental data sets are shown (one biological replicate). Non-specific dsRNA (*GFP*) was used as a negative control and *LRIM1* as a positive control. Either Yaoundé (Y) or Ngousso (Ng) strain mosquitoes were used. *N* = number of individual mosquito midguts. Prevalence is the percentage of guts that contain at least one oocyst or melanised parasite. Mann Whitney U-test was used for infection intensity, comparing to *dsGFP*. If prevalence for one gene was zero, the Wilcoxon Test was used (#). Fisher's exact test was used for prevalence. Significant P-values (< 0.05) are shown in red. Knockdown efficiency was calculated by qRT-PCR. NS = Not significant; ND = Not determined; N/A = Not applicable.

4.3 Discussion

The LRIMs are a novel, mosquito-specific family of LRR-containing proteins recently discovered in *An. gambiae*. LRR-containing proteins play key defensive roles in many phyla, including TLRs in mammals and VLRs in jawless vertebrates (Bent and Mackey, 2007; Guo et al., 2009; Han et al., 2008; Herrin et al., 2008; Matsushima et al., 2007). The LRR domain often mediates pathogen recognition and protein-protein interactions (Bell et al., 2003; Bella et al., 2008). The founding members of the LRIM family, LRIM1 and APL1C, are powerful antagonists of the rodent malaria parasites, *P. berghei* and *P. yoelii* (Jaramillo-Gutierrez et al., 2009; Osta et al., 2004a; Riehle et al., 2006; Riehle et al., 2008), and have an infection intensity-dependent impact on the human parasite, *P. falciparum* (Garver et al., 2012). It was hypothesised that the LRIM family has expanded to mediate recognition of the wide range of pathogens that mosquitoes encounter. As LRIMs are only found in mosquitoes, their function may be associated with blood feeding, perhaps in regulating infections to the various blood-borne pathogens and parasites.

Transcriptional profiling was used to determine whether there is specificity in the responses of different LRIMs to distinct immune challenges. It was hoped the profiling would identify candidates for involvement in defence against particular pathogens. Activation of immune effectors and mechanisms is largely regulated at the transcriptional level in *An. gambiae* (Aguilar et al., 2005b). Previous studies have demonstrated that gene expression and putative function show good correlation (Dimopoulos et al., 2002). The TEP family was included in the analysis as potential interacting partners of the LRIMs. Hierarchical clustering of the transcriptional data was used to provide clues about the functional relationships between LRIMs and TEPs.

Overall, LRIM family members showed distinct transcriptional responses to different immune challenges, such as blood feeding, *Plasmodium* parasites, bacteria, fungi and virus. This correlates well with the hypothesis that the LRIMs are PRRs responding to different pathogens faced by mosquitoes. To a lesser extent, the TEPs also demonstrated transcriptional specificity. Several LRIMs and TEPs seem to be generalists that responded to many challenges and are probably core immune genes. The versatile LRR domain is capable of detecting various structurally unrelated ligands (Bell et al., 2003) and so these LRIMs might recognise several PAMPs or “danger signals”. Alternatively, they might be activated by a range of other immune effectors under different circumstances. The generalist TEPs could be capable of opsonising a variety of pathogen surfaces, signalling their destruction. Upon proteolytic activation, TEPs covalently bind to pathogens via their TE bond (Levashina et al., 2001). TEPs lacking an active TE, like TEP3, are likely to play a regulatory role (Christophides et al., 2002). Core immune LRIMs and TEPs responded most strongly to *Plasmodium*

and bacterial infections. This correlates well with previous studies reporting a significant overlap in mosquito immune responses against malaria parasites and bacteria (Christophides et al., 2002; Dimopoulos et al., 2002; Dong et al., 2006a). Furthermore, midgut bacteria have been demonstrated to prime the mosquito's basal immune response, which can limit *Plasmodium* development (Dong et al., 2009; Meister et al., 2009).

LRIM1, *APL1C* and *TEP1* were upregulated by many challenges, which correlates well with their important role in the mosquito complement-like system. These three genes transcriptionally co-clustered with *TEP3*, *TEP4* and *APL1A*. This strongly supports the previous finding that the LRIM1/APL1C complex interacts with processed forms of TEP3 and TEP4 *in vitro* (Povelones et al., 2011). The transcriptional co-regulation demonstrated in this Chapter suggests these interactions are likely to be functionally important *in vivo*. In addition, *APL1A* has been reported to protect against infection by *P. falciparum* (Mitri et al., 2009). TEP3, TEP4 and APL1A should be further investigated for roles in the mosquito complement-like system. In Chapter 5, the roles of TEP3 and TEP4 in *P. berghei* infections and melanisation will be explored.

Another potential functional group are *LRIM4*, *LRIM17*, *TEP12* and *TEP14*, which showed broad upregulation in response to various challenges. These four genes were hierarchically clustered together, suggesting the proteins might function in the same or related biochemical pathway(s). LRIM4 and LRIM17 have previously been implicated in *P. falciparum* defence (Dong et al., 2006a), which implies TEP12 and TEP14 could be important candidates for activity against this important human pathogen.

Other LRIMs and TEPs responded to specific challenges indicating they might play a more targeted immunity role. Specialists included the Short LRIMs, *LRIM8A*, *LRIM8B*, *LRIM9* and *LRIM10*, which were dramatically upregulated by naïve blood feeding yet unresponsive to most other challenges. These blood feeding specific LRIMs might be adapted to defend against vertebrate proteins, antibodies, viruses or parasites present in the blood meal, tissue damage caused by midgut distension during blood feeding or specific bacteria found in the mosquito gut that proliferate after a blood meal. The response of the Short LRIMs varied with temperature, which is known to impact on mosquito physiology, such as blood metabolism, but also bacterial proliferation. *LRIM6* was the only LRIM specifically upregulated by PBS injection, which might indicate a role in injury responses or maintenance of salt homeostasis.

Some genes, such as *LRIM3*, *LRIM27*, *LRIM16A* and *LRIM16B*, were barely responsive to any of the challenges. This was not due to poor complementarity between the NanoString probes and these

transcripts as NanoString results were verified by qRT-PCR. It is possible that these genes have important functions but are not transcriptionally responsive. They are unlikely to be pseudogenes because they have not accumulated stop codons and it is evolutionarily costly and potentially dangerous to transcribe and translate non-functional genes. Alternatively, these unresponsive genes might be involved in defence against pathogens untested to date, such as filarial worms.

Several LRIMs, such as *LRIM18*, *APL1B*, *LRIM19*, and many TEPs were very poorly expressed with low NanoString reporter counts in all experiments. It is uncertain whether changes in relative expression of these genes are biologically significant or biased by the low expression levels. These genes might be highly specific responders, redundant or pseudogenes, although there is no evidence of accumulation of stop codons in their sequences. TEPs are highly polymorphic (Obbard et al., 2008), which might reduce the efficiency of NanoString probe hybridisation. However, NanoString probes are quite long and so they are expected to tolerate SNPs well. It was difficult to silence the transcripts of *APL1B* (data not shown), *LRIM18* and *LRIM19* by RNAi. In the RNAi screen with *P. berghei*, the knockdown efficiencies for *LRIM18* and *LRIM19* were very low, which supports the hypothesis that these genes are not expressed. Alternatively, they might be expressed at low levels in a tissue refractory to RNAi-mediated gene knockdown.

NanoString results were verified by qRT-PCR and, overall, the comparison was very good. Even when fold changes differed between methods, trends in expression were the same or very similar. Any minor differences could be accounted for by the different templates used: the NanoString utilises unamplified total RNA whereas the template for qRT-PCR is cDNA synthesised from this RNA. cDNA synthesis can introduce gene-specific or 3' biases, particularly affecting low abundance transcripts (Geiss et al., 2008). As qRT-PCR involves multiple steps where tiny volumes are pipetted by hand, there is more opportunity for the introduction of error than with the NanoString assay.

Overall, the NanoString transcriptional profiling correlated well with previous reports. For *Plasmodium*, a previous microarray showed *LRIM7* is induced by *P. berghei* infection (Dong et al., 2006a), which agrees with the NanoString data. The same microarray found *LRIM4*, *LRIM8B*, *LRIM10* and *LRIM17* to be upregulated in the midgut after *P. falciparum* invasion (Dong et al., 2006a). The NanoString also showed minor induction of *LRIM4* and *LRIM8B* in whole mosquitoes after *P. falciparum* infection but not *LRIM10* and *LRIM17*. Perhaps expression in the whole mosquito masks the effect of individual tissues, such as the midgut. Gene silencing of *APL1A* was reported to increase the prevalence of *P. falciparum* infection (Mitri et al., 2009). Indeed, *APL1A* was induced by *P. falciparum* in the current study at the time of ookinete invasion. It was also upregulated by *P. berghei* and weakly by *P. yoelii*. This may indicate that the mechanisms controlling transcriptional

regulation of *APL1A* cannot distinguish between *Plasmodium* species but *APL1A* can only bind to epitopes on the surface of *P. falciparum*. Furthermore, *APL1A* expression is at least partly regulated by Imd and REL2-S (Mitri et al., 2009).

Differences and similarities were evident between the responses of LRIMs to the rodent parasites, *P. berghei* and *P. yoelii*, and the human parasite, *P. falciparum*. *LRIM1*, *APL1C* and *LRIM4* were transcriptionally induced by all *Plasmodium* parasites at approximately the time of ookinete invasion. For *LRIM1* and *APL1C*, this correlates well with their known roles as antagonists of *P. berghei* and *P. yoelii* (Jaramillo-Gutierrez et al., 2009; Osta et al., 2004a; Riehle et al., 2006) and, dependent on infection intensity, *P. falciparum* (Garver et al., 2012). *LRIM4* knockdown did not affect *P. berghei* development but this LRIM is a candidate for involvement in *P. falciparum* defence. Other LRIMs were specifically induced by *P. berghei* (e.g. *LRIM17*) and *P. falciparum* (e.g. *LRIM20*). Previous studies have shown that mosquito responses against *P. berghei* and *P. falciparum* involve both common and species-specific components (Dong et al., 2006a; Tahar et al., 2002). Importantly, the time points used only covered ookinete invasion and early oocyst formation but did not show mosquito responses to sporozoites in the hemolymph, which occurs approximately 2 weeks after *P. berghei* infection (Sinden, 2002). Immune responses against sporozoites are poorly characterised to date. It would be interesting to see if the same LRIMs are induced in response to sporozoite release into the hemolymph and invasion of the mosquito salivary glands. As the parasite displays distinct surface antigens at each developmental stage, it is plausible that different LRIMs could recognise the sporozoite.

Although *P. berghei* is not a natural parasite of *An. gambiae*, it has become a powerful laboratory model to dissect the mosquito immune response to *Plasmodium*. It is often assumed that virulence is artificially high in host-pathogen associations that have not co-evolved (Hogg and Hurd, 1997). This was supported by meta-analysis showing that unnatural *Plasmodium-Anopheles* combinations are more likely to reduce mosquito survival than natural associations (Ferguson and Read, 2002). Unnatural associations often have higher infection levels (Boete, 2005; Hogg and Hurd, 1997). For example, *P. berghei* infections of *An. gambiae* result in higher oocyst levels than *P. falciparum* infections (Tahar et al., 2002), which might contribute to differences in gene expression. Low numbers of oocysts in natural *P. falciparum* infections has been associated with increased mosquito survival (Boete, 2005). *P. falciparum* and *An. gambiae* have a complex relationship that has been finely tuned by co-evolutionary adaptation. The mosquito has adapted to tolerate a certain level of parasitism because excessive immune responses would be detrimental to mosquito fitness (Boete, 2005). Reducing parasite load is beneficial to both the host and parasite by increasing host survival

and reducing competition between individual parasites. In turn, the parasite has evolved to exploit, suppress and evade the mosquito immune system to complete its sexual developmental cycle and be transmitted to a new vertebrate host. Gene silencing often has a stronger effect in unnatural host-pathogen associations. For example, *LRIM1* and *APL1C* display strong RNAi phenotypes with *P. berghei* (Osta et al., 2004a; Riehle et al., 2006; Riehle et al., 2008), but are only antagonists of *P. falciparum* at medium and low infection intensities, respectively (Garver et al., 2012). It seems likely that *P. falciparum* has evolved to avoid particular immune pathways to aid its transmission. In fact, a recent report provided evidence that certain strains of *P. falciparum* evade the mosquito complement-like system in the L3-5 strain of *An. gambiae* (Molina-Cruz et al., 2012). Comparing *LRIM* function in *P. berghei* and *P. falciparum* infections has provided insights into the mechanisms of immune evasion used by *P. falciparum*.

Transcriptional responses to *Plasmodium* parasite infections showed considerable intrinsic variability between replicates. Known partners, *LRIM1*, *APL1C* and *TEP1*, were co-regulated in all replicates, demonstrating that this variation was biological rather than experimental. It could represent the complex interplay between at least four different taxa: vertebrate, parasite, mosquito and endogenous midgut bacteria. Minor uncontrollable changes in any of these systems and additional environmental factors can affect gene expression. Higher infection intensities could result in increased speed and magnitude of gene induction, which is likely to explain the differences between *P. yoelii* replicates 1 and 2. Parasite developmental stages, such as gametocytes, present in the mouse blood can differ considerably depending on time of feed. Blood meal nutrients also vary, which could affect proliferation of midgut bacteria and therefore transcriptional responses. Levels of mosquito midgut bacteria vary between individual mosquitoes and can affect oocyst formation (Dong et al., 2009; Meister et al., 2009). Slight changes in mosquito age and temperature could also play a role.

Several genes, including *LRIM1*, *LRIM7*, *LRIM8A*, *LRIM15*, *TEP3* and *TEP4*, emerged as candidates for involvement in viral defence. These were induced by ONNV infection via blood feeding and injection. The *LRIMs* could be involved in recognition of viral particles in the hemolymph whereas the *TEPs* might be involved in viral opsonisation. Many *LRIMs* responded most strongly after ingestion of virally infected blood, which is the natural infection route. Perhaps it is viral penetration of the mosquito gut wall that induces expression of immune genes as well as the presence of virus particles in the hemolymph. More genes were induced at higher viral load, which could reflect a threshold for gene induction or the increased tissue damage caused by more virus particles. Viral responses were consistent with a previous microarray in which whole mosquitoes were analysed 1, 4 and 9 days

after inoculation with ONNV (Waldock et al., 2012). In this previous study, *LRIM1*, *LRIM4*, *LRIM7*, *LRIM10*, *LRIM17*, *TEP4*, *TEP12*, *TEP10*, *TEP9* and *TEP14* were all induced by ONNV injection. With the exception of *TEP14*, all these genes responded to ONNV infection in this NanoString analysis, although some genes only responded after a viral blood meal rather than injection. Interestingly, *LRIM4*, *LRIM17*, *TEP12* and *TEP14* hierarchically clustered in the present study, suggesting they might function in a viral defence pathway.

Anopheles mosquitoes are poor viral vectors and, to date, are only able to transmit ONNV (Waldock et al., 2012). In contrast, *Aedes* and *Culex* mosquitoes transmit many arboviruses, including dengue, CHIKV and WNV (Tolle, 2009). This leads to the intriguing hypothesis that LRIMs and TEPs in *Anopheles* are more efficient at recognising and killing viral particles than their *Aedes* and *Culex* counterparts. It would therefore be interesting to elucidate the responses of LRIMs and TEPs to viral infection in *Aedes* and *Culex* mosquitoes. If the hypothesis is confirmed, expressing *Anopheles* LRIMs or TEPs in other mosquitoes could reduce their ability to transmit arboviruses, which would be an exciting prospect for arboviral control.

Many LRIMs and TEPs were induced by bacterial challenge, including components of the mosquito complement-like pathway. This was largely concurrent with previous reports. In agreement with the NanoString analysis presented here, a previous microarray reported that *TEP4* is upregulated by gram-negative and gram-positive bacteria and *TEP4* knockdown decreases survival upon bacterial challenge (Dong et al., 2006a; Dong et al., 2009). *LRIM8B*, *LRIM10*, *LRIM17* and *TEP1* were induced by *E. coli* infection in an earlier microarray (Dong et al., 2006a), which agrees with the current data, except all but *LRIM10* were also induced by *S. aureus*. This might reflect differences in the *S. aureus* strains used in the two studies. *APL1* (prior to re-annotation as *APL1A*, *APL1B* and *APL1C*) was induced by both gram-types in the same microarray (Dong et al., 2006a) and all three *APL1* genes were also upregulated in the NanoString analysis. Several LRIMs and TEPs have also been previously implicated in bacterial phagocytosis, which correlates well with the NanoString expression data. *LRIM1* and *TEP3* were shown to be involved in phagocytosis of gram-negative bacteria whereas *TEP1* and *TEP4* are important for phagocytosis of both gram-types (Moita et al., 2005).

There was significant overlap in the transcriptional responses of LRIMs and TEPs to gram-negative and gram-positive bacteria (*E. coli* and *S. aureus*, respectively). This was in agreement with a previous microarray that found similarities in the responses of other immune genes to both gram-types (Dimopoulos et al., 2002). The authors speculated that overstimulation of the immune system or responses to the effects of phagocytosis could be responsible. Induction by both gram-types does not necessarily indicate a defensive role against both gram-types. For example, *CTL4* and *CTLMA2*

are only involved in defence against gram-negative bacteria but are upregulated by both gram-types (Schnitger et al., 2009). It should be noted that the laboratory models, *E. coli* and *S. aureus*, are unlikely to be natural pathogens encountered by *An. gambiae* in the wild. *E. coli* is weakly virulent in *An. gambiae* and injection of high numbers are required to cause lethality (Gupta et al., 2009). Furthermore, *E. coli* is commonly found as part of the endogenous midgut flora of laboratory-reared *An. gambiae* (Dong et al., 2009) and presumably wild mosquitoes too. Therefore, *E. coli* has the potential to invade the hemolymph during malaria parasite invasion. It would be beneficial to compare the responses of LRIMs and TEPs to natural bacterial pathogens, such as *Enterococcus faecalis* and *Enterobacter cloacae*.

Candidates for involvement in defence against fungi include *LRIM1*, *APL1A*, *LRIM4*, *LRIM17* and *TEP3*. Results correlated well with a previous microarray, which found that *LRIM1*, *APL1C*, *LRIM4* and *LRIM17* were induced 48 h after injection of *B. bassiana* spores (Fanny Turlure, personal communication). Interestingly, no genes were uniquely fungal specific. There was a strong association between transcriptional responses to bacteria and fungi whereby all genes induced by fungi were also upregulated by bacteria. This is probably due to the broad spectrum of the mosquito Toll pathway, which largely responds to both fungi and gram-positive bacteria (Hillyer, 2010). There is also considerable crosstalk with the Imd pathway, which is primarily activated by gram-negative bacteria (Lemaitre and Hoffmann, 2007).

Given their strong virulence, responses to injection of *B. bassiana* spores were weaker than anticipated. It is not known whether fungal spores are recognised directly or only after proliferation into hyphae, as suggested by the observation that most genes responded the strongest at 72 h after spore injection. Therefore, time points after 72 h might be more informative in highlighting LRIMs and TEPs defending against fungal infections. It should be noted that injection of spores is an unnatural means of infection as most entomopathogenic fungal spores adhere to the outer cuticle, germinate and invade the hemocoel (Thomas and Read, 2007). The insect immune system is activated upon penetration of the cuticle (Thomas and Read, 2007), presumably by detection of cuticle degradation products in the hemolymph. It would be interesting to see how transcriptional responses vary if fungal spores are added directly to the mosquito cuticle. After application to the surface of *An. stephensi*, *B. bassiana* has been demonstrated to kill 90% of mosquitoes within 14 days (Thomas and Read, 2007).

Hierarchical clustering of the transcriptional data highlighted putative functional relationships between LRIMs and TEPs. Differential responses to the various immune challenges and intrinsic variability between biological replicates were exploited to find co-regulated genes. Genes in the

same cluster might function in the same biochemical pathway or be under the same regulation. They might physically interact with each other, like LRIM1, APL1C and TEP1 (Fraiture et al., 2009; Povelones et al., 2011; Povelones et al., 2009). It was predicted that clustered genes might be involved in defence against the same pathogen(s). As proof of principle, the known functional partners, *LRIM1*, *APL1C* and *TEP1*, clustered tightly together. Although their regulation remains unclear, it has been reported that these genes are basally expressed under the regulation of REL1 and REL2 and regulated by REL1 after an infection (Blandin et al., 2008; Frolet et al., 2006; Mitri et al., 2009). *APL1A*, *TEP3* and *TEP4* were clustered alongside *LRIM1/APL1C/TEP1*, suggesting they might also function in the complement-like pathway. TEP3 and TEP4 are known to be involved in bacterial defence like LRIM1, APL1C and TEP1 (Dong et al., 2006a; Dong and Dimopoulos, 2009). APL1A has been reported to reduce the prevalence of *P. falciparum* infections (Mitri et al., 2009), which suggests the rest of the cluster should be thoroughly investigated for roles in *P. falciparum* defence. A promising cluster, comprised of *LRIM4*, *LRIM17*, *TEP12* and *TEP14*, was induced by *Plasmodium*, bacterial and viral infections. The relationship between these genes should be investigated further as it might represent a novel defence module. Expression clusters formed by meta-analysis of all extant microarray data (Maccallum et al., 2011) are consistent with hierarchical clustering of the NanoString data in this study. *LRIM8B*, *LRIM9* and *LRIM10* clustered in both analyses, as did *LRIM4* and *LRIM17* and also *LRIM1* and *APL1C*.

Preliminary results have provided fascinating insights into the expression profile of *An. gambiae* LRIMs and TEPs during the mosquito developmental stages. Mosquito eggs are deposited on water and larvae and pupae are completely aquatic (Clements, 2000; Reiter, 2001). Larval and pupal habitats are usually small or shallow bodies of water with little current, such as rice fields, marshes, water-filled tree holes and man-made containers (Clements, 2000). Larvae typically filter feed on particulate matter at the water surface, including plant-derived detritus, bacteria, diatoms and algae. Adult mosquitoes have an aerial lifestyle and feed on plant sugar, such as nectar. Females take blood meals from vertebrates to enable egg development. In their extremely contrasting lifestyles, mosquito larvae and adults are subjected to widely different pathogens and parasites. Interestingly, *LRIM1*, *APL1C*, *TEP1*, *LRIM17* and *TEP15* were highly expressed in fourth instar larvae, pupae and adults, suggesting they play an essential immunity role throughout the life of the insect. These five genes were induced by several immune challenges including bacteria, which are likely to be the predominant pathogens encountered by larvae. We would expect the complement-like pathway to be critical for immunity in all life stages. Furthermore, it has been proposed that selection pressure imposed by larval pathogens is more powerful than the pressure exerted by adult pathogens (White et al., 2011). Adaptive divergence in *TEP1* alleles has been attributed to

evolutionary pressure in larval habitats. Other genes were poorly expressed in larvae and pupae but very high in adults, such as the Short LRIMs, *LRIM8B*, *LRIM9* and *LRIM10*. This is in agreement with the hypothesis that these LRIMs are specific to blood feeding, a behaviour exclusive to adult females. As these Short LRIMs were not well expressed in larvae, this suggests they are unlikely to be important for bacterial defence. It is important to verify these results with further replicates, although they correlate well with a previous microarray (Koutsos et al., 2007). It would also be enlightening to investigate other developmental stages, such as eggs, early larvae, young adults and older adults.

Expression in male adult mosquitoes was not investigated in the current study and the sex of larvae and pupae used was undetermined. Expression of LRIMs and TEPs in males and females should be compared in the future. It would be predicted that the core LRIMs, such as *LRIM1* and *APL1C*, would be strongly expressed in both sexes whereas blood feeding specific LRIMs, such as *LRIM9*, would only be expressed in females. Existing microarray data support this hypothesis (Baker et al., 2011; Koutsos et al., 2007; Marinotti et al., 2005).

Several LRIMs were previously shown to be enriched in *An. gambiae* circulating hemocytes (Pinto et al., 2009). As well as mediating phagocytosis and encapsulation, hemocytes are known to secrete a variety of immune factors, including melanisation factors, opsonins and AMPs (Pinto et al., 2009) (Hillyer, 2009). *LRIM1*, *APL1C*, *LRIM4*, *LRIM6*, *LRIM15*, *LRIM16A*, *LRIM16B*, *LRIM17*, *TEP3*, *TEP4*, *TEP12*, *TEP14* and *TEP15* are all hemocyte expressed genes (Pinto et al., 2009). Hemocytes are believed to play an important role in immune responses against *Plasmodium* parasites. TEP1 was previously revealed to be present in hemocytes attached to the midgut and Malpighian tubules (Blandin et al., 2004). As *LRIM15*, *LRIM16A* and *LRIM16B* are Transmembrane LRIMs, they are likely to be inserted into the membrane of circulating hemocytes. The presence of a functional transmembrane domain in these LRIMs has recently been confirmed by immunolocalisation studies in cultured cells (Michael Povelones, personal communication). An attractive hypothesis is that these Transmembrane LRIMs sense pathogens that hemocytes encounter and trigger cellular responses, such as phagocytosis. It is interesting that the complement-like pathway components, *LRIM1*, *APL1C* and TEP1, and their interacting partners, TEP3 and TEP4, are all hemocyte-enriched. The hierarchical cluster of *LRIM4*, *LRIM17*, *TEP12* and *TEP14* are also hemocyte expressed, suggesting they might have a hemocyte-related function. The increase in their transcripts detected after some infections might result from an overproliferation of hemocytes.

To expand the transcriptional profiling of LRIMs and TEPs in *An. gambiae*, it would be interesting to try other immune challenges, such as filarial worms and more pathogenic bacterial species. *An.*

gambiae frequently suffer co-infections with *Plasmodium* parasites and filarial worms (Muturi et al., 2008). Monitoring gene expression might highlight the tripartite interaction between the mosquito immune system, filarial worms and malaria parasites, which is currently poorly understood. It would also be interesting to monitor expression in specific tissues upon the various immune challenges, such as the midgut, fat body and hemocytes. This is because subtle gene regulation in specific tissues could be masked when whole mosquitoes are analysed. Transcriptional responses of LRIMs and TEPs in other disease vector mosquitoes, such as *Aedes* and *Culex*, should also be undertaken to investigate whether the transcriptional programmes and putative functions of orthologues are conserved. Preliminary evidence suggests that the LRIM1/APL1C/TEP1 module is conserved in *Ae. aegypti* as their orthologues are all upregulated by *Wolbachia* infection (Kambris et al., 2009).

Despite the upregulation of several LRIMs by *Plasmodium* infection, the RNAi screen only identified one novel *P. berghei* antagonist: LRIM9. A single experimental replicate was sufficient to rule out other LRIMs having a dramatic phenotype like LRIM1 and APL1C. This provides further evidence that all LRIMs do not behave similarly and supports the theory that different LRIMs defend against specific pathogens. Nevertheless, this preliminary screen warrants repetition as knockdown efficiencies of some LRIMs were very poor. Silencing efficiency is gene-specific depending on their tissue expression characteristics, the efficiency of dsRNA uptake by particular tissues, transcription and protein turnover rates, polymorphisms and the efficiency of the dsRNA probe. It is more informative to monitor gene knockdowns at the protein level (Moita et al., 2005), which was unachievable in this screen. It is also important to consider that a gene knockdown showing no effect on *P. berghei* infection might highlight functional redundancies in the mosquito immune system. In other words, another immune effector might substitute for the role of the absent protein. In particular, LRIM7, LRIM8B, LRIM12, LRIM15 and LRIM16 (A and B silenced concurrently) demonstrated marginal phenotypes with *P. berghei* that warrant further verification.

For LRIM1, APL1C and TEP1, there was a strong functional link between their transcriptional upregulation by *P. berghei* and their RNAi phenotype as *P. berghei* antagonists. Despite acting as a *P. berghei* antagonist, the *LRIM9* transcript was not induced by *P. berghei*, *P. falciparum* or *P. yoelii*. Transcriptional activity of a gene does not necessarily reflect functional specificity to a particular challenge. Nevertheless, *LRIM9* was strongly upregulated by naïve blood feeding, which might function to boost LRIM9 levels in the hemolymph in anticipation of a parasite infection. LRIM9 will be investigated further in Chapter 5.

To continue the functional analysis, candidate LRIMs should be screened for an RNAi phenotype with the human parasite, *P. falciparum*. Survival assays with fungi, bacteria and ONNV should also be performed on candidate LRIMs chosen from the transcriptional profiling presented in this Chapter.

Chapter 5: LRIM9 – a novel antagonist of *Plasmodium berghei*

5 LRIM9 – a novel antagonist of *Plasmodium berghei*

5.1 Background

Increasing our understanding of the mosquito immune system and how it targets and kills malaria parasites could lead to the development of novel malaria control strategies. Two key mosquito immune proteins, LRIM1 and APL1C, mediate killing of *Plasmodium* parasites through their interaction with the complement-like effector, TEP1 (Fraiture et al., 2009; Povelones et al., 2009). We recently discovered a mosquito-specific family of immune proteins related to LRIM1 and APL1C - the LRIMs. This PhD involved examining the roles of uncharacterised LRIMs in mosquito immunity. As presented in Chapter 4, transcriptional profiling and RNAi screens following immune challenge and *Plasmodium* infection identified LRIM9 as a highly promising candidate. This present Chapter describes the thorough characterisation of LRIM9 to learn more about its involvement in parasite killing and mosquito immunity.

LRIM9 is a Short LRIM, with protein domain architecture typical for this LRIM subfamily (Figure 5.1). It has a predicted signal peptide sequence, which suggests it is secreted into the mosquito hemolymph. LRIM9 has seven LRRs predicted to form a shallow horseshoe shape (Waterhouse et al., 2010). The LRRs are preceded by a leucine-rich leader sequence, which is similar to an LRR motif but with higher leucine substitutions and it rarely has the characteristic asparagine (Waterhouse et al., 2010). These leucine-rich leader sequences are common in vertebrate TLRs (Matsushima et al., 2007). LRIM9 has a single coiled-coil domain whereas LRIM1, APL1C and some Short LRIMs have two tightly-linked coiled-coils (Waterhouse et al., 2010). The LRIM1/APL1C coiled-coils interact with TEP proteins (Povelones et al., 2011). LRIMs have well conserved patterns of cysteine residues between the LRRs and coiled-coil and LRIM9 is quite typical. LRIM9 has a leading N-terminal cysteine motif (C-C) and a C-terminal cysteine pattern (C-C-CC) (Waterhouse et al., 2010). In LRIM1 and APL1C, the C-terminal cysteines form two intramolecular disulphide bonds that likely play a role in protein folding (Baxter et al., 2010; Povelones et al., 2011). However, LRIM9 lacks a final C-terminal single cysteine immediately prior to the coiled-coil, which is only found in LRIM1 and the APL1 cluster. The final cysteine of LRIM1 and APL1C is crucial for covalently linking the proteins by a disulphide bond, although this linkage is not essential for the LRIM1/APL1C interaction and their interaction with TEP1 (Povelones et al., 2011).

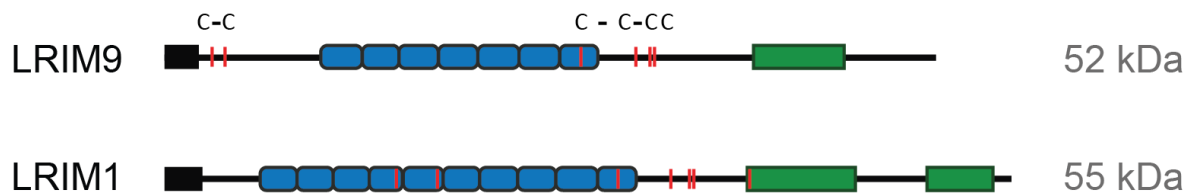


Figure 5.1 Schematic representation of LRIM9 protein structure.

To-scale diagram of LRIM9 protein structure, with LRIM1 shown for comparison. Predicted size of mature proteins is shown in grey. Structures shown are black box: signal peptide, blue box: LRR, green box: coiled-coil domain, red line: cysteine residue. The leading N-terminal (C-C) and C-terminal (C-C-CC) cysteine motifs of LRIM9 are highlighted. The LRIM1 diagram has been adapted from Povelones et al., 2011.

LRIM9 forms a genomic cluster with four other LRIMs in *An. gambiae*: *LRIM7*, *LRIM8A*, *LRIM8B* and *LRIM10* (Waterhouse et al., 2010). Comparative sequence analyses have revealed orthologous clusters in the genomes of *Ae. aegypti* and *C. quinquefasciatus* mosquitoes with evidence of gene duplication and shuffling (Figure 5.2). However, in all three mosquito species, *LRIM9* has been conserved as a single-copy orthologue and has retained its relative location and orientation. In comparison, *LRIM8* has been duplicated in *An. gambiae* and *LRIM10* in *Ae. aegypti*. The orthologous region is approximately four times larger in *Ae. aegypti* due to accumulation of repetitive sequences, which is a common phenomenon in the *Ae. aegypti* genome.

In Chapter 4, the *LRIM9* transcript was found to be unresponsive to *Plasmodium*, bacteria, fungi, ONNV and PBS injection but was induced 24 to 48 h after mouse and human blood feeding, responding more rapidly at higher temperatures. A 1.6-fold induction in *LRIM9* transcript was also observed 24 h after injection of conditioned media from uninfected VERO cells, probably in response to the serum-containing media. Previous transcriptional profiling data have also demonstrated significant differential expression of *LRIM9* after blood feeding, with highest expression at 24 h and lowest at 3 h (Marinotti et al., 2005). Like several other LRIMs, including *LRIM1* and *APL1C*, *LRIM9* showed significantly higher expression in the fat body compared to the midgut or ovaries (Marinotti et al., 2005). Preliminary evidence suggests *LRIM9* is poorly expressed in larvae and pupae.

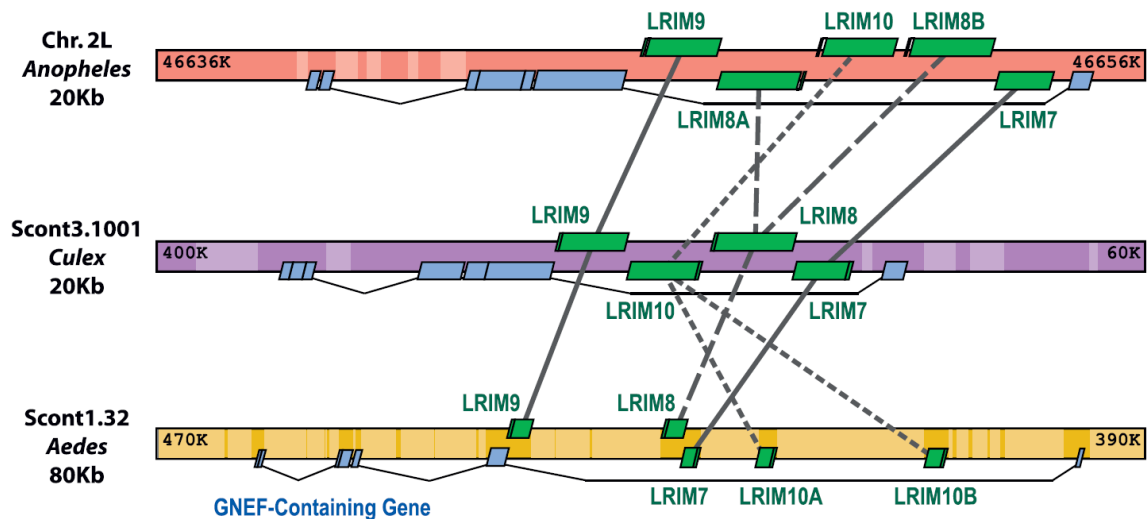


Figure 5.2 Orthologous genomic clusters of Short LRIMs in different mosquito species.

In *An. gambiae*, *LRIM9* is a member of a five gene cluster of Short LRIMs. This cluster is conserved in the other sequenced mosquito species, *Culex* and *Aedes*, with evidence of gene duplication and shuffling of gene order and orientation. The *Anopheles* chromosome (Chr) 2L is shown in red and the orthologous *Culex* and *Aedes* supercontigs (Scont) in purple and yellow, respectively. The LRIM genes (in green) are within the intron of a guanine nuclear exchange factor (GNEF) containing gene (in blue) in all three mosquito species. Orthologues are linked with solid grey lines whereas duplicated genes are linked with dashed lines. Repetitive sequences are lightly shaded. From Waterhouse et al., 2010.

5.2 Results

LRIM9 and *P. berghei* infections

Initially, a dsRNA injection time course was performed to enable optimisation of *LRIM9* silencing, if necessary. Mosquitoes were injected with *dsGFP* (non-specific dsRNA) or *dsLRIM9* and 10 mosquitoes from each group were collected on day 1, 2, 3, 4 and 7. RNA was extracted and cDNA was analysed by qRT-PCR for *LRIM9* expression. *LRIM9* expression was first normalised for total amount of RNA material using expression of *S7*, a gene encoding a ribosomal housekeeping protein. For each time point, levels of *LRIM9* after *dsLRIM9* treatment were calculated relative to the corresponding *dsGFP* treatment. The *LRIM9* transcript was very efficiently silenced at the RNA level, even 7 days after dsRNA injection (Figure 5.3). Knockdown ranged from a minimum of 88% on day 7 to a maximum of 99% on day 2. Therefore, *LRIM9* silencing did not require optimisation and dsRNA was injected 3 or 4 days prior to blood feeding or further treatments in all subsequent experiments.

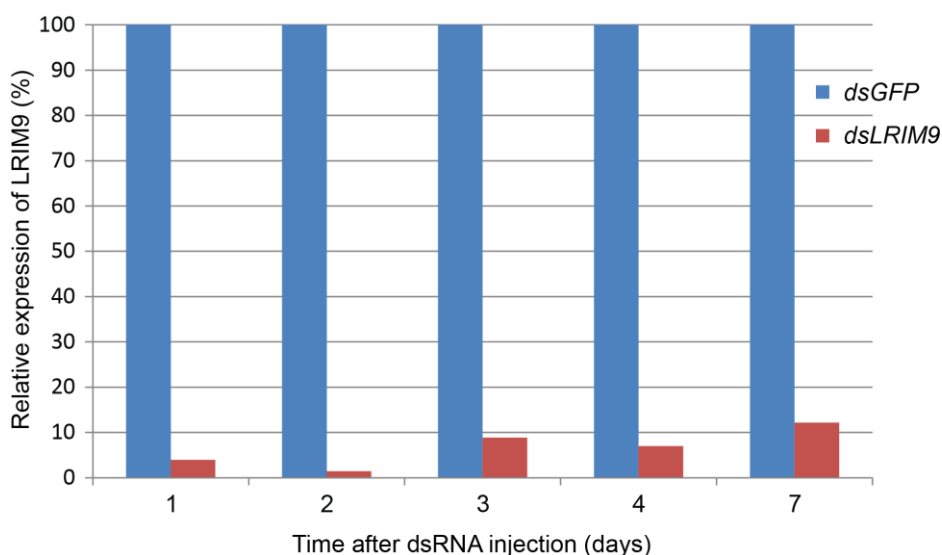


Figure 5.3 Knockdown efficiency time course for *LRIM9* transcript.

RNA was extracted from mosquitoes 1, 2, 3, 4 and 7 days after *dsGFP* or *dsLRIM9* injection. Per time point and group, 10 mosquitoes were pooled for RNA extraction and cDNA synthesis. cDNA was analysed by qRT-PCR to determine *LRIM9* expression, normalising to *S7*, a constitutively expressed housekeeping gene. For each day, *LRIM9* expression in the *LRIM9* knockdown (red) was calculated relative to expression in the *dsGFP*-treated control (blue).

As presented in Chapter 4, *LRIM9* knockdown caused a significant effect on *P. berghei* infection. This initial finding was followed up with further biological replicates to verify the result. Mosquitoes were injected with *dsLRIM9*, *dsLRIM1* (as a positive control) and *dsGFP* (as a negative control). After 3 to 4 days, mosquitoes were allowed to feed on a *P. berghei* infected mouse. Midguts were dissected 7 days later and live GFP-labelled oocysts and dead melanised ookinetes were counted. Silencing *LRIM9* resulted in a highly significant 5-fold increase in live oocysts compared to *dsGFP*-treated controls (Figure 5.4 A and Table 5.1). This result was reproducible in two *An. gambiae* strains (Yaoundé and Ngouso) known to be susceptible to *Plasmodium* infection, suggesting that *LRIM9* is somehow involved in limiting parasite development or killing parasites. The increase in oocysts observed after *LRIM9* silencing was less dramatic than *LRIM1* or *APL1C* silencing, the latter resulting in increases between 3.6-fold and 50-fold (Osta et al., 2004a; Povelones et al., 2009). Knockdown of *LRIM9* also significantly reduced spontaneous ookinete melanisation in susceptible mosquitoes (Figure 5.4 B and Table 5.1), which is also observed upon silencing *LRIM1*, *APL1C* or *TEP1*. The effect on spontaneous melanisation was largely from one biological replicate, although this was sufficient to have a significant effect on the pooled results. As shown in Figure 5.3, the *LRIM9* knockdown phenotype with *P. berghei* is not affected by poor or transient knockdown.

Prevalence of live oocyst infection, the percentage of midguts containing at least one oocyst, was comparable between *dsLRIM9* and *dsGFP* in the pooled experiments (not significant using Fisher's exact test). In contrast, prevalence of live oocyst infection in *dsLRIM1* was significantly higher than in *dsGFP* (P-value < 0.01 using Fisher's exact test). Both *dsLRIM9* and *dsLRIM1* significantly reduced the prevalence of spontaneous melanisation (P-value < 0.05 and < 0.0001, respectively, using Fisher's exact test).

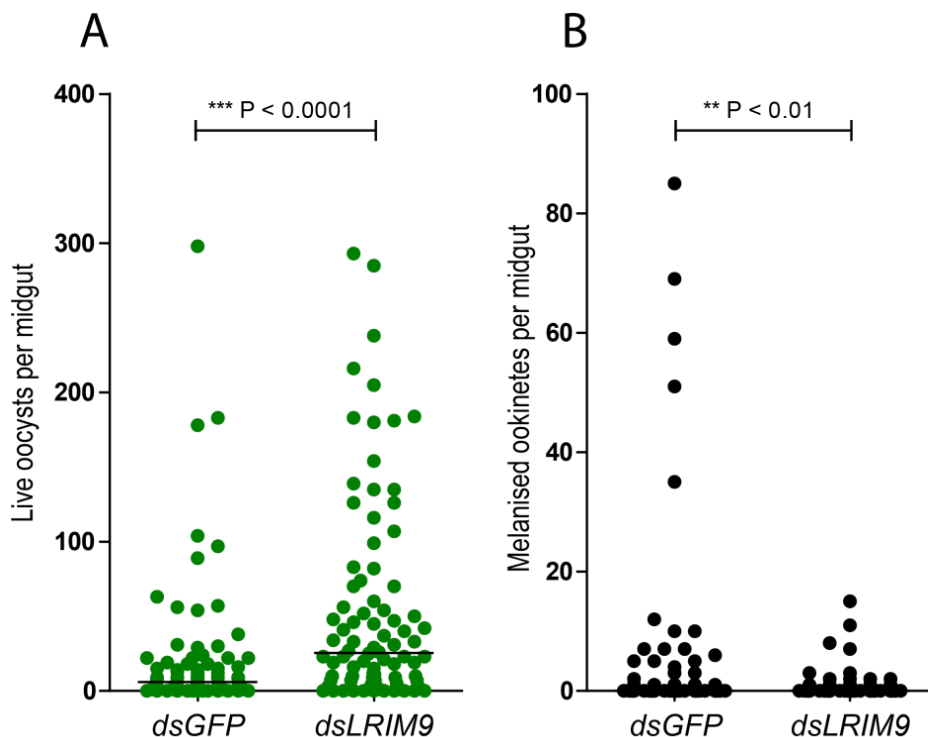


Figure 5.4 *LRIM9* knockdown in susceptible mosquitoes.

LRIM9 was silenced using RNAi, mosquitoes were infected with fluorescent *P. berghei* and parasite load was monitored after 7 days. Non-specific dsRNA (*GFP*) was used as a control. The graphs show pooled data from five independent biological experiments in *Plasmodium* susceptible mosquitoes (two from Yaoundé strain and three from Ngouso strain, see Table 5.1). Horizontal lines represent the median parasite number. Two *LRIM9* knockdown mosquitoes with 403 and 608 oocysts, respectively, were excluded from the graph for presentation purposes. **A)** Live fluorescent oocyst counts (P-value < 0.0001, Mann Whitney U-test). **B)** Melanised (killed) ookinete counts (P-value < 0.01, Mann Whitney U-test).

Table 5.1 The effect of *LRIM9* silencing on *P. berghei* development in susceptible mosquitoes.

Expt (Strain)	Knock-down	N	Live oocysts				Melanised ookinetes				Knockdown efficiency (%)
			Prevalence		Infection intensity		Prevalence		Infection intensity		
			%	P-value	Median (Range)	P-value	%	P-value	Median (Range)	P-value	
1 (Y)	GFP	17	76	N/A	2 (0-89)	N/A	88	N/A	4 (0-85)	N/A	N/A
	LRIM1	10	100	NS	243 (46-805)	< 0.0001	0	< 0.0001	0	< 0.001 [#]	79
	LRIM9	14	93	NS	44 (0-285)	< 0.001	14	< 0.0001	0 (0-2)	< 0.0001	65
2 (Y)	GFP	5	100	N/A	4 (3-63)	N/A	0	N/A	0	N/A	N/A
	LRIM1	7	100	N/A	349 (5-744)	< 0.05	0	N/A	0	N/A	79
	LRIM9	5	80	NS	29 (0-50)	NS	20	NS	0 (0-15)	NS [#]	78
3 (Ng)	GFP	7	86	N/A	6 (0-19)	N/A	14	N/A	0 (0-1)	N/A	N/A
	LRIM1	4	100	NS	519 (307-751)	< 0.01	0	NS	0	NS [#]	72
	LRIM9	10	100	NS	26 (4-608)	< 0.05	30	NS	0 (0-8)	NS	81
4 (Ng)	GFP	16	75	N/A	3.5 (0-22)	N/A	13	N/A	0 (0-3)	N/A	N/A
	LRIM1	13	100	NS	326 (225-748)	< 0.0001	0	NS	0	NS [#]	95
	LRIM9	17	59	NS	1 (0-183)	NS	18	NS	0 (0-2)	NS	86
5 (Ng)	GFP	33	88	N/A	13 (0-298)	N/A	39	N/A	0 (0-10)	N/A	N/A
	TEP1	20	95	NS	240 (0-700)	< 0.0001	15	NS	0 (0-1)	< 0.05	ND
	LRIM9	42	95	NS	43 (0-293)	< 0.01	26	NS	0 (0-11)	NS	ND
Pooled 1-5	GFP	78	83	N/A	6 (0-298)	N/A	40	N/A	0 (0-85)	N/A	N/A
	LRIM1	34	100	< 0.01	317 (5-805)	< 0.0001	0	< 0.0001	0	< 0.0001 [#]	81
	LRIM9	88	88	NS	27 (0-608)	< 0.0001	23	< 0.05	0 (0-15)	< 0.01	78

LRIM9 was silenced using RNAi, mosquitoes were infected with fluorescent *P. berghei* and parasite load was monitored after 7 days. Five biological replicates and pooled data are shown. Non-specific dsRNA (*GFP*) was used as a negative control and *LRIM1* or *TEP1* as a positive control. Either Yaoundé (Y) or Ngousso (Ng) mosquito strains were used. *N* = number of individual mosquito midguts. Prevalence is the percentage of guts that contain at least one oocyst or melanised parasite. Mann Whitney U-test was used for infection intensity, comparing to *dsGFP*. If prevalence for one gene was zero, the Wilcoxon Test was used (#). Fisher's exact test was used for prevalence. Significant P-values (< 0.05) are shown in red. Knockdown efficiency was calculated by qRT-PCR. NS = Not significant; ND = Not determined; N/A = Not applicable.

To further investigate the role of LRIM9 in melanisation, the gene was silenced in L3-5 mosquitoes, a laboratory-selected refractory strain of *An. gambiae* that melanises virtually all invading *P. berghei* ookinetes (Collins et al., 1986). *LRIM9* knockdown in the L3-5 strain caused a significant decrease in melanisation but no parallel increase in live oocysts (Figure 5.5). In contrast, when *LRIM1* or *APL1C* is silenced in L3-5, melanisation is blocked and there is an 80-fold increase in live parasites (Povelones et al., 2009). The *LRIM9* phenotype was verified using two different lines of genetically modified *P. berghei* parasite (EF1 and 507), shown separately in Figure 5.5. These parasites share the same genetic background (ANKA) and EF1 eGFP promoter but have different insertion loci – SSU for EF1 and 230P for 507. Knockdown efficiency of *LRIM9* in L3-5 mosquitoes was 89%.

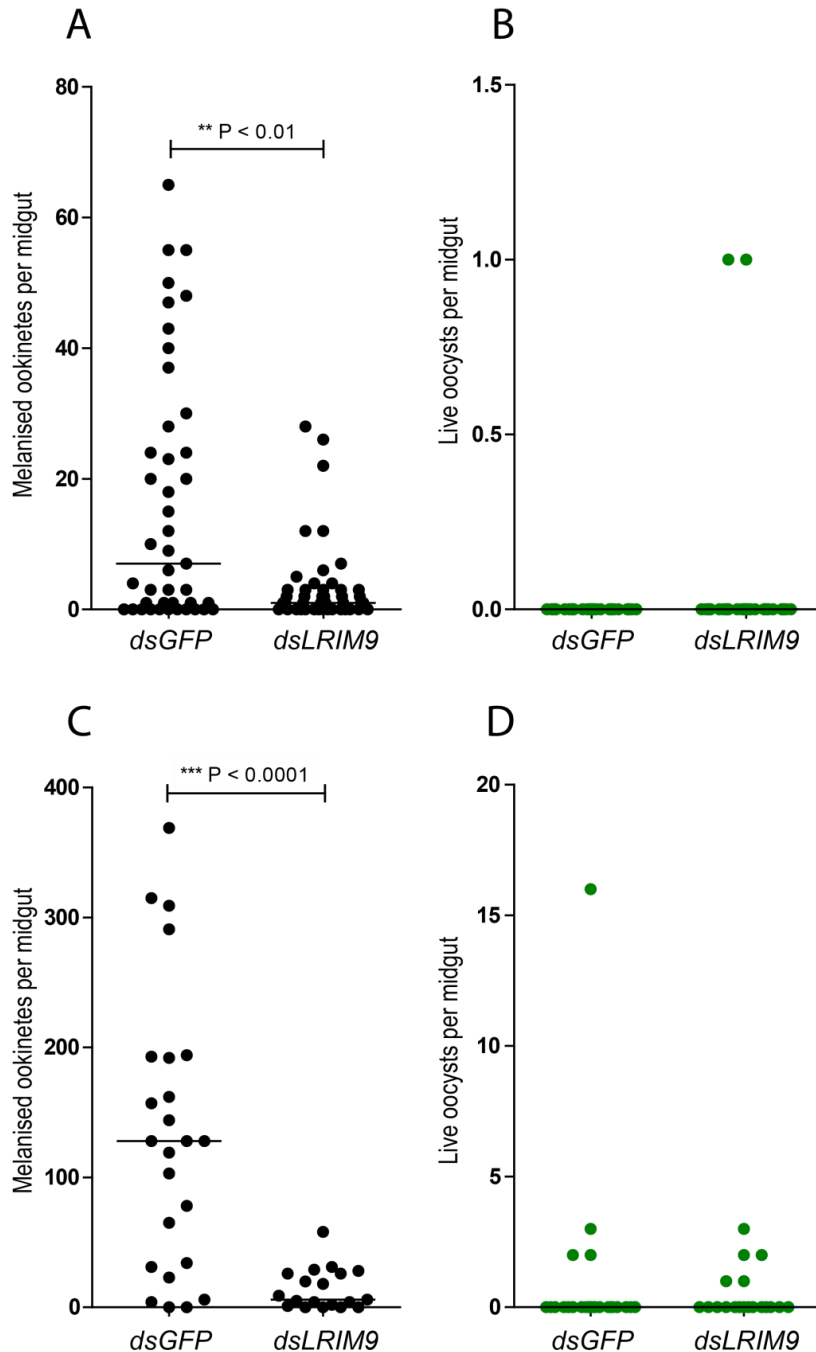


Figure 5.5 *LRIM9* knockdown in L3-5 mosquitoes using two lines of *P. berghei*.

LRIM9 silencing in refractory L3-5 mosquitoes which melanise virtually all invading *P. berghei* parasites. Mosquitoes were infected with two fluorescent *P. berghei* lines and parasite load was monitored after 7 days. Non-specific dsRNA (*GFP*) was used as a control. Horizontal lines represent the median parasite number. **A and B**) Infection with EF1 parasites. **C and D**) Infection with 507 parasites. **A and C**) Melanised (killed) ookinete counts (P-value < 0.01 for **A** and < 0.0001 for **C** using Mann Whitney U-test). **B and D**) Live oocyst counts (no significant differences using Mann Whitney U-test).

To determine the effect of *LRIM9* on parasite melanisation in a different genetic background, *LRIM9* was silenced alongside *CTL4*, a C-type lectin that usually inhibits parasite melanisation in susceptible mosquitoes (Volz et al., 2006). Silencing *CTL4* alone induces dramatic melanisation of invading

ookinetes, inhibiting their development to oocysts, while double knockdown of *LRIM1/CTL4* or *TEP1/CTL4* reverses the *CTL4* phenotype, resulting in negligible melanisation and many live oocysts, which indicates that *LRIM1* and *TEP1* are epistatic to *CTL4* (Osta et al., 2004a). Therefore, silencing *CTL4* and *LRIM9* together can also provide information about epistatic relationships between these two genes in the melanisation cascade. In this experiment, *GFP/GFP* and *GFP/CTL4* double knockdowns served as controls. As expected, *GFP/CTL4* silencing showed increased melanisation and fewer developing oocysts compared to the *GFP/GFP* control (Figure 5.6). However, *LRIM9/CTL4* knockdown showed no significant change in live oocysts or melanised parasites compared to *GFP/CTL4* knockdown. In contrast, as expected, *TEP1/CTL4* knockdown reversed the *CTL4* phenotype. Therefore, the *LRIM9* knockdown phenotype of increased live parasites is suppressed when *LRIM9* is silenced alongside *CTL4*.

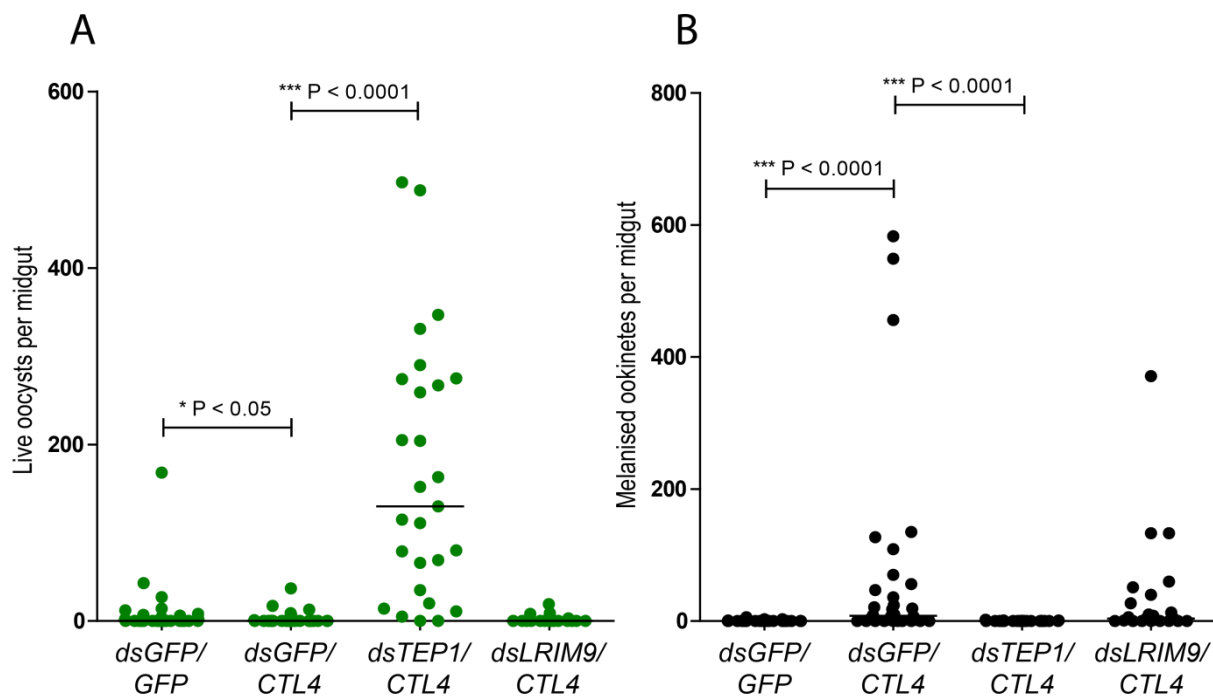


Figure 5.6 *LRIM9* and *CTL4* double knockdown in susceptible mosquitoes.

LRIM9 was silenced with *CTL4*, a known inhibitor of parasite melanisation. Mosquitoes were infected with fluorescent *P. berghei* and parasite load was monitored after 7 days. Double knockdowns of *GFP/GFP*, *GFP/CTL4* and *TEP1/CTL4* were used as controls. All significant results by the Mann Whitney U-test ($P < 0.05$) are highlighted on the graphs. Results shown are representative of two independent biological replicates and the horizontal lines represent the median parasite number. **A)** Live oocyst counts. **B)** Melanised (killed) ookinete counts.

Recombinant LRIM9 in insect cell culture

To analyse the biochemical characteristics of LRIM9 *in vitro*, the gene was cloned into the pEx-10 insect expression vector. This vector adds an N-terminal Strep-tag and a C-terminal His-tag for tandem purification and detection. In an initial experiment, pEx-10-LRIM9 was transfected into two insect cell lines, Lepidopteran Sf9 and *An. gambiae* hemocyte-like Sua4.0, to monitor expression levels, protein mobility and complex formation. Conditioned media were analysed by western blot using the His probe to detect LRIM9. Sf9 cells are excellent secretory cells, contain no endogenous LRIM proteins and can be grown under serum-free conditions, facilitating purification of proteins from the conditioned medium. Sua4.0 cells naturally secrete a subset of mosquito hemolymph proteins and show inducible immune gene expression (Muller et al., 1999). Therefore, LRIM9 expression in Sf9 cells would uncover intrinsic properties of the LRIM9 protein, such as the ability to form homomeric complexes, whereas expression in Sua4.0 cells would allow screening for LRIM9 partners.

Recombinant LRIM9 was highly expressed and secreted as a monomer in both cell lines after transfection (Figure 5.7). The predominant band was at 54 kDa in non-reduced samples, consistent with the predicted size of mature His/Strep-tagged LRIM9. A slight mobility shift (to 60 kDa) was observed in reduced samples, which is common upon reduction of intramolecular disulphide bonds because proteins become less compact with slower electrophoretic mobility. Lower molecular weight bands (25-40 kDa) were visible in conditioned media from Sf9 cells, which were likely to be N-terminally cleaved forms of LRIM9 due to limited protease activity in the samples. Higher molecular weight bands in the conditioned media of Sua4.0 cells were probably non-specific as they were also observed in control transfection using a GFP-expressing plasmid. A band at approximately 120 kDa in the non-reduced LRIM9 sample was perhaps an artefact of overexpression. Overall, LRIM9 does not appear to form a covalent homo- or heteromeric complex when expressed in cultured insect cells. However, it is possible that recombinant LRIM9 behaves differently to the native protein, while the presence and abundance of mosquito proteins is likely to differ between conditioned media and mosquito hemolymph. Therefore, an antibody against LRIM9 was required to investigate complex formation *in vivo*.

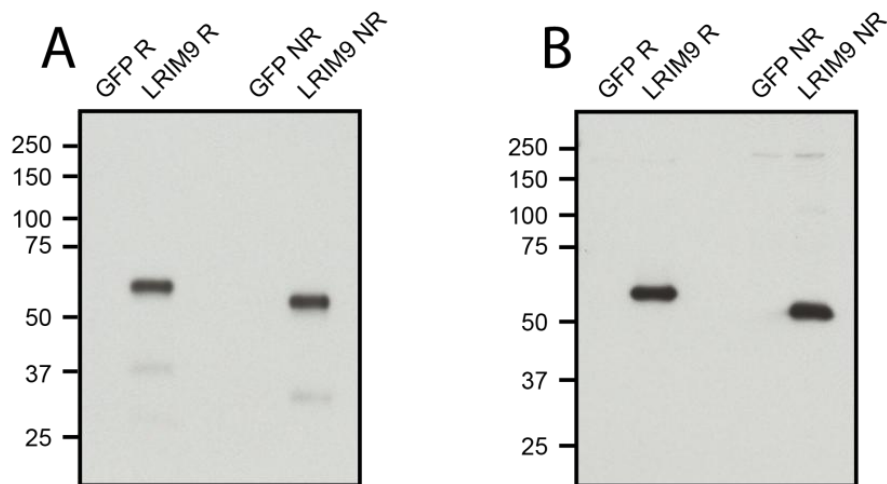


Figure 5.7 Expression of recombinant LRIM9 in insect cell lines.

Recombinant pEx-10-LRIM9 plasmids were transfected into Lepidopteran-derived Sf9 cells **(A)** and mosquito hemocyte-like Sua4.0 cells **(B)**. Cells transfected with a GFP-expressing plasmid were used as a negative control. Cell conditioned media were collected 3 days after transfection and analysed by western blot using an anti-His antibody under reducing (R) and non-reducing (NR) conditions.

Developing an antibody against LRIM9

To investigate the function of the LRIM9 protein, rabbit antibodies were initially raised against two LRIM9 peptides, one at the C-terminus and another located in an internal region between the LRRs and coiled-coil. However, after an initial characterisation, these peptide antibodies were not optimal and showed prominent non-specific bands (Appendix Figure 9.1). As an alternative, polyclonal guinea pig antibodies were raised against the entire LRIM9 protein that was produced in stably transfected Sf9 cells that continually secrete LRIM9 protein into their conditioned media. This cell line was kindly generated by Dr Lavanya Bhagavatula using antibiotic selection after co-transfection of the previously mentioned pIE1-neo and pEx-10-LRIM9 plasmid vectors. Conditioned medium containing tagged LRIM9 was purified by affinity chromatography using the C-terminal 10x His-tag. The purified LRIM9 protein was analysed by Coomassie staining, concentrated and sent to Eurogentec for immunisation of two guinea pigs.

The immune sera were evaluated using conditioned media from pEx-10-LRIM9 transfected Sua4.0 cells. A MiniBlotter was used to optimise the concentration and blocking buffer for western blot (Figure 5.8). Pre-immune serum (collected from the same animal before immunisation) was used to confirm specificity of immunodetection. The antibodies detected LRIM9 as an abundant monomer at 54 kDa, in agreement with the His probe, whereas the pre-immune serum did not. There was no evidence to suggest that LRIM9 is endogenously expressed by Sua4.0 cells under naïve conditions.

Faint bands at approximately 120 and 180 kDa detected in the antisera from both guinea pigs may be an artefact of LRIM9 overexpression.

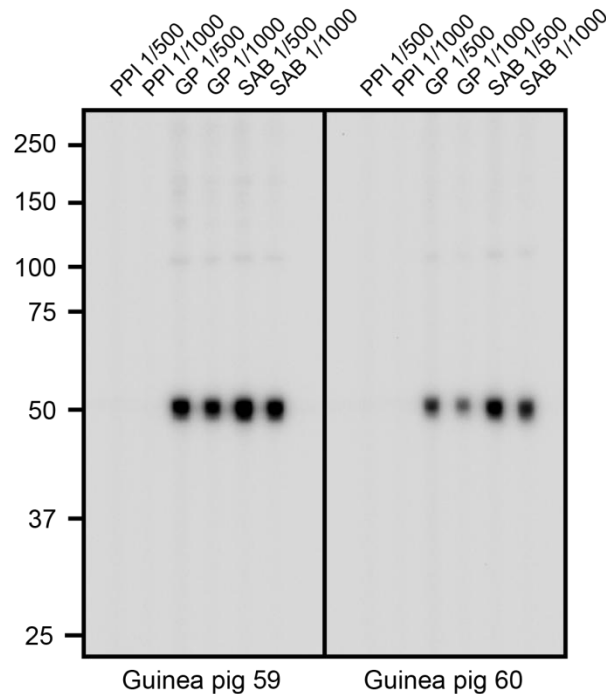


Figure 5.8 Testing LRIM9 whole protein antibody using conditioned media from mosquito cells.

Sera from two guinea pigs (named 59 and 60) were screened for LRIM9 antibodies by western blot of conditioned media collected from LRIM9-expressing Sua4.0 cells. Pre-immune serum (PPI), a large bleed (GP) and final bleed (SAB) were used at 1/500 and 1/1000 dilutions. Molecular weight markers are indicated on the left (kDa).

LRIM9 in the hemolymph

To gain insights into the role of LRIM9 *in vivo*, the next step was to analyse hemolymph using the LRIM9 whole protein antibody. To verify the results from cell culture, the pre-immune serum and final bleed serum from guinea pig 59 (hereafter LRIM9 antibody or α -LRIM9) were used to probe hemolymph collected 4 days after *dsGFP*, *dsLRIM9* or *dsLRIM1* injection (Figure 5.9 A). SRPN3, a protein constitutively present in the hemolymph, was also analysed to confirm equal loading. With the LRIM9 antibody, a unique band just below 50kDa was detected in *dsGFP* and *dsLRIM1* hemolymph but was absent in *dsLRIM9*. This band (shown by red arrow in Figure 5.9) matches the predicted size for an LRIM9 monomer and corresponds well with the observations *in vitro*. A band at approximately 70 kDa and another faint cluster of bands between 180 and 250 kDa were unaffected by *LRIM9* silencing and therefore considered non-specific. None of these bands were detected in the

pre-immune serum, which confirms the LRIM9 antibodies were induced by immunisation and not an artefact of the guinea pig blood. The band detected by the LRIM9 antibody was weaker than anticipated given that LRIM9 was highly transcribed in unchallenged mosquitoes, as described in Chapter 4.

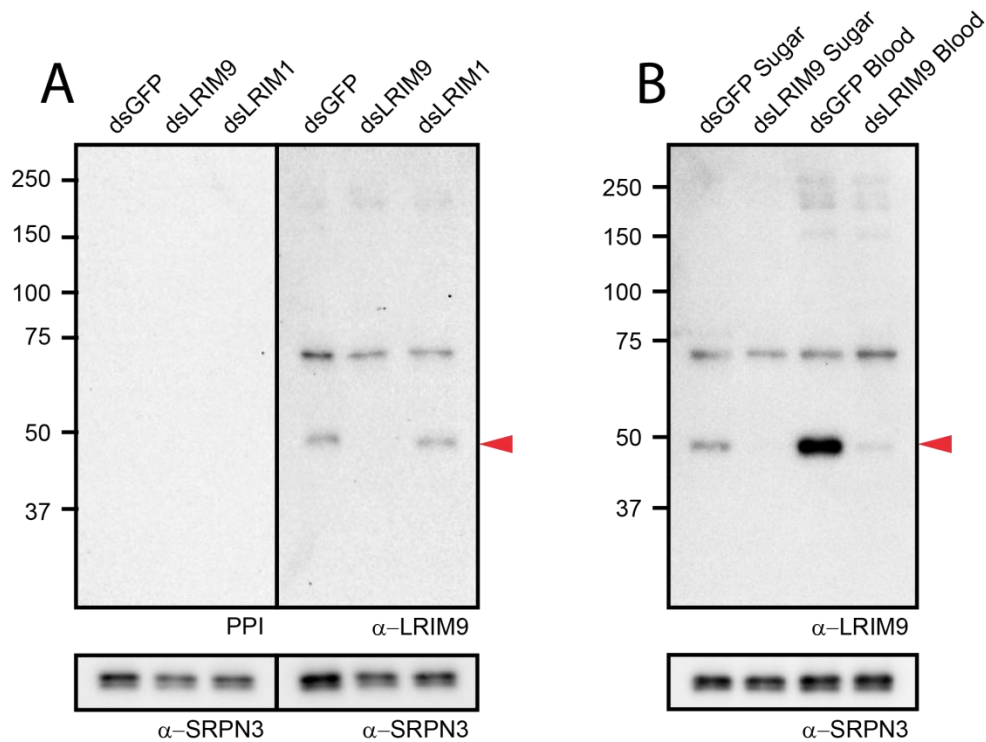


Figure 5.9 Testing LRIM9 antibody with hemolymph after *LRIM9* knockdown.

A) Female Ngousso mosquitoes were injected with *dsGFP*, *dsLRIM9* or *dsLRIM1* and hemolymph was collected after 4 days. Non-reduced hemolymph was analysed by western blot and probed with the pre-immune serum (PPI) or α -LRIM9 antibody. Blots were re-probed with an antibody against constitutively expressed SRPN3 as a loading control. **B)** 3 days after *dsGFP* or *dsLRIM9* injection, mosquitoes were fed either sugar or blood. Hemolymph was collected 24 h later and analysed by western blot using α -LRIM9 and α -SRPN3 antibodies. Molecular weight markers are indicated (kDa). Red arrowheads indicate the position of LRIM9.

As the *LRIM9* transcript was upregulated after naïve blood feeding, it was investigated whether the LRIM9 protein would be more abundant in the hemolymph following a blood meal. Hemolymph collected 24 h after sugar or blood feeding was analysed by western blot using the LRIM9 antibody (Figure 5.9 B). The 50 kDa LRIM9 band was massively enriched in hemolymph collected from blood fed compared to sugar fed mosquitoes, whereas the abundance of SRPN3 was relatively unaffected. The LRIM9 protein was completely absent after *LRIM9* knockdown in the sugar fed mosquitoes but a faint band remained after blood feeding, suggesting RNAi silencing was unable to completely

knockdown the large increase in protein production. Despite this, the remaining band was still much less intense than in the naïve mosquito. Non-specific bands were unaffected by blood feeding.

Next, the temporal dynamics of LRIM9 transcript and protein levels were monitored following a naïve blood meal. Female mosquitoes were allowed to feed on an anaesthetised naïve mouse and hemolymph was collected after 3, 8, 24, 48, 72 and 96 h. Hemolymph was also collected from a group of mosquitoes prior to blood feeding to determine the basal expression ("0 h"). In this experiment, mosquitoes were incubated at 19 °C after blood feeding, which was consistent with the temperature required for *P. berghei* infection. LRIM9 and other hemolymph proteins were analysed by western blot (Figure 5.10 A). Strikingly, the upregulation of LRIM9 after blood feeding was very specific and transient, peaking dramatically at 24 to 48h and rapidly decreasing again by 72h. LRIM9 band intensities were determined and normalised using the SRPN3 loading control to account for total protein in each hemolymph sample (Figure 5.10 B). Levels of LRIM9 protein in naïve hemolymph were relatively low but, by 48 h, this had increased dramatically by over 12-fold. However, it should be noted that enhanced chemiluminescence western blot analysis performed here is only a semi-quantitative technique so this number is provided as an estimate. Analysis of the LRIM1/APL1C complex and LRIM4 demonstrated that not all LRIMs are induced by blood feeding as these proteins remained relatively stable during the time course. The LRIM1/APL1C complex was constitutively present at high levels in naïve hemolymph and further upregulated in response to a challenge. In contrast to LRIM9, levels of TEP1-F and TEP1_{cut} were depleted during a blood meal. Interestingly, the concentration of LRIM9 in the hemolymph at 96 h was still higher than before the blood meal.

LRIM9 transcript abundance was analysed by qRT-PCR over the time course and it correlated very closely with the protein abundance (Figure 5.10 C). This suggests that *LRIM9* is transcribed and secreted when required rather than the protein being stored in large quantities inside the cell. By 72 and 96 h, *LRIM9* transcription returned back to basal levels indicating that the elevated protein levels observed at these time points likely reflect the time required for protein turnover.

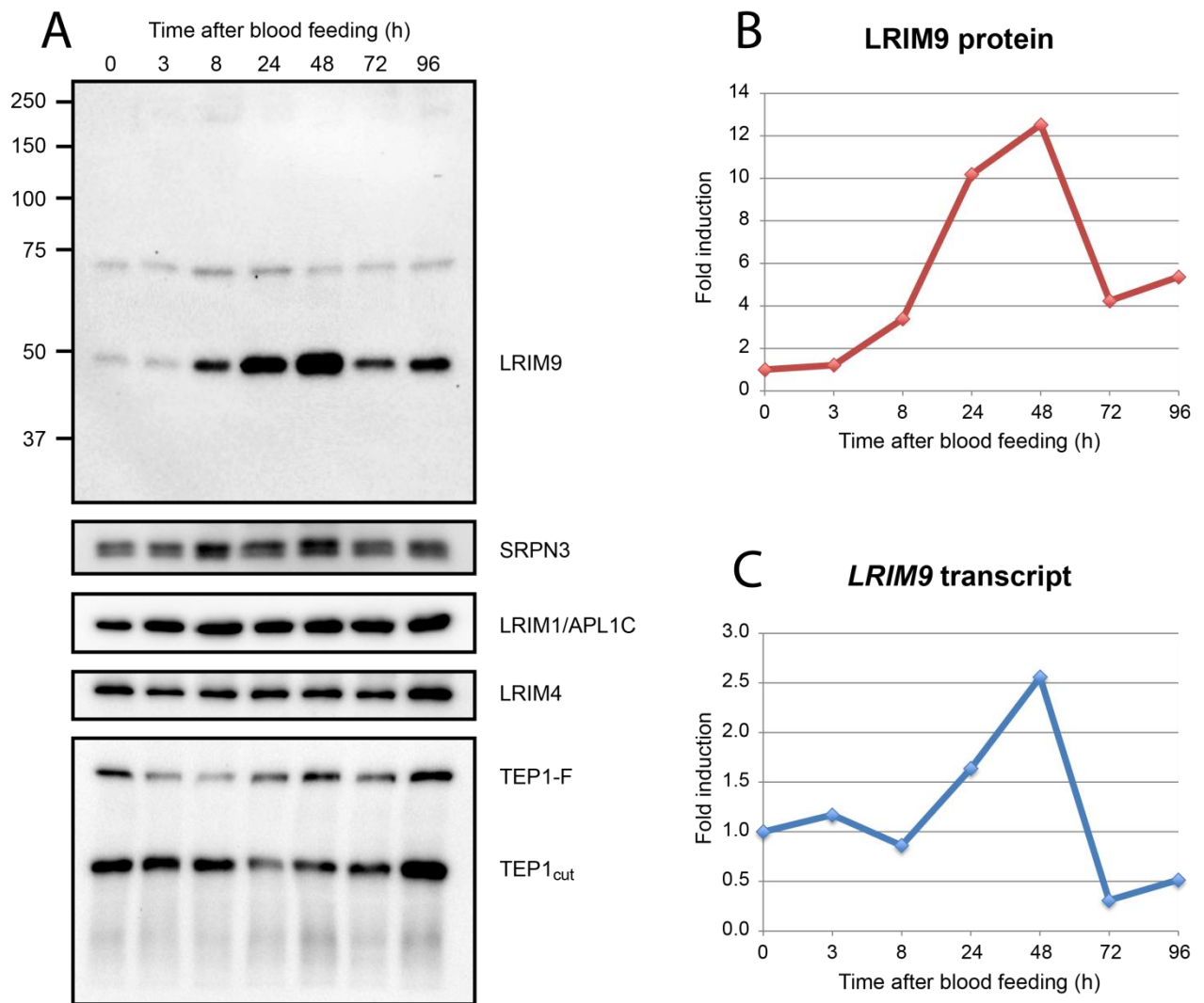


Figure 5.10 LRIM9 transcript and protein expression after feeding on rodent naïve blood.

Mosquitoes were allowed to blood feed on an uninfected mouse and hemolymph and RNA samples were collected after 3, 8, 24, 48, 72 and 96 h. A group of mosquitoes before blood feeding were used to show basal expression levels ("0 h"). **A)** Hemolymph was analysed by western blot under non-reducing conditions and probed with α -LRIM9. The blot was re-probed with α -SRPN3 as a loading control and α -LRIM2-300 to analyse the LRIM1/APL1C complex. Another blot of the same samples was probed with α -LRIM4 and α -TEP1 antibodies. Molecular weight markers are shown (kDa). **B)** LRIM9 protein bands were measured semi-quantitatively and normalised to SRPN3. **C)** LRIM9 transcript was analysed in total RNA isolated from whole mosquitoes by qRT-PCR using LRIM9 primers and normalising to ribosomal S7 gene.

To determine whether feeding on human blood also causes upregulation of LRIM9, mosquitoes were fed through a membrane feeder on human blood warmed to 37 °C. Fed mosquitoes were then kept at their optimal rearing temperature of 27 °C, which is also consistent with infection with the human malaria parasite, *P. falciparum*. Hemolymph was collected after 8, 24, 48 and 72 h, with sugar fed mosquitoes used as “0 h”, and analysed by western blot using the LRIM9 antibody (Figure 5.11 A). Like with mouse blood, the LRIM9 protein showed a dramatic and very transient induction. Upregulation was faster with human blood, peaking at 24 h rather than 48 h for mouse blood, which is probably due to the different temperatures used to rear mosquitoes although it may also reflect batch-to-batch variation in mosquito fitness. In Chapter 4, variation in temporal LRIM9 induction was observed between mosquito batches, either 24 or 48 h. When LRIM9 band intensity was assessed semi-quantitatively and normalised to the SRPN3 control, LRIM9 was found to be upregulated over 20-fold compared to sugar fed mosquitoes (Figure 5.11 B). In summary, mosquitoes responded similarly to murine and human blood, indicating that common mammalian blood components, formation of the blood bolus, distension of the gut or signalling occurring after blood feeding are likely to cause the upregulation of LRIM9.

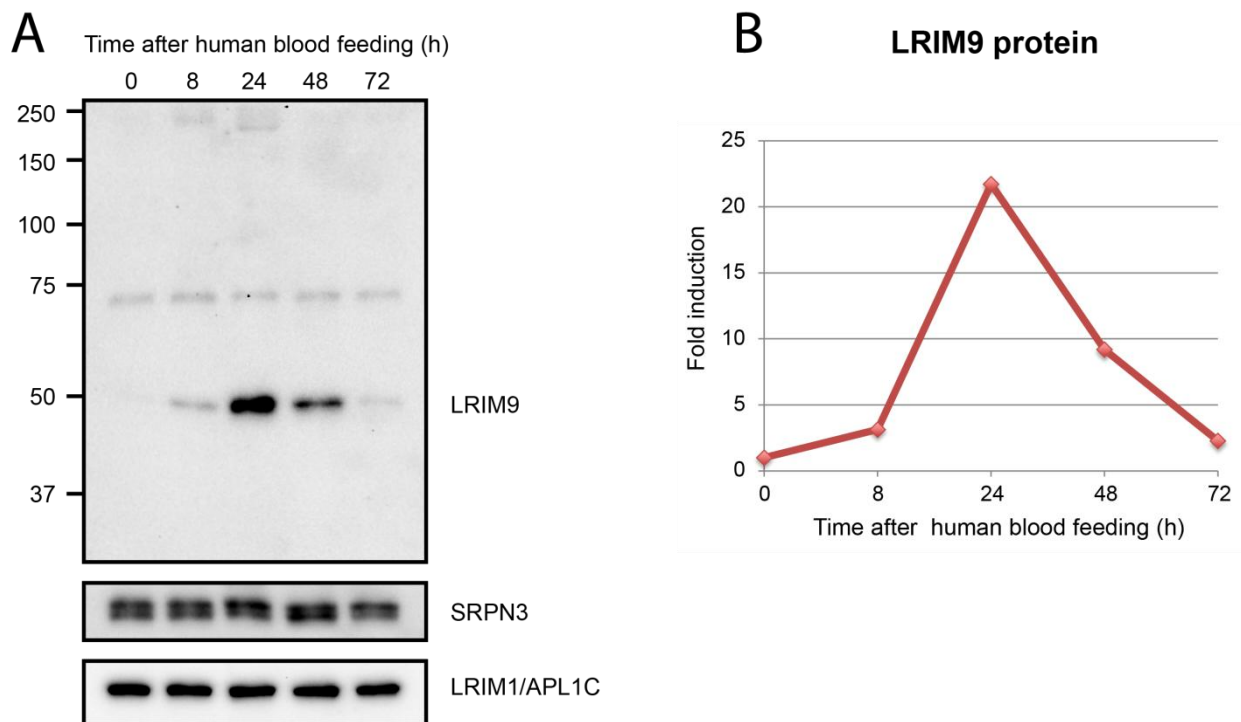


Figure 5.11 LRIM9 protein expression after feeding on human naïve blood.

Mosquitoes were allowed to feed on human blood and hemolymph was collected after 8, 24, 48 and 72 h. **A**) Hemolymph was analysed by western blot under non-reducing conditions and probed with α -LRIM9. The blot was re-probed with α -SRPN3 as a loading control and α -LRIM2-300 to analyse the LRIM1/APL1C complex. Molecular weight markers are indicated (kDa). **B**) LRIM9 protein bands were measured semi-quantitatively and normalised to SRPN3.

LRIM9 expression in the midgut

It was investigated whether LRIM9 is expressed in the mosquito midgut and exerts its role on malaria parasites from the midgut cells. Other parasite-killing immune proteins show midgut expression. For example, SRPN6 is specifically expressed by midgut cells after *P. berghei* invasion (Abraham et al., 2005). The *LRIM9* transcript was monitored in *dsGFP*- or *dsLRIM9*-treated mosquitoes by qRT-PCR 24 h after a *P. berghei* infected blood meal in midguts and carcasses (with midgut removed) (Figure 5.12). *LRIM9* was not or poorly expressed in midgut tissues before or 24 h after an infected blood meal, respectively, compared to corresponding carcass samples that showed strong *LRIM9* expression. This correlates well with previous microarray findings that *LRIM9* is most highly expressed in the fat body (Marinotti et al., 2005). Silencing efficiency of the *LRIM9* transcript in the carcass was very high: 95% after sugar feeding and 91% after blood feeding.

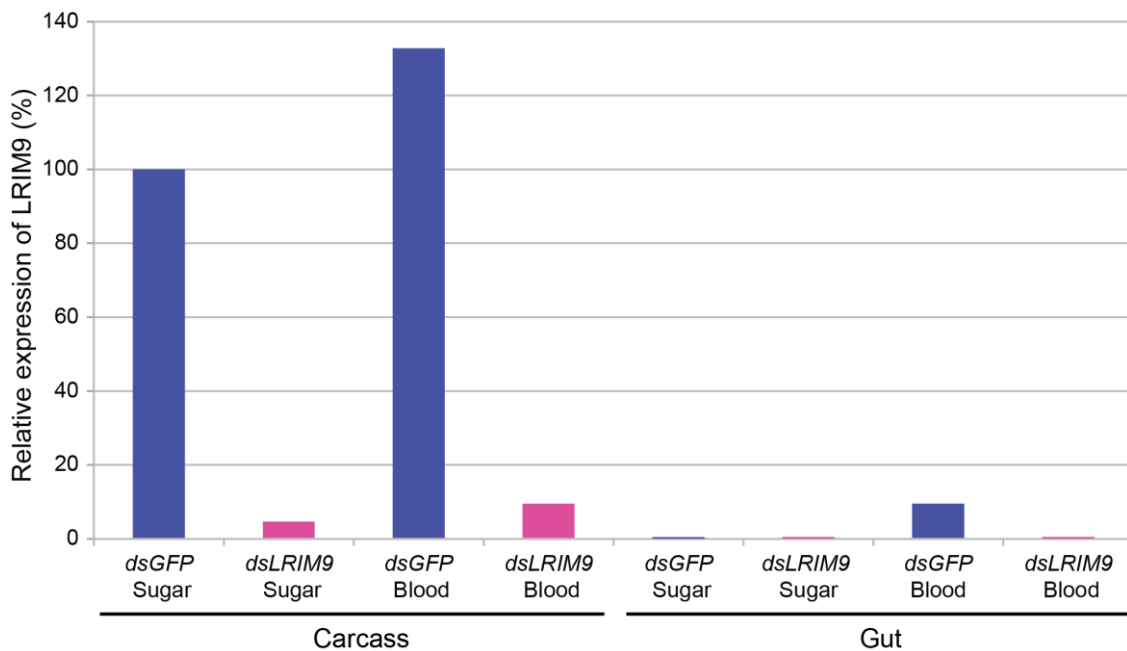


Figure 5.12 *LRIM9* transcript levels in the midgut.

Mosquitoes were injected with *dsGFP* (blue) or *dsLRIM9* (pink) and, 3 days later, some were given a *P. berghei* infected blood meal whereas others were only sugar fed. After 24 h, midguts were dissected and RNA was extracted from 20 guts per group. qRT-PCR was used to analyse *LRIM9* expression, using *S7* for normalisation.

LRIM9 and TEP1-mediated parasite killing

Members of the TEP family of complement C3-like proteins have been shown to interact with LRIMs (Povelones et al., 2011; Povelones et al., 2009). The LRIM1/APL1C complex is involved in parasite killing through its interaction with complement-like effector protein, TEP1. The complex binds to the cleaved form of TEP1, promoting its stabilisation, preventing it from reacting with self-tissues and enabling it to opsonise *P. berghei* parasites (Fraiture et al., 2009; Povelones et al., 2009).

To investigate whether LRIM9 plays a role in TEP1-mediated parasite killing, it was first examined whether LRIM9 interacts with TEP1 or LRIM1/APL1C. Binding assays were performed using recombinant His-tagged LRIM9 expressed in Sua4.0 cells, a hemocyte-like cell line that naturally secretes endogenous TEP1, LRIM1 and APL1C (Povelones et al., 2009) (Figure 5.13). A recombinant secreted His-tagged GFP was used as a negative control whereas His-tagged LRIM1 and APL1C were used as positive controls. Expression of the recombinant proteins in the starting conditioned media was determined by western blot detection of the His-tag to ensure equivalent amounts of protein were used for the binding assay since expression varied between the different proteins, despite being driven by the same viral promoter. His-tagged proteins and their interacting partners were affinity-captured from the conditioned media using cobalt-charged beads. Protein interactions were analysed in the captured material by probing western blots with TEP1, LRIM1 and APL1C antibodies.

As observed previously (Povelones et al., 2009), His-tagged LRIM1 and APL1C were able to interact with their endogenously expressed partner either as a monomer or homodimers. In addition, both recombinant LRIM1 and APL1C captured endogenous TEP1_{cut}. In contrast, no interaction was observed between His-tagged LRIM9 and endogenous TEP1, LRIM1 or APL1C. However, it cannot be ruled out that LRIM9 requires a partner to interact with TEP1, LRIM1 or APL1C and this partner is not produced by Sua4.0 cells.

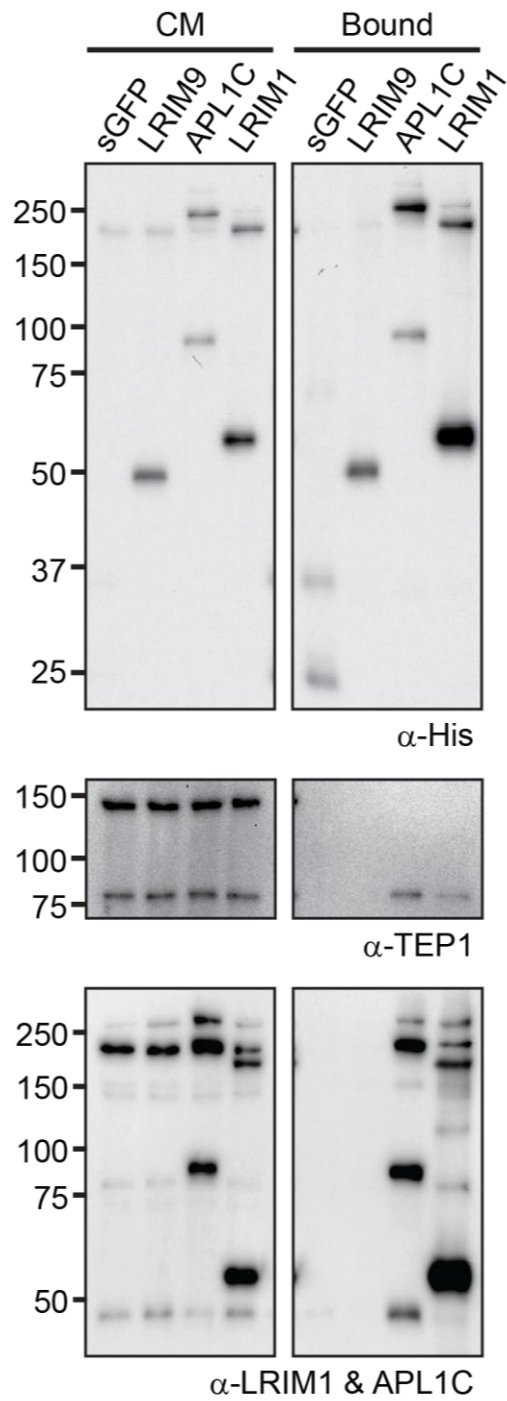


Figure 5.13 Binding assay to test interactions between LRIM9 and TEP1, LRIM1 and APL1C.

Conditioned media (CM) was collected 3.5 days after transfection of Sua4.0 cells with secreted GFP (sGFP), LRIM9, APL1C and LRIM1 constructs. His-tagged proteins and any interacting partners were captured from the conditioned media using metal affinity beads. Starting conditioned media (left panels) and bound material (right panels) were analysed by non-reducing western blot. One blot was incubated with the His probe (top panels). A second blot was probed with an antibody against TEP1 (middle panels) and re-probed with antibodies against LRIM1 and APL1C (bottom panels). Molecular weight markers are indicated (kDa).

Even though LRIM9 did not physically interact with known members of the mosquito complement-like cascade, western blotting of hemolymph was performed to determine whether LRIM9 functionally interacts with these proteins. In the absence of LRIM1 or APL1C, TEP1_{cut} is depleted from the hemolymph (Povelones et al., 2009). Using a C-terminal TEP1 antibody, TEP1-F and TEP1_{cut} were both detected in *GFP* and *LRIM9* knockdown hemolymph whereas TEP1_{cut} was specifically depleted after *LRIM1* knockdown (Figure 5.14 A). This suggests LRIM9 is not involved in the transcription, processing, stabilisation or activity of TEP1 in naïve mosquitoes. Antibodies against LRIM1 and APL1C, which both detect the LRIM1/APL1C complex under non-reducing conditions, demonstrated good silencing efficiency of the complex in the *LRIM1* knockdown.

Given the strong increase in LRIM9 protein upon blood feeding, it was hypothesised that LRIM9 may not be functional in the hemolymph until after the mosquito has blood fed. To examine this possibility, hemolymph was collected 24 h after a blood meal to ensure that sufficient LRIM9 was present and active (Figure 5.14 B). Blood fed mosquitoes were incubated at 27 °C to ensure optimum mosquito physiology. LRIM1/APL1C and LRIM9 were silenced efficiently in their respective knockdowns at the protein level, using the appropriate antibodies. However, like in the naïve hemolymph, *LRIM9* knockdown had no effect on levels of TEP1-F and TEP1_{cut}. Furthermore, there was no difference in the abundance of LRIM9 protein in the *dsGFP*- and *dsLRIM1*-treated mosquitoes, revealing that knockdown of the LRIM1/APL1C complex and concomitant loss of TEP1_{cut} does not affect LRIM9 protein induction following blood feeding (Figure 5.14 B).

In support of these data, an initial experiment found that *LRIM9* knockdown did not affect TEP1 localisation to the surface of *P. berghei* parasites during an infection (Figure 5.15). Although only a single experimental replicate, this result is consistent with the other findings and suggests that LRIM9 does not interact with TEP1 or affect its stability or activity.

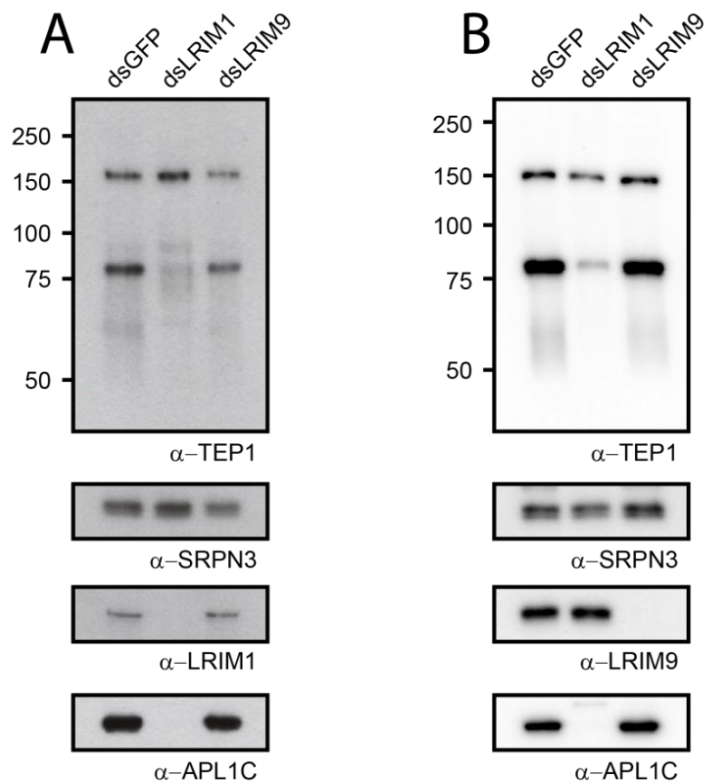


Figure 5.14 Investigating the involvement of LRIM9 in TEP1 activity in the hemolymph.

Hemolymph was collected from naïve (A) and blood fed (B) mosquitoes after injection with *dsGFP*, *dsLRIM1* and *dsLRIM9*. Samples were analysed by non-reducing western blot using α -TEP1, α -SRPN3, α -LRIM1, α -APL1C and α -LRIM9 antibodies.

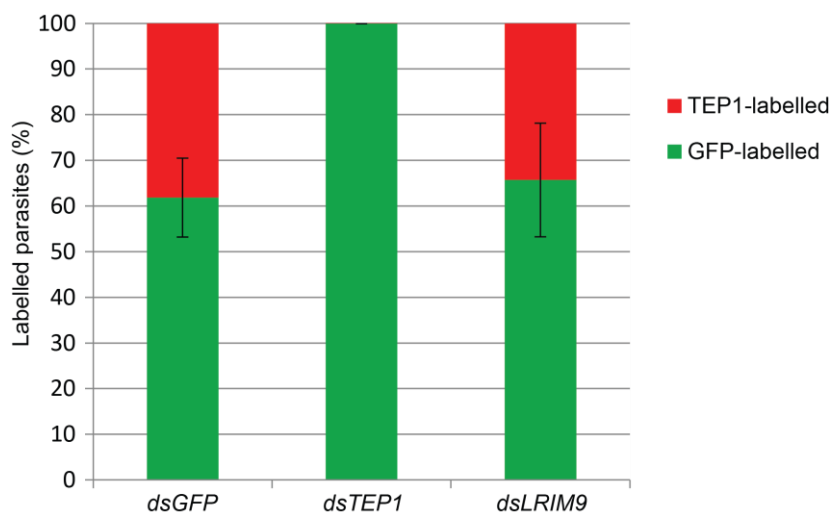


Figure 5.15 TEP1 localisation to *P. berghei* ookinetes after LRIM9 silencing.

Midguts were dissected from *dsGFP*-, *dsTEP1*- and *dsLRIM9*-treated mosquitoes 27-30 h after infection with GFP-expressing *P. berghei*. The blood meal was carefully removed and midgut epithelia were stained with TEP1 antibody and an Alexa Fluor 546 conjugated secondary antibody. A representative photograph was taken per gut and the number of GFP-labelled (live) and TEP1-labelled (dead) parasites were counted. In a single experiment, 7, 5 and 4 guts were analysed for *dsGFP*, *dsTEP1* and *dsLRIM9*, respectively. The graph shows the mean percentage of GFP-labelled (green) and TEP1-labelled (red) parasites with standard error bars.

It was previously established that TEP1-F is lost in the hemolymph after challenge with bacterial bioparticles (see Appendix Figure 9.2). Bioparticles are heat-killed bacteria which are very convenient for assaying rapid responses of complement proteins without the complication of bacterial proliferation. It was examined whether *LRIM9* silencing affects the depletion of TEP1-F after *E. coli* bioparticles challenge (Figure 5.16). Western blot analysis was performed on hemolymph collected 2 h after challenge with bioparticles, the time point with the strongest effect on TEP1. *LRIM9* silencing had no effect on TEP1-F or TEP1_{cut}. As observed previously, there was cross-reactivity with *E. coli* proteins in the SRPN3 control, resulting in a fuzzy band, because this antibody was raised against a SRPN3 protein fragment produced in *E. coli*.

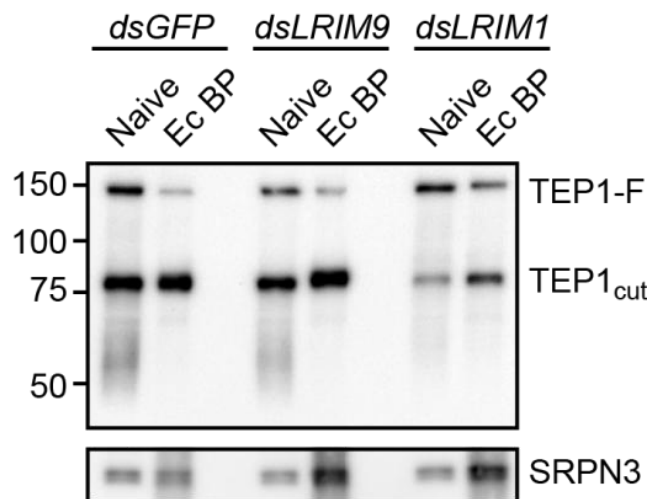


Figure 5.16 TEP1 protein levels after *E. coli* bioparticle challenge after *LRIM9* silencing.

Mosquitoes were injected with *dsGFP*, *dsLRIM9* and *dsLRIM1*. After 4 days, hemolymph was collected from half these mosquitoes (naïve) and half were injected with *E. coli* bioparticles and hemolymph was collected 2 h post challenge (Ec BP). Samples were analysed by non-reducing western blot, probing with α -TEP1 and α -SRPN3 antibodies. Molecular weight markers are indicated (kDa).

LRIM9 and other TEP family members

It was next examined whether LRIM9 might function together with other TEP family members in eliminating invading *P. berghei* parasites. Apart from TEP1, the LRIM1/APL1C complex has been shown to interact with TEP3, TEP4 and TEP9 in the conditioned media of *An. gambiae* cultured cells (Povelones et al., 2011). Of these proteins, TEP3 and TEP4 also emerged as interesting candidates from the transcriptional profiling presented in Chapter 4. They were induced by a broad spectrum of pathogens, including *P. berghei*, *P. yoelii*, *P. falciparum*, ONNV (especially by oral infection), bacteria

and fungi. This suggests that TEP3 and TEP4 are important core immune genes with a generalised role in mosquito defence.

To investigate potential interactions between LRIM9 and TEP3 and/or TEP4, it was attempted to create C-terminal antibodies against TEP3 and TEP4, using the same approach that produced the C-terminal TEP1 antibody. Fusion proteins of TEP3 and TEP4 C-terminal fragments with GST were generated and sequence verified. Plasmids containing the GST-fusion proteins were transformed into BL21-pLysS cells, which are IPTG inducible and excellent for protein expression. Unfortunately, small and large scale IPTG inductions and His purifications were unsuccessful. The C-terminal fragments were poorly induced and not very soluble under both native and denaturing conditions (data not shown). Due to time constraints, this problem was unable to be resolved. Peptide antibodies previously generated in the laboratory were not successful.

In the absence of antibodies against TEP3 and TEP4, phenotypic analyses were carried out to investigate whether knockdown phenotypes of *TEP3* and *TEP4* are similar to that of *LRIM9*, i.e. significant increase of *P. berghei* oocysts and inhibition of parasite melanisation in susceptible mosquitoes, but no effect on parasite melanisation in *CTL4* knockdown mosquitoes. This could suggest a functional relationship between LRIM9 and TEP3 and/or TEP4. The following findings were recently published (Povelones et al., 2011).

TEP3 and *TEP4* were silenced alongside known antagonist *TEP1* in susceptible mosquitoes to investigate the effect on *P. berghei* development (Figure 5.17). The results showed that TEP3 is a *Plasmodium* antagonist, like LRIM9. *TEP3* silencing resulted in a highly significant increase in developing oocysts. The increase of median infection intensity after *dsTEP3*-treatment was higher than *dsLRIM9* but much lower than *dsTEP1*, which was more comparable to *dsLRIM1*. There was a modest trend towards more oocysts after *TEP4* silencing but the increase was not statistically significant.

To further investigate the phenotypic relationship between *LRIM9*, *TEP3* and *TEP4*, they were silenced in double knockdowns with *CTL4*, a known inhibitor of *P. berghei* melanisation (Figure 5.18). In this experiment, the *GFP/CTL4* knockdown showed increased melanisation and fewer developing oocysts compared to the *GFP/GFP* control. *TEP1/CTL4* knockdown fully reversed the *CTL4* phenotype, greatly increasing the number of live oocysts and completely abolishing ookinete melanisation. *TEP3/CTL4* knockdown gave an intermediate phenotype whereby numbers of live oocysts increased whilst maintaining high levels of melanisation. Silencing *TEP4/CTL4* caused no

significant change in either live oocysts or melanised ookinetes compared to *GFP/CTL4*, although there was a marginal non-significant increase in ookinete melanisation.

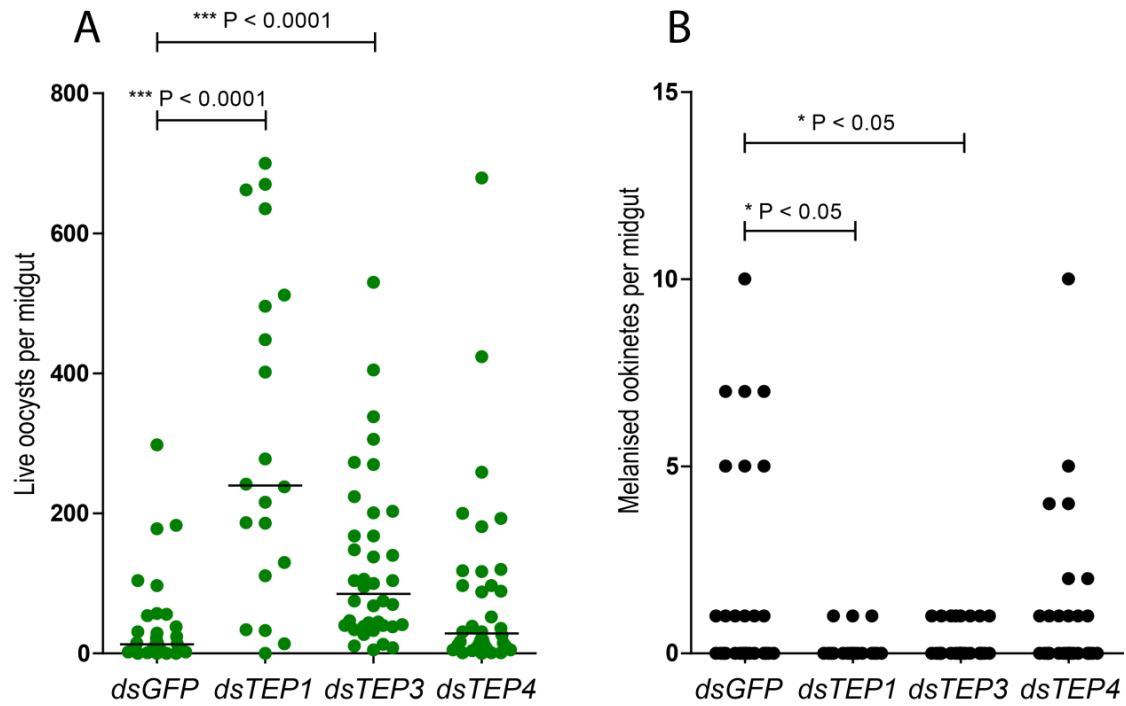


Figure 5.17 The effect of *TEP3* and *TEP4* knockdown on *P. berghei* development.

TEP3 and *TEP4* were silenced, mosquitoes were infected with GFP-expressing *P. berghei* and parasite load was monitored after 7 days. *GFP* and antagonist *TEP1* were used as controls. Horizontal lines indicate the median parasite number and all significant results ($P < 0.05$, Mann Whitney U-test) are highlighted. A representative experiment of three independent biological replicates is shown. **A**) Live oocyst counts. **B**) Melanised (killed) ookinete counts.

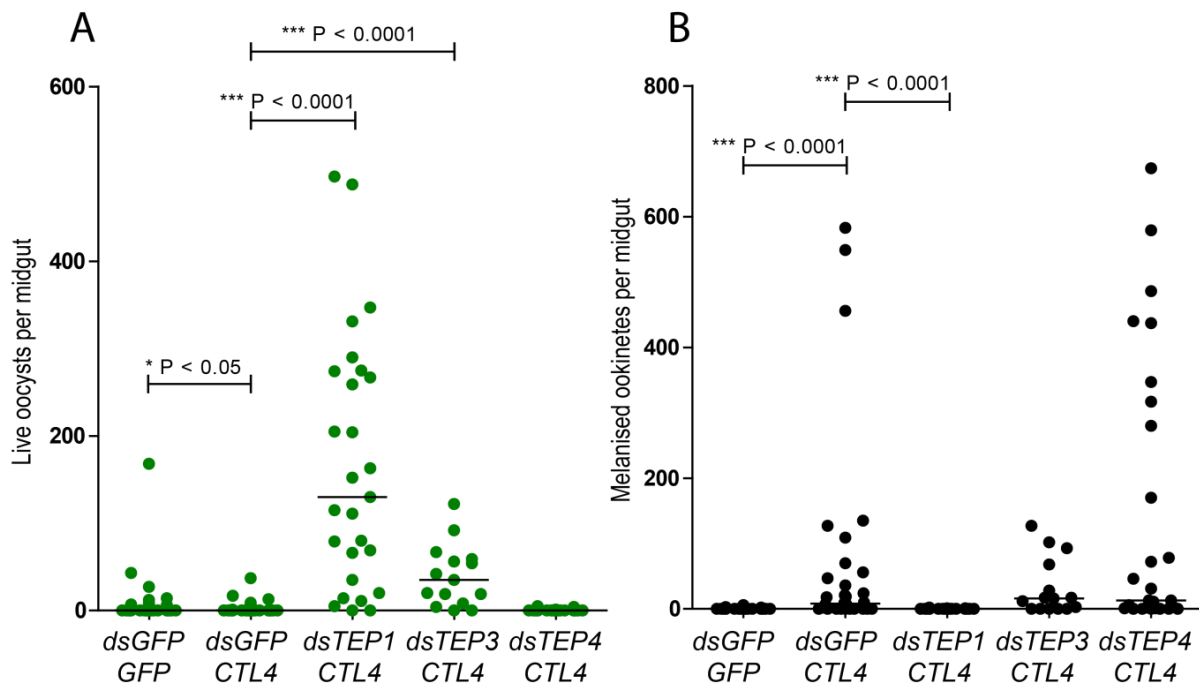


Figure 5.18 Double knockdowns of *CTL4* with *TEP3* and *TEP4*.

TEP3 and *TEP4* were silenced using RNAi in double knockdowns with *CTL4*, a known inhibitor of parasite melanisation. Mosquitoes were infected with fluorescent *P. berghei* and parasite load was monitored after 7 days. Double knockdowns of *GFP/GFP*, *GFP/CTL4* and *TEP1/CTL4* were used as controls. All significant results ($P < 0.05$, Mann Whitney U-test) are highlighted. Results shown are representative of two independent biological replicates. **A**) Live oocyst counts. **B**) Melanised (killed) ookinete counts.

Involvement of *LRIM9* in antibacterial defence

As *LRIM9* responds strongly to blood feeding, it was examined whether it functions in antibacterial defence. Although the blood meal itself is sterile, the influx of nutrients upon blood feeding causes dramatic proliferation of endogenous bacteria within the mosquito midgut (Kumar et al., 2010; Meister et al., 2009). The midgut undergoes extreme distension, which could damage the gut epithelia and allow midgut bacteria to invade the hemolymph, leading to systemic infection. The mosquito innate immune system constitutively and actively controls midgut bacterial load (Dong et al., 2009). Thus, *LRIM9* induction after blood feeding might be a response to signalling triggered by the increase in midgut bacteria or detection of bacteria in the hemolymph. Parasite melanisation is also dependent on levels of commensal bacteria (Fanny Turlure, personal communication), which strengthens the hypothesis given the previously described role for *LRIM9* in parasite melanisation.

To test this hypothesis, it was investigated whether *LRIM9* knockdown affects mosquito survival after *E. coli* injection. Although *E. coli* is not a natural pathogen of *An. gambiae*, it is a typical gram-negative bacterium and conveniently ampicillin-resistant. *LRIM9* was silenced by RNAi, mosquitoes were injected with live *E. coli* 4 days later and survival monitored for 10 days. In naïve (non-blood

fed) mosquitoes, *LRIM9* knockdown had no significant effect on mosquito survival compared to the *dsGFP* control (Figure 5.19 A), using the Log-rank (Mantel-Cox) test. Silencing the positive control, *LRIM1*, which has a known role in defence against *E. coli* infection (Moita et al., 2005), resulted in significantly higher mosquito mortality compared to *dsGFP*. As *LRIM9* was present at low levels in the hemolymph before blood feeding, the survival assay was repeated using mosquitoes that were blood fed 24 h before *E. coli* injection (Figure 5.19 B). Again, *LRIM9* knockdown did not affect mosquito survival indicating that *LRIM9* does not protect mosquitoes from dying during an *E. coli* infection in both naïve and blood fed mosquitoes.

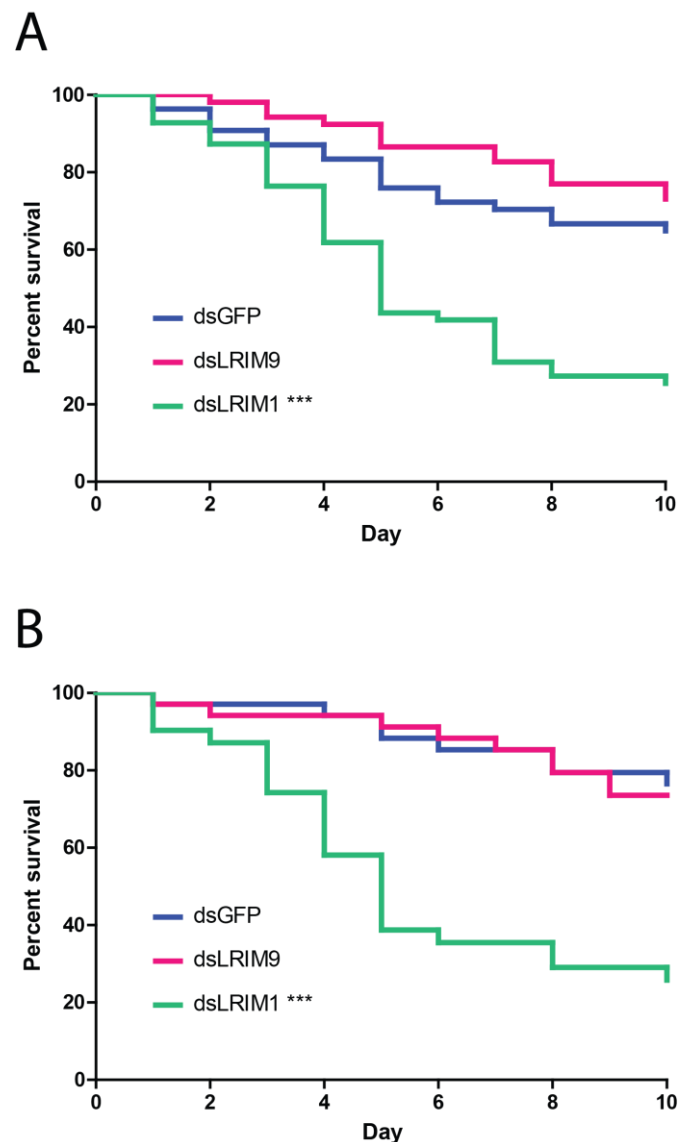


Figure 5.19 Survival after *E. coli* injection in naïve and blood fed mosquitoes.

A) Mosquitoes were injected with *dsGFP*, *dsLRIM9* and *dsLRIM1* and inoculated with live *E. coli* 4 days later. Mosquito survival was monitored daily for 10 days. Survival was compared to *dsGFP* using the Log-rank (Mantel-Cox) test (***) = P-value < 0.0001). **B)** As above, but mosquitoes were blood fed 24 h prior to *E. coli* injection.

Since survival is not always connected with bacterial proliferation (Ayres et al., 2008), it was investigated whether LRIM9 affects bacterial proliferation when *E. coli* is injected into the hemocoel (Figure 5.20). *GFP*, *LRIM9* and *LRIM1* were silenced and mosquitoes were inoculated with live ampicillin-resistant *E. coli*. After 24 h, batches of 10 mosquitoes were surface-sterilised, washed and homogenised. The resulting suspension was plated onto ampicillin agar, incubated overnight at 37 °C and colonies were counted the next day to measure bacterial proliferation. Uninjected mosquitoes were homogenised as additional controls and showed no colony formation on ampicillin plates. The results showed that *LRIM9* knockdown had no significant impact on proliferation of injected *E. coli* compared to control *dsGFP*-treated mosquitoes (P-value = 0.804, Meta-Analysis). A sample of the injected bacteria was plated to ensure comparable viability between experiments. In contrast, *LRIM1* knockdown resulted in a consistently higher number of CFU per mosquito.

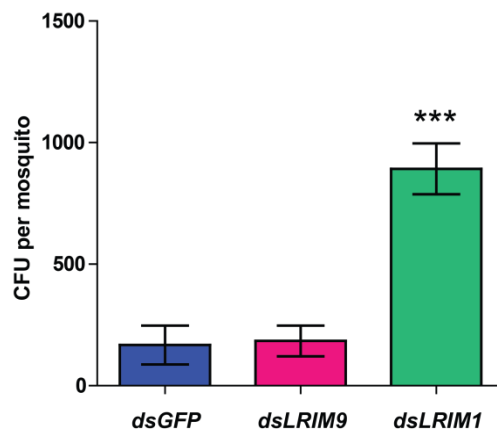


Figure 5.20 The effect of *LRIM9* knockdown on bacterial proliferation.

Mosquitoes were injected with *dsGFP*, *dsLRIM9* and *dsLRIM1* and after 4 days inoculated with live ampicillin-resistant *E. coli*. After 24 h, batches of 10 mosquitoes were collected per group, surface-sterilised, homogenised and plated onto ampicillin agar. After incubation at 37 °C overnight, CFU were counted. Mean CFU per mosquito from three independent experiments is shown, with standard error bars. *dsLRIM9* and *dsLRIM1* were compared to *dsGFP* using Meta-Analysis (***) = P-value < 0.0001).

Antibiotics were used to investigate whether LRIM9 upregulation after blood feeding is dependent on the massive proliferation of midgut bacteria. It was hypothesised that antibiotics would prevent the induction of LRIM9. Mosquitoes were fed on a spectrum of antibiotics dissolved in sterile sugar to significantly reduce their midgut flora. To confirm antibiotic efficacy, surface-sterilised mosquitoes were homogenised and plated on agar. The antibiotics were very effective at significantly reducing the midgut flora. Four days into the treatment, some mosquitoes were allowed to blood feed whereas others were only given antibiotic sugar. Hemolymph was collected 24 h later

and analysed by non-reducing western blot (Figure 5.21 A) for LRIM9 and SRPN3. Untreated mosquitoes, which were fed sterile sugar with or without blood feeding, acted as controls. LRIM9 was low in sugar fed hemolymph irrespective of antibiotic treatment. Interestingly, LRIM9 was still dramatically induced at the protein level after blood feeding, even with a significantly reduced midgut flora. This suggests that the upregulation of LRIM9 after blood feeding is independent of the endogenous bacteria.

In Chapter 4, *E. coli* or *S. aureus* injection did not affect *LRIM9* transcript levels. It was decided to verify this result at the protein level by collecting hemolymph 24 h after injection of live *E. coli* or *S. aureus*. Hemolymph was analysed by western blot under non-reducing conditions and probed with antibodies against LRIM9 and SRPN3 (Figure 5.21 B). LRIM9 protein was not upregulated after *E. coli* or *S. aureus* injection, consistent with the transcriptional results. Levels of LRIM9 in the hemolymph were comparable to naïve mosquitoes. Even the injury at the site of injection did not affect LRIM9. Therefore, LRIM9 did not respond to bacteria at both the transcript and protein level. Overall, it can be concluded that LRIM9 is unlikely to be involved in antibacterial immunity.

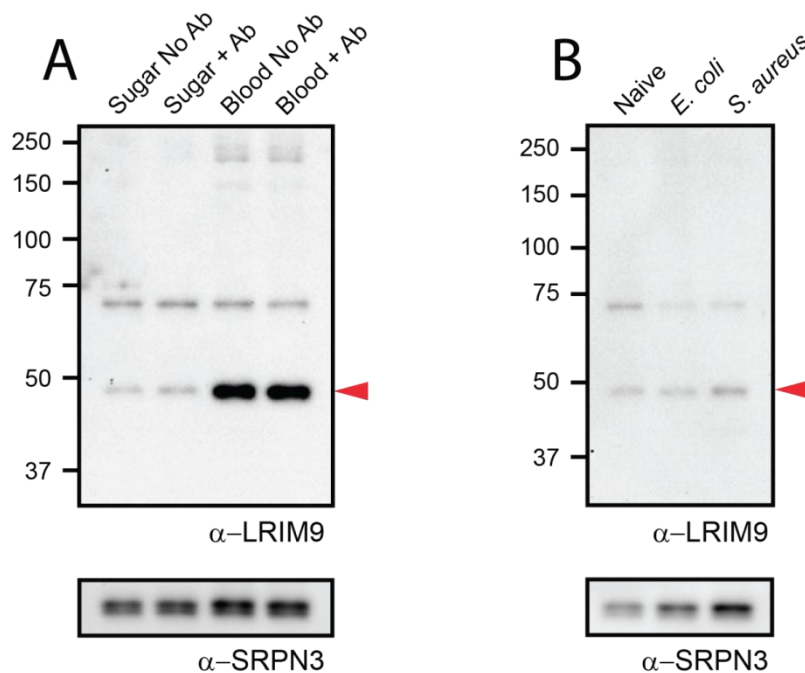


Figure 5.21 The effect of antibiotics and bacterial injection on LRIM9 expression.

A) Newly emerged mosquitoes were fed either sterile sugar solution (No Ab) or a cocktail of antibiotics dissolved in sugar (+ Ab) for the entire experiment. After 4 days of treatment, mosquitoes were either fed on naïve blood or kept on sugar. 24 h later, hemolymph was collected and analysed by non-reducing western blot, probing with α -LRIM9 and α -SRPN3 antibodies. **B)** Hemolymph was collected from naïve mosquitoes 24 h after injection with live *E. coli* or *S. aureus*. Samples were analysed by western blot and probed with α -LRIM9 and α -SRPN3 antibodies. Molecular weight markers are shown (kDa) and LRIM9 is indicated with a red arrowhead.

LRIM9 and the melanisation pathway

After showing an interesting parasite melanisation phenotype, it was decided to investigate the functional role played by LRIM9 in melanisation, a powerful innate immune response of arthropods (Cerenius and Soderhall, 2004; Christensen et al., 2005; Jiravanichpaisal et al., 2006). Melanisation is triggered by a clip-domain serine protease cascade that culminates in proteolytic activation of the inactive PPO into the active PO. Active PO then catalyses the rate-limiting step in the production of melanin that is deposited on the surfaces of invading parasites and pathogens and at tissue wound sites, crosslinking surrounding proteins. CLIPA8, a noncatalytic clip-domain SPH, is a vital regulator of PO activation in *An. gambiae*. It is essential for ookinete and bacterial melanisation (Schnitger et al., 2007; Volz et al., 2006). CLIPA8 circulates in the hemolymph and is rapidly activated by cleavage after wounding and bacterial challenge (Schnitger et al., 2007). It has been shown to bind to the surface of bacteria (Hassan Yassine, personal communication).

Firstly, it was examined whether CLIPA8 activation requires LRIM9 (Figure 5.22). To this end, mosquitoes were injected with *dsGFP*, *dsLRIM9*, *dsTEP1* or *dsLRIM1*. TEP1 and LRIM1 used as positive controls because both have striking effects on CLIPA8 activation cleavage. *TEP1* silencing blocks CLIPA8 cleavage whereas *LRIM1* silencing leads to spontaneous CLIPA8 cleavage, even in unchallenged mosquitoes (Michael Povelones, personal communication). Four days after injection of dsRNA, hemolymph was collected from naïve mosquitoes (dsRNA injected only) and 2 h after injection with *S. aureus* bioparticles (heat-killed bacteria). *S. aureus* was chosen because it is a potent inducer of CLIPA8 cleavage (Schnitger et al., 2007). Western blot analysis of hemolymph under reducing conditions was performed using a CLIPA8 monoclonal antibody. In *dsGFP*-treated mosquitoes, only a 47 kDa band was observed in naïve hemolymph, which corresponds to full-length CLIPA8. After *S. aureus* challenge, a cleaved form of CLIPA8 at 38 kDa was also detected. Interestingly, the full-length CLIPA8 was less abundant after *S. aureus* challenge, probably due to CLIPA8 cleavage and binding of CLIPA8 to bacterial surfaces and mosquito tissues. CLIPA8 appeared unchanged by *LRIM9* silencing compared to *GFP* silencing. As expected, *TEP1* silencing blocked CLIPA8 cleavage after *S. aureus* challenge and full-length CLIPA8 was very strong in both lanes. There was mild spontaneous cleavage observed after *LRIM1* knockdown, in both naïve and challenged hemolymph, which was not further enhanced by *S. aureus*. Interestingly, compared to the *dsGFP*-treated control group, full-length CLIPA8 was considerably less abundant in hemolymph isolated from both naïve and *S. aureus* challenged *dsLRIM1*-treated mosquitoes. Therefore, these data suggest LRIM9 is not involved in CLIPA8 activation. The blot was re-probed with antibodies against TEP1 and LRIM9, which both revealed good knockdown efficiencies. As seen in Figure 5.16, LRIM9

was also not involved in the loss of TEP1-F after bioparticle challenge. LRIM9 was unchanged in the hemolymph after bioparticle challenge.

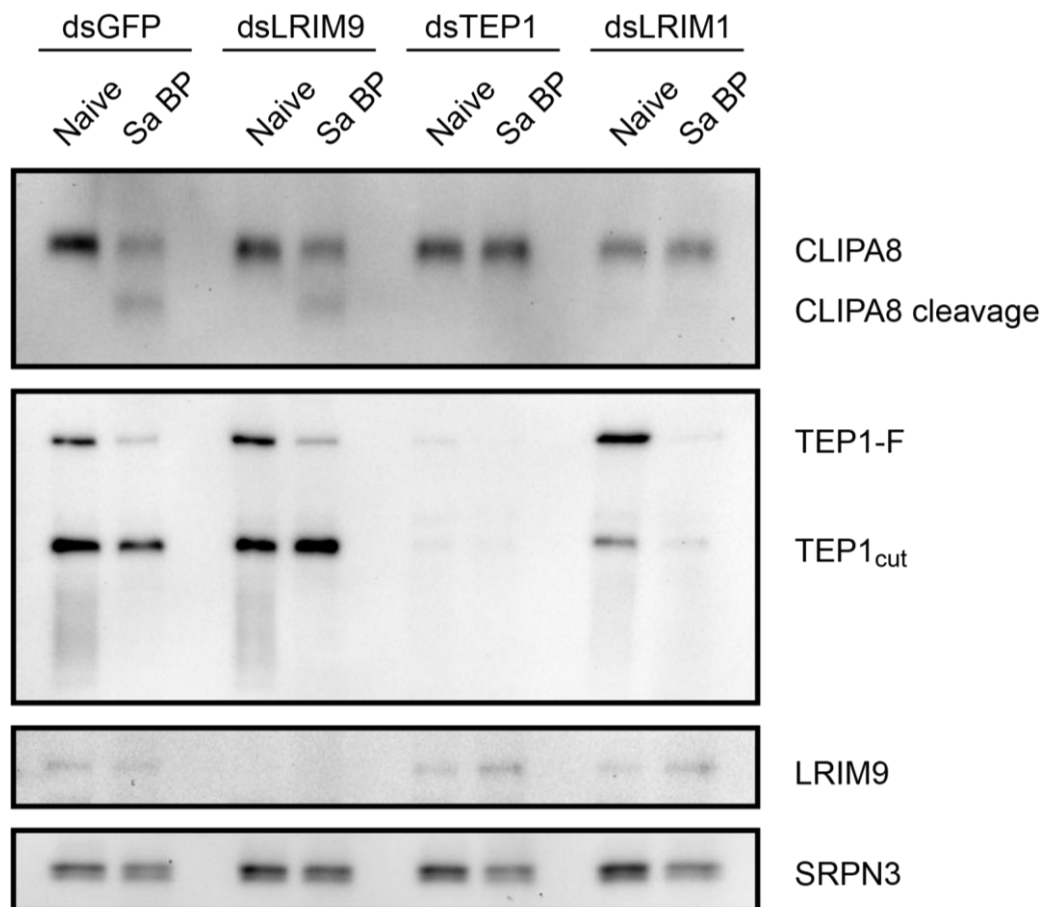


Figure 5.22 Investigating the involvement of LRIM9 in CLIPA8 activation cleavage.

Mosquitoes were injected with *dsGFP*, *dsLRIM9*, *dsTEP1* and *dsLRIM1*. After 4 days, hemolymph was collected from half these mosquitoes (naïve) and half were injected with *S. aureus* bioparticles and hemolymph was collected 2 h post challenge (Sa BP). Hemolymph was normalised to 1.5 mosquitoes/ μ L (to boost CLIPA8 signal) and analysed by reducing western blot. The blot was probed with α -CLIPA8, α -SRPN3, α -LRIM9 and α -TEP1 antibodies. This blot is representative of two independent experiments.

It was next investigated whether LRIM9 functions downstream of CLIPA8 in the melanisation pathway and affects PO activation. To test this, live bacteria were injected into the hemocoel of *dsGFP*, *dsLRIM9* and *dsLRIM1* mosquitoes and hemolymph was collected 5 h after injection (Figure 5.23). Equivalent amounts of hemolymph proteins were incubated with L-DOPA, a key PO substrate, and absorbance at 490 nm was measured at kinetic intervals. Absorbance at 490 nm detects

dopachrome production by PO and gives an indication of systemic melanisation after bacterial challenge.

Despite variation between replicates, there was significant indication that *LRIM9* knockdown reduces PO activity. Hemolymph from *dsGFP* controls showed consistently high PO activity after bacterial challenge, with dopachrome production continuing to increase throughout the 90 minute assay. In the first replicate using naïve non-blood fed mosquitoes, *LRIM9* knockdown blocked PO activity to the same extent as *LRIM1*, a known regulator of melanisation (Figure 5.23 A). In the second replicate, *LRIM9* silencing inhibited PO activity but did not completely block activity to basal levels like *LRIM1* silencing (Figure 5.23 B). Next, the assay was repeated using blood fed mosquitoes to determine whether boosting *LRIM9* concentration would make the effect of *LRIM9* more pronounced. Although basal PO activity was higher after blood feeding and the resolution poorer, a similar trend was observed (Figure 5.23 C). *LRIM9* silencing reduced PO activity without blocking it. It was concluded that *LRIM9* knockdown partially inhibits PO activity, even after blood feeding.

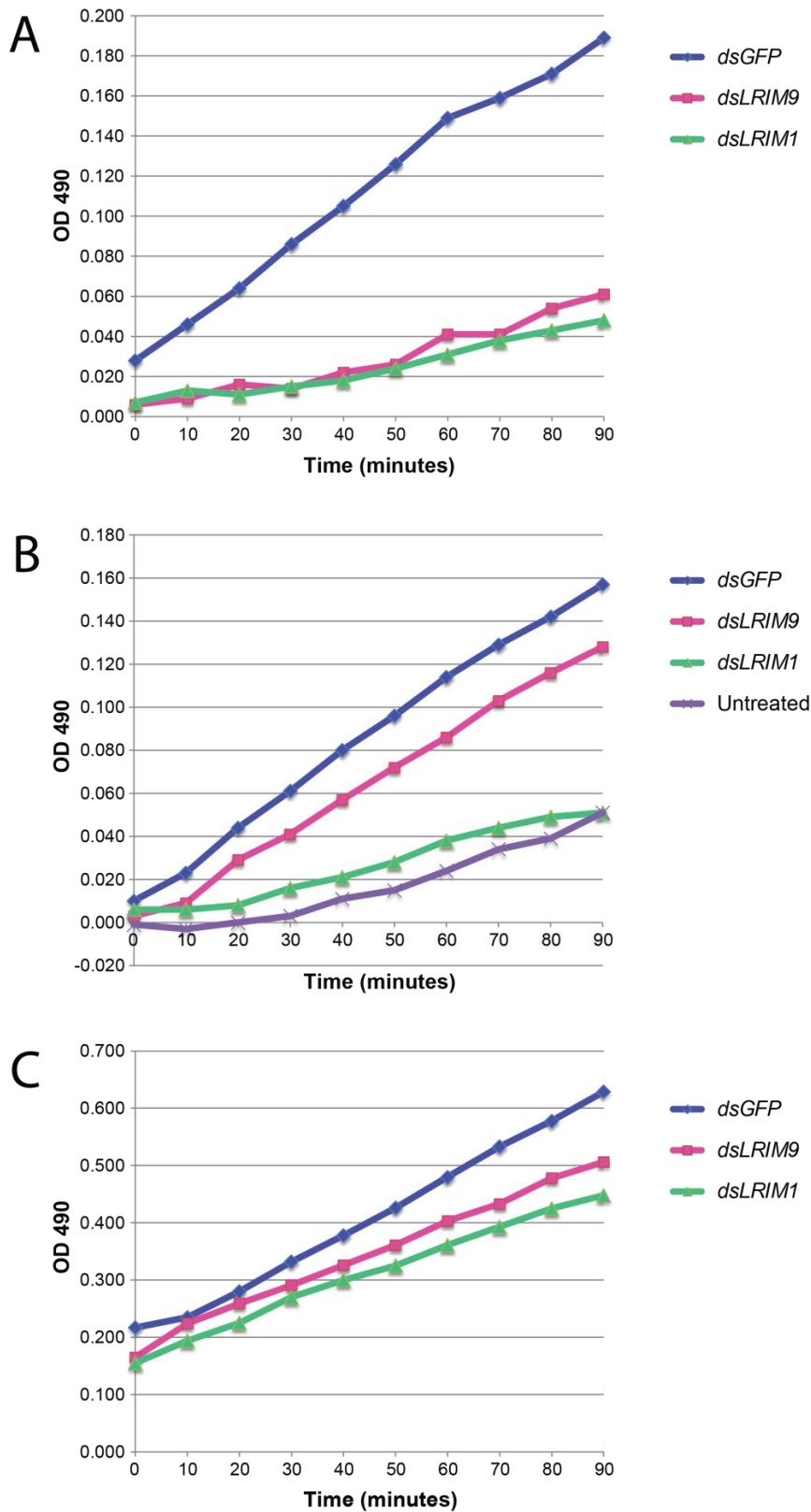


Figure 5.23 LRIM9 and phenoloxidase activity.

PO enzymatic activity was measured in hemolymph from *dsGFP*, *dsLRIM9* and *dsLRIM1* injected mosquitoes 5 h after injection of *E. coli* and *S. aureus*. To measure PO activity, hemolymph was normalised for protein content and incubated with L-DOPA, the substrate of PO. Absorbance at 490 nm (OD 490) was measured at kinetic intervals of 10 minutes. **A)** Replicate 1 in naïve mosquitoes. **B)** Replicate 2 in naïve mosquitoes, including untreated mosquitoes (not challenged with bacteria) to show basal activity. **C)** Replicate 3 in mosquitoes challenged 24 h after blood feeding.

Tissue melanisation at the site of wounding is another distinct insect defence response. It plays a physiological role in wound healing and cuticle sclerotisation (Asano and Ashida, 2001a, b). In *Ae. aegypti*, it has been reported that immune melanisation and tissue melanisation have distinct mechanisms of PPO activation (Zou et al., 2010). In fact, CLIPA8 is dispensable for wound melanisation (Schnitger et al., 2007), which suggests a similar system in *An. gambiae*. To determine whether LRIM9 influences tissue melanisation, dsRNA-treated mosquitoes were pricked with a sterile needle 24 h after blood feeding. Melanisation of the epidermis at the site of injury was visualised in immobilised mosquitoes 24 h later. Wound melanisation was equally efficient in *dsGFP* and *dsLRIM9* mosquitoes, suggesting that LRIM9 is not involved in this process (Figure 5.24).

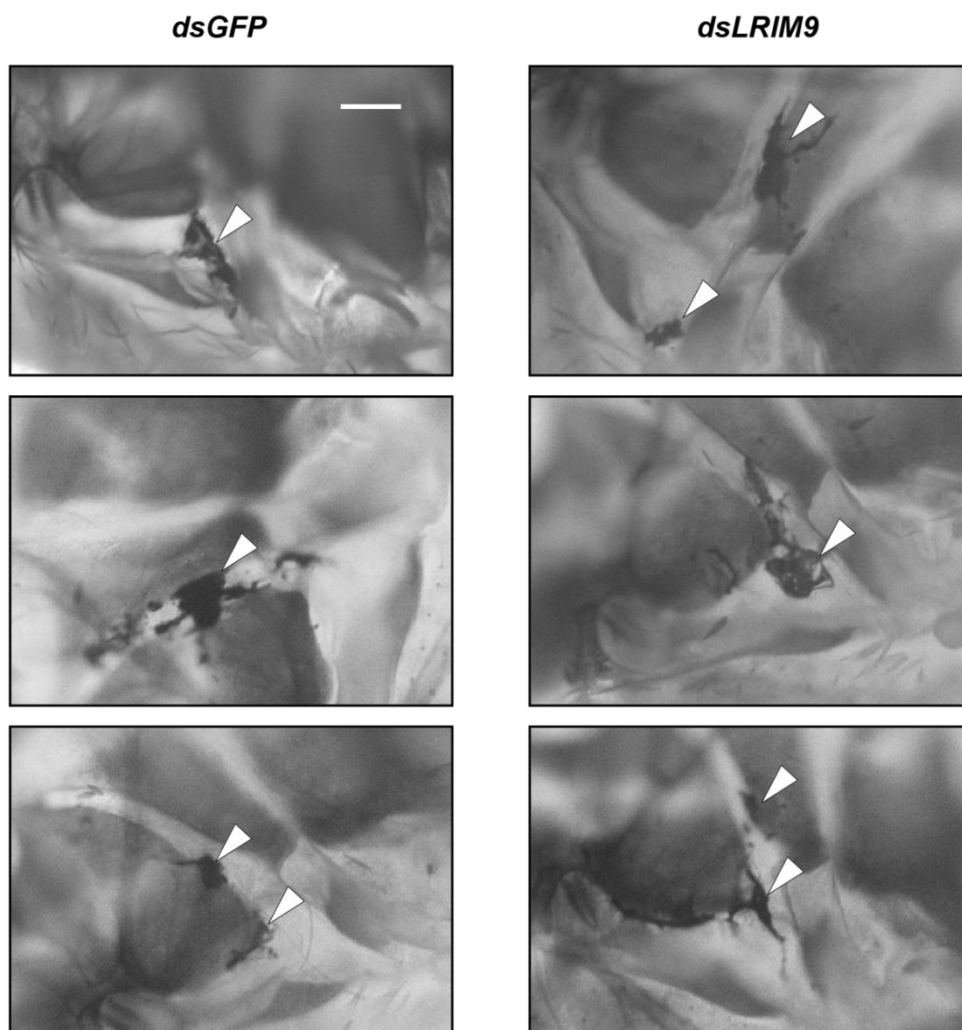


Figure 5.24 The effect of *LRIM9* knockdown on tissue melanisation.

Mosquitoes were blood fed 3 days after *dsGFP* or *dsLRIM9* injection. 24 h later, mosquito thoraxes were pricked several times with a sterile needle. The thoraxes of live immobilised mosquitoes were imaged 24 h after wounding. White arrowheads indicate sites of tissue melanisation. The scale bar in the top left panel represents 100 μ M.

LRIM9 and mosquito fecundity

Female mosquitoes take a blood meal to obtain nutrients that activate egg development (oogenesis) in their ovaries. In anautogenous mosquitoes, like *An. gambiae*, the reproductive system remains dormant until after blood feeding (Attardo et al., 2005; Hansen et al., 2004). A key physiological event in egg maturation is vitellogenesis, the production and secretion of yolk protein precursors (YPPs) by the fat body (Raikhel et al., 2002). Amino acids and lipids from a blood meal are transported through the midgut cells into the hemolymph where they stimulate the nutrient-sensitive target of rapamycin (TOR) pathway (Hansen et al., 2004). This initiates YPP production, which are transported to the ovaries for oogenesis. Vitellogenesis is also regulated by the ecdysteroid hormone, 20-hydroxyecdysone. It has been previously shown that apolipoprotein II/I (ApoII/I; also known as lipophorin) and vitellogenin, two key YPPs that transport nutrients to the developing mosquito oocytes, reduce the efficiency of TEP1-mediated parasite killing (Rono et al., 2010). This demonstrates that there is a trade-off between mosquito immunity and reproduction. Modulating the immune response to block mosquito reproduction has exciting prospects for malaria control.

As LRIM9 was so strongly induced by blood feeding, it was hypothesised that LRIM9 might play a role in mosquito fecundity. To examine this possibility, mosquitoes were allowed to mate in a large cage for 3 days before being injected with *dsGFP* or *dsLRIM9* and blood fed 3 days later. After 72 h, individual blood fed females were placed in dishes with wet filter paper and encouraged to lay eggs in darkness for 24 h. The number of eggs laid and larvae hatched were counted (Table 5.2). A few mosquitoes from both treatment groups were dissected 72 h after blood feeding and, in both groups, the ovaries were well developed and the blood meal was well digested (data not shown).

LRIM9 silencing had no impact on mosquito fecundity (Table 5.2). There was no significant difference between the number of eggs laid (P-value = 0.6842) and the number of larvae hatched (P-value = 0.6596) between *dsGFP* and *dsLRIM9*, using the Mann Whitney U-test. Total eggs laid, mean eggs laid per female, proportion of eggs that hatched into larvae and percentage of fertile females (laying at least one egg and hatching at least one larva) were equivalent between *dsGFP* and *dsLRIM9*.

Table 5.2 The effect of *LRIM9* knockdown on egg laying and larval hatching.

Gene knockdown	Females at start	Females laid eggs	Total eggs laid	Mean eggs per female	% Females laid eggs	% Hatchability	% Fertile females
GFP	46	27	1809	67	59	62	50
LRIM9	46	29	1958	68	63	64	52

Mosquitoes were allowed to mate, treated with *dsGFP* and *dsLRIM9* and then blood fed. After 72 h, individual females were placed in dishes with wet filter paper and encouraged to lay eggs in the dark. Eggs laid and larvae hatched were counted. % Hatchability is the percentage of eggs that hatched into larvae. Fertile females were defined as those that laid at least one egg and produced at least one larva.

5.3 Discussion

LRIM9 is a member of the LRIM family, a novel group of LRR-containing proteins exclusively found in mosquitoes. The family are predicted to be pathogen recognition proteins but most LRIMs are largely uncharacterised. The founding members of the family, LRIM1 and APL1C, are components of the *An. gambiae* complement-like system alongside the complement-like effector, TEP1 (Blandin et al., 2008; Fraiture et al., 2009; Povelones et al., 2009). These three proteins are powerful antagonists of *Plasmodium* infections of *An. gambiae*. In Chapter 4, LRIM9 was identified as a new *P. berghei* antagonist that was massively upregulated by naïve blood feeding. The role of LRIM9 in mosquito innate immunity and parasite killing was investigated in this Chapter.

LRIM9 was discovered to be a novel antagonist of *P. berghei* infections of *An. gambiae*. Silencing *LRIM9* in susceptible mosquitoes resulted in a 5-fold increase in live oocysts. The *LRIM9* knockdown phenotype was less dramatic than *LRIM1*, *APL1C* or *TEP1*. This moderate phenotype cannot be explained by poor knockdown of the *LRIM9* transcript as expression was demonstrated to be significantly reduced for at least 7 days after dsRNA injection. Alternatively, there could be independent pathways involved in parasite recognition and killing and impairing one pathway would have a moderate impact on parasite survival (Blandin et al., 2008). Furthermore, different parasite recognition pathways might take precedence depending on the basal immune status of individual mosquitoes.

Evidence suggests that LRIM9 is not directly involved in the mosquito complement-like pathway. Recombinant LRIM9 did not interact with TEP1, LRIM1 or APL1C in binding assays *in vitro*. However, it cannot be excluded that LRIM9 requires another mosquito partner to enable interaction with TEP1/LRIM1/APL1C, which was not secreted by the mosquito cell line used. Also, recombinant LRIM9

may not have the same functional properties as the native protein. Unlike the LRIM1/APL1C complex, LRIM9 showed no involvement in TEP1 stability, processing or activity in naïve mosquitoes, after blood feeding and after injection of *E. coli* bioparticles. An initial experiment suggested that LRIM9 was not required for TEP1 localisation to the surface of *P. berghei* parasites. Together, this evidence implies that LRIM family members can exhibit different behaviours and can function in distinct immune pathways.

TEP3 and TEP4 showed interesting transcriptional profiles and therefore were investigated as putative interacting partners of LRIM9. Phenotypic characterisation revealed that TEP3 is another novel antagonist of *P. berghei* infections of *An. gambiae* (Povelones et al., 2011), demonstrating a moderate phenotype similar to LRIM9. However, in double knockdowns with *CTL4*, *TEP3* silencing results in a significant increase in live parasites without blocking melanisation. In contrast, *LRIM9* had no effect in *CTL4* double knockdowns. By comparison, *TEP4* silencing does not impact *P. berghei* infections in susceptible mosquitoes or when silenced alongside *CTL4*. TEP3 and TEP4 antibodies and *in vitro* binding assays are required to conclusively determine whether these TEPs function alongside LRIM9. Nonetheless, evidence so far suggests an interaction is unlikely. Both *TEP3* and *TEP4* are highly upregulated by bacteria, as shown in Chapter 4 and previous microarrays (Dimopoulos et al., 2002; Dong et al., 2006a). Furthermore, TEP4 is required for survival of bacterial infections (Dong et al., 2006a) and is known to function in bacterial phagocytosis (Moita et al., 2005). In comparison, LRIM9 does not seem to be involved in antibacterial defence. Additionally, TEP3 and TEP4 interact with the LRIM1/APL1C complex *in vitro* and there is no evidence linking LRIM9 to the mosquito complement-like pathway.

LRIM9 demonstrated an atypical role in melanisation. Its silencing reduced the intensity and prevalence of spontaneous parasite melanisation in susceptible mosquitoes. In refractory L3-5 mosquitoes, which usually melanise virtually all invading ookinetes, *LRIM9* knockdown resulted in a significant reduction in melanisation but no corresponding increase in live oocysts. In other words, parasites were not melanised but were still killed successfully. This was in contrast to the phenotypes of *LRIM1*, *APL1C* and *TEP1*, which fully reverse the refractory L3-5 phenotype: melanisation is blocked and there is a massive increase in live parasites (Blandin et al., 2004; Povelones et al., 2009). This suggests that parasite lysis and/or TEP1-mediated killing are blocked when *LRIM1*, *APL1C* or *TEP1* are silenced but not when *LRIM9* is silenced. Therefore, LRIM9 might be independent of these lysis/killing mechanisms, which correlates with the lack of evidence linking LRIM9 to the complement-like pathway. The unusual phenotype of *LRIM9* knockdown in L3-5 mosquitoes is shared by some other mosquito proteins: CLIPA8, Apoll/I, Frizzled2 (Fz2) and Cell

division cycle 42 (*Cdc42*) (Mendes et al., 2008; Shiao et al., 2006; Volz et al., 2006). CLIPA8, a non-catalytic SPH, is an essential regulator of melanisation (Volz et al., 2006) and recent data place CLIPA8 downstream of the complement-like pathway (Hassan Yassine, personal communication). *Apoll/I* is a key nutrient transport protein that delivers lipids and fatty acids to various target tissues, including developing mosquito oocytes (Atella et al., 2006; Rono et al., 2010). Silencing *Apoll/I* in susceptible mosquitoes decreases oocyst levels by enhancing the efficiency of TEP1-mediated killing and aborts egg development (Mendes et al., 2008; Rono et al., 2010; Vlachou et al., 2005). Unlike *LRIM9*, silencing *CLIPA8*, *Fz2* or *Cdc42* does not affect oocyst levels in susceptible mosquitoes (Shiao et al., 2006; Volz et al., 2006).

In susceptible mosquitoes, *LRIM9* had no effect on parasite melanisation when silenced alongside *CTL4*, a known repressor of melanisation. This suggested there is no genetic interaction between *LRIM9* and the *CTL4* module. Even so, the increase in live oocysts usually seen upon *LRIM9* silencing in susceptible mosquitoes was suppressed, which suggests *CTL4* might be upstream of *LRIM9* in the melanisation cascade. *CTL4* is known to be downstream of TEP1 (Michael Povelones, personal communication). The function of melanisation is thought to vary depending on the mosquito genetic background. Interestingly, melanisation has been proposed as a killing mechanism after *CTL4* knockdown and a clearance mechanism of dead parasites in L3-5 mosquitoes (Volz et al., 2006). This suggests that *LRIM9* might be involved in the disposal of parasites rather than killing *per se*. With its LRR domain, *LRIM9* could recognise dead or dying parasites and promote their melanisation. For instance, *LRIM9* might recognise parasites damaged by ROS or NO. In contrast to *LRIM9*, *CLIPA8* is essential for melanisation in both L3-5 and *CTL4* knockdown genetic backgrounds (Volz et al., 2006). *CLIPA8* is activated by cleavage in response to injury and bacterial infection (Schnitger et al., 2007). Curiously, *LRIM9* knockdown did not affect *CLIPA8* cleavage after injection of *S. aureus* bioparticles, unlike *TEP1* and *LRIM1*. This could mean that *LRIM9* functions downstream of *CLIPA8* in the melanisation cascade or *LRIM9* might be involved in an unidentified tributary pathway, independent of *CLIPA8* activation. Alternatively, *LRIM9* could have a minor, regulatory role in melanisation that does not affect *CLIPA8* cleavage. It would be informative to test whether *LRIM9* knockdown inhibits *CLIPA8* cleavage in L3-5 mosquitoes.

LRIM9 was shown to influence the activity of PO, a fundamental enzyme required for melanin synthesis. *LRIM9* knockdown partially inhibited PO activity, even after blood feeding. The extent of this inhibition varied between biological replicates from complete blockage to a reduction in PO activity. Apart from one biological replicate, the inhibitory effect of *LRIM1* knockdown was more robust than *LRIM9*. *LRIM1* and the complement-like pathway are master regulators of melanisation

(Warr et al., 2006) and so LRIM9 is likely to play a less central or partially redundant role in promoting melanisation. For instance, LRIM9 might improve the efficiency of melanisation without being essential. Furthermore, the *An. gambiae* genome encodes nine PPO genes (Christophides et al., 2002), which have distinct transcriptional profiles during mosquito development (Muller et al., 1999). For example, *PPO2*, *PPO3* and *PPO9* are strongly induced after blood feeding (Christophides et al., 2004; Christophides et al., 2002; Muller et al., 1999). Perhaps LRIM9 only affects the activity of particular PPOs, such as those induced by blood feeding, which could explain the partial inhibition of PO activity. It should be noted that the PO assay is an artificial system that measures systemic melanisation in collected hemolymph after bacterial challenge. Melanisation is usually tightly controlled and only deployed in discrete locations to minimise self-damage from highly toxic intermediates (Christensen et al., 2005). Therefore, this assay does not conclusively prove that LRIM9 regulates PO activity on the parasite surface *in vivo*.

LRIM9 knockdown had no effect on melanisation of cuticular wound sites or egg sclerotisation. Therefore, LRIM9 is probably only involved in immune melanisation. This is in agreement with recent studies suggesting immune and tissue melanisation have distinct pathways of PPO activation in *Ae. aegypti* (Zou et al., 2010). The same is thought to apply in *An. gambiae* as CLIPA8 is not required for wound melanisation but is critical for parasite and bacterial melanisation (Schnitger et al., 2007).

LRIM9 was dramatically induced at the transcript and protein level 24 to 48 h after an uninfected blood meal. This correlated well with whole-genome transcriptomics analysis (Marinotti et al., 2005). Upregulation of LRIM9 proceeded faster at higher temperatures, which is probably due to increased metabolic rate. Analysis of hemolymph revealed that normally there were low levels of LRIM9 circulating in naïve hemolymph and that its levels were massively boosted upon blood feeding. This is unusual for most mosquito immune proteins, which are typically constitutively expressed and secreted at high levels. For example, *LRIM1* and *APL1C* are basally expressed at high levels and further upregulated during infection, perhaps to replenish utilised protein (Fraiture et al., 2009). It was hypothesised that LRIM9 is a blood feeding specific LRIM, which was reinforced by preliminary data suggesting it is very poorly expressed in larvae and pupae. The blood feeding hypothesis correlates well with previous microarrays showing significantly higher expression of *LRIM9* in females than adult male mosquitoes (Baker et al., 2011; Koutsos et al., 2007; Marinotti et al., 2005). It is unknown whether *LRIM9* is expressed at low levels in males or not expressed at all. Ongoing work is aimed at investigating further the developmental and sex specific expression patterns of *LRIM9*.

Blood feeding has a profound effect on mosquito physiology and several hypotheses were tested to explain the massive increase in LRIM9 after a blood meal. Firstly, the purpose of blood feeding is to provide amino acids and nutrients to enable egg development (Attardo et al., 2005). The mosquito's vitellogenic period lasts until 30 h post blood feeding (Kokoza et al., 2001), which corresponds well with the LRIM9 induction. Secondly, a major consequence of blood feeding is a dramatic rise in levels of endogenous midgut bacteria, which subsequently must be controlled by the mosquito immune system (Cirimotich et al., 2010; Kumar et al., 2010; Meister et al., 2009). Therefore, it was predicted that LRIM9 could play a role in mosquito fecundity or antibacterial defence. However, *LRIM9* silencing had no impact on the mosquito's ability to produce eggs or viable larvae. *LRIM9* knockdown also had no effect on survival during *E. coli* infections (in both naïve and blood fed mosquitoes) or *E. coli* proliferation in the hemocoel. Furthermore, antibiotic treatment did not affect LRIM9 levels in the hemolymph after blood feeding. These results suggest that LRIM9 is probably not involved in mosquito reproduction or antibacterial responses. As bacteria are the predominant larval pathogens, the results correlate well with poor expression of *LRIM9* in larvae. Although LRIM9 was not shown to be involved in tissue melanisation, a further hypothesis is that LRIM9 could be involved in injury responses caused by gut distension during blood feeding. This could be investigated by feeding mosquitoes low melting point agarose to mimic gut distension in the absence of blood feeding (Oliveira et al., 2011) and monitoring LRIM9 in the hemolymph.

There was an intriguing discrepancy in LRIM9 expression at the transcript and protein level in naïve mosquitoes. Based on NanoString reporter counts, *LRIM9* transcripts were very abundant in naïve mosquitoes and further upregulated upon blood feeding. In fact, the average reporter count for *LRIM9* was ranked 8th highest of all genes tested. However, western blot analysis of hemolymph showed that LRIM9 was low in naïve hemolymph and dramatically boosted upon a blood meal. This is unlikely to be a technical issue with the NanoString probes because qRT-PCR analysis confirmed high levels of *LRIM9* in naïve mosquitoes. The discrepancy between the transcript and protein might suggest that LRIM9 is subject to translational repression. There might also be a high turnover of LRIM9 protein in the hemolymph of naïve mosquitoes. Perhaps LRIM9 protein is constitutively produced at high levels but retained in fat body or hemocyte cell vesicles and secreted when required, such as upon blood feeding. The *Anopheles* PPOs are an interesting example of immune proteins that are constitutively expressed and sequestered in cytoplasmic granules of circulating oenocytoid hemocytes (Castillo et al., 2006). The majority of PPOs lack a signal peptide and are degranulated upon hemocyte activation (Castillo et al., 2006; Christophides et al., 2002). This allows melanisation activity to be tightly controlled, both spatially and temporally. To investigate whether LRIM9 is also sequestered, fat body and hemocytes collected before and after blood feeding should

be stained with the LRIM9 antibody to determine whether LRIM9 is sequestered in these cells and released upon blood feeding. It would be informative to undergo a more fine-tuned analysis of how LRIM9 transcript and protein levels change after blood feeding. For example, if hemolymph protein levels are regulated at the level of secretion, then LRIM9 protein should accumulate in the hemolymph at time points preceding transcriptional upregulation.

Unlike LRIM1 and APL1C, LRIM9 was detected as a monomer in cell culture and in the hemolymph by non-reducing western blot. Therefore, LRIM9 does not seem to form stable, covalent homo- or heterocomplexes *in vitro* or *in vivo*. The LRIM family has a conserved pattern of cysteine residues between the LRR domains and the coiled-coil (Waterhouse et al., 2010). Mutational analyses revealed that the LRIM1/APL1C complex is held together by a covalent linkage between orthologous cysteine residues in LRIM1 (C352) and APL1C (C562) (Baxter et al., 2010; Povelones et al., 2011). These cysteines are directly opposite each other in the LRIM1/APL1C crystal structure (Baxter et al., 2010) and are the last conserved cysteines in the characteristic LRIM pattern, immediately upstream of the coiled-coil domain (see Figure 5.1). Interestingly, LRIM9 is missing this cysteine, which is consistent with monomer formation although, as discussed in detail in Chapter 6, the position of the dimerising cysteine residue is very flexible (Povelones et al., 2011). Nevertheless, LRIM9 might interact non-covalently with other proteins or other LRIM9 molecules. These interactions are disrupted by denaturing SDS-PAGE analysis. To investigate LRIM9 protein interactions further, hemolymph should be analysed by gel filtration or native PAGE, which electrophoretically separates proteins under gentle non-denaturing conditions. His-tagged LRIM9 could be captured from the conditioned media of transfected mosquito cells. Proteins captured alongside LRIM9 could be separated by non-reducing SDS-PAGE, visualised by Coomassie staining and any interesting protein bands identified using mass spectrometry. This approach successfully revealed that the LRIM1/APL1C complex interacts with TEP3, TEP4 and TEP9 (Povelones et al., 2011). Immunoprecipitation is also an important tool for identifying interacting partners. In this approach, the LRIM9 antibody would be immobilised on beads and used to capture LRIM9 and any interacting partners from the hemolymph of blood fed mosquitoes. Protein bands specific to the LRIM9 immunoprecipitation and not present in a control immunoprecipitation performed with pre-immune serum would be identified by mass spectrometry. Any candidate partners could be tested in direct binding assays performed in cell culture and for a knockdown phenotype similar to *LRIM9* with *P. berghei*.

The tissue localisation of LRIM9 expression is still an open question that warrants further investigation. Analysis of the *LRIM9* transcript in *An. gambiae* midguts showed *LRIM9* was poorly

expressed in the midgut, even after blood feeding. Although this needs to be confirmed at the protein level by western blot, this result was consistent with a previous microarray analysis that reported significantly higher expression of *LRIM9* in the fat body compared to the midgut and ovaries (Marinotti et al., 2005). The fat body and hemocytes should be investigated as the probable source of *LRIM9* expression and secretion. *LRIM9* was not found to be enriched in circulating hemocytes (Pinto et al., 2009) but the majority of hemocytes are largely sedentary and attached to visceral surfaces, such as the trachea and Malpighian tubules (Blandin and Levashina, 2007). Most immune effectors, such as TEP1, *LRIM1* and *APL1C*, are secreted by hemocytes and the fat body and encounter malaria parasites in hemolymph bathing the basal labyrinth (Blandin et al., 2004; Blandin et al., 2008; Frolet et al., 2006). The *LRIM9* antibody could be used to analyse fat body samples by western blot and to stain hemocytes.

The precise function of *LRIM9* in mosquito immunity, particularly *Plasmodium* defence, remains unclear and requires further investigation. The characteristic LRR and coiled-coil domains of *LRIM9* are good indicators for involvement in pathogen recognition and interactions with other immune proteins (Waterhouse et al., 2010). The effect of *LRIM9* on *P. berghei* development might be indirect and related to its putative role in melanisation. In *Drosophila*, melanisation has been shown to increase the efficiency of other immune reactions (Tang et al., 2006) and the same has been proposed in *An. gambiae* (Schnitger et al., 2007). Therefore, reduced efficiency of *P. berghei* parasite detection, killing or clearance could explain the moderate increase in infection intensity observed upon *LRIM9* knockdown. To further investigate the role of *LRIM9* in parasite defence, *P. berghei* infected midguts should be stained with the *LRIM9* antibody to see if *LRIM9* localises to parasite surfaces. *In vitro* ookinete binding assays could also be used to determine whether *LRIM9* interacts directly with *P. berghei* parasites. To examine whether *LRIM9* is involved in ookinete killing or clearance of dead ookinetes, numbers of live and dead ookinetes should be compared in *GFP* and *LRIM9* knockdown mosquitoes 30 h after an infectious blood meal. To this end, midguts infected with the *P. berghei* *CON_{GFP}* strain (Franke-Fayard et al., 2004) should be stained with an antibody against the *P. berghei* surface antigen, Pbs28. In this experiment, live parasites would show GFP fluorescence and Pbs28 staining whereas dead parasites would show only Pbs28 staining. The *LRIM9* antibody could also be used to determine if *LRIM9* localises to the surface of live or dead parasites. Furthermore, many oocysts are known to die between 3 and 12 days post infection and then be cleared by the mosquito (Gupta et al., 2009; Dina Vlachou, personal communication). To elucidate whether *LRIM9* plays a role in their disposal, the ratio of live to dead oocysts should be compared at days 4 and 10 post infection in *GFP* and *LRIM9* knockdown midguts. If *LRIM9* is involved, an accumulation of dead oocysts would be expected after *LRIM9* is silenced. As *P. berghei*-*An. gambiae*

is an unnatural combination, the role of LRIM9 in *P. falciparum* infections should be investigated using RNAi to determine whether LRIM9 is also an antagonist of this important human pathogen.

A favourable hypothesis is that LRIM9 is an immune factor induced in anticipation of blood-borne infections. The ability to anticipate infection is a novel concept in mosquito immunity. Some immune genes, like the complement-like pathway components, are constitutively expressed and permanently circulate in the hemolymph poised to defend against invaders (Frolet et al., 2006). This basal immunity provides a front-line of attack that is critical in antiparasitic responses. *LRIM1*, *APL1C* and *TEP1* are subsequently induced by the Imd pathway, possibly to replenish utilised protein. Other immune genes are transiently induced upon detection of a pathogen, such as the induction of AMPs in response to a microbial infection (Lemaitre and Hoffmann, 2007). In contrast, *LRIM9* is induced after blood feeding to defend against potential blood-borne invaders or dangers. Although vital for egg production, feeding on vertebrate blood potentially exposes mosquitoes to ingestion of parasites, viruses and other “foreign” substances. *Plasmodium* parasites and filarial worms both penetrate the mosquito midgut, resulting in considerable tissue damage (Aliota et al., 2011; Vlachou et al., 2006). Immunoglobulins and other host proteins could be detrimental to the mosquito and have even been found to permeate the gut into the hemolymph (Vaughan and Azad, 1988). Although blood is typically sterile, diseased vertebrates can be bacteremic and mosquitoes could become exposed to these bacteria upon blood feeding. As LRIM9 is induced after both uninfected and infected blood meals, this suggests it is upregulated in anticipation of infection rather than in response to infection. It is unknown whether LRIM9 is fully functional prior to blood feeding, although silencing *LRIM9* inhibited PO activity in naïve hemolymph. It would be interesting to elucidate whether the same induction of LRIM9 occurs after multiple blood meals. It should also be determined whether *LRIM9* orthologues are blood feeding specific in other mosquitoes, such as *Ae. aegypti* and *C. quinquefasciatus*.

Using the genome-wide expression map available for *An. gambiae* (Maccallum et al., 2011), LRIM9 is found to cluster to the same node as vitellogenin, the major YPP that delivers nutrients to developing oocytes. Therefore, based on the extant microarray data, *LRIM9* and *vitellogenin* are co-regulated. Expression of both genes is significantly higher in females and induced 24 h after an uninfected blood meal (Baker et al., 2011; Koutsos et al., 2007; Marinotti et al., 2005). It is tempting to speculate that transcription of these two genes is under the same regulatory mechanism and the proteins function in the same pathway. However, *LRIM9* and *vitellogenin* are located on different chromosomes (2L and 2R, respectively), so they are unlikely to share the same regulatory sequences. Vitellogenin is produced specifically by fat body and secreted into the hemolymph where it travels to

oocytes, is internalised and transformed into vitellin crystals (Clements, 2000). Vitellogenin is regulated by the steroid hormone, 20-hydroxyecdysone (20E), which is produced 10-36 h post blood feeding (Clements, 2000). The prohormone, ecdysone, is secreted by the ovaries and hydroxylated into 20E by the fat body (Clements, 2000). Interestingly, vitellogenin interferes with TEP1-mediated killing of *Plasmodium* parasites by reducing the efficiency of TEP1 binding to parasite surfaces (Rono et al., 2010). This is a clear example of a trade-off between immunity and reproduction. Apoll/I, a lipid transporter and YPP, is required for full induction of vitellogenin after blood feeding and indirectly impacts TEP1-killing (Rono et al., 2010). Like vitellogenin, Apoll/I is regulated by 20E and produced by the fat body (Sun et al., 2000). Exciting preliminary evidence indicates that LRIM9 is also under 20E regulation (Michael Povelones, personal communication). 20E regulation of immune genes has been observed previously and there seems to be a link between melanisation, 20E and vitellogenesis. Melanisation pathway components, such as PPO, are also under 20E regulation in *Anopheles* (Ahmed et al., 1999; Muller et al., 1999) and other blood feeding insects (Genta et al., 2010). Furthermore, Apoll/I was shown to immunoprecipitate PPO2 *in vitro* (Rono et al., 2010). As mentioned earlier, *LRIM9* and *Apoll/I* share the same knockdown phenotype in L3-5 mosquitoes (Mendes et al., 2008). However, unlike vitellogenin and Apoll/I, LRIM9 was not shown to be required for mosquito fecundity.

An interesting hypothesis is that LRIM9 might inhibit vitellogenin or Apoll/I to readdress the balance between immunity and reproduction. After blood feeding, LRIM9 could reduce the activity of vitellogenin or Apoll/I, which increases the efficiency of TEP1 binding to ookinetes and parasite killing. In the absence of LRIM9, the activity of vitellogenin or Apoll/I could increase, which reduces the efficiency of TEP1 binding and results in more surviving oocysts (i.e. the *LRIM9* knockdown phenotype). If the efficiency of TEP1 binding was reduced but not blocked, this could explain the moderate increase in oocysts upon *LRIM9* knockdown. The only caveat to this hypothesis is an initial experiment showed LRIM9 did not affect TEP1 accumulation on *P. berghei* parasites. Therefore, this theory requires further investigation. To examine this hypothesis, epistasis experiments could be performed to explore any putative interactions between *LRIM9*, *vitellogenin* and *Apoll/I*. For example, the effect of *vitellogenin* or *Apoll/I* silencing on LRIM9 levels in the hemolymph could be investigated, and vice versa. Proteins captured from blood fed hemolymph using the LRIM9 antibody could be analysed by western blot, probing for vitellogenin or Apoll/I. It is unknown whether *LRIM9* is directly activated by the ecdysone receptor or indirectly via an ecdysone-regulated transcription factor. This could be resolved using an electrophoretic mobility-shift assay (EMSA). The 5' regulatory region of vitellogenin possesses a functional ecdysteroid-responsive element (EcRE) and the gene is both directly and indirectly regulated by 20E (Martin et al., 2001; Raikhel et al., 2002). It seems

parsimonious that *LRIM9* is transcriptionally regulated by 20E, like vitellogenin (Kokoza et al., 2001). Alternatively, if *LRIM9* is sequestered inside cells, 20E could trigger its release. *LRIM9* is likely to be under additional forms of regulation because it is expressed at lower levels prior to blood feeding and 20E induction.

Exploiting *LRIM9* and its promoter could have exciting prospects for vector control. Blood meal inducible promoters are highly desirable for driving expression of anti-pathogen factors in GM mosquitoes, increasing refractoriness to blood-borne pathogens (Raikhel et al., 2002). With the help of a gene drive system, it is hoped these GM mosquitoes could replace natural populations and reduce disease transmission (Christophides, 2005). Overexpression of effectors can be deleterious to mosquito fitness (Marrelli et al., 2006) and the local ecology (Christophides, 2005) so it is advantageous to only express the desired gene after blood feeding. The *LRIM9* promoter could be used to drive expression of an anti-*Plasmodium* effector in response to blood feeding in GM *An. gambiae*. This would be effective if *LRIM9* is expressed at very low levels in naïve hemolymph and massively induced upon blood feeding (as shown by the antibody) rather than constitutively expressed and sequestered. The vitellogenin promoter has already been exploited to produce *An. stephensi* overexpressing REL2 after blood feeding, which enhanced resistance to *P. falciparum* infection (Dong et al., 2011). *Ae. aegypti* co-expressing the AMPs defensin and cecropin under the control of the vitellogenin promoter also blocked *P. gallinaceum* infection (Kokoza et al., 2010). If the *LRIM9* promoter behaves similarly in *Aedes* and *Culex*, the same approach could be applied to arboviral control. *Ae. aegypti* expressing an anti-dengue effector transgene, *Mnp*, was recently shown to suppress dengue infection (Mathur et al., 2010).

Alternatively, if *LRIM9* is expressed at high levels in naïve females (as shown by the NanoString) but not in males, the *LRIM9* promoter could be utilised for RIDL mosquito control strategies (Alphey et al., 2008; Labbe et al., 2012; Thomas et al., 2000). Preliminary NanoString data suggested that *LRIM9* transcription commences in late pupae. The *LRIM9* promoter could be linked to a dominant lethal gene, resulting in death of female mosquitoes upon emergence as adults. Male mosquitoes would survive and could be released into the field to mate with wild females and pass on the lethal gene. As all female offspring would die and male offspring would continue to spread the lethal gene, this would suppress the natural vector population and reduce disease transmission. The lethal gene should be under tetracycline-dependent repression so mosquitoes can be reared to adulthood in the laboratory and females are killed in the absence of tetracycline (i.e. immediately prior to mosquito release and subsequently in the wild) (Thomas et al., 2000). The *Ae. aegypti* OX513A transgenic line

is the most successful example of a female-specific tetracycline-repressible dominant lethal and field trials are underway (Bargielowski et al., 2011; Harris et al., 2011; Phuc et al., 2007).

Chapter 6: Functional analysis of other LRIMs

6 Functional analysis of other LRIMs

6.1 Background

The LRIMs are a novel mosquito-specific family recently discovered in the malaria vector, *An. gambiae* (Povelones et al., 2009; Waterhouse et al., 2010). The founding members, LRIM1 and APL1C, play a key role in killing malaria parasites via a TEP1-mediated pathway (Fraiture et al., 2009; Povelones et al., 2009). LRIM1 and APL1C circulate in the mosquito hemolymph as an obligate heterodimer and stabilise the mature form of TEP1 (Baxter et al., 2010; Povelones et al., 2011). The LRIM1/APL1C complex delivers TEP1 to the surface of *P. berghei* parasites, which labels the invaders for destruction by lysis and melanisation.

The other 22 LRIMs were largely uncharacterised at the start of this PhD project. LRIM family members share similar protein domain architecture that comprises a signal peptide, a region of LRR domains, a conserved pattern of cysteines and an optional coiled-coil domain. There are four subfamilies of LRIMs based on variations to this core structure (Povelones et al., 2009; Waterhouse et al., 2010). Long LRIMs, including LRIM1 and APL1C, have 10 or more LRRs whereas Short LRIMs possess 6 or 7 LRRs. Transmembrane LRIMs have a predicted C-terminal transmembrane region. Coil-less LRIMs are missing the C-terminal coiled-coil domain but exhibit all other characteristics of the LRIM family.

In this Chapter, a representative from each LRIM subfamily was further characterised to investigate its biochemical, functional and structural properties. It was hoped this would provide insights into the evolution and function of the LRIM family in mosquito immunity. LRIM4 (Long), LRIM17 (Coil-less) and LRIM15 (Transmembrane) were chosen because of their interesting transcriptional profiles, as described in Chapter 4. LRIM4 and LRIM17 were also previously implicated in malaria parasite defence (Dong et al., 2006a). The representative Short subfamily member, LRIM9, was covered in detail in Chapter 5. Representatives of the Long subfamily, LRIM1 and APL1C, were previously characterised (Baxter et al., 2010; Fraiture et al., 2009; Povelones et al., 2011; Povelones et al., 2009).

LRIM4 is a typical Long LRIM, with 11 LRRs and two closely spaced coiled-coil domains (Waterhouse et al., 2010). As described in Chapter 4, LRIM4 showed strong basal expression and was upregulated by various challenges, including *P. berghei*, *P. yoelii*, *P. falciparum*, ONNV, bacteria and fungi; however, knockdown of *LRIM4* had no effect on *P. berghei* development. In agreement, a previous study found *LRIM4* (referred to as LRRD5) was significantly induced in the mosquito midgut upon *P.*

falciparum ookinete invasion (Dong et al., 2006a). However, the same report showed *LRIM4* was not induced by *P. berghei* invasion, which conflicts with the data presented in Chapter 4.

LRIM17 is the longest Coil-less LRIM and has previously been implicated in immune defence against *P. falciparum*, *P. berghei* and bacteria (Dong et al., 2006a; Dong et al., 2009; Garver et al., 2012). It has 13 LRRs and is without a coiled-coil domain (Waterhouse et al., 2010). *LRIM17* has also been referred to in the literature as *LRRD7* (Dong et al., 2006a; Dong et al., 2011; Dong et al., 2009) and *APL2* (Riehle et al., 2006). It was originally identified together with *APL1* in an *Anopheles* population survey as both mapped to a genetic locus that controls mosquito infections with *P. falciparum* (Riehle et al., 2006). With a similar transcriptional profile to *LRIM4*, *LRIM17* was upregulated by a range of challenges in Chapter 4. The *LRIM17* transcript was induced by *P. berghei*, *P. yoelii*, ONNV after blood feeding, bacteria and fungi but not *P. falciparum*. Interestingly, a previous microarray reported the opposite effect: *LRIM17* was upregulated 8-fold in the midgut during *P. falciparum* invasion but not after *P. berghei* infection (Dong et al., 2006a). Previous RNAi experiments reported that *LRIM17* is a major antagonist of *P. berghei* and *P. falciparum* in the *An. gambiae* Keele strain (Dong et al., 2006a). However, knockdown of *LRIM17* in *An. gambiae* G3 strain did not result in any change in *P. berghei* infection (Riehle et al., 2006). Similarly, as shown in Chapter 4, *LRIM17* silencing did not affect *P. berghei* development in the *An. gambiae* Yaoundé strain. Also in G3 mosquitoes, *LRIM17* knockdown did not affect oocyst development after *P. falciparum* infection (Michael Povelones, personal communication). *LRIM17* was also implicated in defence against opportunistic bacterial infection and gene silencing significantly increased bacterial load in the midgut (Dong et al., 2009) and reduced survival to *E. coli* and *S. aureus* infections (Dong et al., 2006a). A previous microarray found it was only responsive to gram-negative and not gram-positive bacterial infection (Dong et al., 2006a).

As *LRIM4* and *LRIM17* share a similar transcriptional profile in Chapter 4 (see Figure 4.3), it was hypothesised that these LRIMs may function together. Previous microarrays have shown that *LRIM4* and *LRIM17* were induced after injection of ONNV virus (Waldock et al., 2012) and *B. bassiana* spores (Fanny Turlure, personal communication). The hypothesis that *LRIM4* and *LRIM17* work in the same biochemical pathway and interact, directly or indirectly, was investigated in this Chapter.

Prior to this PhD project, relatively little was known about *LRIM15*. *LRIM15* is the smallest of the Transmembrane LRIMs and possesses 13 LRRs (Waterhouse et al., 2010). Instead of the characteristic double cysteine motif, *LRIM15* and the other Transmembrane LRIMs have a tyrosine-cysteine motif. In Chapter 4, preliminary results indicated that *LRIM15* was not a *P. berghei* antagonist. The *LRIM15* transcript was induced by naïve blood feeding, *Plasmodium* (especially *P.*

berghei), conditioned media injection and ONNV. It was not responsive to *E. coli*, *S. aureus* or *B. bassiana* infection at the time points used.

6.2 Results

Recombinant LRIM4, LRIM15 and LRIM17 in insect cell culture

Expression constructs for LRIM4, LRIM15 and LRIM17 were generated to facilitate their biochemical characterisation in order to elucidate whether any of these LRIMs formed complexes *in vitro*. LRIM4, LRIM15 and LRIM17 genes were cloned into the pEx-10 insect expression vector, which adds an N-terminal Strep-tag and a C-terminal His-tag. pEx-10-LRIM4, -LRIM15 and -LRIM17 were transfected into Sf9 cells, which lack endogenous LRIM expression, to test for secretion and complex formation. pEx-10-GFP (secreted GFP) and pEx-10-LRIM9 were used as controls. Proteins in the conditioned media were analysed by western blot under non-reducing and reducing conditions, probing for His or Strep (Figure 6.1 A and B). Interestingly, LRIM4 migrated at approximately 124 kDa under non-reducing conditions, which is the predicted size of a homodimer. Upon reduction, LRIM4 was detected as a monomer at approximately 62 kDa, which demonstrates that LRIM4 forms a disulphide-bonded homodimer *in vitro*. Lower molecular weight LRIM4 bands in the reducing blot were probably N-terminal cleavage products. Under both non-reducing and reducing conditions, LRIM17 migrated at approximately 51 kDa, consistent with the expected size of a monomer and comparable to LRIM9. LRIM15 was not detected in the conditioned media, which is consistent with the prediction that it is a transmembrane protein and not secreted. Subsequently, LRIM15 was detected as a monomer in cell lysate (Michael Povelones, personal communication).

LRIM4 and LRIM17 constructs were next transfected into mosquito Sua4.0 cells, which secrete an array of hemolymph proteins, to determine whether they interact with other mosquito proteins. As LRIM4 and LRIM17 have a similar transcriptional profile and showed expression-based clustering in Chapter 4, it was predicted that they might function together. LRIM4 and LRIM17 were co-transfected to elucidate whether they form a heterocomplex. Functional partners LRIM1 and APL1C were co-transfected as a positive control of heterocomplex formation. Conditioned media were analysed by non-reducing western blot using the His probe (Figure 6.1 C). Again, LRIM4 was expressed as a homodimer, although expression levels were much lower than in Sf9 cells. LRIM17 migrated predominantly as a monomer but a fainter band was visible at approximately 150 kDa after His purification, which could be a LRIM17 trimer or indicate interaction with another protein (data not shown). However, this could also be an artefact of overexpression *in vitro*. No disulphide-bonded complex between LRIM4 and LRIM17 was observed in the co-transfection as only the LRIM17

monomer and LRIM4 homodimer were detected. However, this does not rule out a non-covalent interaction between the two proteins.

Using a strategy similar to that described for LRIM9, a whole protein polyclonal antibody was generated against recombinant LRIM4. Using this antibody, LRIM4 was also shown to circulate as a disulphide-bonded homodimer in hemolymph (Figure 6.1 D). A fainter higher molecular weight band was also visible in both hemolymph and after His purification from Sf9 conditioned media, which could represent a tetrameric complex (a dimer of homodimers).

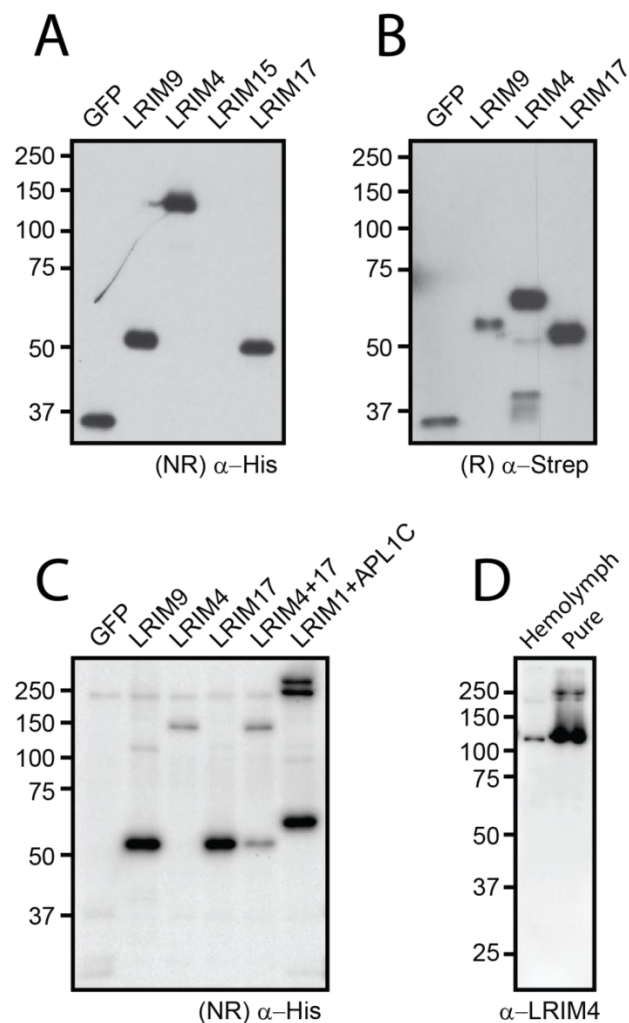


Figure 6.1 LRIM4 and LRIM17 expression in cell culture and hemolymph.

LRIM4, *LRIM15* and *LRIM17* were cloned into pEx-10, transfected into Sf9 or Sua4.0 cells and conditioned media were collected after 3 days. pEx-10-GFP and -LRIM9 were used as controls. **A)** Conditioned media from Sf9 cells were analysed by western blot under non-reducing (NR) conditions with the His probe. **B)** The same samples were analysed under reducing (R) conditions with a Strep antibody. **C)** pEx-10-LRIM4 and -LRIM17 were transfected into Sua4.0 cells, both separately and co-transfected to test for an interaction. LRIM1 and APL1C were co-transfected as an additional control for heterocomplex formation. Conditioned media were analysed by NR western blot using the His probe. **D)** Hemolymph and His purified recombinant LRIM4 (from Sf9 cells) were analysed by NR western blot using an LRIM4 antibody (this blot was kindly provided by Michael Povelones).

Analysing the role of cysteine residues in LRIM4 homodimerisation

The role of the cysteine residues in LRIM4 homodimer formation was investigated. The LRIM1/APL1C heterodimer is held together by a disulphide bond between LRIM1 C352 and APL1C C562 (Baxter et al., 2010; Povelones et al., 2011). These homologous cysteines are found just N-terminal to the coiled-coil domain, as highlighted by yellow stars in Figure 6.2 A. Mutating either cysteine prevents LRIM1/APL1C complex formation and only LRIM1 and APL1C monomers are secreted in cell culture. LRIM4 lacks a homologous cysteine to either LRIM1 C352 or APL1C C562 but it does have an additional cysteine residue (C535) at its extreme C-terminus (Figure 6.2 A). It was hypothesised that C535 is responsible for covalently linking two LRIM4 molecules in the homodimer. To test this theory, a cysteine to serine missense mutation of C535 was generated (C535S) by site-directed mutagenesis and verified by sequencing. Wild-type LRIM4 and the C535S mutant were expressed in Sf9 cells and conditioned media were analysed by western blot using the His probe (Figure 6.2 B). When analysed under reducing conditions, both wild-type LRIM4 and the C535S mutant migrated at approximately 62 kDa, the predicted monomeric size for LRIM4. Under non-reducing conditions, wild-type LRIM4 migrated as a homodimer at 124 kDa, whereas the C535S mutant remained a monomer. These results showed that C535 is crucial for LRIM4 homodimer formation. Furthermore, LRIM4 C535 is functionally equivalent to LRIM1 C352 and APL1C C562, which demonstrates that there is inherent flexibility in the position of the cysteine responsible for dimerising two LRIM molecules. This work and the subsequent experiments for LRIM4 were published in Povelones et al., 2011.

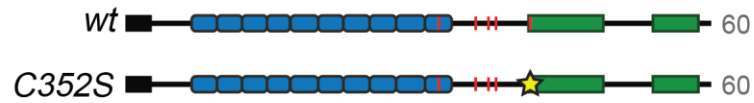
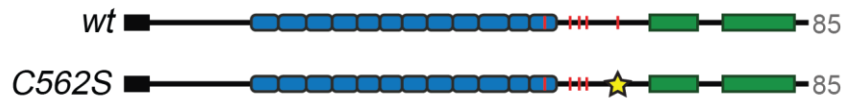
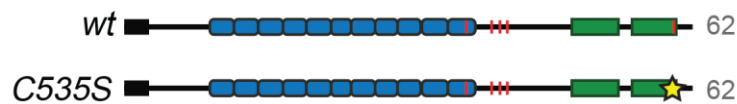
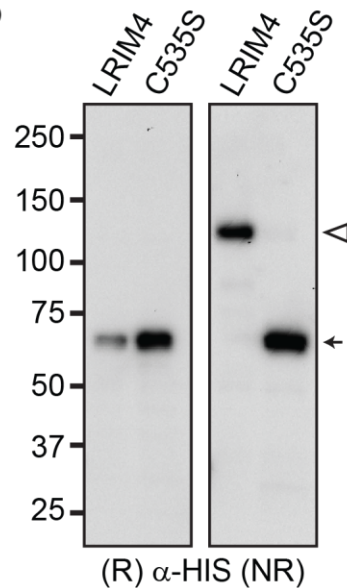
A*LRIM1* alleles*APL1C* alleles*LRIM4* alleles**B**

Figure 6.2 Investigating the cysteine residue responsible for LRIM4 homodimer formation.

A) Schematic representation of wild-type (wt) and cysteine mutant alleles for *LRIM1*, *APL1C* and *LRIM4*. Predicted size of mature His/Strep-tagged proteins in kDa is shown in grey. Structures shown are black box: signal peptide, blue box: LRR, green box: coiled-coil domain, red line: cysteine residue, yellow star: cysteine to serine missense mutation. Mutations indicated are C352S in *LRIM1*, C562S in *APL1C* and C535S in *LRIM4*. **B)** *LRIM4* wt and C535S mutant were transfected into Sf9 cells and conditioned media were collected after 3.5 days. Conditioned media were analysed by western blot under non-reducing (NR) and reducing (R) using the His probe. *LRIM4* monomer and homodimer are shown by a small black arrow and white arrowhead, respectively. Adapted from Povelones et al., 2011.

LRIM4 and parasite killing

The interaction between the LRIM1/APL1C heterodimer and TEP1 plays an important role in the mosquito complement-like pathway. It was investigated whether the LRIM4 homodimer can also interact with TEP1. Binding assays were performed using recombinant LRIM4 expressed in Sua4.0 cells, which secrete endogenous TEP1, LRIM1 and APL1C. Secreted GFP, LRIM1 and APL1C were chosen as controls. Expression of the tagged proteins in the conditioned media was determined by western blot using the His probe to ensure equivalent amounts of protein were used for the binding assay. His-tagged proteins were captured from the conditioned media using cobalt-charged beads. The captured material was analysed by western blot for interactions with TEP1, LRIM1 and APL1C using antibodies.

No interaction was observed between LRIM4 and endogenous TEP1, LRIM1 or APL1C (Figure 6.3). Nevertheless, it is possible that LRIM4 requires an additional protein partner to interact with these proteins and that this partner is not expressed by Sua4.0 cells. As expected, LRIM1 and APL1C were able to interact with their endogenously expressed partner, form the LRIM1/APL1C heterodimer and capture TEP1_{cut} from the conditioned media. These data demonstrated the specificity of the LRIM1/APL1C interaction with TEP1 and showed that it is not common to all LRIM dimers.

The initial RNAi screen in Chapter 4 revealed that *LRIM4* knockdown had no effect on *P. berghei* development. *LRIM4* silencing and *P. berghei* infection was repeated since a modest phenotype might have been overlooked in the first replicate. However, upon repetition, *LRIM4* knockdown did not affect infection intensity or prevalence (Figure 6.4). Both live oocysts and melanised ookinetes were unaffected. It can therefore be concluded that, although the *LRIM4* transcript was induced by *P. berghei* infection, LRIM4 is not involved in *P. berghei* defence.

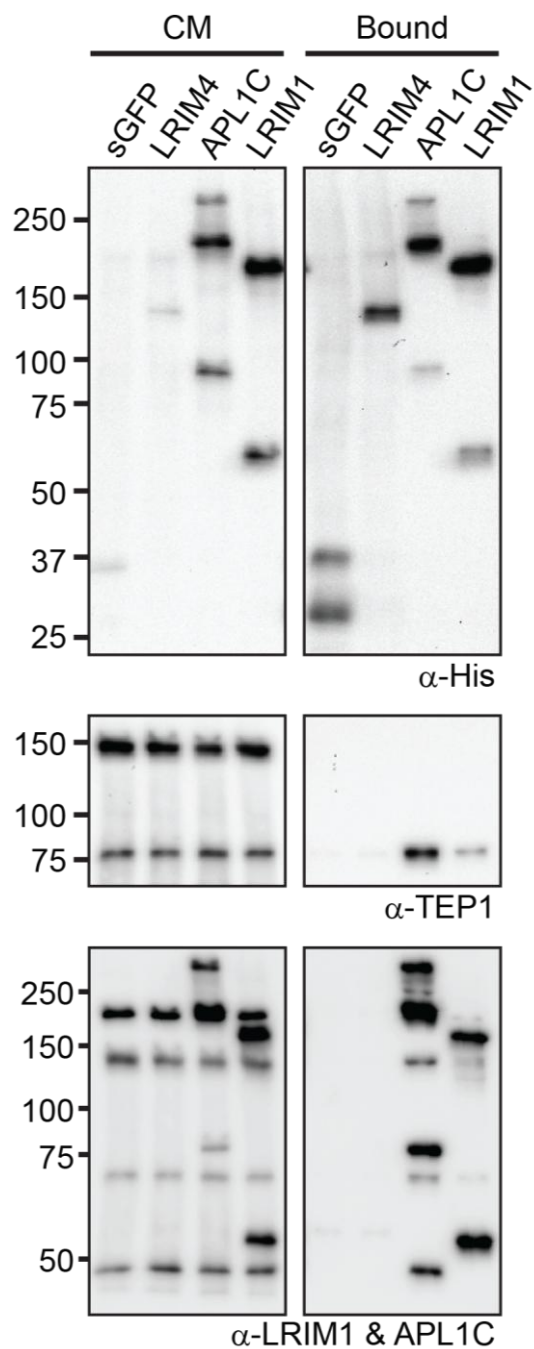


Figure 6.3 Binding assay to investigate whether LRIM4 interacts with TEP1 and LRIM1/APL1C.

Conditioned media (CM) were collected 3.5 days after transfection of Sua4.0 cells with secreted GFP (sGFP), LRIM4, APL1C and LRIM1 constructs. His-tagged proteins were captured from the conditioned media using metal affinity beads. Starting conditioned media (left panels) and bound material (right panels) were analysed by non-reducing western blot. One blot was incubated with the His probe (top panels). A second blot was probed with an antibody against TEP1 (middle panels) and re-probed with antibodies against LRIM1 and APL1C (bottom panels). Adapted from Povelones et al., 2011.

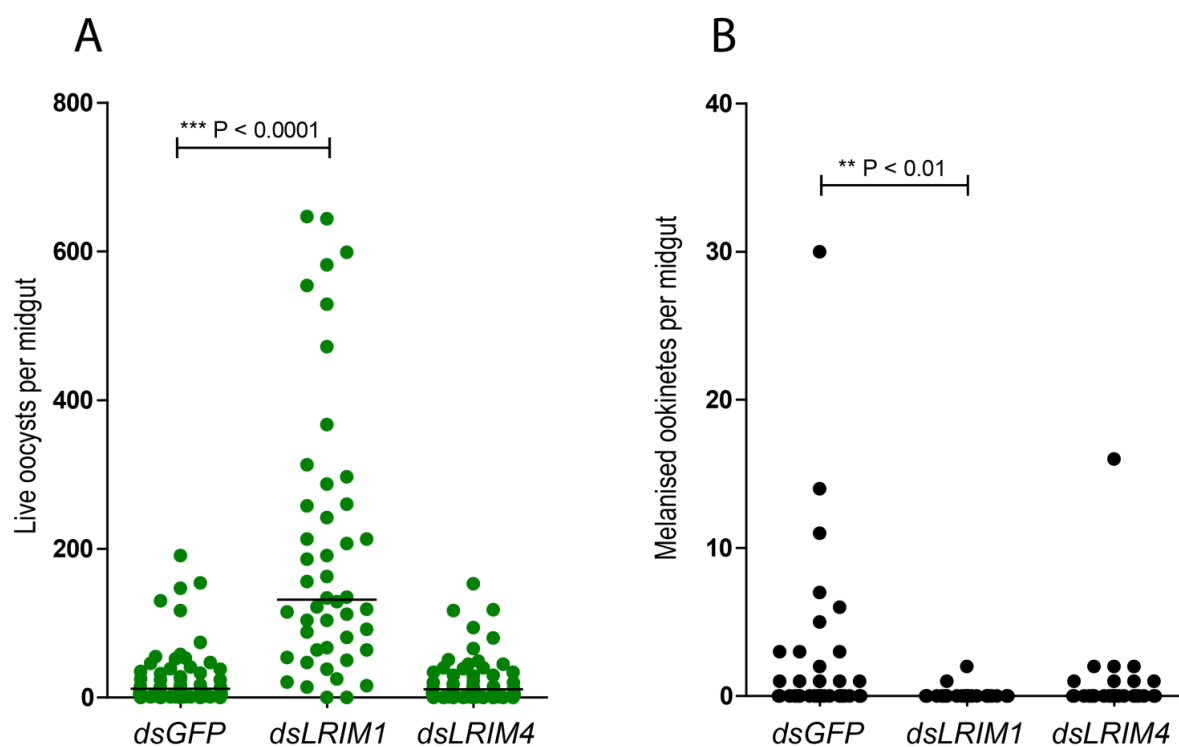


Figure 6.4 *LRIM4* silencing and *P. berghei* infection.

LRIM4 was silenced, mosquitoes were infected with fluorescent *P. berghei* and parasite load was monitored after 7 days. *dsGFP* and *dsLRIM1* were injected as controls. The graphs display pooled data from two independent biological experiments in *Plasmodium* susceptible mosquitoes (one from Yaoundé strain and one from Ngouso strain). Horizontal lines represent the median parasite number. Significant differences in infection intensity by Mann Whitney U-test are shown. **A)** Live fluorescent oocyst counts. Prevalence of live oocysts for *dsGFP*, *dsLRIM1* and *dsLRIM4* was 92, 98 and 83%, respectively (all comparisons non-significant, Fisher's exact test). **B)** Melanised (killed) ookinete counts. Prevalence of melanisation for *dsGFP*, *dsLRIM1* and *dsLRIM4* was 26, 4 and 17%, respectively. Only prevalence for *LRIM1* was significant (< 0.01, Fisher's exact test). Adapted from Povelones et al., 2011.

LRIM17 and parasite killing

The role of *LRIM17* in *P. berghei* defence was questionable due to conflicting results from different laboratories. In the RNAi screen presented in Chapter 4, *LRIM17* silencing had no effect on infection intensity or prevalence in the Yaoundé strain of *An. gambiae*. This supports other reports using G3 strain mosquitoes (Riehle et al., 2006). However, *LRIM17* was reported as a major *Plasmodium* antagonist in the Keele strain of *An. gambiae* (Dong et al., 2006a; Dong et al., 2011; Dong et al., 2009; Garver et al., 2012). It was decided to silence *LRIM17* in Keele mosquitoes to try to replicate the findings of Dong et al. in another laboratory using the same dsRNA fragment. Interestingly, it was found that *LRIM17* knockdown did not affect *P. berghei* development in Keele mosquitoes in two independent experiments (Figure 6.5). Infection intensity and prevalence of live oocysts and

melanised ookinetes were unaffected by *LRIM17* knockdown. The efficiency of *LRIM17* silencing in Keele mosquitoes was determined to be 83%.

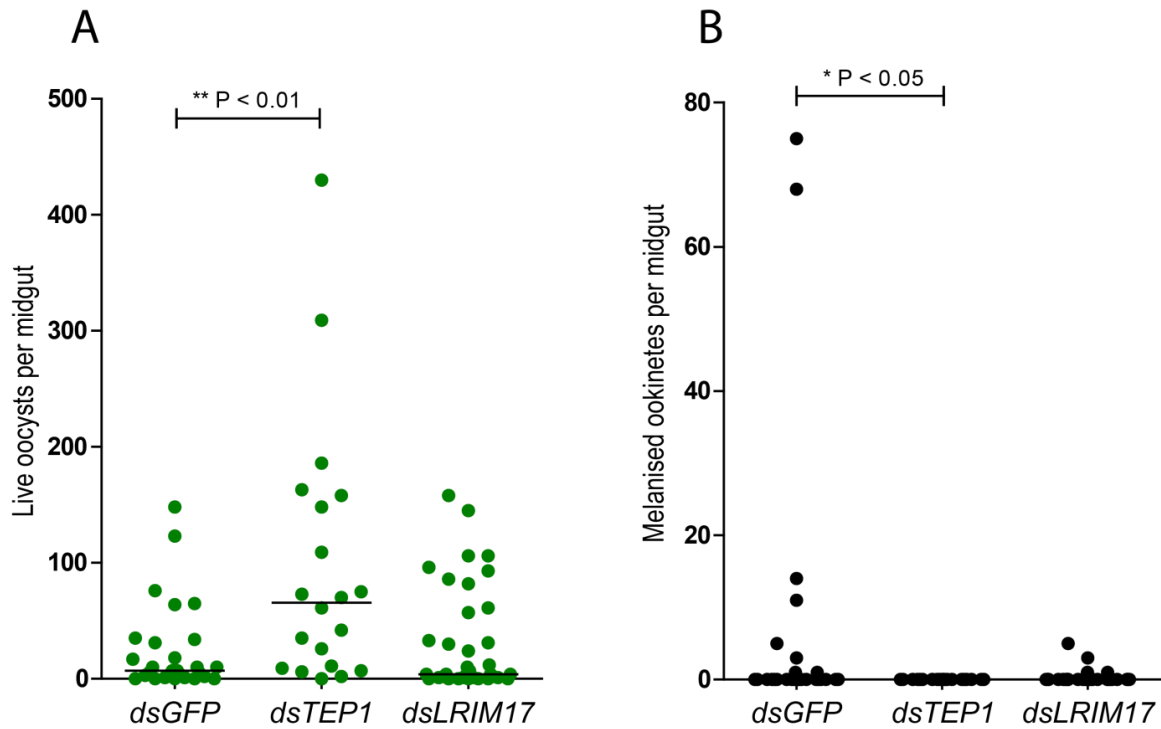


Figure 6.5 *LRIM17* silencing and *P. berghei* development in Keele mosquitoes.

LRIM17 was silenced in Keele strain *An. gambiae*, using *GFP* and *TEP1* as controls. Mosquitoes were infected with fluorescent *P. berghei* and infection intensity and prevalence were monitored 7 days later. The graphs display pooled data from two independent biological experiments, with horizontal lines representing the median parasite number. Significant differences in infection intensity by Mann Whitney U-test are shown. **A)** Live fluorescent oocyst counts. Prevalence of live oocysts for *dsGFP*, *dsTEP1* and *dsLRIM17* was 82, 95 and 81%, respectively (all comparisons non-significant, Fisher's exact test). **B)** Melanised (killed) ookinete counts. Prevalence of melanisation for *dsGFP*, *dsTEP1* and *dsLRIM17* was 29, 0 and 11%, respectively. Only prevalence for *TEP1* was significant (< 0.05, Fisher's exact test).

6.3 Discussion

Members of the mosquito-specific LRIM family in *An. gambiae* share similar protein domain architecture and are divided into four subfamilies. This Chapter aimed to characterise a representative member of the Long, Transmembrane and Coil-less subfamilies: LRIM4, LRIM15 and LRIM17, respectively. These three LRIMs demonstrated interesting transcriptional profiles in Chapter 4. Furthermore, LRIM4 and LRIM17 have previously been implicated in *Plasmodium* defence (Dong et al., 2006a; Dong et al., 2011; Garver et al., 2012).

The Long subfamily member LRIM4 seems likely to play a core role in *An. gambiae* immunity based on its diverse transcriptional profile. The *LRIM4* transcript was induced by a wide range of challenges, including *Plasmodium*, ONNV, bacteria and fungi. Despite being upregulated by all three *Plasmodium* species tested, *LRIM4* knockdown has no impact on *P. berghei* infections (Povelones et al., 2011), which demonstrates that transcriptional induction does not always correlate with function. Interestingly, the lack of RNAi phenotype with *P. berghei* matches a lack of transcriptional response to this rodent parasite reported in a previous microarray (Dong et al., 2006a). The same microarray showed that *LRIM4* was induced by *P. falciparum*, in agreement with Chapter 4. An exciting possibility is that LRIM4 might function exclusively in defence against *P. falciparum*. Furthermore, the effect of *LRIM4* silencing might only be detectable under certain *Plasmodium* infection intensities, which have been shown to modulate antiparasitic responses (Garver et al., 2012; Mendes et al., 2011). Another indicator that LRIM4 is an important immune effector is that it is enriched in circulating *An. gambiae* hemocytes, like LRIM1 and APL1C (Pinto et al., 2009). This might suggest LRIM4 is part of the mosquito's basal immune response, poised ready to attack invaders. However, there is no evidence linking LRIM4 to the mosquito complement-like pathway and it does not interact with LRIM1, APL1C or TEP1 *in vitro* (Povelones et al., 2011). Preliminary evidence suggests that LRIM4 is fairly well expressed in larvae and pupae, which is consistent with a generalist immunity role.

Further investigation is required to determine the precise function of LRIM4 in mosquito immunity. As the *LRIM4* transcript responds to bacterial and fungal infection, it would be enlightening to perform bacterial and fungal survival assays after *LRIM4* silencing. As described for LRIM9, the LRIM4 polyclonal antibody could be used to immunoprecipitate interacting proteins from hemolymph. This approach would highlight covalent and non-covalent interactions, providing new insights into the function of LRIM4.

Evidence suggests that the Coil-less LRIM17 is also a core immune protein involved in defence against a range of pathogens, although its exact role is unknown. *LRIM17* was induced by many

challenges in Chapter 4, including *P. berghei*, *P. yoelii*, ONNV after blood feeding, bacteria and fungi but not *P. falciparum*. This correlates well with previous reports that *LRIM17* silencing reduces mosquito survival during *E. coli* and *S. aureus* infections (Dong et al., 2006a) and significantly increases bacterial load in the midgut (Dong et al., 2009). Curiously, a previous microarray reported *LRIM17* upregulation after *P. falciparum* but not *P. berghei* infection (Dong et al., 2006a). Like *LRIM4*, *LRIM17* is also highly expressed by circulating hemocytes (Pinto et al., 2009), suggesting it could play a role in the mosquito's basal immune response. Furthermore, preliminary data suggests it is highly expressed in larvae and pupae, which implies it is important for immunity in all life stages.

The role of *LRIM17* in *Plasmodium* defence remains uncertain due to conflicting results between different laboratories and mosquito strains. *LRIM17* was reported to be a major antagonist of *P. berghei* and *P. falciparum* in the *An. gambiae* Keele strain (Dong et al., 2006a; Garver et al., 2012) and *An. stephensi* (Dong et al., 2011). Like *APL1A-C*, *LRIM17* maps to a genetic locus in *An. gambiae* controlling *P. falciparum* infections (Riehle et al., 2006). However, *LRIM17* knockdown was shown to have no effect on *P. berghei* development in *An. gambiae* G3 (Riehle et al., 2006) and Yaoundé (Chapter 4). Furthermore, knockdown experiments using G3 showed no effect on *P. falciparum* infections (Michael Povelones, personal communication). In an attempt to resolve this discrepancy, *LRIM17* was silenced in Keele mosquitoes in this Chapter but no impact on *P. berghei* development was observed. Crucially, the same RNAi primers as Dong et al. were utilised and the knockdown was highly efficient. This could suggest the effect of *LRIM17* silencing is dependent upon laboratory conditions rather than mosquito strain. The discrepancy between laboratories could be explained by differences in mosquito midgut microbiota. Microbiota have been shown to modulate parasite infections by stimulating the mosquito's basal immune response or directly inhibiting parasite development (Cirimotich et al., 2011a; Dong et al., 2009; Meister et al., 2009). Furthermore, it is unknown whether laboratory colonies of Keele mosquitoes have been inadvertently "contaminated" by interbreeding with other mosquito strains. It would be interesting to sequence *LRIM17* from different laboratory colonies of Keele mosquitoes to rule out significant polymorphism. In addition, *LRIM17* in hemolymph collected from various Keele colonies could be analysed by western blot to determine whether the protein migrates at different molecular weights or forms different complexes. The intensity of parasite infections could also influence results as *LRIM17* silencing has been shown to significantly affect *P. falciparum* development at low and medium but not high intensities in Keele mosquitoes (Garver et al., 2012). Importantly, lower intensities are more consistent with infections in the field.

If LRIM17 is involved in *Plasmodium* killing under certain circumstances, the mechanism remains unknown. *LRIM17* is known to be regulated by the Imd pathway, like *TEP1* (Garver et al., 2009). However, preliminary evidence suggests LRIM17 does not interact with TEP1, LRIM1 or APL1C so it might not be directly involved in the complement-like system. As the LRIM1/APL1C complex binds TEP1 via its intertwined coiled-coil domains (Povelones et al., 2011), it is perhaps unsurprising that the Coil-less LRIM17 is unable to interact with TEP1. It would be useful to determine whether *LRIM17* silencing affects the processing of TEP1-F into mature TEP1_{cut}. Also, it should be investigated whether *LRIM17* knockdown affects TEP1 localisation to ookinete surfaces. LRIM17 might function in a TEP1-independent parasite killing mechanism that is only active under particular circumstances. Identification of LRIM17 interacting partners would provide important clues to its function. A polyclonal antibody against LRIM17 is being developed to facilitate this investigation.

As LRIM4 and LRIM17 were transcriptionally co-regulated, it was hypothesised that they function together. However, no disulphide-bonded complex between LRIM4 and LRIM17 was observed upon co-transfection of cultured cells. Nevertheless, LRIM4 and LRIM17 might still interact non-covalently, which could be investigated by western blot analysis of hemolymph proteins immunoprecipitated by His-tagged LRIM17, probing with the LRIM4 antibody. Alternatively, LRIM4 and LRIM17 could function in the same or related biochemical pathway(s) without physically interacting. Interestingly, both *LRIM4* and *LRIM17* hierarchically clustered with *TEP12* and *TEP14* in Chapter 4, based on their transcriptional regulation. This could be a novel functional relationship in the mosquito immune system. It would be interesting to determine whether LRIM4 or LRIM17 can pull-down TEP12 or TEP14 from hemolymph. Preliminary evidence suggests that *LRIM4*, *LRIM17*, *TEP12* and *TEP14* are not endogenously expressed by mosquito Sua4.0 cells (data not shown). If the presence of all four proteins is required for normal functionality, this could explain why LRIM4 and LRIM17 did not interact with each other, TEP1, LRIM1 or APL1C in experiments using these cells. Curiously, TEP12 and TEP14 are phylogenetically clustered in the *An. gambiae* TEP family, based on protein sequence, but do not seem to originate by a recent gene duplication (Christophides et al., 2002). Both lack an active thioester motif, like most *An. gambiae* TEPs.

Unfortunately, time constraints prevented a thorough analysis of LRIM15 and this Transmembrane LRIM requires further investigation. It was recently shown that LRIM15 is a true transmembrane protein (Michael Povelones, personal communication). After transfection of recombinant LRIM15, the protein was immunolocalised to the cell surface after staining with a Strep antibody. As its expression is hemocyte-enriched (Pinto et al., 2009), it is tempting to speculate that LRIM15 could be a PRR on the surface of circulating hemocytes, poised to recognise invaders in the hemolymph.

Furthermore, the intracellular region of LRIM15 is very small, which could be another strong indication. Little is known about the properties of Transmembrane LRIMs. Although membrane-bound TLRs in mammals dimerise upon ligand binding (Botos et al., 2011), LRIM15 has been observed as a monomer in lysate from cultured cells (Michael Povelones, personal communication).

Evidence presented in this Chapter has provided new insights into complex formation in the LRIM family. Whereas LRIM1 and APL1C form a disulphide-linked heterodimer (Baxter et al., 2010; Povelones et al., 2011), it was shown that LRIM4 forms a homodimer *in vitro* and *in vivo*. Interestingly, these three LRIMs are all Long subfamily members (Povelones et al., 2009). LRIM1 and APL1C are linked by a single intermolecular disulphide-bond between homologous cysteines located just upstream of the coiled-coil domains (Baxter et al., 2010; Povelones et al., 2011). LRIM4 lacks a cysteine in this position but has an additional cysteine at its extreme C-terminus, downstream of the coiled-coils (Waterhouse et al., 2010). Site-directed mutagenesis demonstrated that this additional cysteine residue is responsible for covalently-linking the LRIM4 homodimer (Povelones et al., 2011). This demonstrates an intrinsic flexibility in the position of the cysteine capable of bridging two LRIM molecules. It would be intriguing to determine how the three-dimensional structure of the LRIM4 homodimer compares to the LRIM1/APL1C complex (Baxter et al., 2010).

LRIM17 is secreted as a monomer in cell culture but its behaviour in the hemolymph is undetermined. LRIM17 lacks a terminal cysteine residue homologous to the bridging cysteine in LRIM1, APL1C or LRIM4 (Waterhouse et al., 2010), suggesting it is unlikely to form covalent interactions with other molecules. Nevertheless, it was shown that the disulphide bond between LRIM1 and APL1C is not essential for their heterodimerisation as they can form non-covalent complexes (Povelones et al., 2011). Therefore, LRIM17 could still be capable of forming non-covalent homo- and heterocomplexes. Interestingly, LRIM17 forms a weak band at the predicted size of a homotrimer after His purification *in vitro*, in addition to the predominant monomer. Perhaps LRIM17 functions as a trimer when at very high concentrations, such as on pathogen surfaces. Although the coiled-coil domains are largely dispensable for LRIM1/APL1C heterodimer formation, the most C-terminal coiled-coil domain seems to contribute to the specificity of their interaction (Povelones et al., 2011). Therefore, LRIM17 and the other coil-less LRIMs might be more promiscuous in their protein-protein interactions (Waterhouse et al., 2010).

Chapter 7: Final discussion and conclusions

7 Final discussion and conclusions

This PhD thesis has provided new insights into the LRIM family in *An. gambiae* and its role in mosquito immunity. It has demonstrated that the LRIMs show differential transcriptional responses to various immune challenges, including blood feeding and infections with *Plasmodium*, bacteria, fungi and virus. Some LRIMs are induced by a wide variety of challenges and seem to play a core immune function, such as LRIM1 and APL1C in a complement-like pathway. In contrast, other LRIMs respond exclusively to specific challenges, including LRIM9, which was strongly induced by blood feeding. LRIM9 was discovered to be a novel antagonist of *P. berghei* infections of *An. gambiae*, with a putative role in parasite melanisation. We hypothesise that LRIM9 is induced in anticipation of blood-borne infections, which is an original concept in *An. gambiae* immunity. Finally, this project has increased our understanding of complex formation in the LRIM family. In particular, mutational studies using LRIM4 showed that there is intrinsic flexibility in the ability of LRIMs to form disulphide-bonded dimers.

We propose that the LRIMs are a novel, mosquito-specific family of pathogen recognition proteins. LRR proteins are involved in pathogen sensing in many phyla, including TLRs and NLRs in mammals and NB-LRRs in plants (Istomin and Godzik, 2009; Padmanabhan et al., 2009; Sirard et al., 2007). They are hypothesised to link the mosquito complement-like system to pathogens, with different LRIMs responding to distinct pathogens and immune challenges. This thesis suggests that the LRIM family has diversified to respond to the wide variety of pathogens that mosquitoes encounter in their blood feeding lifestyle. The variability and structural flexibility of the LRR domains within the LRIM family could enable diverse interactions (Waterhouse et al., 2010). The LRIMs might directly interact with pathogen surfaces with their LRR domains. Those LRIMs that interact with TEP proteins via their coiled-coil domains might deliver their TEP cargo to the pathogen surface, opsonising the pathogen. Indeed, the LRIM1/APL1C complex is known to stabilise mature TEP1_{cut}, promote its opsonisation of pathogen surfaces and prevent it from reacting with self-tissues (Fraiture et al., 2009; Povelones et al., 2009). It remains to be determined whether other LRIM family members bind TEP proteins. Alternatively, the LRIMs might recruit other immune proteins and mediate pathogen recognition indirectly. The LRIMs do not possess known signalling domains and so they are probably not involved in immune signal transduction, unlike the TLR, NLR and NB-LRR proteins (Waterhouse et al., 2010). However, the existence of novel signalling domains cannot be ruled out. In particular, the Transmembrane LRIMs possess a small intracellular domain and seem the most likely candidates to play a signalling role. There remains much to learn about how LRIMs interact with each other in the hemolymph. As LRIM1/APL1C form a heterodimer and LRIM4 forms a homodimer (Povelones et

al., 2011), it can be predicted that other LRIMs form complexes, perhaps under different circumstances.

The evolutionary history of the LRIMs is very interesting as it remains unknown how this mosquito-specific family originated. To date, no LRIM-like genes have been discovered in the sequenced genome of any non-mosquito organism. Attempts to find LRIM orthologues or ancestral LRIM genes in other organisms have been hampered by the extensive amino acid sequence divergence in the LRIM family (Povelones et al., 2009; Waterhouse et al., 2010). A more thorough bioinformatic search might find the ancestor of mosquito LRIMs in another insect, although the characteristics of such a protein are unknown. It can be envisaged that a founder LRR protein gained a coiled-coil, or vice versa, and subsequently expanded. As LRR proteins and coiled-coil proteins are common, the original protein that gave rise to the LRIMs might not be identifiable, presuming it is still intact today. Although *Drosophila* has LRR proteins and coiled-coil proteins, the exact LRIM domain organisation is not present. Nevertheless, mosquitoes (Diptera: Culicidae) are lower Diptera, one of the earliest fly lineages, and are thought to have diverged from *Drosophila* (Diptera: Drosophilidae) approximately 250 million years ago (Waterhouse et al., 2007; Wiegmann et al., 2011). Therefore, an ancestral LRIM gene might be unrecognisable in *Drosophila*. It would be expected that the ancestral LRIM would be found in species more closely related to mosquitoes, such as sandflies (Diptera: Psychodidae). Very preliminary genome assemblies of the sandflies, *Lutzomyia longipalpis* and *Phlebotomus papatasi*, are becoming available but there is currently no evidence of LRIM-like genes. These sandflies are also blood feeders but, interestingly, hematophagy is thought to have arisen independently at least 12 times in Dipteran evolution (Wiegmann et al., 2011).

It will be interesting to investigate how the orthologous LRIM proteins behave in *Ae. aegypti* and *C. quinquefasciatus*. In particular, it should be determined whether the role of LRIM9 is conserved, as *LRIM9* exists as a single orthologue in these other mosquitoes (Waterhouse et al., 2010). Evidence suggests that the functional relationship between LRIM1, APL1C and TEP1 is conserved in *Ae. aegypti* as their orthologues are induced by *Wolbachia* infection (Kambris et al., 2009).

Several LRIMs are involved in defence against the deadliest human malaria parasite, *P. falciparum*, which highlights the significance of the LRIM family. The mosquito complement-like pathway is thought to play an important role in *P. falciparum* defence, dependent on parasite infection intensity. TEP1 is consistently shown to be a major *P. falciparum* antagonist whereas LRIM1 and APL1C are known to be most effective at medium and low infection intensities, respectively (Dong et al., 2006a; Garver et al., 2012). Interestingly, several strains of *P. falciparum* have been demonstrated to evade the mosquito complement-like system to aid their transmission (Molina-Cruz

et al., 2012). Furthermore, LRIM17 has been reported to be a *P. falciparum* antagonist in the *An. gambiae* Keele strain, particularly at medium and low infection intensities (Dong et al., 2006a; Garver et al., 2012). The paralogues of APL1C have also been implicated in responses against *P. falciparum*. APL1A has been reported to influence the prevalence of *P. falciparum* infections (Mitri et al., 2009) and *APL1B* knockdown increases oocyst levels at medium infection intensities (Garver et al., 2012). It is possible that several LRIMs cooperate in *P. falciparum* defence responses or different LRIMs might take precedence in specific contexts. This PhD thesis has provided new candidate LRIMs for involvement in *P. falciparum* defence, such as LRIM4 and LRIM7. Although LRIM9 is not upregulated in response to *P. falciparum*, its suggested role in anticipatory immunity triggered by blood feeding may also be important during *P. falciparum* infections. TEP3 is another promising contender as it is a novel antagonist of *P. berghei* and interacts with the LRIM1/APL1C complex (Povelones et al., 2011).

Hematophagous insects, like mosquitoes, are at high risk of infection from blood-borne pathogens, including parasites and viruses. The blood meal also promotes dramatic proliferation of midgut bacterial flora (Cirimotich et al., 2010; Kumar et al., 2010). The proposed theory of anticipatory immunity in mosquitoes would be a highly important defence mechanism against infections arising after blood feeding. By assuming every blood meal is infectious and inducing immune effectors, like LRIM9, in anticipation, the mosquito does not need to specifically recognise each pathogen but is prepared for imminent danger. Some pathogens, like viruses, can infect mosquito cells within hours of blood meal ingestion, which would allow little time for pathogen recognition and specific immune induction. Furthermore, anticipatory defence could even help kill pathogens evading immune recognition because the blood meal alone is sufficient to trigger the deployment of killing mechanisms. Anticipatory immunity has not, to our knowledge, been reported in the innate immune response of another organism. Innate immunity is traditionally considered to be poorly specific and non-anticipatory. However, the adaptive immune response of vertebrates has been previously proposed as “anticipatory”. In a distinct mechanism to mosquitoes, vertebrates generate diverse repertoires of T and B lymphocyte receptors by rearrangement of gene segments to enable recognition of any potential antigen (Pancer and Cooper, 2006).

LRIM1 and APL1C function differently to LRIM9 as they constitutively circulate at high levels in the mosquito hemolymph poised to attack invaders, which has been described as basal immunity (Frolet et al., 2006). Unlike LRIM9, they are not specific to blood-borne infections because they are also involved in antibacterial defence and phagocytosis (Moita et al., 2005). Both the complement-like system discovered in *An. gambiae* and the proposed mechanism of anticipatory defence seem to be

mosquito-specific and involve LRIMs. Therefore, it can be postulated that the LRIM family is mosquito-specific because it evolved to defend against the distinct blood-borne pathogens faced by these insects. Importantly, many pathogens are only transmitted by mosquitoes, such as *Plasmodium* parasites, filarial worms and numerous viruses. In contrast to the LRIMs, the TEPs have ancient evolutionary origins and related proteins are found in many phyla, including the C3/C4/C5 factors of the mammalian complement system (Blandin and Levashina, 2004). As well as mosquitoes, TEPs with complement-like activity have been discovered in horseshoe crabs (Tagawa et al., 2012; Zhu et al., 2005). We propose that the functions of TEP and LRIM proteins were combined to create the mosquito complement-like system whereas certain LRIMs, like LRIM9, have retained their ancestral function in blood-borne infections. It is unknown whether LRIM9 plays a generalised role or is specific to particular blood-borne pathogens. LRIM9 functions against *P. berghei* despite being transcriptionally unresponsive to malaria parasite infections, which demonstrates that transcriptional responses can be independent of protein activity. Therefore, LRIM9 should be investigated for RNAi phenotypes with other blood-borne pathogens, such as ONNV and filarial worms. Furthermore, other Short LRIMs with a similar induction post blood feeding (i.e. LRIM8A, LRIM8B and LRIM10) should also be examined for roles in defence against blood-borne infections.

Understanding the mosquito immune system and how it interacts with *Plasmodium* parasites is an important challenge with exciting prospects for malaria control (Chen et al., 2008). The most successful malaria control strategies to date have all targeted the mosquito vector (Catteruccia, 2007). The mosquito immune system could be exploited to create GM mosquitoes refractory to *P. falciparum* or *P. vivax*, which could be employed to replace wild mosquito populations (Christophides, 2005). Ideally, multiple *Plasmodium* antagonists could be overexpressed in the same GM mosquito to achieve 100% blockade of malaria transmission and reduce the risk of parasite resistance. The mosquito-specific LRIM family and the complement-like system are potential candidates for malaria control strategies and this PhD study has increased our understanding of the role of LRIMs in mosquito immunity. Future work is needed to elucidate precise mechanisms of parasite killing, the involvement of LRIMs and TEPs and immune evasion strategies used by *P. falciparum*. Furthermore, promoters of genes with blood feeding and/or female specific expression, potentially like LRIM9, are highly desirable for driving gene expression in GM mosquitoes. Finally, if members of the LRIM family are involved in limiting viral infections, as suggested by the transcriptional profiling in this study, the family could also be used to control arboviral disease.

Chapter 8: Bibliography

8 Bibliography

Abraham, E.G., Pinto, S.B., Ghosh, A., Vanlandingham, D.L., Budd, A., Higgs, S., Kafatos, F.C., Jacobs-Lorena, M., and Michel, K. (2005). An immune-responsive serpin, SRPN6, mediates mosquito defense against malaria parasites. *Proc Natl Acad Sci U S A* 102, 16327-16332.

Agnandji, S.T., Lell, B., Soulanoudjingar, S.S., Fernandes, J.F., Abossolo, B.P., Conzelmann, C., Methogo, B.G., Doucka, Y., Flamen, A., Mordmuller, B., *et al.* (2011). First results of phase 3 trial of RTS,S/AS01 malaria vaccine in African children. *The New England journal of medicine* 365, 1863-1875.

Aguilar, R., Dong, Y., Warr, E., and Dimopoulos, G. (2005a). Anopheles infection responses; laboratory models versus field malaria transmission systems. *Acta Trop* 95, 285-291.

Aguilar, R., Jedlicka, A.E., Mintz, M., Mahairaki, V., Scott, A.L., and Dimopoulos, G. (2005b). Global gene expression analysis of *Anopheles gambiae* responses to microbial challenge. *Insect Biochem Mol Biol* 35, 709-719.

Ahmed, A., Martin, D., Manetti, A.G., Han, S.J., Lee, W.J., Mathiopoulos, K.D., Muller, H.M., Kafatos, F.C., Raikhel, A., and Brey, P.T. (1999). Genomic structure and ecdysone regulation of the prophenoloxidase 1 gene in the malaria vector *Anopheles gambiae*. *Proc Natl Acad Sci U S A* 96, 14795-14800.

Akachi, Y., and Atun, R. (2011). Effect of investment in malaria control on child mortality in sub-Saharan Africa in 2002-2008. *PLoS ONE* 6, e21309.

Akman-Anderson, L., Olivier, M., and Luckhart, S. (2007). Induction of nitric oxide synthase and activation of signaling proteins in *Anopheles* mosquitoes by the malaria pigment, hemozoin. *Infect Immun* 75, 4012-4019.

Alavi, Y., Arai, M., Mendoza, J., Tufet-Bayona, M., Sinha, R., Fowler, K., Billker, O., Franke-Fayard, B., Janse, C.J., Waters, A., *et al.* (2003). The dynamics of interactions between *Plasmodium* and the mosquito: a study of the infectivity of *Plasmodium berghei* and *Plasmodium gallinaceum*, and their transmission by *Anopheles stephensi*, *Anopheles gambiae* and *Aedes aegypti*. *Int J Parasitol* 33, 933-943.

Aliota, M.T., Chen, C.C., Dagoro, H., Fuchs, J.F., and Christensen, B.M. (2011). Filarial worms reduce *Plasmodium* infectivity in mosquitoes. *PLoS neglected tropical diseases* 5, e963.

Alphey, L. (2009). Natural and engineered mosquito immunity. *Journal of biology* 8, 40.

Alphey, L., Beard, C.B., Billingsley, P., Coetzee, M., Crisanti, A., Curtis, C., Eggleston, P., Godfray, C., Hemingway, J., Jacobs-Lorena, M., *et al.* (2002). Malaria control with genetically manipulated insect vectors. *Science* 298, 119-121.

Alphey, L., Nimmo, D., O'Connell, S., and Alphey, N. (2008). Insect population suppression using engineered insects. *Advances in experimental medicine and biology* 627, 93-103.

Aly, A.S., Vaughan, A.M., and Kappe, S.H. (2009). Malaria parasite development in the mosquito and infection of the mammalian host. *Annual review of microbiology* 63, 195-221.

Ao, J., Ling, E., and Yu, X.Q. (2007). *Drosophila* C-type lectins enhance cellular encapsulation. *Molecular immunology* 44, 2541-2548.

Asano, T., and Ashida, M. (2001a). Cuticular pro-phenoloxidase of the silkworm, *Bombyx mori*. Purification and demonstration of its transport from hemolymph. *J Biol Chem* 276, 11100-11112.

Asano, T., and Ashida, M. (2001b). Transepithelially transported pro-phenoloxidase in the cuticle of the silkworm, *Bombyx mori*. Identification of its methionyl residues oxidized to methionine sulfoxides. *J Biol Chem* 276, 11113-11125.

Atella, G.C., Silva-Neto, M.A., Golodne, D.M., Arefin, S., and Shahabuddin, M. (2006). *Anopheles gambiae* lipophorin: characterization and role in lipid transport to developing oocyte. *Insect Biochem Mol Biol* 36, 375-386.

Atieli, H.E., Zhou, G., Afrane, Y., Lee, M.C., Mwanzo, I., Githeko, A.K., and Yan, G. (2011). Insecticide-treated net (ITN) ownership, usage, and malaria transmission in the highlands of western Kenya. *Parasites & vectors* 4, 113.

Attardo, G.M., Hansen, I.A., and Raikhel, A.S. (2005). Nutritional regulation of vitellogenesis in mosquitoes: implications for anautogeny. *Insect Biochem Mol Biol* 35, 661-675.

Ayres, J.S., Freitag, N., and Schneider, D.S. (2008). Identification of *Drosophila* mutants altering defense of and endurance to *Listeria monocytogenes* infection. *Genetics* 178, 1807-1815.

Baird, J.K. (2005). Effectiveness of antimalarial drugs. *The New England journal of medicine* 352, 1565-1577.

Baker, D.A., Nolan, T., Fischer, B., Pinder, A., Crisanti, A., and Russell, S. (2011). A comprehensive gene expression atlas of sex- and tissue-specificity in the malaria vector, *Anopheles gambiae*. *BMC Genomics* 12, 296.

Bargielowski, I., Nimmo, D., Alpey, L., and Koella, J.C. (2011). Comparison of life history characteristics of the genetically modified OX513A line and a wild type strain of *Aedes aegypti*. *PLoS ONE* *6*, e20699.

Barillas-Mury, C., and Kumar, S. (2005). Plasmodium-mosquito interactions: a tale of dangerous liaisons. *Cell Microbiol* *7*, 1539-1545.

Bass, C., Williamson, M.S., Wilding, C.S., Donnelly, M.J., and Field, L.M. (2007). Identification of the main malaria vectors in the *Anopheles gambiae* species complex using a TaqMan real-time PCR assay. *Malar J* *6*, 155.

Baton, L.A., Garver, L., Xi, Z., and Dimopoulos, G. (2008). Functional genomics studies on the innate immunity of disease vectors. *Insect Science* *15*, 15-27.

Baxter, R.H., Chang, C.I., Chelliah, Y., Blandin, S., Levashina, E.A., and Deisenhofer, J. (2007). Structural basis for conserved complement factor-like function in the antimalarial protein TEP1. *Proc Natl Acad Sci U S A* *104*, 11615-11620.

Baxter, R.H., Steinert, S., Chelliah, Y., Volohonsky, G., Levashina, E.A., and Deisenhofer, J. (2010). A heterodimeric complex of the LRR proteins LRIM1 and APL1C regulates complement-like immunity in *Anopheles gambiae*. *Proc Natl Acad Sci U S A*.

Bell, J.K., Mullen, G.E., Leifer, C.A., Mazzoni, A., Davies, D.R., and Segal, D.M. (2003). Leucine-rich repeats and pathogen recognition in Toll-like receptors. *Trends Immunol* *24*, 528-533.

Bella, J., Hindle, K.L., McEwan, P.A., and Lovell, S.C. (2008). The leucine-rich repeat structure. *Cell Mol Life Sci* *65*, 2307-2333.

Bent, A.F., and Mackey, D. (2007). Elicitors, effectors, and R genes: the new paradigm and a lifetime supply of questions. *Annu Rev Phytopathol* *45*, 399-436.

Besansky, N.J., Powell, J.R., Caccone, A., Hamm, D.M., Scott, J.A., and Collins, F.H. (1994). Molecular phylogeny of the *Anopheles gambiae* complex suggests genetic introgression between principal malaria vectors. *Proc Natl Acad Sci U S A* *91*, 6885-6888.

Bian, G., Xu, Y., Lu, P., Xie, Y., and Xi, Z. (2010). The endosymbiotic bacterium *Wolbachia* induces resistance to dengue virus in *Aedes aegypti*. *PLoS Pathog* *6*, e1000833.

Billker, O., Lindo, V., Panico, M., Etienne, A.E., Paxton, T., Dell, A., Rogers, M., Sinden, R.E., and Morris, H.R. (1998). Identification of xanthurenic acid as the putative inducer of malaria development in the mosquito. *Nature* *392*, 289-292.

Billker, O., Shaw, M.K., Margos, G., and Sinden, R.E. (1997). The roles of temperature, pH and mosquito factors as triggers of male and female gametogenesis of *Plasmodium berghei* in vitro. *Parasitology* 115 (Pt 1), 1-7.

Bisi, D.C., and Lampe, D.J. (2011). Secretion of anti-*Plasmodium* effector proteins from a natural *Pantoea agglomerans* isolate by using PelB and HlyA secretion signals. *Applied and environmental microbiology* 77, 4669-4675.

Black, W.C.t., Alpey, L., and James, A.A. (2011). Why RIDL is not SIT. *Trends Parasitol* 27, 362-370.

Blandin, S., and Levashina, E.A. (2004). Thioester-containing proteins and insect immunity. *Molecular immunology* 40, 903-908.

Blandin, S., Moita, L.F., Kocher, T., Wilm, M., Kafatos, F.C., and Levashina, E.A. (2002). Reverse genetics in the mosquito *Anopheles gambiae*: targeted disruption of the Defensin gene. *EMBO Rep* 3, 852-856.

Blandin, S., Shiao, S.H., Moita, L.F., Janse, C.J., Waters, A.P., Kafatos, F.C., and Levashina, E.A. (2004). Complement-like protein TEP1 is a determinant of vectorial capacity in the malaria vector *Anopheles gambiae*. *Cell* 116, 661-670.

Blandin, S.A., and Levashina, E.A. (2007). Phagocytosis in mosquito immune responses. *Immunol Rev* 219, 8-16.

Blandin, S.A., Marois, E., and Levashina, E.A. (2008). Antimalarial responses in *Anopheles gambiae*: from a complement-like protein to a complement-like pathway. *Cell Host Microbe* 3, 364-374.

Blandin, S.A., Wang-Sattler, R., Lamacchia, M., Gagneur, J., Lycett, G., Ning, Y., Levashina, E.A., and Steinmetz, L.M. (2009). Dissecting the genetic basis of resistance to malaria parasites in *Anopheles gambiae*. *Science* 326, 147-150.

Blanford, S., Chan, B.H., Jenkins, N., Sim, D., Turner, R.J., Read, A.F., and Thomas, M.B. (2005). Fungal pathogen reduces potential for malaria transmission. *Science* 308, 1638-1641.

Boete, C. (2005). Malaria parasites in mosquitoes: laboratory models, evolutionary temptation and the real world. *Trends Parasitol* 21, 445-447.

Boissiere, A., Tchioffo, M.T., Bachar, D., Abate, L., Marie, A., Nsango, S.E., Shahbazkia, H.R., Awono-Ambene, P.H., Levashina, E.A., Christen, R., *et al.* (2012). Midgut microbiota of the malaria mosquito vector *Anopheles gambiae* and interactions with *Plasmodium falciparum* infection. *PLoS Pathog* 8, e1002742.

Botos, I., Segal, D.M., and Davies, D.R. (2011). The structural biology of Toll-like receptors. *Structure* 19, 447-459.

Brault, A.C., Foy, B.D., Myles, K.M., Kelly, C.L., Higgs, S., Weaver, S.C., Olson, K.E., Miller, B.R., and Powers, A.M. (2004). Infection patterns of o'nyong nyong virus in the malaria-transmitting mosquito, *Anopheles gambiae*. *Insect Mol Biol* 13, 625-635.

Broderick, N.A., Welchman, D.P., and Lemaitre, B. (2009). Recognition and response to microbial infection in *Drosophila*. In *Insect Infection and Immunity: Evolution, Ecology, and Mechanisms*, J. Rolff, and S.E. Reynolds, eds. (Oxford Biology).

Buchanan, S.G., and Gay, N.J. (1996). Structural and functional diversity in the leucine-rich repeat family of proteins. *Progress in biophysics and molecular biology* 65, 1-44.

Bukhari, T., Middelman, A., Koenraadt, C.J., Takken, W., and Knols, B.G. (2010). Factors affecting fungus-induced larval mortality in *Anopheles gambiae* and *Anopheles stephensi*. *Malar J* 9, 22.

Carlton, J.M., Adams, J.H., Silva, J.C., Bidwell, S.L., Lorenzi, H., Caler, E., Crabtree, J., Angiuoli, S.V., Merino, E.F., Amedeo, P., *et al.* (2008). Comparative genomics of the neglected human malaria parasite *Plasmodium vivax*. *Nature* 455, 757-763.

Carlton, J.M., Angiuoli, S.V., Suh, B.B., Kooij, T.W., Perteau, M., Silva, J.C., Ermolaeva, M.D., Allen, J.E., Selengut, J.D., Koo, H.L., *et al.* (2002). Genome sequence and comparative analysis of the model rodent malaria parasite *Plasmodium yoelii yoelii*. *Nature* 419, 512-519.

Carta, S., Castellani, P., Delfino, L., Tassi, S., Vene, R., and Rubartelli, A. (2009). DAMPs and inflammatory processes: the role of redox in the different outcomes. *J Leukoc Biol* 86, 549-555.

Castillo, J.C., Robertson, A.E., and Strand, M.R. (2006). Characterization of hemocytes from the mosquitoes *Anopheles gambiae* and *Aedes aegypti*. *Insect Biochem Mol Biol* 36, 891-903.

Catteruccia, F. (2007). Malaria vector control in the third millennium: progress and perspectives of molecular approaches. *Pest Manag Sci* 63, 634-640.

Catteruccia, F., Nolan, T., Blass, C., Muller, H.M., Crisanti, A., Kafatos, F.C., and Loukeris, T.G. (2000). Toward *Anopheles* transformation: Minos element activity in anopheline cells and embryos. *Proc Natl Acad Sci U S A* 97, 2157-2162.

Cerenius, L., and Soderhall, K. (2004). The prophenoloxidase-activating system in invertebrates. *Immunol Rev* 198, 116-126.

Chen, Y., Weng, Z.-H., and Zheng, L. (2008). Innate immunity against malaria parasites in *Anopheles gambiae*. *Insect Science* 15, 45-52.

Christensen, B.M., Li, J., Chen, C.C., and Nappi, A.J. (2005). Melanization immune responses in mosquito vectors. *Trends Parasitol* 21, 192-199.

Christophides, G.K. (2005). Transgenic mosquitoes and malaria transmission. *Cell Microbiol* 7, 325-333.

Christophides, G.K., Vlachou, D., and Kafatos, F.C. (2004). Comparative and functional genomics of the innate immune system in the malaria vector *Anopheles gambiae*. *Immunol Rev* 198, 127-148.

Christophides, G.K., Zdobnov, E., Barillas-Mury, C., Birney, E., Blandin, S., Blass, C., Brey, P.T., Collins, F.H., Danielli, A., Dimopoulos, G., *et al.* (2002). Immunity-related genes and gene families in *Anopheles gambiae*. *Science* 298, 159-165.

Cirimotich, C.M., Dong, Y., Clayton, A.M., Sandiford, S.L., Souza-Neto, J.A., Mulenga, M., and Dimopoulos, G. (2011a). Natural microbe-mediated refractoriness to *Plasmodium* infection in *Anopheles gambiae*. *Science* 332, 855-858.

Cirimotich, C.M., Dong, Y., Garver, L.S., Sim, S., and Dimopoulos, G. (2010). Mosquito immune defenses against *Plasmodium* infection. *Dev Comp Immunol* 34, 387-395.

Cirimotich, C.M., Ramirez, J.L., and Dimopoulos, G. (2011b). Native microbiota shape insect vector competence for human pathogens. *Cell Host Microbe* 10, 307-310.

Clements, A.N. (2000). *The Biology of Mosquitoes. Volume 1, Development, Nutrition and Reproduction* (CABI Publishing).

Clements, A.N. (2012). *The Biology of Mosquitoes. Volume 3, Transmission of viruses and interactions with bacteria* (CABI Publishing).

Coetzee, M., Craig, M., and le Sueur, D. (2000). Distribution of African malaria mosquitoes belonging to the *Anopheles gambiae* complex. *Parasitol Today* 16, 74-77.

Cohuet, A., Osta, M.A., Morlais, I., Awono-Ambene, P.H., Michel, K., Simard, F., Christophides, G.K., Fontenille, D., and Kafatos, F.C. (2006). *Anopheles* and *Plasmodium*: from laboratory models to natural systems in the field. *EMBO Rep* 7, 1285-1289.

Collins, F.H., Sakai, R.K., Vernick, K.D., Paskewitz, S., Seeley, D.C., Miller, L.H., Collins, W.E., Campbell, C.C., and Gwadz, R.W. (1986). Genetic selection of a *Plasmodium*-refractory strain of the malaria vector *Anopheles gambiae*. *Science* 234, 607-610.

Coluzzi, M., Sabatini, A., della Torre, A., Di Deco, M.A., and Petrarca, V. (2002). A polytene chromosome analysis of the *Anopheles gambiae* species complex. *Science* *298*, 1415-1418.

Crompton, P.D., Pierce, S.K., and Miller, L.H. (2010). Advances and challenges in malaria vaccine development. *The Journal of clinical investigation* *120*, 4168-4178.

Davidson, G. (1964). *Anopheles Gambiae*, a Complex of Species. *Bulletin of the World Health Organization* *31*, 625-634.

DeJong, R.J., Miller, L.M., Molina-Cruz, A., Gupta, L., Kumar, S., and Barillas-Mury, C. (2007). Reactive oxygen species detoxification by catalase is a major determinant of fecundity in the mosquito *Anopheles gambiae*. *Proc Natl Acad Sci U S A* *104*, 2121-2126.

Delves, M., Plouffe, D., Scheurer, C., Meister, S., Wittlin, S., Winzeler, E.A., Sinden, R.E., and Leroy, D. (2012). The activities of current antimalarial drugs on the life cycle stages of *Plasmodium*: a comparative study with human and rodent parasites. *PLoS medicine* *9*, e1001169.

Dimopoulos, G. (2003). Insect immunity and its implication in mosquito-malaria interactions. *Cell Microbiol* *5*, 3-14.

Dimopoulos, G., Christophides, G.K., Meister, S., Schultz, J., White, K.P., Barillas-Mury, C., and Kafatos, F.C. (2002). Genome expression analysis of *Anopheles gambiae*: responses to injury, bacterial challenge, and malaria infection. *Proc Natl Acad Sci U S A* *99*, 8814-8819.

Dinglasan, R.R., Kalume, D.E., Kanzok, S.M., Ghosh, A.K., Muratova, O., Pandey, A., and Jacobs-Lorena, M. (2007). Disruption of *Plasmodium falciparum* development by antibodies against a conserved mosquito midgut antigen. *Proc Natl Acad Sci U S A* *104*, 13461-13466.

Dong, Y., Aguilar, R., Xi, Z., Warr, E., Mongin, E., and Dimopoulos, G. (2006a). *Anopheles gambiae* immune responses to human and rodent *Plasmodium* parasite species. *PLoS Pathog* *2*, e52.

Dong, Y., Das, S., Cirimotich, C., Souza-Neto, J.A., McLean, K.J., and Dimopoulos, G. (2011). Engineered *Anopheles* immunity to *Plasmodium* infection. *PLoS Pathog* *7*, e1002458.

Dong, Y., and Dimopoulos, G. (2009). *Anopheles* fibrinogen-related proteins provide expanded pattern recognition capacity against bacteria and malaria parasites. *J Biol Chem* *284*, 9835-9844.

Dong, Y., Manfredini, F., and Dimopoulos, G. (2009). Implication of the mosquito midgut microbiota in the defense against malaria parasites. *PLoS Pathog* *5*, e1000423.

Dong, Y., Taylor, H.E., and Dimopoulos, G. (2006b). AgDscam, a hypervariable immunoglobulin domain-containing receptor of the *Anopheles gambiae* innate immune system. *PLoS Biol* 4, e229.

Eastman, R.T., and Fidock, D.A. (2009). Artemisinin-based combination therapies: a vital tool in efforts to eliminate malaria. *Nat Rev Microbiol* 7, 864-874.

Enayati, A., and Hemingway, J. (2010). Malaria management: past, present, and future. *Annual review of entomology* 55, 569-591.

Enserink, M. (2010). If artemisinin drugs fail, what's plan B? *Science* 328, 846.

Erlanger, T.E., Weiss, S., Keiser, J., Utzinger, J., and Wiedenmayer, K. (2009). Past, present, and future of Japanese encephalitis. *Emerging infectious diseases* 15, 1-7.

Fanello, C., Santolamazza, F., and della Torre, A. (2002). Simultaneous identification of species and molecular forms of the *Anopheles gambiae* complex by PCR-RFLP. *Medical and veterinary entomology* 16, 461-464.

Feachem, R.G., Phillips, A.A., Hwang, J., Cotter, C., Wielgosz, B., Greenwood, B.M., Sabot, O., Rodriguez, M.H., Abeyasinghe, R.R., Ghebreyesus, T.A., *et al.* (2010). Shrinking the malaria map: progress and prospects. *Lancet* 376, 1566-1578.

Ferguson, H.M., and Read, A.F. (2002). Why is the effect of malaria parasites on mosquito survival still unresolved? *Trends Parasitol* 18, 256-261.

Ferrandon, D., Imler, J.L., Hetru, C., and Hoffmann, J.A. (2007). The *Drosophila* systemic immune response: sensing and signalling during bacterial and fungal infections. *Nature reviews Immunology* 7, 862-874.

Fidock, D.A. (2010). Drug discovery: Priming the antimalarial pipeline. *Nature* 465, 297-298.

Fortina, P., and Surrey, S. (2008). Digital mRNA processing. *Nat Biotechnol* 26, 293-294.

Fraiture, M., Baxter, R.H., Steinert, S., Chelliah, Y., Frolet, C., Quispe-Tintaya, W., Hoffmann, J.A., Blandin, S.A., and Levashina, E.A. (2009). Two mosquito LRR proteins function as complement control factors in the TEP1-mediated killing of *Plasmodium*. *Cell Host Microbe* 5, 273-284.

Franke-Fayard, B., Trueman, H., Ramesar, J., Mendoza, J., van der Keur, M., van der Linden, R., Sinden, R.E., Waters, A.P., and Janse, C.J. (2004). A *Plasmodium berghei* reference line that constitutively expresses GFP at a high level throughout the complete life cycle. *Mol Biochem Parasitol* 137, 23-33.

Frech, C., and Chen, N. (2011). Genome comparison of human and non-human malaria parasites reveals species subset-specific genes potentially linked to human disease. *PLoS computational biology* 7, e1002320.

Frolet, C., Thoma, M., Blandin, S., Hoffmann, J.A., and Levashina, E.A. (2006). Boosting NF-kappaB-dependent basal immunity of *Anopheles gambiae* aborts development of *Plasmodium berghei*. *Immunity* 25, 677-685.

Ganesan, S., Aggarwal, K., Paquette, N., and Silverman, N. (2011). NF-kappaB/Rel proteins and the humoral immune responses of *Drosophila melanogaster*. *Current topics in microbiology and immunology* 349, 25-60.

Gardner, M.J., Hall, N., Fung, E., White, O., Berriman, M., Hyman, R.W., Carlton, J.M., Pain, A., Nelson, K.E., Bowman, S., *et al.* (2002). Genome sequence of the human malaria parasite *Plasmodium falciparum*. *Nature* 419, 498-511.

Garver, L.S., Bahia, A.C., Das, S., Souza-Neto, J.A., Shiao, J., Dong, Y., and Dimopoulos, G. (2012). *Anopheles imd* pathway factors and effectors in infection intensity-dependent anti-*Plasmodium* action. *PLoS Pathog* 8, e1002737.

Garver, L.S., Dong, Y., and Dimopoulos, G. (2009). Caspar controls resistance to *Plasmodium falciparum* in diverse anopheline species. *PLoS Pathog* 5, e1000335.

Garver, L.S., Xi, Z., and Dimopoulos, G. (2008). Immunoglobulin superfamily members play an important role in the mosquito immune system. *Dev Comp Immunol* 32, 519-531.

Geiss, G.K., Bumgarner, R.E., Birditt, B., Dahl, T., Dowidar, N., Dunaway, D.L., Fell, H.P., Ferree, S., George, R.D., Grogan, T., *et al.* (2008). Direct multiplexed measurement of gene expression with color-coded probe pairs. *Nat Biotechnol* 26, 317-325.

Genta, F.A., Souza, R.S., Garcia, E.S., and Azambuja, P. (2010). Phenol oxidases from *Rhodnius prolixus*: temporal and tissue expression pattern and regulation by ecdysone. *Journal of insect physiology* 56, 1253-1259.

Ghosh, A.K., Dinglasan, R.R., Ikadai, H., and Jacobs-Lorena, M. (2010). An improved method for the *in vitro* differentiation of *Plasmodium falciparum* gametocytes into ookinetes. *Malar J* 9, 194.

GlaxoSmithKline, and PATH, M. (2012). Fact Sheet: RTS,S Malaria Vaccine Candidate.

Gould, E.A., and Solomon, T. (2008). Pathogenic flaviviruses. *Lancet* 371, 500-509.

Govind, S. (2008). Innate immunity in *Drosophila*: Pathogens and pathways. *Insect Sci* 15, 29-43.

Greenwood, B. (2010). Anti-malarial drugs and the prevention of malaria in the population of malaria endemic areas. *Malar J* 9 *Suppl* 3, S2.

Greenwood, B.M., Bojang, K., Whitty, C.J., and Targett, G.A. (2005). Malaria. *Lancet* 365, 1487-1498.

Greenwood, B.M., Fidock, D.A., Kyle, D.E., Kappe, S.H., Alonso, P.L., Collins, F.H., and Duffy, P.E. (2008). Malaria: progress, perils, and prospects for eradication. *The Journal of clinical investigation* 118, 1266-1276.

Greenwood, B.M., and Targett, G.A. (2011). Malaria vaccines and the new malaria agenda. *Clinical microbiology and infection : the official publication of the European Society of Clinical Microbiology and Infectious Diseases* 17, 1600-1607.

Grossman, G.L., Rafferty, C.S., Clayton, J.R., Stevens, T.K., Mukabayire, O., and Benedict, M.Q. (2001). Germline transformation of the malaria vector, *Anopheles gambiae*, with the piggyBac transposable element. *Insect Mol Biol* 10, 597-604.

Guo, P., Hirano, M., Herrin, B.R., Li, J., Yu, C., Sadlonova, A., and Cooper, M.D. (2009). Dual nature of the adaptive immune system in lampreys. *Nature* 459, 796-801.

Gupta, L., Molina-Cruz, A., Kumar, S., Rodrigues, J., Dixit, R., Zamora, R.E., and Barillas-Mury, C. (2009). The STAT pathway mediates late-phase immunity against *Plasmodium* in the mosquito *Anopheles gambiae*. *Cell Host Microbe* 5, 498-507.

Guttery, D.S., Holder, A.A., and Tewari, R. (2012). Sexual development in *Plasmodium*: lessons from functional analyses. *PLoS Pathog* 8, e1002404.

Habtewold, T., Povelones, M., Blagborough, A.M., and Christophides, G.K. (2008). Transmission blocking immunity in the malaria non-vector mosquito *Anopheles quadriannulatus* species A. *PLoS Pathog* 4, e1000070.

Hall, N., Karras, M., Raine, J.D., Carlton, J.M., Kooij, T.W., Berriman, M., Florens, L., Janssen, C.S., Pain, A., Christophides, G.K., *et al.* (2005). A comprehensive survey of the *Plasmodium* life cycle by genomic, transcriptomic, and proteomic analyses. *Science* 307, 82-86.

Han, B.W., Herrin, B.R., Cooper, M.D., and Wilson, I.A. (2008). Antigen recognition by variable lymphocyte receptors. *Science* 321, 1834-1837.

Han, Y.S., Thompson, J., Kafatos, F.C., and Barillas-Mury, C. (2000). Molecular interactions between *Anopheles stephensi* midgut cells and *Plasmodium berghei*: the time bomb theory of ookinete invasion of mosquitoes. *EMBO J* 19, 6030-6040.

Hansen, I.A., Attardo, G.M., Park, J.H., Peng, Q., and Raikhel, A.S. (2004). Target of rapamycin-mediated amino acid signaling in mosquito anautogeny. *Proc Natl Acad Sci U S A* 101, 10626-10631.

Haq, S., and Yadav, R.S. (2011). Geographical distribution and evaluation of mosquito larvivorous potential of *Aphanius dispar* (Ruppell), a native fish of Gujarat, India. *Journal of vector borne diseases* 48, 236-240.

Harris, A.F., Nimmo, D., McKemey, A.R., Kelly, N., Scaife, S., Donnelly, C.A., Beech, C., Petrie, W.D., and Alphey, L. (2011). Field performance of engineered male mosquitoes. *Nat Biotechnol* 29, 1034-1037.

Hay, S.I., Guerra, C.A., Tatem, A.J., Noor, A.M., and Snow, R.W. (2004). The global distribution and population at risk of malaria: past, present, and future. *The Lancet infectious diseases* 4, 327-336.

Hemingway, J., Beaty, B.J., Rowland, M., Scott, T.W., and Sharp, B.L. (2006). The Innovative Vector Control Consortium: improved control of mosquito-borne diseases. *Trends Parasitol* 22, 308-312.

Herrin, B.R., Alder, M.N., Roux, K.H., Sina, C., Ehrhardt, G.R., Boydston, J.A., Turnbough, C.L., Jr., and Cooper, M.D. (2008). Structure and specificity of lamprey monoclonal antibodies. *Proc Natl Acad Sci U S A* 105, 2040-2045.

Hill, A.V. (2011). Vaccines against malaria. *Philosophical transactions of the Royal Society of London Series B, Biological sciences* 366, 2806-2814.

Hill, C.A., Kafatos, F.C., Stansfield, S.K., and Collins, F.H. (2005). Arthropod-borne diseases: vector control in the genomics era. *Nat Rev Microbiol* 3, 262-268.

Hillyer, J.F. (2009). Transcription in mosquito hemocytes in response to pathogen exposure. *Journal of biology* 8, 51.

Hillyer, J.F. (2010). Mosquito Immunity. In *Invertebrate Immunity*, K. Soderhall, ed. (Landes Bioscience and Springer Science+Business Media, LLC).

Hillyer, J.F., Barreau, C., and Vernick, K.D. (2007). Efficiency of salivary gland invasion by malaria sporozoites is controlled by rapid sporozoite destruction in the mosquito haemocoel. *Int J Parasitol* 37, 673-681.

Hillyer, J.F., and Estevez-Lao, T.Y. (2010). Nitric oxide is an essential component of the hemocyte-mediated mosquito immune response against bacteria. *Dev Comp Immunol* 34, 141-149.

Hoffmann, A.A., Montgomery, B.L., Popovici, J., Iturbe-Ormaetxe, I., Johnson, P.H., Muzzi, F., Greenfield, M., Durkan, M., Leong, Y.S., Dong, Y., *et al.* (2011). Successful establishment of *Wolbachia* in *Aedes* populations to suppress dengue transmission. *Nature* 476, 454-457.

Hoffmann, J.A. (2003). The immune response of *Drosophila*. *Nature* 426, 33-38.

Hogg, J.C., and Hurd, H. (1997). The effects of natural *Plasmodium falciparum* infection on the fecundity and mortality of *Anopheles gambiae* s. l. in north east Tanzania. *Parasitology* 114 (Pt 4), 325-331.

Holt, R.A., Subramanian, G.M., Halpern, A., Sutton, G.G., Charlab, R., Nusskern, D.R., Wincker, P., Clark, A.G., Ribeiro, J.M., Wides, R., *et al.* (2002). The genome sequence of the malaria mosquito *Anopheles gambiae*. *Science* 298, 129-149.

Horn, T., and Boutros, M. (2010). E-RNAi: a web application for the multi-species design of RNAi reagents - 2010 update. *Nucleic Acids Research* 38, W-332-229.

Hughes, G.L., Koga, R., Xue, P., Fukatsu, T., and Rasgon, J.L. (2011). *Wolbachia* infections are virulent and inhibit the human malaria parasite *Plasmodium falciparum* in *Anopheles gambiae*. *PLoS Pathog* 7, e1002043.

Hunt, R.H., Coetzee, M., and Fettene, M. (1998). The *Anopheles gambiae* complex: a new species from Ethiopia. *Transactions of the Royal Society of Tropical Medicine and Hygiene* 92, 231-235.

Hurd, H., Taylor, P.J., Adams, D., Underhill, A., and Eggleston, P. (2005). Evaluating the costs of mosquito resistance to malaria parasites. *Evolution; international journal of organic evolution* 59, 2560-2572.

Isaacs, A.T., Jasinskiene, N., Tretiakov, M., Thiery, I., Zettor, A., Bourgooin, C., and James, A.A. (2012). Transgenic *Anopheles stephensi* coexpressing single-chain antibodies resist *Plasmodium falciparum* development. *Proc Natl Acad Sci U S A*.

Isaacs, A.T., Li, F., Jasinskiene, N., Chen, X., Nirmala, X., Marinotti, O., Vinetz, J.M., and James, A.A. (2011). Engineered resistance to *Plasmodium falciparum* development in transgenic *Anopheles stephensi*. *PLoS Pathog* 7, e1002017.

Istomin, A.Y., and Godzik, A. (2009). Understanding diversity of human innate immunity receptors: analysis of surface features of leucine-rich repeat domains in NLRs and TLRs. *BMC Immunol* 10, 48.

Ito, J., Ghosh, A., Moreira, L.A., Wimmer, E.A., and Jacobs-Lorena, M. (2002). Transgenic anopheline mosquitoes impaired in transmission of a malaria parasite. *Nature* 417, 452-455.

Jaramillo-Gutierrez, G., Molina-Cruz, A., Kumar, S., and Barillas-Mury, C. (2010). The *Anopheles gambiae* oxidation resistance 1 (OXR1) gene regulates expression of enzymes that detoxify reactive oxygen species. *PLoS ONE* 5, e11168.

Jaramillo-Gutierrez, G., Rodrigues, J., Ndikuyeze, G., Povelones, M., Molina-Cruz, A., and Barillas-Mury, C. (2009). Mosquito immune responses and compatibility between *Plasmodium* parasites and anopheline mosquitoes. *BMC microbiology* 9, 154.

Jiravanichpaisal, P., Lee, B.L., and Soderhall, K. (2006). Cell-mediated immunity in arthropods: hematopoiesis, coagulation, melanization and opsonization. *Immunobiology* 211, 213-236.

Jomori, T., and Natori, S. (1992). Function of the lipopolysaccharide-binding protein of *Periplaneta americana* as an opsonin. *FEBS Lett* 296, 283-286.

Kambris, Z., Blagborough, A.M., Pinto, S.B., Blagrove, M.S., Godfray, H.C., Sinden, R.E., and Sinkins, S.P. (2010). *Wolbachia* stimulates immune gene expression and inhibits plasmodium development in *Anopheles gambiae*. *PLoS pathogens* 6, e1001143.

Kambris, Z., Cook, P.E., Phuc, H.K., and Sinkins, S.P. (2009). Immune activation by life-shortening *Wolbachia* and reduced filarial competence in mosquitoes. *Science* 326, 134-136.

Kim, W., Koo, H., Richman, A.M., Seeley, D., Vizioli, J., Klocko, A.D., and O'Brochta, D.A. (2004). Ectopic expression of a cecropin transgene in the human malaria vector mosquito *Anopheles gambiae* (Diptera: Culicidae): effects on susceptibility to *Plasmodium*. *Journal of medical entomology* 41, 447-455.

Kiszewski, A., Mellinger, A., Spielman, A., Malaney, P., Sachs, S.E., and Sachs, J. (2004). A global index representing the stability of malaria transmission. *The American journal of tropical medicine and hygiene* 70, 486-498.

Kiszewski, A.E. (2011). Blocking *Plasmodium falciparum* Malaria Transmission with Drugs: The Gametocytocidal and Sporontocidal Properties of Current and Prospective Antimalarials. *Pharmaceuticals* 4, 44-68.

Kobe, B., and Kajava, A.V. (2001). The leucine-rich repeat as a protein recognition motif. *Curr Opin Struct Biol* 11, 725-732.

Kokoza, V., Ahmed, A., Woon Shin, S., Okafor, N., Zou, Z., and Raikhel, A.S. (2010). Blocking of *Plasmodium* transmission by cooperative action of Cecropin A and Defensin A in transgenic *Aedes aegypti* mosquitoes. *Proc Natl Acad Sci U S A* 107, 8111-8116.

Kokoza, V.A., Martin, D., Mienaltowski, M.J., Ahmed, A., Morton, C.M., and Raikhel, A.S. (2001). Transcriptional regulation of the mosquito vitellogenin gene via a blood meal-triggered cascade. *Gene* 274, 47-65.

Koutsos, A.C., Blass, C., Meister, S., Schmidt, S., MacCallum, R.M., Soares, M.B., Collins, F.H., Benes, V., Zdobnov, E., Kafatos, F.C., *et al.* (2007). Life cycle transcriptome of the malaria mosquito *Anopheles gambiae* and comparison with the fruitfly *Drosophila melanogaster*. *Proc Natl Acad Sci U S A* 104, 11304-11309.

Kuehn, A., and Pradel, G. (2010). The coming-out of malaria gametocytes. *Journal of biomedicine & biotechnology* 2010, 976827.

Kumar, S., Christophides, G.K., Cantera, R., Charles, B., Han, Y.S., Meister, S., Dimopoulos, G., Kafatos, F.C., and Barillas-Mury, C. (2003). The role of reactive oxygen species on *Plasmodium melanotic* encapsulation in *Anopheles gambiae*. *Proc Natl Acad Sci U S A* 100, 14139-14144.

Kumar, S., Gupta, L., Han, Y.S., and Barillas-Mury, C. (2004). Inducible peroxidases mediate nitration of anopheles midgut cells undergoing apoptosis in response to *Plasmodium* invasion. *J Biol Chem* 279, 53475-53482.

Kumar, S., Molina-Cruz, A., Gupta, L., Rodrigues, J., and Barillas-Mury, C. (2010). A peroxidase/dual oxidase system modulates midgut epithelial immunity in *Anopheles gambiae*. *Science* 327, 1644-1648.

Kyle, J.L., and Harris, E. (2008). Global spread and persistence of dengue. *Annual review of microbiology* 62, 71-92.

Labbe, G.M., Scaife, S., Morgan, S.A., Curtis, Z.H., and Alphey, L. (2012). Female-Specific Flightless (fsRIDL) Phenotype for Control of *Aedes albopictus*. *PLoS neglected tropical diseases* 6, e1724.

Lawniczak, M.K., Emrich, S.J., Holloway, A.K., Regier, A.P., Olson, M., White, B., Redmond, S., Fulton, L., Appelbaum, E., Godfrey, J., *et al.* (2010). Widespread divergence between incipient *Anopheles gambiae* species revealed by whole genome sequences. *Science* 330, 512-514.

Lawson, D., Arensburger, P., Atkinson, P., Besansky, N.J., Bruggner, R.V., Butler, R., Campbell, K.S., Christophides, G.K., Christley, S., Dialynas, E., *et al.* (2009). VectorBase: a data resource for invertebrate vector genomics. *Nucleic Acids Res* *37*, D583-587.

Lemaitre, B., and Hoffmann, J. (2007). The host defense of *Drosophila melanogaster*. *Annual review of immunology* *25*, 697-743.

Lengeler, C. (2004). Insecticide-treated bed nets and curtains for preventing malaria (Review) (Cochrane Database of Systematic Reviews).

Levashina, E.A., Moita, L.F., Blandin, S., Vriend, G., Lagueux, M., and Kafatos, F.C. (2001). Conserved role of a complement-like protein in phagocytosis revealed by dsRNA knockout in cultured cells of the mosquito, *Anopheles gambiae*. *Cell* *104*, 709-718.

Lim, J., Gowda, D.C., Krishnegowda, G., and Luckhart, S. (2005). Induction of nitric oxide synthase in *Anopheles stephensi* by *Plasmodium falciparum*: mechanism of signaling and the role of parasite glycosylphosphatidylinositols. *Infect Immun* *73*, 2778-2789.

Luckhart, S., Vodovotz, Y., Cui, L., and Rosenberg, R. (1998). The mosquito *Anopheles stephensi* limits malaria parasite development with inducible synthesis of nitric oxide. *Proc Natl Acad Sci U S A* *95*, 5700-5705.

Maccallum, R.M., Redmond, S.N., and Christophides, G.K. (2011). An expression map for *Anopheles gambiae*. *BMC Genomics* *12*, 620.

Manguin, S., Bangs, M.J., Pothikasikorn, J., and Chareonviriyaphap, T. (2010). Review on global co-transmission of human *Plasmodium* species and *Wuchereria bancrofti* by *Anopheles* mosquitoes. *Infection, genetics and evolution : journal of molecular epidemiology and evolutionary genetics in infectious diseases* *10*, 159-177.

Marinotti, O., Nguyen, Q.K., Calvo, E., James, A.A., and Ribeiro, J.M. (2005). Microarray analysis of genes showing variable expression following a blood meal in *Anopheles gambiae*. *Insect Mol Biol* *14*, 365-373.

Marois, E. (2011). The multifaceted mosquito anti-*Plasmodium* response. *Curr Opin Microbiol* *14*, 429-435.

Marrelli, M.T., Moreira, C.K., Kelly, D., Alphey, L., and Jacobs-Lorena, M. (2006). Mosquito transgenesis: what is the fitness cost? *Trends Parasitol* *22*, 197-202.

Martin, D., Wang, S.F., and Raikhel, A.S. (2001). The vitellogenin gene of the mosquito *Aedes aegypti* is a direct target of ecdysteroid receptor. *Molecular and cellular endocrinology* *173*, 75-86.

Mathur, G., Sanchez-Vargas, I., Alvarez, D., Olson, K.E., Marinotti, O., and James, A.A. (2010). Transgene-mediated suppression of dengue viruses in the salivary glands of the yellow fever mosquito, *Aedes aegypti*. *Insect Mol Biol* 19, 753-763.

Matsushima, N., Tanaka, T., Enkhbayar, P., Mikami, T., Taga, M., Yamada, K., and Kuroki, Y. (2007). Comparative sequence analysis of leucine-rich repeats (LRRs) within vertebrate toll-like receptors. *BMC Genomics* 8, 124.

Mazier, D., Renia, L., and Snounou, G. (2009). A pre-emptive strike against malaria's stealthy hepatic forms. *Nature reviews Drug discovery* 8, 854-864.

McGavin, G.C. (2001). *Essential Entomology. An Order-by Order Introduction* (Oxford University Press).

McMeniman, C.J., Lane, R.V., Cass, B.N., Fong, A.W., Sidhu, M., Wang, Y.F., and O'Neill, S.L. (2009). Stable introduction of a life-shortening *Wolbachia* infection into the mosquito *Aedes aegypti*. *Science* 323, 141-144.

Meister, S., Agianian, B., Turlure, F., Religio, A., Morlais, I., Kafatos, F.C., and Christophides, G.K. (2009). *Anopheles gambiae* PGRPLC-mediated defense against bacteria modulates infections with malaria parasites. *PLoS Pathog* 5, e1000542.

Meister, S., Kanzok, S.M., Zheng, X.L., Luna, C., Li, T.R., Hoa, N.T., Clayton, J.R., White, K.P., Kafatos, F.C., Christophides, G.K., *et al.* (2005). Immune signaling pathways regulating bacterial and malaria parasite infection of the mosquito *Anopheles gambiae*. *Proc Natl Acad Sci U S A* 102, 11420-11425.

Meister, S., Koutsos, A.C., and Christophides, G.K. (2004). The *Plasmodium* parasite--a 'new' challenge for insect innate immunity. *Int J Parasitol* 34, 1473-1482.

Mendes, A.M., Awono-Ambene, P.H., Nsango, S.E., Cohuet, A., Fontenille, D., Kafatos, F.C., Christophides, G.K., Morlais, I., and Vlachou, D. (2011). Infection intensity-dependent responses of *Anopheles gambiae* to the African malaria parasite *Plasmodium falciparum*. *Infect Immun* 79, 4708-4715.

Mendes, A.M., Schlegelmilch, T., Cohuet, A., Awono-Ambene, P., De Iorio, M., Fontenille, D., Morlais, I., Christophides, G.K., Kafatos, F.C., and Vlachou, D. (2008). Conserved mosquito/parasite interactions affect development of *Plasmodium falciparum* in Africa. *PLoS Pathog* 4, e1000069.

Meredith, J.M., Basu, S., Nimmo, D.D., Larget-Thierry, I., Warr, E.L., Underhill, A., McArthur, C.C., Carter, V., Hurd, H., Bourgoign, C., *et al.* (2011). Site-specific integration and expression of an anti-malarial gene in transgenic *Anopheles gambiae* significantly reduces *Plasmodium* infections. *PLoS ONE* 6, e14587.

Michel, K., Budd, A., Pinto, S., Gibson, T.J., and Kafatos, F.C. (2005). *Anopheles gambiae* SRPN2 facilitates midgut invasion by the malaria parasite *Plasmodium berghei*. *EMBO Rep* 6, 891-897.

Michel, K., and Kafatos, F.C. (2005). Mosquito immunity against *Plasmodium*. *Insect Biochem Mol Biol* 35, 677-689.

Mitri, C., Jacques, J.C., Thiery, I., Riehle, M.M., Xu, J., Bischoff, E., Morlais, I., Nsango, S.E., Vernick, K.D., and Bourgooin, C. (2009). Fine pathogen discrimination within the APL1 gene family protects *Anopheles gambiae* against human and rodent malaria species. *PLoS Pathog* 5, e1000576.

Moita, L.F., Wang-Sattler, R., Michel, K., Zimmermann, T., Blandin, S., Levashina, E.A., and Kafatos, F.C. (2005). In vivo identification of novel regulators and conserved pathways of phagocytosis in *A. gambiae*. *Immunity* 23, 65-73.

Molina-Cruz, A., DeJong, R.J., Charles, B., Gupta, L., Kumar, S., Jaramillo-Gutierrez, G., and Barillas-Mury, C. (2008). Reactive oxygen species modulate *Anopheles gambiae* immunity against bacteria and *Plasmodium*. *J Biol Chem* 283, 3217-3223.

Molina-Cruz, A., Dejong, R.J., Ortega, C., Haile, A., Abban, E., Rodrigues, J., Jaramillo-Gutierrez, G., and Barillas-Mury, C. (2012). Some strains of *Plasmodium falciparum*, a human malaria parasite, evade the complement-like system of *Anopheles gambiae* mosquitoes. *Proc Natl Acad Sci U S A* 109, E1957-1962.

Moreira, L.A., Iturbe-Ormaetxe, I., Jeffery, J.A., Lu, G., Pyke, A.T., Hedges, L.M., Rocha, B.C., Hall-Mendelin, S., Day, A., Riegler, M., *et al.* (2009). A *Wolbachia* symbiont in *Aedes aegypti* limits infection with dengue, Chikungunya, and *Plasmodium*. *Cell* 139, 1268-1278.

Muller, H.M., Dimopoulos, G., Blass, C., and Kafatos, F.C. (1999). A hemocyte-like cell line established from the malaria vector *Anopheles gambiae* expresses six prophenoloxidase genes. *J Biol Chem* 274, 11727-11735.

Muturi, E.J., Jacob, B.G., Kim, C.H., Mbogo, C.M., and Novak, R.J. (2008). Are coinfections of malaria and filariasis of any epidemiological significance? *Parasitology research* 102, 175-181.

Neafsey, D.E., Lawniczak, M.K., Park, D.J., Redmond, S.N., Coulibaly, M.B., Traore, S.F., Sagnon, N., Costantini, C., Johnson, C., Wiegand, R.C., *et al.* (2010). SNP genotyping defines complex gene-flow boundaries among African malaria vector mosquitoes. *Science* 330, 514-517.

Newton, K., and Dixit, V.M. (2012). Signaling in innate immunity and inflammation. *Cold Spring Harbor perspectives in biology* 4.

Obbard, D.J., Callister, D.M., Jiggins, F.M., Soares, D.C., Yan, G., and Little, T.J. (2008). The evolution of TEP1, an exceptionally polymorphic immunity gene in *Anopheles gambiae*. *BMC Evol Biol* 8, 274.

Okumu, F.O., and Moore, S.J. (2011). Combining indoor residual spraying and insecticide-treated nets for malaria control in Africa: a review of possible outcomes and an outline of suggestions for the future. *Malar J* 10, 208.

Oliveira Gde, A., Lieberman, J., and Barillas-Mury, C. (2012). Epithelial nitration by a peroxidase/NOX5 system mediates mosquito antiplasmodial immunity. *Science* 335, 856-859.

Oliveira, J.H., Goncalves, R.L., Lara, F.A., Dias, F.A., Gandara, A.C., Menna-Barreto, R.F., Edwards, M.C., Laurindo, F.R., Silva-Neto, M.A., Sorgine, M.H., *et al.* (2011). Blood meal-derived heme decreases ROS levels in the midgut of *Aedes aegypti* and allows proliferation of intestinal microbiota. *PLoS Pathog* 7, e1001320.

Ono, T., Tadakuma, T., and Rodriguez, A. (2007). *Plasmodium yoelii yoelii* 17XNL constitutively expressing GFP throughout the life cycle. *Exp Parasitol* 115, 310-313.

Osta, M.A., Christophides, G.K., and Kafatos, F.C. (2004a). Effects of mosquito genes on *Plasmodium* development. *Science* 303, 2030-2032.

Osta, M.A., Christophides, G.K., Vlachou, D., and Kafatos, F.C. (2004b). Innate immunity in the malaria vector *Anopheles gambiae*: comparative and functional genomics. *J Exp Biol* 207, 2551-2563.

Padmanabhan, M., Cournoyer, P., and Dinesh-Kumar, S.P. (2009). The leucine-rich repeat domain in plant innate immunity: a wealth of possibilities. *Cell Microbiol* 11, 191-198.

Pancer, Z., and Cooper, M.D. (2006). The evolution of adaptive immunity. *Annual review of immunology* 24, 497-518.

Paskewitz, S.M., Andreev, O., and Shi, L. (2006). Gene silencing of serine proteases affects melanization of Sephadex beads in *Anopheles gambiae*. *Insect Biochem Mol Biol* 36, 701-711.

Pham, L.N., Dionne, M.S., Shirasu-Hiza, M., and Schneider, D.S. (2007). A specific primed immune response in *Drosophila* is dependent on phagocytes. *PLoS Pathog* 3, e26.

Phuc, H.K., Andreasen, M.H., Burton, R.S., Vass, C., Epton, M.J., Pape, G., Fu, G., Condon, K.C., Scaife, S., Donnelly, C.A., *et al.* (2007). Late-acting dominant lethal genetic systems and mosquito control. *BMC biology* 5, 11.

Pierro, D.J., Myles, K.M., Foy, B.D., Beaty, B.J., and Olson, K.E. (2003). Development of an orally infectious Sindbis virus transducing system that efficiently disseminates and expresses green fluorescent protein in *Aedes aegypti*. *Insect Mol Biol* 12, 107-116.

Pinto, S.B., Lombardo, F., Koutsos, A.C., Waterhouse, R.M., McKay, K., An, C., Ramakrishnan, C., Kafatos, F.C., and Michel, K. (2009). Discovery of *Plasmodium* modulators by genome-wide analysis of circulating hemocytes in *Anopheles gambiae*. *Proc Natl Acad Sci U S A* 106, 21270-21275.

Povelones, M., Upton, L.M., Sala, K.A., and Christophides, G.K. (2011). Structure-Function Analysis of the *Anopheles gambiae* LRIM1/APL1C Complex and its Interaction with Complement C3-Like Protein TEP1. *PLoS Pathog* 7, e1002023.

Povelones, M., Waterhouse, R.M., Kafatos, F.C., and Christophides, G.K. (2009). Leucine-rich repeat protein complex activates mosquito complement in defense against *Plasmodium* parasites. *Science* 324, 258-261.

Powers, A.M., Brault, A.C., Tesh, R.B., and Weaver, S.C. (2000). Re-emergence of Chikungunya and O'nyong-nyong viruses: evidence for distinct geographical lineages and distant evolutionary relationships. *The Journal of general virology* 81, 471-479.

Price, R.N., Tjitra, E., Guerra, C.A., Yeung, S., White, N.J., and Anstey, N.M. (2007). Vivax malaria: neglected and not benign. *The American journal of tropical medicine and hygiene* 77, 79-87.

Prudencio, M., Rodriguez, A., and Mota, M.M. (2006). The silent path to thousands of merozoites: the *Plasmodium* liver stage. *Nat Rev Microbiol* 4, 849-856.

Raghavendra, K., Barik, T.K., Reddy, B.P., Sharma, P., and Dash, A.P. (2011). Malaria vector control: from past to future. *Parasitology research* 108, 757-779.

Raikhel, A.S., Kokoza, V.A., Zhu, J., Martin, D., Wang, S.F., Li, C., Sun, G., Ahmed, A., Dittmer, N., and Attardo, G. (2002). Molecular biology of mosquito vitellogenesis: from basic studies to genetic engineering of antipathogen immunity. *Insect Biochem Mol Biol* 32, 1275-1286.

Ramirez, J.L., Souza-Neto, J., Torres Cosme, R., Rovira, J., Ortiz, A., Pascale, J.M., and Dimopoulos, G. (2012). Reciprocal tripartite interactions between the *Aedes aegypti* midgut microbiota, innate immune system and dengue virus influences vector competence. *PLoS neglected tropical diseases* 6, e1561.

Ranson, H., N'Guessan, R., Lines, J., Moiroux, N., Nkuni, Z., and Corbel, V. (2011). Pyrethroid resistance in African anopheline mosquitoes: what are the implications for malaria control? *Trends Parasitol* 27, 91-98.

Reiter, P. (2001). Climate change and mosquito-borne disease. *Environmental health perspectives* 109 Suppl 1, 141-161.

Riehle, M.M., Guelbeogo, W.M., Gneme, A., Eiglmeier, K., Holm, I., Bischoff, E., Garnier, T., Snyder, G.M., Li, X., Markianos, K., *et al.* (2011). A cryptic subgroup of *Anopheles gambiae* is highly susceptible to human malaria parasites. *Science* 331, 596-598.

Riehle, M.M., Markianos, K., Niare, O., Xu, J., Li, J., Toure, A.M., Podiougou, B., Oduol, F., Diawara, S., Diallo, M., *et al.* (2006). Natural malaria infection in *Anopheles gambiae* is regulated by a single genomic control region. *Science* 312, 577-579.

Riehle, M.M., Xu, J., Lazzaro, B.P., Rottschaefer, S.M., Coulibaly, B., Sacko, M., Niare, O., Morlais, I., Traore, S.F., and Vernick, K.D. (2008). *Anopheles gambiae* APL1 is a family of variable LRR proteins required for Rel1-mediated protection from the malaria parasite, *Plasmodium berghei*. *PLoS One* 3, e3672.

Rodrigues, J., Brayner, F.A., Alves, L.C., Dixit, R., and Barillas-Mury, C. (2010). Hemocyte differentiation mediates innate immune memory in *Anopheles gambiae* mosquitoes. *Science* 329, 1353-1355.

Rono, M.K., Whitten, M.M., Oulad-Abdelghani, M., Levashina, E.A., and Marois, E. (2010). The major yolk protein vitellogenin interferes with the anti-plasmodium response in the malaria mosquito *Anopheles gambiae*. *PLoS Biol* 8, e1000434.

Rozen, S., and Skaletsky, H. (2000). Primer3 on the WWW for general users and for biologist programmers. In *Bioinformatics Methods and Protocols: Methods in Molecular Biology*, S. Krawetz, and S. Misener, eds. (Totowa, NJ.: Humana Press), pp. 365-386.

Schlitzer, M. (2007). Malaria chemotherapeutics part I: History of antimalarial drug development, currently used therapeutics, and drugs in clinical development. *ChemMedChem* 2, 944-986.

Schmid-Hempel, P. (2005). Evolutionary ecology of insect immune defenses. *Annual review of entomology* 50, 529-551.

Schnitger, A.K., Kafatos, F.C., and Osta, M.A. (2007). The melanization reaction is not required for survival of *Anopheles gambiae* mosquitoes after bacterial infections. *J Biol Chem* 282, 21884-21888.

Schnitger, A.K., Yassine, H., Kafatos, F.C., and Osta, M.A. (2009). Two C-type lectins cooperate to defend *Anopheles gambiae* against Gram-negative bacteria. *J Biol Chem* 284, 17616-17624.

Scholte, E.J., Ng'habi, K., Kihonda, J., Takken, W., Paaijmans, K., Abdulla, S., Killeen, G.F., and Knols, B.G. (2005). An entomopathogenic fungus for control of adult African malaria mosquitoes. *Science* 308, 1641-1642.

Schwartz, A., and Koella, J.C. (2002). Melanization of *Plasmodium falciparum* and C-25 sephadex beads by field-caught *Anopheles gambiae* (Diptera: Culicidae) from southern Tanzania. *Journal of medical entomology* 39, 84-88.

Shiao, S.H., Whitten, M.M., Zachary, D., Hoffmann, J.A., and Levashina, E.A. (2006). Fz2 and cdc42 mediate melanization and actin polymerization but are dispensable for *Plasmodium* killing in the mosquito midgut. *PLoS Pathog* 2, e133.

Sim, C., Hong, Y.S., Vanlandingham, D.L., Harker, B.W., Christophides, G.K., Kafatos, F.C., Higgs, S., and Collins, F.H. (2005). Modulation of *Anopheles gambiae* gene expression in response to o'nyong-nyong virus infection. *Insect Mol Biol* 14, 475-481.

Sinden, R.E. (1999). *Plasmodium* differentiation in the mosquito. *Parassitologia* 41, 139-148.

Sinden, R.E. (2002). Molecular interactions between *Plasmodium* and its insect vectors. *Cell Microbiol* 4, 713-724.

Sinden, R.E., Alavi, Y., and Raine, J.D. (2004). Mosquito--malaria interactions: a reappraisal of the concepts of susceptibility and refractoriness. *Insect Biochem Mol Biol* 34, 625-629.

Sinden, R.E., Butcher, G.A., and Beetsma, A.L. (2002). Maintenance of the *Plasmodium berghei* life cycle. *Methods Mol Med* 72, 25-40.

Singh, B., Kim Sung, L., Matusop, A., Radhakrishnan, A., Shamsul, S.S., Cox-Singh, J., Thomas, A., and Conway, D.J. (2004). A large focus of naturally acquired *Plasmodium knowlesi* infections in human beings. *Lancet* 363, 1017-1024.

Sinka, M.E., Bangs, M.J., Manguin, S., Rubio-Palis, Y., Chareonviriyaphap, T., Coetzee, M., Mbogo, C.M., Hemingway, J., Patil, A.P., Temperley, W.H., *et al.* (2012). A global map of dominant malaria vectors. *Parasites & vectors* 5, 69.

Sinkins, S.P., and Gould, F. (2006). Gene drive systems for insect disease vectors. *Nat Rev Genet* 7, 427-435.

Sirard, J.C., Vignal, C., Dessein, R., and Chamaillard, M. (2007). Nod-like receptors: cytosolic watchdogs for immunity against pathogens. *PLoS Pathog* 3, e152.

Somboon, P., Prapanthadara, L., and Suwonkerd, W. (1999). Selection of *Anopheles dirus* for refractoriness and susceptibility to *Plasmodium yoelii nigeriensis*. *Medical and veterinary entomology* *13*, 355-361.

Steinert, S., and Levashina, E.A. (2011). Intracellular immune responses of dipteran insects. *Immunol Rev* *240*, 129-140.

Sun, J., Hiraoka, T., Dittmer, N.T., Cho, K.H., and Raikhel, A.S. (2000). Lipophorin as a yolk protein precursor in the mosquito, *Aedes aegypti*. *Insect Biochem Mol Biol* *30*, 1161-1171.

Surachetpong, W., Pakpour, N., Cheung, K.W., and Luckhart, S. (2011). Reactive oxygen species-dependent cell signaling regulates the mosquito immune response to *Plasmodium falciparum*. *Antioxidants & redox signaling* *14*, 943-955.

Suwanchaichinda, C., and Kanost, M.R. (2009). The serpin gene family in *Anopheles gambiae*. *Gene* *442*, 47-54.

Tagawa, K., Yoshihara, T., Shibata, T., Kitazaki, K., Endo, Y., Fujita, T., Koshiba, T., and Kawabata, S. (2012). Microbe-specific C3b deposition in the horseshoe crab complement system in a C2/factor B-dependent or -independent manner. *PLoS ONE* *7*, e36783.

Tahar, R., Boudin, C., Thiery, I., and Bourgooin, C. (2002). Immune response of *Anopheles gambiae* to the early sporogonic stages of the human malaria parasite *Plasmodium falciparum*. *EMBO J* *21*, 6673-6680.

Tang, H., Kambris, Z., Lemaitre, B., and Hashimoto, C. (2006). Two proteases defining a melanization cascade in the immune system of *Drosophila*. *J Biol Chem* *281*, 28097-28104.

Tanne, J.H. (2011). Trial shows vaccine halves malaria episodes in children in Africa. *BMJ* *343*, d6832.

Tchuinkam, T., Mulder, B., Dechering, K., Stoffels, H., Verhave, J.P., Cot, M., Carnevale, P., Meuwissen, J.H., and Robert, V. (1993). Experimental infections of *Anopheles gambiae* with *Plasmodium falciparum* of naturally infected gametocyte carriers in Cameroon: factors influencing the infectivity to mosquitoes. *Trop Med Parasitol* *44*, 271-276.

Thomas, D.D., Donnelly, C.A., Wood, R.J., and Alphey, L.S. (2000). Insect population control using a dominant, repressible, lethal genetic system. *Science* *287*, 2474-2476.

Thomas, M.B., and Read, A.F. (2007). Can fungal biopesticides control malaria? *Nat Rev Microbiol* *5*, 377-383.

Tolle, M.A. (2009). Mosquito-borne diseases. Current problems in pediatric and adolescent health care 39, 97-140.

Vaughan, J.A., and Azad, A.F. (1988). Passage of Host Immunoglobulin G From Blood Meal into Hemolymph of Selected Mosquito Species (Diptera: Culicidae) Journal of medical entomology 25, 472-474.

Vernick, K.D., Fujioka, H., Seeley, D.C., Tandler, B., Aikawa, M., and Miller, L.H. (1995). Plasmodium gallinaceum: a refractory mechanism of ookinete killing in the mosquito, Anopheles gambiae. Exp Parasitol 80, 583-595.

Vijay, S., Rawat, M., Adak, T., Dixit, R., Nanda, N., Srivastava, H., Sharma, J.K., Prasad, G.B., and Sharma, A. (2011). Parasite killing in malaria non-vector mosquito Anopheles culicifacies species B: implication of nitric oxide synthase upregulation. PLoS ONE 6, e18400.

Vlachou, D., and Kafatos, F.C. (2005). The complex interplay between mosquito positive and negative regulators of Plasmodium development. Curr Opin Microbiol 8, 415-421.

Vlachou, D., Schlegelmilch, T., Christophides, G.K., and Kafatos, F.C. (2005). Functional genomic analysis of midgut epithelial responses in Anopheles during Plasmodium invasion. Curr Biol 15, 1185-1195.

Vlachou, D., Schlegelmilch, T., Runn, E., Mendes, A., and Kafatos, F.C. (2006). The developmental migration of Plasmodium in mosquitoes. Curr Opin Genet Dev 16, 384-391.

Vlachou, D., Zimmermann, T., Cantera, R., Janse, C.J., Waters, A.P., and Kafatos, F.C. (2004). Real-time, in vivo analysis of malaria ookinete locomotion and mosquito midgut invasion. Cell Microbiol 6, 671-685.

Vogel, G. (2010). The 'do unto others' malaria vaccine. Science 328, 847-848.

Volohonsky, G., Steinert, S., and Levashina, E.A. (2010). Focusing on complement in the antiparasitic defense of mosquitoes. Trends Parasitol 26, 1-3.

Volz, J., Muller, H.M., Zdanowicz, A., Kafatos, F.C., and Osta, M.A. (2006). A genetic module regulates the melanization response of Anopheles to Plasmodium. Cell Microbiol 8, 1392-1405.

Volz, J., Osta, M.A., Kafatos, F.C., and Muller, H.M. (2005). The Roles of Two Clip Domain Serine Proteases in Innate Immune Responses of the Malaria Vector Anopheles gambiae. J Biol Chem 280, 40161-40168.

Waldock, J., Olson, K.E., and Christophides, G.K. (2012). *Anopheles gambiae* Antiviral Immune Response to Systemic O'nyong-nyong Infection. *PLoS neglected tropical diseases* *6*, e1565.

Walker, T., Johnson, P.H., Moreira, L.A., Iturbe-Ormaetxe, I., Frentiu, F.D., McMeniman, C.J., Leong, Y.S., Dong, Y., Axford, J., Kriesner, P., *et al.* (2011). The wMel Wolbachia strain blocks dengue and invades caged *Aedes aegypti* populations. *Nature* *476*, 450-453.

Wang, Y., Gilbreath, T.M., 3rd, Kukutla, P., Yan, G., and Xu, J. (2011). Dynamic gut microbiome across life history of the malaria mosquito *Anopheles gambiae* in Kenya. *PLoS ONE* *6*, e24767.

Warr, E., Das, S., Dong, Y., and Dimopoulos, G. (2008). The Gram-negative bacteria-binding protein gene family: its role in the innate immune system of *Anopheles gambiae* and in anti-*Plasmodium* defence. *Insect Mol Biol* *17*, 39-51.

Warr, E., Lambrechts, L., Koella, J.C., Bourgouin, C., and Dimopoulos, G. (2006). *Anopheles gambiae* immune responses to Sephadex beads: involvement of anti-*Plasmodium* factors in regulating melanization. *Insect Biochem Mol Biol* *36*, 769-778.

Waterhouse, R.M., Kriventseva, E.V., Meister, S., Xi, Z., Alvarez, K.S., Bartholomay, L.C., Barillas-Mury, C., Bian, G., Blandin, S., Christensen, B.M., *et al.* (2007). Evolutionary dynamics of immune-related genes and pathways in disease-vector mosquitoes. *Science* *316*, 1738-1743.

Waterhouse, R.M., Povelones, M., and Christophides, G.K. (2010). Sequence-structure-function relations of the mosquito leucine-rich repeat immune proteins. *BMC Genomics* *11*, 531.

Weaver, S.C., and Reisen, W.K. (2010). Present and future arboviral threats. *Antiviral research* *85*, 328-345.

Wen-Yue, X., Jian, Z., Tao-Li, Z., Fu-Sheng, H., Jian-Hua, D., Ying, W., Zhong-Wen, Q., and Li-Sha, X. (2007). *Plasmodium yoelii*: contribution of oocysts melanization to natural refractoriness in *Anopheles dirus*. *Exp Parasitol* *116*, 433-439.

White, B.J., Lawniczak, M.K., Cheng, C., Coulibaly, M.B., Wilson, M.D., Sagnon, N., Costantini, C., Simard, F., Christophides, G.K., and Besansky, N.J. (2011). Adaptive divergence between incipient species of *Anopheles gambiae* increases resistance to *Plasmodium*. *Proc Natl Acad Sci U S A* *108*, 244-249.

Whitten, M.M., Shiao, S.H., and Levashina, E.A. (2006). Mosquito midguts and malaria: cell biology, compartmentalization and immunology. *Parasite Immunol* *28*, 121-130.

WHO (2010). Global report on antimalarial drug efficacy and drug resistance: 2000-2010 (Switzerland).

WHO (2011a). World Health Statistics, 2011 (Geneva).

WHO (2011b). World Malaria Report 2011 (Geneva).

WHO (2012a). Dengue and severe dengue Fact Sheet No. 117 (WHO Media Centre).

WHO (2012b). Lymphatic filariasis Fact Sheet No. 102 (WHO Media Centre).

WHO (2012c). Malaria Fact Sheet No. 94 (WHO Media Centre).

WHO (2012d). Yellow fever Fact Sheet No. 100 (WHO Media Centre).

Wiegmann, B.M., Trautwein, M.D., Winkler, I.S., Barr, N.B., Kim, J.W., Lambkin, C., Bertone, M.A., Cassel, B.K., Bayless, K.M., Heimberg, A.M., *et al.* (2011). Episodic radiations in the fly tree of life. *Proc Natl Acad Sci U S A* 108, 5690-5695.

Wilmanski, J.M., Petnicki-Ocwieja, T., and Kobayashi, K.S. (2008). NLR proteins: integral members of innate immunity and mediators of inflammatory diseases. *J Leukoc Biol* 83, 13-30.

Wirth, D.F. (2002). Biological revelations. *Nature* 419, 495-496.

Xi, Z., Ramirez, J.L., and Dimopoulos, G. (2008). The *Aedes aegypti* toll pathway controls dengue virus infection. *PLoS Pathog* 4, e1000098.

Yassine, H., and Osta, M.A. (2010). *Anopheles gambiae* innate immunity. *Cell Microbiol* 12, 1-9.

Zaim, M., Aitio, A., and Nakashima, N. (2000). Safety of pyrethroid-treated mosquito nets. *Medical and veterinary entomology* 14, 1-5.

Zheng, L., Cornel, A.J., Wang, R., Erfle, H., Voss, H., Ansorge, W., Kafatos, F.C., and Collins, F.H. (1997). Quantitative trait loci for refractoriness of *Anopheles gambiae* to *Plasmodium cynomolgi* B. *Science* 276, 425-428.

Zheng, L., Wang, S., Romans, P., Zhao, H., Luna, C., and Benedict, M.Q. (2003). Quantitative trait loci in *Anopheles gambiae* controlling the encapsulation response against *Plasmodium cynomolgi* Ceylon. *BMC genetics* 4, 16.

Zhu, Y., Thangamani, S., Ho, B., and Ding, J.L. (2005). The ancient origin of the complement system. *EMBO J* 24, 382-394.

Zieler, H., and Dvorak, J.A. (2000). Invasion in vitro of mosquito midgut cells by the malaria parasite proceeds by a conserved mechanism and results in death of the invaded midgut cells. *Proc Natl Acad Sci U S A* 97, 11516-11521.

Zou, Z., Shin, S.W., Alvarez, K.S., Kokoza, V., and Raikhel, A.S. (2010). Distinct melanization pathways in the mosquito *Aedes aegypti*. *Immunity* 32, 41-53.

Chapter 9: Appendix

9 Appendix

9.1 Supplementary figures

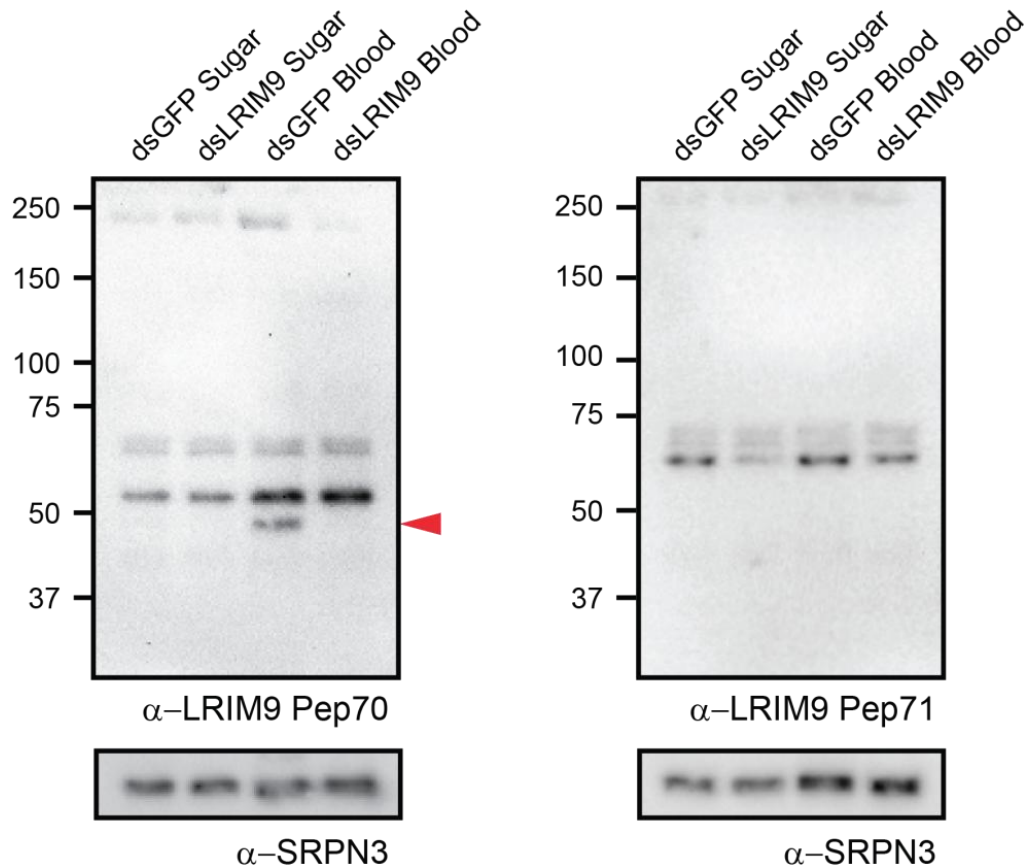


Figure 9.1 Evaluating LRIM9 peptide antibodies using blood fed hemolymph.

Rabbit polyclonal antibodies were generated against two LRIM9 peptides: peptide 70 (α -LRIM9 Pep70; located at the C-terminus) and peptide 71 (α -LRIM9 Pep71; located between the LRRs and coiled-coil). Mosquitoes were injected with *dsGFP* or *dsLRIM9* and, after 3 days, they were either sugar or blood fed. Hemolymph was collected 24 h later and analysed by non-reducing western blot, probing with α -LRIM9 Pep70 (left panel) or α -LRIM9 Pep71 (right panel) followed by SRPN3 as a loading control. The red arrow shows the true LRIM9 band in the *dsGFP* blood fed lane. Molecular weight markers are indicated (kDa).

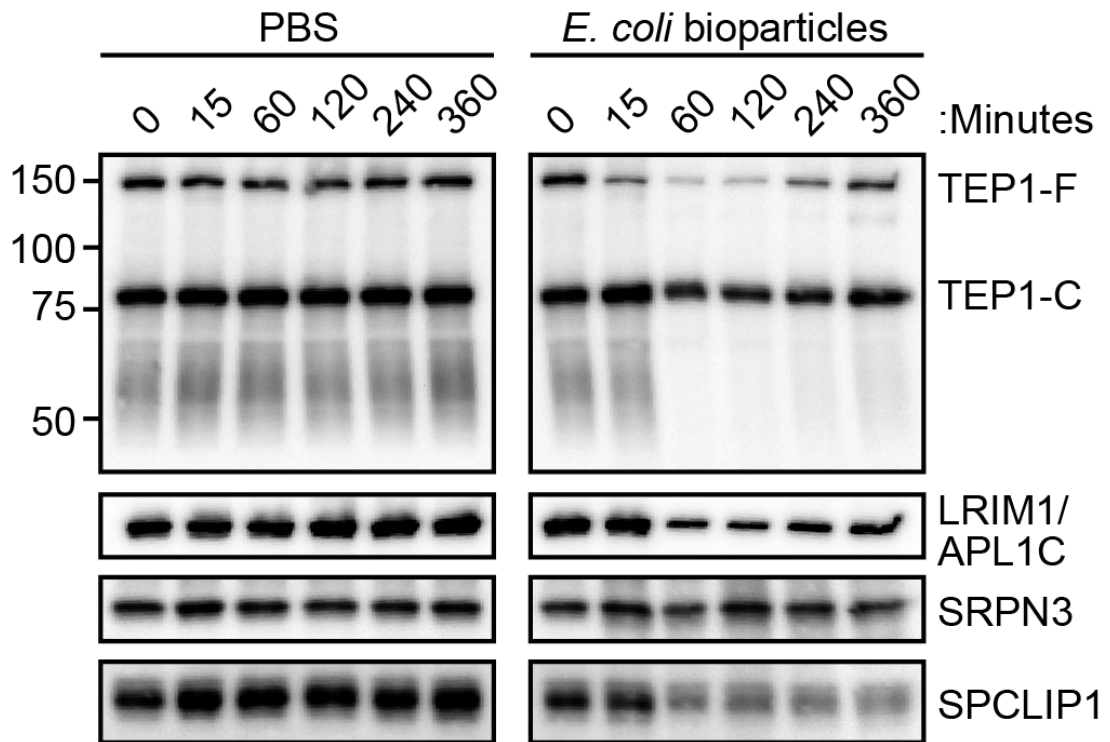


Figure 9.2 Temporal profiling of LRIM1/APL1C and TEP1 protein levels after *E. coli* bioparticle challenge in naïve mosquitoes.

Non-reducing western blot was performed on hemolymph collected 15, 60, 120, 240 and 360 minutes after challenge with PBS or *E. coli* bioparticles. Blots were probed with antibodies against TEP1, the LRIM1/APL1C complex and SPCLIP1. SRPN3 was used as a control to ensure equal loading. Molecular weight markers are indicated (kDa).

9.2 Tables of primers

Table 9.1 RNAi primer sequences.

Gene	Primer name	Sequence	Amplicon size (bp)
<i>GFP</i>	5' GFP1 T7 pove	taatacgactcactatagggACGTAAACGGCCACAAGTTC	535
	3' GFP1 T7 pove	taatacgactcactatagggTGTCTGCTGGTAGTGGTCG	
<i>LRIM1</i>	LRIM1 T7 forward	taatacgactcactatagggAATATCTATCTCGCAACAATAA	529
	LRIM1 T7 reverse	taatacgactcactatagggTGGCACGGTACACTCTTCC	
<i>APL1A</i>	APL1A_dsRNA_F	taatacgactcactatagggCTACCACCTGCCGAAAGATG	350
	APL1A_dsRNA_R	taatacgactcactatagggTCTGGTCTTGATAGTACAATGG	
<i>APL1B</i>	APL1B_dsRNA_F	taatacgactcactatagggACTCGCAAAGCTCAGCAAACAC	224
	APL1B_dsRNA_R	taatacgactcactatagggTGAGAACAAATAAGTTCAAAGTCC	
<i>APL1C</i>	APL1C_dsRNA_F	taatacgactcactatagggCCAAGAAGAACCACAATCC	241
	APL1C_dsRNA_R	taatacgactcactatagggTACAGTGATTTCAAGGTGTGC	
<i>LRIM3</i>	LRIM2 A T7 F	taatacgactcactatagggTGCGAAGTCAACGACACC	459
	LRIM2 A T7 R	taatacgactcactatagggGTTGATCTCCTTGATGCGGT	
<i>LRIM4</i>	LRIM4 f1 T7 F	taatacgactcactatagggATCTGGAGCTGCACGAAAAT	501
	LRIM4 f1 T7 R	taatacgactcactatagggCCCTCCTGAAGGCTTTTAC	
<i>LRIM5</i>	LRIM5 R28 RNAi T7 F	taatacgactcactatagggCATACGCACGTGTGAAAAGT	279
	LRIM5 R28 RNAi T7 R	taatacgactcactatagggTCATGCTAAACGAACGTGCT	
<i>LRIM6</i>	AGAP006327 LRIM6 RNAi T7 F	taatacgactcactatagggATATCCGCTTCCTAGTCGGG	248
	AGAP006327 LRIM6 RNAi T7 R	taatacgactcactatagggACAACGCCAGCTTGTCTT	
<i>LRIM7</i>	AGAP007457 RNAi T7 F	taatacgactcactatagggATCTGGCCGTTGTGATAAG	284
	AGAP007457 RNAi T7 R	taatacgactcactatagggCGCTGCAGGGTGAGTATCTT	
<i>LRIM8A</i>	AGAP007454 RNAi T7 F	taatacgactcactatagggCCGAAGTGTGCAGAGTGAAG	274
	AGAP007454 RNAi T7 R	taatacgactcactatagggTAGCGTTATCTACCGCGAT	
<i>LRIM8B</i>	AGAP007456 RNAi T7 F	taatacgactcactatagggATGGGCATTCGGAAGATGTA	269
	AGAP007456 RNAi T7 R	taatacgactcactatagggACGAGTCGAGTGCTACCTCC	
<i>LRIM9</i>	AGAP007453 RNAi T7 F	taatacgactcactatagggACTGGCAGAAAAGCTTCAA	323
	AGAP007453 RNAi T7 R	taatacgactcactatagggTGGCATTCTCGAACACAG	
<i>LRIM10</i>	AGAP007455 RNAi T7 F	taatacgactcactatagggCAAAGATCCGCGGACTAAAG	274
	AGAP007455 RNAi T7 R	taatacgactcactatagggCAAGCTTTTGTCCAACCTCC	
<i>LRIM11</i>	LRIM11 AGAP007034 T7 F	taatacgactcactatagggGTACCGCTGGTGTCTGCTC	204
	LRIM11 AGAP007034 T7 R	taatacgactcactatagggACGTCACTGCCGAGGTACAC	
<i>LRIM12</i>	AGAP005496 LRIM12 RNAi T7 F	taatacgactcactatagggGGCGTCCAAGACTTCAAAC	304
	AGAP005496 LRIM12 RNAi T7 R	taatacgactcactatagggAAGTTCCTCCACCTCGTCG	
<i>LRIM15</i>	AGAP007045 LRIM15 RNAi T7 F	taatacgactcactatagggTCGATCGGATGATCCTCTTC	302
	AGAP007045 LRIM15 RNAi T7 R	taatacgactcactatagggTGAGCAGCAGTTATCGGAGA	
<i>LRIM16A+B</i>	LRIM16A+B T7 F	taatacgactcactatagggGCCTTGCAAAGCTAGCCAAT	234
	LRIM16A+B T7 R	taatacgactcactatagggCCGATTACCGTCCAGAAAGA	
<i>LRIM17</i>	LRRD7 APL2 T7 F	taatacgactcactatagggTCGGTGAGCAACAGTTTGAC	397
	LRRD7 APL2 T7 R	taatacgactcactatagggCTTCACTCCCGCTAATGCTC	
<i>LRIM18</i>	LRIM18 AGAP010675 T7 F	taatacgactcactatagggGCCTGTTGGGTTTTGACAAG	218
	LRIM18 AGAP010675 T7 R	taatacgactcactatagggGCACTCGTCCCAAGTTCA	
<i>LRIM19</i>	LRIM19 AGAP011117 T7 F	taatacgactcactatagggCGAGATGGAGTGCAAAATCT	224
	LRIM19 AGAP011117 T7 R	taatacgactcactatagggGATCTCGAGCTTCTCGGTCTG	
<i>LRIM20</i>	AGAP002542 LRIM20 RNAi T7 F	taatacgactcactatagggGTTGGCCGACTGCAAAAT	246
	AGAP002542 LRIM20 RNAi T7 R	taatacgactcactatagggGTATCGAGCGTGTGGGAATG	
<i>LRIM26</i>	AGAP005744 LRIM26 RNAi T7 F	taatacgactcactatagggGGTGTCTGGATGTCTGGTA	240
	AGAP005744 LRIM26 RNAi T7 R	taatacgactcactatagggCCACCAGCAGTTTGCAGTTA	
<i>LRIM27</i>	LRIM27 T7 F	taatacgactcactatagggACCTGGCATTGGAGCTT	257
	LRIM27 T7 R	taatacgactcactatagggACAGGTCGAGCAGTTTACAGG	
<i>TEP1</i>	TEP1 T7 F	taatacgactcactatagggTTTGTGGCCCTTAAAGCGCTG	435
	TEP1 T7 R	taatacgactcactatagggACCACGTAACCGCTCGGTAAG	
<i>TEP3</i>	TEP3 T7 F	taatacgactcactatagggCGAGAAGGAACCCATTTAAGG	321
	TEP3 T7 R	taatacgactcactatagggGCTGCTGGAATGGCATAAGT	

<i>TEP4</i>	TEP4 T7 F Lav	taatacgactcactatagggTCTTCTGGGAGGATGTTGG	410
	TEP4 T7 R Lav	taatacgactcactatagggACGGTGGTCAATTGAAGAGG	
<i>CTL4</i>	CTL4 T7 F	taatacgactcactatagggTGGTTTATGATGCCGTGCCT	342
	CTL4 T7 R	taatacgactcactatagggAATAAATTGTCTCGGTTTCATCATC	

Primer sequences used to amplify RNAi fragments from cDNA or plasmid template. T7 tags are shown in lower-case. Amplicon size includes the T7 tags.

Table 9.2 qRT-PCR primer sequences.

Gene	Primer name	Sequence	Concentration (nM)
<i>S7</i>	AgS7 AGAP010592 qRT-PCR F	GTGCGCGAGTTGGAGAAGA	300
	AgS7 AGAP010592 qRT-PCR R	ATCGGTTTGGGCAGAATGC	900
<i>LRIM1</i>	AGAP6348 LRIM1 QPCR F	CATCCGCGATTGGGATATGT	900
	AGAP6348 LRIM1 QPCR R	CTTCTTGAGCCGTGCATTTTC	900
<i>APL1A</i>	APL1A_qPCRu_F	CCATTTGCATGAGTTGGGTA	900
	APL1A_qPCRu_R	TCCATCTGGTCCTTGAGCTT	300
<i>APL1B</i>	APL1B_qPCRI_F	TGCAGATTCTGTTGAGACAGC	300
	APL1B_qPCRI_R	AATTGCTTTATTTGTTGACGCTT	300
<i>APL1C</i>	APL1C_qPCRI_F	CAGGCTGAGTTGAGACAGGA	300
	APL1C_qPCRI_R	GCTTCACTTTTGGCGCT	300
<i>LRIM3</i>	AGAP7037 LRIM2A QPCR F (LRIM3)	GCAGATGGAGGAGATTGAGC	900
	AGAP7037 LRIM2A QPCR R (LRIM3)	AGGTTGATGCAGTCCCAGTC	900
<i>LRIM4</i>	AGAP7039 LRIM4 QPCR F	CTGTTTACCGTGCAGACCAC	900
	AGAP7039 LRIM4 QPCR R	AGCACGGTCAGGAAGTTGTT	900
<i>LRIM5</i>	AgROB2-R28 QPCR F	CTGTGCTGTTACGAGGGTCA	900
	AgROB2-R28 QPCR R	CCCAAAGTGTCTCGTTCAT	900
<i>LRIM6</i>	AGAP6327 QPCR F	CGTACTTCGGCAAGGACATT	300
	AGAP6327 QPCR R	TGGTCACCGGTATGAACAGA	300
<i>LRIM7</i>	AGAP7457 QPCR F	ATCTCGATACCGGACTGTGG	900
	AGAP7457 QPCR R	AGCTCTCCAGAAACGTCAA	900
<i>LRIM8A</i>	AGAP7454 QPCR F	TAATCTCGCCCAATTTCCAG	900
	AGAP7454 QPCR R	ACCATCAGCAACCACTCACA	900
<i>LRIM8B</i>	AGAP7456 QPCR F	GGATTGATCGTGGTGGAGTC	300
	AGAP7456 QPCR R	AAGCCAACGAGAGGTGCTTA	300
<i>LRIM9</i>	AGAP7453-2 QPCR F	TTCAGCATGCACTGGAAAAG	900
	AGAP7453-2 QPCR R	GTCGGTACCATCGGTTGACT	300
<i>LRIM10</i>	AGAP7455 QPCR F	TCGGTCTGAAGGAGCTTTGT	300
	AGAP7455 QPCR R	CACGTGCAGTGTCTGATTTC	300
<i>LRIM12</i>	AGAP5496 QPCR F	CACGCTCGATCTTTGTGTGT	300
	AGAP5496 QPCR R	GCCAGATTGTTGCTGGAAAG	300
<i>LRIM15</i>	AGAP7045 QPCR F	ATCTGGAAGCCACCAATCTG	900
	AGAP7045 QPCR R	ACACATCCAGCCAGGTAAGG	300
<i>LRIM16A</i>	AGAP7758-R42 QPCR F (LRIM16A)	AGCAACATTGTGAGCACGAG	300
	AGAP7758-R42 QPCR R (LRIM16A)	CAACCCTATTAGGACACAAAGCAT	300
<i>LRIM16B</i>	AGAP7758-R44 QPCR F (LRIM16B)	ATAGGCTGCCAATCCATCAG	300
	AGAP7758-R44 QPCR R (LRIM16B)	TTCCCATCATGAGACACATCAC	300
<i>LRIM17</i>	AGAP5693 LRRD7 APL2 QPCR F	ATTCACCTCACGGCGCTAAAC	900
	AGAP5693 LRRD7 APL2 QPCR R	CTCGCGTCAATCAAATCAAA	900
<i>LRIM18</i>	AgLRIM18 QPCR F	GCTACGGGAGCTAGATGTGC	300
	AgLRIM18 QPCR R	AGCATCAGGGTCAGCAGTTT	900
<i>LRIM19</i>	AgLRIM19 QPCR F	ACGCTCTACCTGGACGAGAA	300
	AgLRIM19 QPCR R	CTGGTCTCCGTGTCGTAGT	300

<i>LRIM20</i>	AgLRIM20 QPCR F	CCCGTACGAAAAGCTACGAA	900
	AgLRIM20 QPCR R	AGCTCGATGTGGGTTAGCTG	900
<i>LRIM26</i>	AgLRIM26 QPCR F	CGCAAGTGAAGGAAAAGGAG	300
	AgLRIM26 QPCR R	AAACCGATCAAAGCACCAC	300
<i>LRIM27</i>	AgLRIM27 QPCR F	CTGTCCAAATCGACCACTT	900
	AgLRIM27 QPCR R	TGCCAAATTTTCTCCCTCAC	900
<i>TEP1</i>	TEP1 QPCR F	AAAGCTGTTGCGTCAGGG	900
	TEP1 QPCR R	TTCTCCACACACCAAACGAA	300
<i>TEP3</i>	TEP3 QPCR F	GGAAAGCATTGCGGATGTAT	300
	TEP3 QPCR R	TTGGTAGCGATTCCCAGTTC	300
<i>TEP4</i>	TEP4 QPCR F	GCTGAAGGCATTACCAAGC	900
	TEP4 QPCR R	CGCGAAACTCTTCTTACGG	300

After optimisation, gene-specific primers were used for qRT-PCR at the indicated final concentration. 3 μ M or 9 μ M working primer stocks were prepared and used at 1/10 dilution in a 20 μ L reaction.

Table 9.3 NanoString probe sequences.

Gene	Target sequence
<i>S7</i>	GTGTACAAGAAGCTGACTGGCCGTGACGTTACGTTTCAATTCCAGAGAACTACCTGTAAAATATAAGGGTTGCGTGCTAGTGAATAGCCGAAGTTTGCA
<i>LRIM1</i>	CTCGAGCACTTTGACCTGCGCGGCAACGGGTTTCACTGTGGAACGTTGCGTGATTTCTTTCAGCAAAAACCAACGCGTGCAAACGGTCGCAAAAACAAACCG
<i>APL1A</i>	CGCCGTATCACAATAAGTGAATTTTTTTCAGCCTGTACCAACGGAGGACAGCCATCCTACAGGAGTCAGCCAATTTACGGAAATAAACAACGCTACTAC
<i>APL1B</i>	ACGCGCCGTATCTTAATCAGTATGATCTTTTTCAGCCAGTACCTACGGAGGACAGCTATCTACAAAAGTATGCACTTGACTCCTTTCACCTTTGAGTGCT
<i>APL1C</i>	TCCAACCCATATAGGTCAAACAATCTACAGAAGTCAGCCAAATTACGGAGGTGAGCAACGCTACAACGCAAGACCACGACAGCTAGAATACAAATGCATT
<i>LRIM3</i>	CGAACATTAACAACATCTTCAAGTTCCGCAACCTGATCGAGCTGGACGTGTCGTACAACGAGCTGGTAACGCTGGACTTTGTCATCTTCGCCTTCATGAA
<i>LRIM4</i>	GCGTTTCGATTTTCGCTCTCGTGCGCAATATGCGCTCCCTGGTGACGTTGAATCTGGCGCACAATCGGCTGTTTACCGTGCAGACCACCGGCGGTTACCCGC
<i>LRIM5</i>	AGGGCTGTGCTGTTACGAGGGTCAAGAGCCGTTAATGAGCTGGACGGTGGTTTGGAGCGGGAGGCGAAAGGTGACGATGAACGAGGACAGTTGGGAAG
<i>LRIM6</i>	GCCGGATTTTGCTTCATCGAGAATGTGCACCTGGACGTTTCCACCAACGGCATCGGGGGTGATTTCGATACAGTTTCCACGCCACCCGACGCTGCTCATCA
<i>LRIM7</i>	CTCTTTCAGCCACTCGCCACGTTGAAAACCTGATGATCCATCGGCTGCAGATAGAGCAGCTCGATCTGGCCGGTTGTGATAAGCTCGACATCCTGTTCCG
<i>LRIM8A</i>	AAACAAGCTGCCCGCATTTTTCGACCTCACCGTCGATAAGTTGGGCATAGTGCAGCTCTTCATACGCTCCTAGCCTGGTGCATCTATCGGCGGTAGATAAC
<i>LRIM8B</i>	CTCGATCTATCGAACAATGATCTCTACCTACTGCTTACGAGGGCGACCAGCTTGGTTCAGTTCCGGTGCAGTCTGCTGGAAGTTTCTACGCCGGGAACGATT
<i>LRIM9</i>	TTCCAACAGTCGACAGTGAGCTACCGGATTTGTCCAACGAACCACAGTGCGCATATTGGAAGGATCACTGGCCAATCTTACTGTGAACTGGCAGAAAA
<i>LRIM10</i>	TGATTGCTTCTACCGTTAGTGAGCTATCACTTCCCGCCCTGAGTGTGCTGGCGCTCCAGAACAACACGCTGACCGTGTGATCTGCGCACATGGTCATT
<i>LRIM11</i>	TCTGTAACACTAGAAAAGTTCCACCTGTTTCGACAGCATGTACCGGCCGCGACGGACAACCTCTCGCTGTTTAAACGACGTGTACCTCGGCAGTGACGTGAA
<i>LRIM12</i>	CGGCTGCTCGATCTTTCAGCAACAATCTGGCGCTGGTGCAGCTCGATCGGTGCCGAGAAGCTTGCCTCACTGACAGTATTATATCTGAACGATAACC
<i>LRIM15</i>	ACGATCGACTTCCGGGAGACGGGCATCGAGAACATCAACAAGTTCACGTTCCGAGAACGCCAAGCAGCTTCCGGCATCTGTTTCTGCGCCGCAACAAGCTTA
<i>LRIM16A</i>	AGCACGAGTGGTATGTTGGGGCAGGATCGGTTACTAGTCCATCAGAGTGCAGCACAAGTTGAAGGTAGCGGTGGA AATGGCAATGGAGTGAATATTGCAG

<i>LRIM16B</i>	GGTGCTGCTGGTATGTTGGGTATGATAGGCTGCCAATCCATCAGAGTGCAGCACAAGTTGAAGTCAGCAGCGGAA ATGGCAATGGGCTGATTATTGCAA
<i>LRIM17</i>	GTGTCCTCGGACGAGATTCTAACCACCACCTTTGCCAGCTCTAATCCCTCCACCCTATCCACCGTCCAGTTTGCACGCT CTTCGCTCACCGGCATCCAC
<i>LRIM18</i>	CACAGCCGGCGGTCTCCAGCCAAAACGGACGATGGCCACAGCATGGCTTCGATGGCTCCGTTAGGCAACAGCTGG CTGCTAGCCGGTCTGGCGCGGGT
<i>LRIM19</i>	GTTTTCTAGTGACGGTTGCTTGC GGCGCCAGCGCTACGGCCGAAAGCTGGAGTGCAGCGAGCACCGCGAGATGG AGTGCGAAATCTCCAACTTTACCAT
<i>LRIM20</i>	TGTGACACTTACCAACGGACCTTTCCGCGATGGCTCAAACGGGCGGTGGCGGTGAACTCTCGCTCGACGGCTGCC AGATTGACCACCTCGGGCCGGCA
<i>LRIM26</i>	AACTGTTTCTCGGTGACGCGAGCATGACGGATCTATCCGTAACGGACATCCGGCGTGACATGCCCGCGTCAAGCGT ATCCATCTCGGGGGTAACGATTT
<i>LRIM27</i>	CCGGCCGAACGTTACATGTGGACACCGACGACGGTGTCCCGGAAGCAGGAAGAGCACGAGGAAGTTTGCATC ATCGCGAGTCCCCGACTGAACAGCA
<i>TEP1</i>	TTGATGGGTTCCATGCAATCAATGAGAACGAGTTTGACATATTCCACAGCTTGGGTCTGTTCCGCCAGGACATTGGAC GATATCTTGTTCGACAGTGCAA
<i>TEP2</i>	TATGTCAGCGTGGAGGTGAAATACCGTGGGAAGGATTATTATGTGCAAGGCATCACGAAACCTCGAGATTACGAGG AAGCATTGATGAGAGTGCGGCTTT
<i>TEP3</i>	GCCCACAGTTCCTCGGGGACTCCTTTCAAGTGTACGCTAACGCTAATCTATCACGATGGCAGACCCGCTGGACAC GTTCCCTTCTTTGTAATGTGCA
<i>TEP4</i>	TCTCGAATCTTGGCTGTGGAAAACGGACAAAATTGGTTCTCGGGAAGCGCAACGACCAAGGAGAGCGTTCCAGAT ACGATCACAGCATGGCATTGACA
<i>TEP5</i>	CCACACCGCAAGACTTAAGGAAGATTAATAAACAGTTGAGGGTATTGGGGTGGGGCTCCTGGAGGTGATGTATAA ATACAGATTGAATCTCGTGAACCT
<i>TEP6</i>	TTCGAATTATCGACTTCAGTATTCCGGATAGTCTGTCTCTGGGAACATAAAAATTACCATTGATGGGCTGCAAGGTT TCAACTTTACGAGGAGGCAGA
<i>TEP9</i>	CAAGCTCAGATTCAATCCAACCTTACTTATCACCGTGAAGGACAACCTGAACGATATTCGCACTGATTGGAGTAGAT GTAACGAAGGCATAAGAGGCACG
<i>TEP10</i>	TCGTTGTTTCATGACTACCTGGTTGCCATTGGGTCAACACATCCATATGAATCCAACGATAATAAATGCATCAAATCCA ATGGTTCATGGCGGAATCAGGT
<i>TEP11</i>	TTTTCATGGACTCGCACCAGAATCGAACGTTGTACCGTCCACGAGACGGAGGAGCCATAGAACTTACAGGATCA AGAGCGATCGGGTTTAGAGTTAAT
<i>TEP12</i>	CACCGTGATATTGGAAGTCAGTTTTGGATTCTACCGTCAACCACGACGGTCCAGCTTACCATTGAAGGACGAT TTCGGGAGCGTTACGCATACACT
<i>TEP13</i>	CGTACAATCCGCGCACCTCGTTCCGGCGAGCATCAGTTCTACATCTACCTGAACGCGCAGGACTCGACTAACGTGTAT CTGCCGATCGTGCCGACACGGTT
<i>TEP14</i>	TGCTCGATGGCAACGAAGTATTCTATCCGGGGCTGGCGATGCGATTAAATGGTGAAGCTTGCAACGATTGATGAGAA ACCGCTTGTGAATCAACCTGTTAC
<i>TEP15</i>	TTATCGGGCCTAACCTTTAAGAACGAAACCGATTTGGAGTATCAGCAGAAGAGCTTCTCGGTATTTGTGCAAACGGA CAAATCCATCTACAAGCCGGGCG
<i>Actin5C</i>	TCGGAGCGGATTGCGCCGCTATTATCATTTTTCCCTATTGCGCCACCTACTTCTGCGCAACAGAGAGGGTGAA GGGTTATATGATGTCTGACGCTA
<i>Polyubiquitin</i>	GAAGGAATCCACCCTTCTATCTGGTTCTCCGCTGCGTGGTGGTATGCAGATTTTCGTGAAAACCTGACCGGAAAGA CCATCACTCTGGAAGTTGAGCCA

100 bp of coding sequence for each gene was targeted using NanoString analysis. For each gene, one capture probe and one labelled reporter probe (~50 bp each) were used to target this 100 bp region.

Table 9.4 Ek/LIC cloning primer sequences.

Gene	Primer name	Sequence
<i>LRIM4</i>	LRIM4 LIC for	gacgacgacaagatgAAGCCATTGCAGTTTGCGTGC
	LRIM4 LIC rev	gaggagaagcccggtttCTGAATAATGACCGTTTGTCC
<i>LRIM9</i>	gLRIM9 forA #	TGCAATTTTCGATTCAAGTGC
	tLRIM9 revA #	AAAGGACCCACATCTCAACG
	LRIM9 LIC for	gacgacgacaagatgGAGATTTCAGCTCCGTGGTG
	LRIM9 LIC rev	gaggagaagcccggtttGGCAGACGGTTCGGACGCCAC
<i>LRIM15</i>	LRIM15 LIC for	gacgacgacaagatgGTCATCTATCAGTGCGATCATTAC
	LRIM15 LIC rev	gaggagaagcccggtttCAAATCCTCGTGAGTCCGTTTG
<i>LRIM17</i>	LRIM17 LIC for	gacgacgacaagatgAAGCAGCTGAGCTGCACAATG
	LRIM17 LIC rev	gaggagaagcccggtttCGAGCAGCAAATGCCATCGATCAG
<i>TEP3</i>	TEP3C gst LIC F	gacgacgacaagatgGGGATAAGGGCACTCGCCGCG
	TEP3C gst LIC R	gaggagaagcccggtttGTCGAGGTAGCTCTGGATATC
<i>TEP4</i>	TEP4Cnew gst LIC F	gacgacgacaagatgGGGCTGAAGGCACTTACCAAG
	TEP4Cnew gst LIC R	gaggagaagcccggtttGTCGTCCTTGGTACATCTT

The open reading frames of *LRIM4*, *LRIM9*, *LRIM15* and *LRIM17* (without the endogenous signal peptides) were cloned into the pEx-10 insect expression vector. C-terminal fragments of *TEP3* and *TEP4* were cloned into the pET41a(+) expression vector. Ek/LIC cloning overhangs are shown in lower-case. All inserts were amplified by PCR from cDNA or plasmid template, except *LRIM9*, which was first amplified from genomic DNA using the primers marked # before LIC ends were added with the LIC for and rev primers.